

Impact of the 2015-2016 El Niño on tropical forests

Amy Clare Bennett

Submitted in accordance with the requirements for the degree of Doctor of Philosophy

The University of Leeds

School of Geography

April 2020

The candidate confirms that the work submitted is her own and that appropriate credit has been given where reference has been made to the work of others.

This copy has been supplied on the understanding that it is copyright material and that no quotation from this thesis may be published without proper acknowledgement.

The right of Amy C. Bennett to be identified as Author of this work has been asserted by her in accordance with the Copyright, Designs and Patents Act 1988.

© 2020 The University of Leeds and Amy C. Bennett

This is not our world with trees in it. It's a world of trees where humans have only just arrived.

— Richard Powers, *The Overstory*

Acknowledgements

First, I thank my supervisors, Simon Lewis and Oliver Phillips, from whom I have learnt so much. For the opportunity to conduct this research, for your ideas and guidance and for teaching me the power of a strong narrative, I am so grateful.

At the University of Leeds I thank the members of the Ecology and Global Change cluster. To work among this exceptional group everyday has been a great privilege. Thanks to Martin Sullivan for his kind insights and thanks to Georgia Pickavance and Aurora Levesley for their assistance with the Forest Plots Database and to the many peers, postdocs and friends who made each day brighter.

To my friends and mentors near and far, I thank each of you for your sustaining friendship and encouragement that endures beyond continents. To my mum, my dad and my sister Emily, thank you for your unyielding love and support.

It takes many people to measure a tree and I am indebted to a long list of people who make the long-term measurement of field plots possible. I acknowledge all who have contributed to the datasets in this thesis and I extend special thanks to those who led or participated in El Niño remeasurement campaigns.

I have special thanks for my field teams for their hard work in Liberia and Ghana. I thank the Forest Development Authority (FDA) of Liberia and the Forestry Commission (FC) and Forestry Research Institute of Ghana (FORIG) for allowing me to conduct field research and Armandu Daniels, Paul Duo, Kofi Affum-Baffoe and Ernest Foli for their logistical support. Thank you to Simon Lewis for training me in the field. Gratitude to my wonderful field crew in Ghana who worked tirelessly and looked out for me as one of their own; Samuel Asamoah, Francis Addai and Yaw Nkrumah. To Sylvester Chenikan, master botanist and friend, who, incredibly, has participated in the establishment (1978) and all four remeasurement campaigns of the plots in Liberia - thank you for sharing your wisdom and for bearing with such a newcomer to the jungle.

For the first time in my life I set foot in a tropical forest, an experience I will never forget. I extend my sincere thanks the communities of Garley Town, Zwedru and Glaro Freetown in Liberia and Akotakrom, Ankasa, Bobiri, Boekrom, and Dadieso in Ghana. Thank you for embracing me. I am proud to have gained two new names during fieldwork. In Ghana, it is an Ashanti tradition to have a name based on the day you were born, and born on a Friday, I was called Afia. In Liberia my house gave me a Grebo name, Dewonyon, which means doing something good from the heart. I hope this name will always be true.

Abstract

Tropical forests comprise an important long-term carbon sink. Loss of carbon and biomass following severe droughts across Borneo in 1997-98 and Amazonia in 2005 and 2010 suggest this sink is sensitive to drought, but recent evidence also identifies a shift in species composition to more drought tolerant species and thus the exact climate sensitivity of the tropical carbon sink remains unclear. Uncertainty in how the world's most biodiverse and productive ecosystems will respond to increasing temperatures and altered precipitation is a major limitation for predicting future climate.

The El Niño Southern Oscillation causes anomalies of high temperature and drought in tropical regions and the responses of tropical forests to these climate anomalies gives us an insight into whether and how key carbon pools, dynamics and species might endure the hotter and periodically drier conditions predicted for the end of the century. Therefore, the record hot and dry climate caused by the 2015-16 El Niño offers a novel opportunity to understand the response of the tropical sink to temperature and drought as it was the first very strong El Niño to be captured by the African Tropical Rainforest Observation Network (AfriTRON) and the Amazon Forest Inventory Network (RAINFOR) that monitor structurally intact forests. This thesis combines climate data with measurements from long-term forest monitoring plots across tropical Africa (100 plots) and South America (137 plots) over the El Niño climate anomaly to investigate the impacts of the unprecedented temperatures and droughts on tropical forests.

For the first time, the resistance of intact African tropical forests to short-term drought is assessed and despite record temperatures and drought, the El Niño was insufficient to reverse the longstanding biomass carbon sink which reduced but was still a sink of $0.52 \pm 0.20 \text{ Mg C ha}^{-1} \text{ yr}^{-1}$ in the El Niño. South American tropical forests were a carbon sink prior to the El Niño and became a small carbon source of $-0.1 \pm 0.40 \text{ Mg C ha}^{-1} \text{ yr}^{-1}$ in the El Niño. The negative responses of African and South American tropical forests to high temperatures were similar, but the negative impacts of drought differed between the continents' forests. Overall, the results indicate some resistance to environmental change in the short-term and potential resilience in the long-term in African forests, although hotter drier forests in South America are vulnerable to carbon sink reversal. The results in this thesis provide evidence that much of the world's intact tropical

forests have the capacity to resist climate anomalies only if conservation efforts succeed in keeping forests intact and global temperature increases are limited.

Table of Contents

Chapter 1	14
1.1 Tropical forests on two continents	16
1.1.1 Climate.....	17
1.1.2 Paleoclimate	18
1.1.3 Structure	18
1.1.4 Floristics.....	19
1.1.5 Soils	20
1.2 Uptake, storage and release of carbon with global change	21
1.2.1 Carbon dioxide.....	21
1.2.2 Temperature	22
1.2.3 Drought	24
1.2.4 Drought Metrics	25
1.3 What kills trees?	26
1.3.1 Carbon starvation	29
1.3.2 Hydraulic Failure.....	30
1.4 El Niño	30
1.4.1 Temperature impacts.....	31
1.4.2 Precipitation impacts.....	31
1.4.3 Fires.....	32
1.4.4 The tropical carbon cycle during El Niño	32
1.4.5 The 1982-83 El Niño.....	33
1.4.6 The 1997-98 El Niño.....	33
1.4.7 The 2015-16 El Niño.....	34
1.5 Capturing the impacts of the 2015-16 El Niño with long-term forest plots	34
1.6 Aims and Objectives	35
1.6.1 Objectives	36
1.7 Thesis Outline	37
Chapter 2	38
Abstract	38
2.1 Introduction	39

2.2	Methods	41
2.2.1	Climate Analysis	41
2.2.2	Temperature, Precipitation and Drought Estimation.....	42
2.2.3	Plot Data Collection and Analysis.....	43
2.3	Results	48
2.3.1	Climate.....	48
2.3.2	Drivers of Biomass Carbon Dynamics	53
2.3.3	El Niño impact on Biomass Carbon Dynamics	55
2.3.4	Stem Dynamics.....	59
2.4	Discussion	61
2.4.1	Forest Responses.....	62
2.4.2	Regional Carbon Implications.....	64
Chapter 3	67
Abstract	67
3.1	Introduction	68
3.2	Methods	71
3.2.1	Climate Data	71
3.2.2	Plot Data Collection and Analysis.....	72
3.3	Results	74
3.4	Discussion	92
Chapter 4	97
Abstract	97
4.1	Introduction	98
4.2	Methods	100
4.2.1	Climate Data	100
4.2.2	Plot Data Collection and Analysis.....	101
4.3	Results	102
4.4	Discussion	123
Chapter 5	127
5.1	Research Synthesis	127
5.1.1	Climate and climate change in the tropical forest biome	129
5.1.2	Temperature and drought impacts on carbon and stem dynamics.....	130

5.1.3	Baseline climate can modulate climate anomaly response	130
5.1.4	Are El Niño responses to temperature and drought consistent across two continents?	131
5.2	Research Implications	131
5.3	Future Directions	133
5.4	Summary	134
	References	136
	Appendices	154

List of Equations

The maximum cumulative water deficit, MCWD, is calculated as in (Aragão et al. 2007):

if $WD_{n-1} - ET_n + P_n < 0$;

then $WD_n = WD_{n-1} - ET_n + P_n$;

else $WD_n = 0$

Where WD =water deficit (mm), n = month, ET =evapotranspiration (mm), P =precipitation (mm)

Aboveground biomass = $0.0673 \times (\rho D^2H)^{0.976}$ (Chave et al. 2014)

Where ρ = stem wood density (g cm^{-3}), D = stem diameter (cm) at 1.3 m or above buttresses, H = height (m)

Annual plot-level per-capita stem mortality rate:

$N_{s,t-1} = (1 - m_a) N_{s,t}$ (Kohyama et al. 2018)

Where N_s = the number of surviving trees and m_a = annual mortality

List of Tables

Table 2.1 Climate anomalies of three very strong El Niños for the African tropical forest region and plot locations.....	50
Table 3.1 Climate anomalies of five drought events, including three very strong El Niño events, for the South American tropical forest region and plot locations.....	76
Table 4.1 Mean plot-level per capita stem mortality rates of 237 plots.....	123
Table 5.1 Summary of the key impacts of the 2015-16 El Niño climate anomaly on carbon dynamics of tropical forests	129

List of Figures

Figure 1.1 Mean annual temperature in tropical forests of South America and Africa.....	23
Figure 1.2 Hypothesized tree mortality threshold	29
Figure 1.3 Typical temperature impacts of El Niño	31
Figure 1.4 Typical precipitation impacts of El Niño	31
Figure 2.1 Plot locations within African tropical forest region and climate for plot locations and the African tropical forest region	51
Figure 2.2 Climate anomalies of 100 long-term inventory plots.....	52
Figure 2.3 Temperature and drought impacts on aboveground biomass carbon dynamics of 100 long-term forest plots	54
Figure 2.4 Trends in net aboveground biomass carbon, carbon gains to the system from woody productivity and carbon losses from biomass mortality, for 100 long-term plots in Africa.....	56
Figure 2.5 Carbon and stem dynamics, pre- and during the 2015-16 El Niño.....	57
Figure 2.6 Temperature and drought impacts on stem dynamics of 100 long-term forest plots	58
Figure 2.7 Effect sizes of change in carbon and stems in 100 African tropical forest plots over the 2015-16 El Niño	60

Figure 3.1 Climate for plot locations and the South American tropical forest region	77
Figure 3.2 Intensity of droughts and locations of forest monitoring plots in South America	78
Figure 3.3 Intensity of temperature and drought anomalies in 2015-16	80
Figure 3.4 Carbon and stem dynamics, pre- and during the 2015-16 El Niño.....	81
Figure 3.5 Carbon dynamics, pre- and during the 2015-16 El Niño and in the context of 2005 and 2010 Amazon drought-responses	82
Figure 3.6 Temperature and drought impacts on aboveground biomass carbon dynamics	84
Figure 3.7 Baseline temperature and baseline drought and anomalies of aboveground biomass carbon dynamics	85
Figure 3.8 Temperature-productivity thresholds	86
Figure 3.9 Effect sizes of change in carbon in South American tropical forest plots over the 2015-16 El Niño	89
Figure 3.10 Aboveground carbon change in neotropical moist forests.....	91
Figure 4.1 Climate anomalies of 237 long-term forest plots	104
Figure 4.2 El Niño climate anomalies at 237 plots.....	105
Figure 4.3 Mean pre-El Niño climate at 237 plots.....	106
Figure 4.4 Carbon and stem dynamics, pre- and during the 2015-16 El Niño.....	107
Figure 4.5 Temperature and drought impacts on aboveground biomass carbon dynamics	110
Figure 4.6 Baseline temperature and drought and aboveground biomass carbon dynamics	112
Figure 4.7 Temperature-productivity thresholds	113
Figure 4.8 Temperature and drought impacts on stem dynamics of 237 long-term forest plots	116
Figure 4.9 Baseline temperature and drought and stem dynamics.	118
Figure 4.10 Effect sizes of change in carbon and stems in tropical forest plots over the 2015-16 El Niño	121

Figure 4.11 | Temperature and drought impacts on per capita stem mortality rate. 122

Appendices

Figure A2.1 | Monthly correlation coefficients for temperature

Figure A2.2 | Monthly correlation coefficients for precipitation

Table A2.1 | Parameters used to estimate tree height from tree diameter

Table A2.2 | Coefficients of model-averaged multiple regression models of net carbon, carbon gains and carbon losses

Table A2.3 | Coefficients of model-averaged multiple regression models of net stems, recruitment and stem mortality

Abbreviations

A – altitude

AGB – aboveground biomass

AGWP – aboveground woody productivity

AfriTRON – African Tropical Rainforest Observation Network

ANOVA – analysis of variance

C – carbon

DGVM – dynamic global vegetation model

MCWD – maximum cumulative water deficit

POM – point of measurement

RAINFOR – Amazon Forest Inventory Network

SST – sea surface temperature

T – temperature

VPD – vapour pressure deficit

Chapter 1

Introduction

Since the start of the Industrial Revolution the concentration of atmospheric carbon dioxide has been rising, leading to an increase in surface air temperature (Stocker et al. 2013, IPCC 2018). Tree-dominated ecosystems worldwide are affected by this environmental change alongside deforestation, forest degradation and fire. Tropical forests comprise 44 % of global forest area (Keenan et al. 2015), are highly carbon rich (Sullivan et al. 2017) and house many species and communities (Barlow et al. 2007) so the impacts of such anthropogenic change on tropical forests may be particularly important. Thus, environmental changes that impact tropical forests may have globally significant effects on carbon, climate and biodiversity.

Forest cover is rapidly decreasing in the tropics, disturbance levels are increasing and human impacts are modifying even intact tropical forests (Lewis et al. 2015). Current rates of tropical deforestation are high (Hansen et al. 2010, Baccini et al. 2012), forest loss is increasing by $2101 \text{ km}^2 \text{ yr}^{-1}$ (Hansen et al. 2013) and though estimates vary widely, deforestation leads to loss of biodiversity, hydrological impacts, loss of carbon storage and sequestration (Foley et al. 2007). Deforestation is the most pervasive land-use-change process and emissions from land use change contribute 1.3 Gt C yr^{-1} , 12 % of global anthropogenic CO_2 emissions (Le Quéré et al. 2018). As forests are a major carbon sink deforestation lowers the capacity of forests to uptake CO_2 emissions (Pan et al. 2011, Hubau et al. 2020). In carbon terms, there is a near neutral exchange of carbon across the terrestrial tropics as the large carbon losses from deforestation and degradation are almost entirely offset by the significant carbon uptake from intact tropical forests and tropical forest regrowth (Gaubert et al. 2019). Independently, long-term measurements of structurally intact old-growth tropical forests also show this uptake with forest biomass carbon increasing across remaining African (Lewis et al. 2009), Amazonian (Brienen et al. 2015), and Asian (Qie et al. 2017) forests. Yet, the tropical carbon sink may be vulnerable: there are indications that the Amazon carbon sink is declining, driven by a

combination of accelerating tree mortality and a stalling of past increases of woody productivity (Brienen et al. 2015). Recent evidence suggests the African carbon sink is beginning to decline too, with high temperatures and drought impacting both tree growth and tree mortality pan-tropically (Hubau et al. 2020).

One possible cause of the decline in sink strength may be increasing surface air temperatures, because both photosynthesis and respiration are temperature dependent. Above optimal temperatures plants reduce their carbon uptake (Lloyd and Farquhar 2008), closing stomata to avoid water loss, reducing internal CO₂ concentrations and reducing carbon assimilation in the leaf (Slot and Winter 2017). One study from La Selva, Costa Rica has suggested a decline of up to 20 % in tree biomass growth per degree of warming (Clark et al. 2013). Respiration rates also tend to increase with short-term increases in temperature at both the leaf-level (Heskel et al. 2016) and in tropical forest communities (Clark et al. 2010), again reducing tree growth. So, rising global temperatures may be compromising the tropical carbon sink.

Droughts may also be causing the decline in carbon sink strength. Carbon gains from biomass growth are expected to decrease during drought and tree mortality is expected to increase, which means that drought may decrease the amount of carbon stored and negatively feedback to reduce the carbon sink of tropical forests. Without sufficient water plants cannot maintain photosynthesis (Doughty et al. 2014), increase respiration (Metcalfe et al. 2010) and if droughts are strong enough or long enough trees die and tree mortality may be widespread (McDowell et al. 2018). As hotter temperatures exacerbate water deficits by increasing the evaporative demands for plants (Trenberth et al. 2014), even if drought intensity itself is not increasing, recent droughts may have been stronger and had greater impacts on forests simply due to hotter temperatures.

El Niño is a recurring stochastic climate phenomenon whereby changes in the magnitude and spatial distribution of Pacific sea surface temperatures impact climate conditions across most of the tropics for up to a year or more (Cai et al. 2015). Typically, El Niño events lead to widespread drought across Amazonia, droughts in east Africa, and below average precipitation over the Indian subcontinent and Southeast Asia (Dai and Wigley 2000). El Niño events vary in strength but sea surface temperature anomalies amplify land temperatures (Tyrrell et al. 2015) and strongly determine interannual variation in climate. Against a background of rising atmospheric CO₂ and warming, the El Niño of

2015-16 led to record atmospheric CO₂ concentrations, record global temperatures and the hottest conditions across the tropics in modern times (Liu et al. 2017). Therefore, El Niño presents a potential insight into the ecological impacts of the more extreme climate conditions predicted for the future.

Long-term measurements of forests capture their responses to a changing climate. Three very strong El Niño events have occurred in the last 50 years, 1982-83, 1997-98 and 2015-16, but only the latter occurred after networks of long-term inventory plots had been established in Africa and South America and were poised to capture an El Niño event. The 2015-16 El Niño event provides a first opportunity to assess the impact of high temperatures and strong water deficits on African and South American tropical forests. Climate data is combined with measurements from inventory plots to gain a quantitative impact of the 2015-16 El Niño event on African and Amazonian forests.

In sum, (1) tropical forests have a potentially important role to play in slowing climate change, to the extent that atmospheric CO₂ increases continue to support enhanced autotrophic carbon uptake, and yet (2) climate change itself threatens to stop, and even reverse, the tropical carbon sink and in so doing may damage the integrity of tropical forests themselves. There are several ways to reduce the scientific uncertainties surrounding these changes and threats. Arguably, one of the simplest is to try to exploit natural variations in the climate to quantitatively assess how higher temperature and water availability affect tropical forests over shorter, measurable periods. Using the recent record extreme high temperature anomalies across the tropics that were associated with the 2015-16 El Niño event in combination with measurements from networks of long-term monitoring plots across large areas of tropical forest may significantly improve our understanding of how the biome responds to large-scale perturbation. Quantifying how the tropical biome responds to such large-scale perturbation is an important component to help us understand the contemporary carbon cycle, with implications for the future temporal evolution of the tropical forest carbon sink.

1.1 Tropical forests on two continents

Tropical forests are ecosystems characterised by dense, tall, closed canopies dominated by trees (Putz and Redford 2010). They occur in the region surrounding the equator from the Tropic of Cancer in the Northern Hemisphere at 23.43702° North, to

the Tropic of Capricorn in the Southern Hemisphere at 23.43702° South. Tropical forests occur on four continents, but this thesis and literature review contends with tropical forests in two major regions; Africa and South America. Tropical forests on these two continents differ in terms of climate, paleoclimate, structure and floristics.

1.1.1 Climate

Temperatures vary by continent. Africa is on average the coolest of the major tropical regions, due to lowland forested regions being at higher altitudes (Malhi and Wright 2004). South American tropical forests are warmer and recent trends indicate temperatures are rising faster in South American than in African tropical forest regions (Hubau et al. 2020).

Tropical forests are generally hot and wet, but total annual rainfall and rainfall seasonality vary regionally. The tropical moist forest biome is largely constrained by total annual rainfall. Africa is on average the driest major tropical region with approximately 1800 mm yr⁻¹ precipitation while South America has approximately 2400 mm yr⁻¹ (Malhi and Wright 2004). The intertropical convergence zone, where northern and southern trade winds meet and produce a narrow zone of low pressure, dominates the precipitation regimes of the tropics. Rainfall varies with latitudinal distance from the equator and dry seasons are strongest and longest further from the equator, at the edge of the tropical forest biome. Precipitation is also highly regional due to orography, coastline shape and distance from the sea (McGregor and Nieuwolt 1998). About 90 % of African tropical forests receive less than 2,000 mm yr⁻¹ precipitation, the approximate amount to sustain high levels of photosynthesis throughout the year (Guan et al. 2015). By contrast just 41 % of South American forests have precipitation below 2,000 mm yr⁻¹. So African tropical forests tend to be drier than South American tropical forests.

There can be strong seasonality of rainfall in the tropics and African forests may have two dry and two wet seasons. The intensity, length and arrival date of seasonal rainfall is becoming more variable with increases in interannual variability of seasonality over the dry tropics (Feng et al. 2013). The hydrological cycle of the Amazon is intensifying with wet seasons getting wetter, particularly in the Northwest Amazon (Gloor et al. 2013), and the dry season getting drier in the Amazon (Fu et al. 2013). In Africa the dry season in the Congo basin is increasing in length with earlier onset due to long-term drought (Jiang et al. 2019). The Amazon and Congo basins are hydrologically connected and floods in the

Amazon tend to coincide with droughts over the Congo and vice versa (Eltahir et al. 2004). Overall, there are greater seasonal water deficits in South America than in Africa (Hubau et al. 2020).

1.1.2 Paleoclimate

The palaeoclimate history of South America and Africa differ considerably and the species present today reflect these environmental changes of the past. In Amazonia, according to oxygen isotope records from the centre of the eastern Amazon, the climate was drier during the last glacial with less plant transpiration and water recycling, but the tropical forest remained (Wang et al. 2017). Pollen records also suggest that forests of the western Amazon were resilient to past climate change with only a few species replacements and minor fluctuations in abundance in the Mid-Holocene Dry Event (Nascimento et al. 2019). So, tropical forests probably persisted across Amazonia, despite drier conditions, with any forest changes restricted to forest fringes (Malhi et al. 2014). African climate has oscillated between wetter conditions in interglacial periods, and cooler and drier conditions in glacial periods (deMenocal 2004), when forests retreated to refugia (Malhi et al. 2014). The paleo-filtering of African species may have eliminated much of the most mesic-adapted biodiversity and the lower plant diversity of African forests today reflects their more variable climate history (Parmentier et al. 2007). African tropical forest diversity is actually similar to or higher than that of the Amazon when comparing equivalent forests with similar dry season lengths (Parmentier et al. 2007), suggesting that in Africa most wet-adapted species have been lost and the dry-adapted species remain and perhaps these xeric lineages have diversified, conferring drought resistance.

1.1.3 Structure

Neotropical forests tend to have more smaller stems in a given area than African forests (Lewis et al. 2013). Amazonian forests have approximately 600 trees per hectare greater than 100 mm diameter while African forests have about 425 (Lewis et al. 2013, Hubau et al. 2020). So, African tropical forests are more dominated by large trees (Enquist et al. 2020) and thus while tree biodiversity is lower, carbon density is greater in Africa (Sullivan et al. 2017). South American plots have lower carbon storage per unit area than African forests (Sullivan et al. 2017) but both diversity and carbon vary greatly

within South America. Carbon residence times are also shorter in South American forests compared to African forests (Galbraith et al. 2013, Hubau et al. 2020). South American forests tend to have higher recruitment, higher stem mortality and faster stem turnover than African forests. So overall, high biomass is typically found in forests in Africa, high diversity in South America and low diversity in Africa, although carbon storage and tropical tree species diversity vary widely across the tropical biome and within continents.

1.1.4 Floristics

Forest composition and diversity differs in Africa and South America. Evidence from pollen and molecular studies suggests that most extant tropical genera first appeared after the supercontinent Gondwana split (Donoghue and Donoghue 2008), so species on each continent represent evolutionary responses to the physical environment on each continent. Indeed, forest plots from different continents tend not to share genera (Dexter et al. 2015), and only 4 % of species are shared between Africa, America and Asia (Slik et al. 2015) with the most speciose tropical families overlapping across continents (Gentry 1988). The Dipterocarpaceae dominate in Asian forests but are very rare in South American and African forests (Dexter et al. 2015). In Amazonia areas with geologically younger soils tend to have more phylogenetically diverse and species-rich tree communities (Honorio Coronado et al. 2015) with local communities assembled from lineages that span the whole Amazon (Dexter et al. 2017). Seasonally dry neotropical forests have more closely related species from lineages that tend to be geographically more restricted (Dexter et al. 2017, Slik et al. 2018).

There are some phylogenetic links between African and South American forests. The genera present in Africa and South America are similar due to the shared origin and Cenozoic plate of these tropical forests alongside some transatlantic dispersal (Slik et al. 2018). South American tropical forests can be divided into humid forests and dry forests, with dry tropical forests relatively compositionally distinct (Slik et al. 2018). Within Africa forests are compositionally very similar and this is thought to be because of the paleoclimate history of the continent and repeated retreat of the forest to refugia.

There is also contemporary evidence of the composition of ecosystems moving towards drought tolerance. Forest composition in Amazonia has shifted to include more dry affiliated genera (Esquivel-Muelbert et al. 2019) and drought-induced mortality in

Amazonia has been greater for wetter-affiliated genera (Esquivel-Muelbert et al. 2017). Additionally trees are distributed according to drought sensitivity in Panama (Engelbrecht et al. 2007) and in West Africa drier forests are responding more to changes in climate than wetter forests (Aguirre-Gutiérrez et al. 2019). In West Africa deciduous species have increased in response to long-term drought (Fauset et al. 2012), and these forests have undergone a series of other trait-based changes including an increase in nitrogen-fixing species and light-demanding species (Aguirre-Gutiérrez et al. 2019). In South America as mortality rates in the wet-affiliated genera increase, the shift towards drought resistance is among newly recruited trees, but this shift to potentially greater drought-tolerance is not yet evident in community composition (Esquivel-Muelbert et al. 2019). On both continents a long-term carbon sink has persisted even as species composition has shifted (Brienen et al. 2015, Hubau et al. 2020).

1.1.5 Soils

Soils of tropical moist forests are typically weathered and nutrient poor as erosion and leaching are promoted by hot and humid climates (Richards et al. 1996). Though nutrient poor, the dominant soils under tropical forests are often deep and store water effectively making them physically good for tree growth. With a relatively closed nutrient cycle, it is often the trees that supply the forest with nutrients through litterfall, throughfall and stemflow (Vitousek and Sanford 1986). Rapid decomposition and efficient uptake by plants and microorganisms makes the nutrients available to return to the vegetation, but nutrient cycling is diverse among tropical forests (Vitousek and Sanford 1986).

South America has a strong east to west soil gradient with more fertile soils in the west than the east Amazon (Quesada et al. 2012). In the western Amazon soils are younger and have higher nutrient availability and cation exchange capacity due to relatively recent deposition from Andean uplift (Hoorn et al. 2010, Quesada et al. 2010). In the eastern Amazon soils are more weathered (Quesada et al. 2010). The Amazon soil gradient is an important determinant for vegetation. Africa does not have a strong soil fertility gradient (Lewis et al. 2013), but regions of the Ivory Coast, Ghana and Nigeria tend to have relatively more nutrient rich soils than the rest of the continent (IUSS Working Group WRB 2006) and East African forests tend to have younger more fertile soils than Central African forests (Lewis et al. 2013).

1.2 Uptake, storage and release of carbon with global change

There has been a strong global carbon sink in forests in recent decades, especially in tropical forests (Pan et al. 2011), but there is evidence that the carbon sink capacity in South America (Brienen et al. 2015) and Africa (Hubau et al. 2020) has recently saturated. Growth rates in the Amazon have stalled while biomass mortality has increased, reducing carbon residence times (Brienen et al. 2015) with some evidence that carbon losses have increased in Africa since 2010 (Hubau et al. 2020).

Forests are under increasing anthropogenic pressure; carbon dioxide concentrations are rising, temperatures are rising, and precipitation patterns are changing, all of which affect the processes of photosynthesis and respiration. These three pressures will be focused on here, but it is important to note the other global change effects on tropical forests: increasing nutrient deposition (Lewis et al. 2004), increasing solar radiation (Willson and Mordvinov 2003) (especially at higher elevations (Cabrol et al. 2014)), increasing liana loads (Phillips et al. 2002, Schnitzer and Bongers 2011, Jones et al. 2017), shifting fire regimes (Aragão et al. 2018, Yin et al. 2020) and land use change including deforestation and forest degradation (Barlow et al. 2016).

1.2.1 Carbon dioxide

The global atmospheric concentration of CO₂ reached 399.4 ppm in 2015 (Le Quéré et al. 2016) and 402.8 in 2016 (Le Quéré et al. 2018) and continues to rise. This rise is strongly correlated with the increase in global consumption of fossil fuels with significant contributions from the clearing of forests, especially in the tropics (Le Quéré et al. 2016). Atmospheric increases in CO₂ increase annual global temperatures, and atmospheric concentrations of other greenhouse gases, e.g. water vapour and methane are also changing, feeding back to further alter climate.

Across multiple scales, photosynthesis increases with increasing atmospheric carbon dioxide concentration. Higher concentrations of CO₂ reduce the competition from O₂ for the active site of RuBisCO and reduce photorespiration. A synthesis of results from CO₂ fertilisation experiments showed an increase of 5.0 ± 1.2 % in tropical carbon stocks per 100 ppm of CO₂, but included no data from mature tropical forests (Terrer et al. 2019). Long term tropical plots in Africa and Amazonia link increased CO₂ to large increases in productivity (Hubau et al. 2020). Currently increased uptake from CO₂ fertilisation is

greater than the negative impacts of rising temperatures (Piao et al. 2013) and drought (Gloor et al. 2015, Jiang et al. 2019). Long-term observations of increases in tropical greenness measured by satellites in areas without major land-use-change (Nemani 2003, Smith et al. 2016) and in central Africa this decade (Chen et al. 2019) also indicate increases in tropical forest productivity. Thus, the increased carbon sink capacity is widespread.

As well as direct fertilization effects, higher CO₂ also often leads to large decreases in leaf conductance (Field et al. 1995) and increases in water use efficiency and at both the leaf and canopy scale (Bonan et al. 2014). The increased water use efficiency gained under higher CO₂ may buffer plants to drought (Keenan et al. 2013), but it is likely the coincident negative effects of temperature and drought could outweigh this positive effect of CO₂ as illustrated by the saturation of the tropical carbon sink (Hubau et al. 2020).

1.2.2 Temperature

Global and regional temperatures are increasing, and in 2016 the world was about a degree warmer than the 20th century average temperature (NOAA 2018). Basal respiration increased with temperature, but shows some acclimation at both short- and long-term scales (Tjoelker et al. 2001, Wythers et al. 2005). However, warming increases autotrophic respiration rates (Lloyd and Farquhar 2008) and could compromise forest carbon sinks (Clark et al. 2003, Anderegg et al. 2015a). Tree growth models also suggest maximum temperatures increase respiration and so can have a strong negative effect on stem growth (Schippers et al. 2015). Vegetation productivity and respiration both increase with higher precipitation and thus can offset each other when it is wetter and hotter (Wang 2013). With the higher temperatures and variable precipitation of El Niño it is difficult to predict a respiration response. If trees have already acclimated to increasing temperatures, there should be very little, if any, temperature driven respiration increases seen in the plot data.

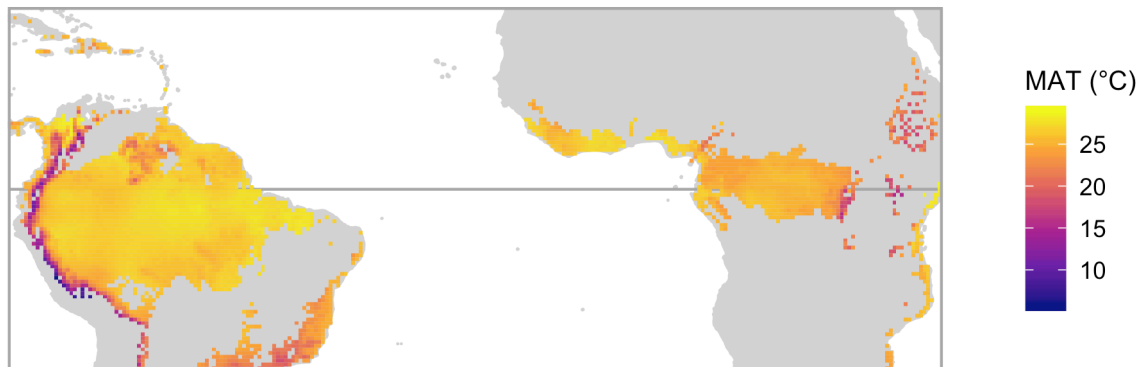


Figure 1.1 | Mean annual temperature in tropical forests of South America and Africa
Mean annual temperature (CRU 4.03 (University of East Anglia Climatic Research Unit et al. 2020)) of tropical moist forest region (Olson et al. 2001) for the thirty year reference period 1989-2018.

Tropical forest productivity responses to temperature are complex; to an extent increasing temperature should increase productivity. If plants can tightly regulate stomatal conductance and increase water use efficiency then they should be able to perform better under high temperatures, but higher temperatures also pose greater risks of thermal damage (Schreiber and Berry 1977) and greater hydraulic risks, as vapour pressure deficits increase with temperature (Trenberth et al. 2014). Warmer climates have higher productivity across tropical elevation gradients (Raich et al. 1997, Fyllas et al. 2017) and more widely across ecosystems (Del Grosso et al. 2008), but tropical forest responses to temperature have not been well-documented. In tropical forests, 30-year mean maximum temperatures predict aboveground biomass as maximum temperatures limit productivity, particularly in the hottest forests (Sullivan et al. 2020).

The full impact of high temperatures and increased atmospheric CO₂ on tropical ecosystems is unlikely to result from direct thermal effects alone, but also from interactions with other environmental variables. Notably, increasing temperatures increase vapour pressure deficits and decrease the amount of plant-available water, while transpiration rates from plant canopies increase. Temperature increases alone can lead to water deficits but the frequency of severe droughts is also increasing in many regions as a result of climate change (IPCC 2012, Settele et al. 2014, Trenberth et al. 2014). Although

episodic mortality occurs in the absence of climate change, studies suggest that at least some of the world's forested ecosystems may already be responding to climate change (Allen et al. 2010, Hubau et al. 2020), raising concerns that forests may become increasingly vulnerable to higher background tree mortality rates in response to warming and drought, even in environments that are not normally considered water limited. This would lead to the loss of sequestered forest carbon and associated atmospheric feedback. If climate change increases drought duration and intensity, drought induced mortality is likely to increase (Allen et al. 2015), Figure 1.2).

1.2.3 Drought

Anomalous droughts can threaten the tropical forest carbon sink. Increasing plant-available water is usually beneficial for tropical forests, except where soils are saturated (Sousa et al. 2020), or productivity is light-limited (Schoor 2003). In these regions drought can increase productivity (Sousa et al. 2020). Lack of water mostly impacts forests through tree mortality and water deficits increase mortality risk for most of the climate space (Allen et al. 2010, Phillips et al. 2010b). There is also evidence that larger trees might be more vulnerable to drought as they face greater hydraulic challenges (Bennett et al. 2015). So, it is expected that regions with more anomalous drought should have greater biomass mortality and a disproportionate number of large trees dying.

Responses to increased vapour pressure deficits also suggest that strong droughts reduce aboveground growth. VPD is higher in tropical canopies than in the relatively buffered understory (Fetcher et al. 1985) and tropical trees respond to VPD by closing stomata, decreasing midday xylem pressure and leaf conductance (Fetcher 1979). Tropical drought experiments also suggest strongly reduced water pressures and lower conductance during high VPD episodes (Rowland et al. 2015). So, forests may be able to withstand short periods of drought, by reducing growth when hydraulic demands are high.

Hydraulic pressures in forests are greatest for taller trees with exposed crowns as they experience greater vapour pressure deficits and more solar radiation (Roberts et al. 1990a). These large trees may lose their leaves in drought and their drought deciduousness may change the structure of tropical forests during the drought. Small trees could benefit from the drought deciduousness of larger trees as they are released from competition for light (Slik 2004). Understory trees could also have a relative

advantage during drought with lower leaf temperatures, vapour pressure deficits, and wind speeds. Thus, if the extra light more than compensates for the higher air temperatures in El Niño, growth and recruitment of small trees may increase. In a meta-analysis of forests, the growth rate of small trees increased in response to drought, and was presumed to be due to increased solar radiation reaching the understory from increased deciduousness of large trees during drought, although that study included no plots in Africa (Bennett et al. 2015). Furthermore, a recent analysis of the carbon sink contribution of different size classes of trees in African forests highlights the aperiodic growth of understory trees and shows a large relative response to small changes in the growing conditions of small understory stems (Hubau et al. 2019), consistent with the idea that small trees could benefit in drought.

1.2.4 Drought Metrics

Defining drought is vital to assessing its impact on tropical forests. A recent meta-analysis of drought found ecologists consistently struggle to quantify drought (Slette et al. 2019), and in this thesis I use a drought metric to allow comparisons across regions and continents. Standard indices of drought include Palmer's Drought Severity Index (PDSI), standardised precipitation index (SPI), standardised precipitation evapotranspiration index (SPEI) and maximum cumulative water deficit (MCWD).

The PDSI uses a temperature and water balance model to quantify long-term drought, but does not capture droughts shorter than 12 months, and PDSI is not comparable across regions. The SPI is closely related to soil moisture in the short term and groundwater storage in the long term but cannot incorporate changes in evapotranspiration. The SPEI takes into account evapotranspiration as well as precipitation so captures the main impacts of increased temperatures on water demand but requires a long base period of fifty or more years.

Another useful metric to compare precipitation seasonality and intensity of dry seasons is MCWD. Water deficit is the difference between monthly rainfall and monthly evapotranspiration which can be approximated as about $100 \text{ mm month}^{-1}$ (Aragão et al. 2007) or estimated on a monthly basis with seasonally estimated evapotranspiration. Cumulative water deficit is calculated beginning with the wettest month of the year and the

maximum or most negative value is assigned to that hydrological year. The maximum cumulative water deficit, MCWD, is calculated as in (Aragão et al. 2007):

if $WD_{n-1} - ET_n + P_n < 0$;

then $WD_n = WD_{n-1} - ET_n + P_n$;

else $WD_n = 0$.

Where WD =water deficit, n = month, ET =evapotranspiration, P =precipitation

MCWD is a useful indicator of water stress as it captures duration and intensity of drought through accumulated water stress across dry seasons, although it does not include local soil characteristics that determines water storage capacity or temperature or overlying vegetation characteristics that may alter evapotranspiration. MCWD is commonly used in tropical forest ecology and reflects the distribution of tropical forests better than annual rainfall (Zelazowski et al. 2011). The analytical priorities of this thesis involve comparing droughts across regions with more than one dry season, and comparing droughts pantropically, so MCWD is the best drought intensity metric for these purposes.

The assumption of 100 mm month⁻¹ evapotranspiration for tropical forests in Africa and South America is based on measurements from Amazonia (Aragão et al. 2007, 2014), more limited measurements from West Africa (Kume et al. 2011) and use in past studies on both continents (Phillips et al. 2009, James et al. 2013, Hubau et al. 2020). With constant evapotranspiration MCWD represents a precipitation-driven dry season water deficit. This thesis uses MCWD with 100 mm month⁻¹ to calculate water deficits in Africa and South America.

1.3 What kills trees?

Logically, factors that tend to increase growth also tend to decrease mortality, and conversely factors that decrease growth tend to increase mortality. Increased tree size or age brings increased mortality risks through greater hydraulic challenges, increased risk of embolism, and greater pest and pathogen pressure (Ryan et al. 2006, Zhang et al. 2009, McDowell and Allen 2015). At the inter-species level trees that grow fast tend to die sooner, completing their life cycle more quickly, as the faster a plant grows the faster it may get to the risk zone (Sterck et al. 2016).

Widespread global warming is a robust climate prediction and temperature impacts tree mortality. Few studies disentangle the impact of temperature from the impact of drought and hardly any of these studies focus on the tropics. Temperature impacts on vegetation are largely through vapour pressure deficits as they increase nonlinearly with temperature (Breshears et al. 2013). Trees die faster from hotter drought (McDowell and Allen 2015). Experimentally increased temperatures made trees die faster in the southwestern US (Adams et al. 2009), temperature was significantly correlated with tree mortality rates in the Western US (van Mantgem et al. 2009) and tree ring records from the same region indicate maximum temperatures are closely associated with tree mortality (Williams et al. 2013). However, it is unlikely such large temperature related mortality increases will occur in non-conifers (McDowell et al. 2016).

Trees have many adaptations to persist in drought, for example wood density and deciduousness (Condit 1998). Presumably following a severe drought, the surviving individuals have adaptations that are advantageous and will be inherited by the next generation (Allen et al. 2010). Hence drought resistance might increase over time and areas exposed past strong drought may contain species adapted avoid cavitation. However, the adaptation of a tree species to a new local climate may be too slow if generation time is long and climate change is rapid.

Wood density is a key functional trait that varies within individuals and species as wood acts as a mechanical support, water store and sap flow conduit. Wood traits are based on functional trade-offs as one of the main roles of the wood is providing mechanical stability whilst plants compete for light, and transport water in spite of hazards such as pathogens, pests, water deficits and cavitation. Experimental evidence from non-tropical trees suggests that plants with greater drought tolerance, i.e. those that can withstand more negative xylem pressure without cavitation, are those of greater wood density (Hacke et al. 2001).

Plants at the greatest risk of drought mortality tend to be tall trees of old-growth forests, with implications for terrestrial carbon storage (McDowell and Allen 2015). Trees that are tall with isohydric stomatal regulation, low hydraulic conductance, and high leaf area are most likely to die from future drought stress (Anderegg et al. 2014). In addition, in closed-canopy forests the taller trees have a more challenging hydraulic environment as crowns are exposed to higher solar radiation and higher leaf-to-air vapour pressure deficits

than the relatively buffered understory (Roberts et al. 1990a). Tree mortality occurs when an essential metabolic resource need is not met. Drought induced mortality at the regional scale is often associated with increased temperature (Allen et al. 2010) and the hypotheses of carbon starvation (failure to maintain metabolism due to prolonged negative carbon balance) and hydraulic failure (desiccation from failed water transport) have stimulated debate (Sevanto et al. 2014).

Several other factors cause tree mortality in tropical forests. Lightning is thought to be a major cause of tree mortality for tropical forests in Panama, responsible for 40 % of large tree mortality (Yanoviak et al. 2019) and as lightning incidence increases in El Niño (Guha et al. 2017), lightning may be responsible for increased tree mortality in El Niño. Drought typically makes trees more susceptible to pests and pathogens (Mattson and Haack 1987), though outbreaks in the tropics are not usually severe because of high tree species diversity (Anderegg et al. 2015b). Tree mortality is stochastic and it is possible that any extra mortality during the El Niño may be just as stochastic (Mori 2019), so rather than predominant mortality of certain species, size classes or functional types, the trees that die might continue to be random. Trees may die via senescence but tree life histories vary and some trees can potentially be very long lived (Issartel and Coiffard 2011, Lindenmayer and Laurance 2017).

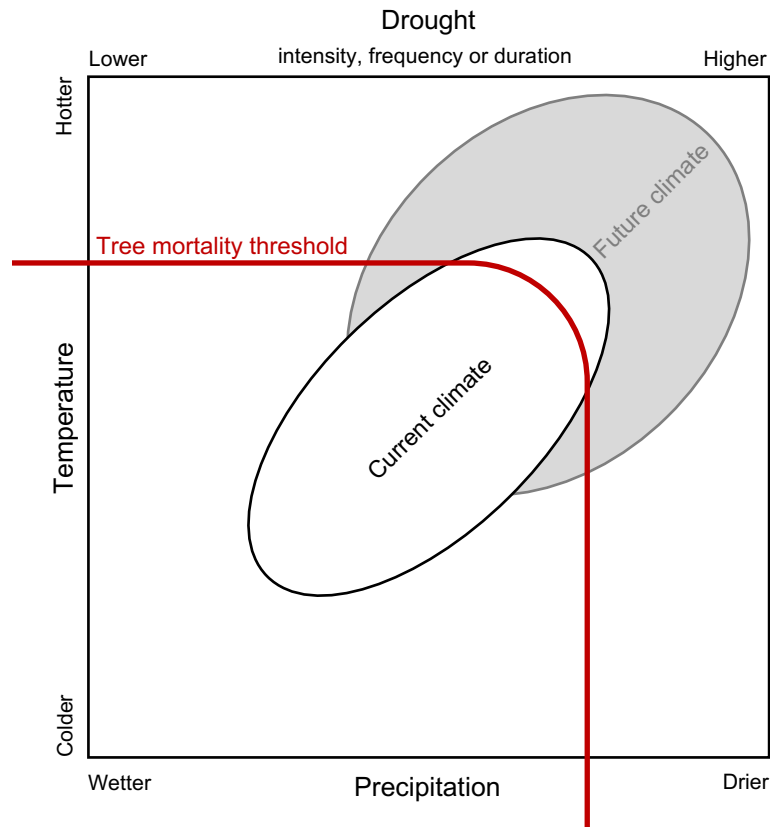


Figure 1.2 | Hypothesized tree mortality threshold

Warming alone can drive climate to exceed the mortality threshold, without declines in precipitation. Adapted from (Allen et al. 2010).

1.3.1 Carbon starvation

When water is limiting and evaporative demands high, plants rely on stored carbon (Jackson 2005) and keep their stomata closed to avoid water loss and so must rely on a limited supply of stored carbohydrates. Hot and dry conditions often make it impossible for leaves to maintain hydraulic safety while opening stomata, so leaves may be unable to simultaneously maintain a positive carbon balance while regulating temperatures through transpirative cooling. Vapour pressure deficits increase with temperature as the water potential gradient between atmosphere and leaf mesophyll increases, so with rising temperatures, droughts that previously would have been tolerable may become deadly (Trenberth et al. 2014). Some support for carbon starvation is that surviving plants exhibit the same carbohydrate storage patterns as dying plants, supporting the idea that carbon starvation is a threat to survival during drought (McDowell 2011).

1.3.2 Hydraulic Failure

Reduced soil water supply plus high evaporative demand causes xylem vessels to fill with air and cavitate, stopping water flow and desiccating plant tissues (McDowell et al. 2008). Hydraulic failure can lead to plant mortality and is likely if drought is sufficiently intense that plants run out of water before they run out of carbon. Hydraulic safety margins vary with species because vessel architecture varies and areas exposed to past strong drought may contain species adapted avoid cavitation. Carbon metabolism and hydraulics are coupled so there is higher risk of mortality for species that maintain narrow margins of hydraulic safety (McDowell 2011). Species that maintain narrow margins of hydraulic safety might be deciduous or drought deciduous, sacrificing leaves in drought, have denser wood and xylem structure that avoids embolism or are able to release stored water to maintain xylem tension (Meinzer et al. 2009). On the other hand, drought tolerant canopy trees tend to have wide hydraulic safety margins (Ziegler et al. 2019).

1.4 El Niño

The El Niño Southern Oscillation is a climate phenomenon responsible for much of the inter-annual variation in climate and weather globally. During El Niño sea surface temperatures and atmospheric pressures shift in the Pacific Ocean, weakening easterly trade winds and influencing regional weather patterns. Normally, in non-El Niño years, there are high sea surface temperatures in the western Pacific (Glantz 2001) but during an El Niño event the weaker trade winds cause warmer waters and associated rainfall move to the central Pacific and the Western coast of South America. Atmospheric circulation is altered via the Walker Cell and dry weather prevails in much of the tropics (McGregor and Nieuwolt 1998). In the opposite phase, La Niña, trade winds strengthen and warm waters are pushed further east (McGregor and Nieuwolt 1998). Of course, each El Niño event is unique, varying in spatial extent, intensity and duration, and occurring at the same time as other climatic events. Hence, not all of the possible El Niño climate impacts occur in all events, and impacts may not be confined to the regions indicated in the figures below.

1.4.1 Temperature impacts

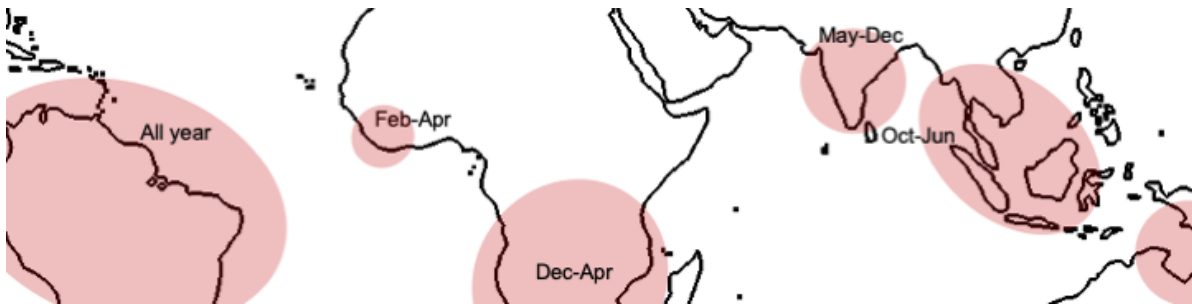


Figure 1.3 | Typical temperature impacts of El Niño

Regions that tend to be hotter during an El Niño year are shaded in red. Adapted from (Met Office 2020)

Almost all tropical regions experience higher temperatures during El Niño events (Figure 1.4), independent of any change in rainfall (Malhi and Wright 2004) and temperature peaks are associated with the last three very strong El Niño events in 1982-83, 1997-98 and 2015-16 across the tropics (Liu et al. 2017). Land surface temperature peaks about 3 months after sea surface temperatures peak in the Niño 3.4 region (Trenberth et al. 2002). High temperatures particularly affect the Amazon (Malhi and Wright 2004), but stronger temperature anomalies are associated with locations closer to the equator for all continents (Malhi and Wright 2004). West African tropical forests are also typically hotter during an El Niño, but for a shorter period of time and it is notable that the Congo is not highlighted as a region with typical temperature increases in El Niño (Figure 1.4). There is some evidence that El Niño temperature anomalies are increasing as global temperatures rise, with the most severe El Niño events for more than a century being the most recent (Fedorov and Philander 2000).

1.4.2 Precipitation impacts

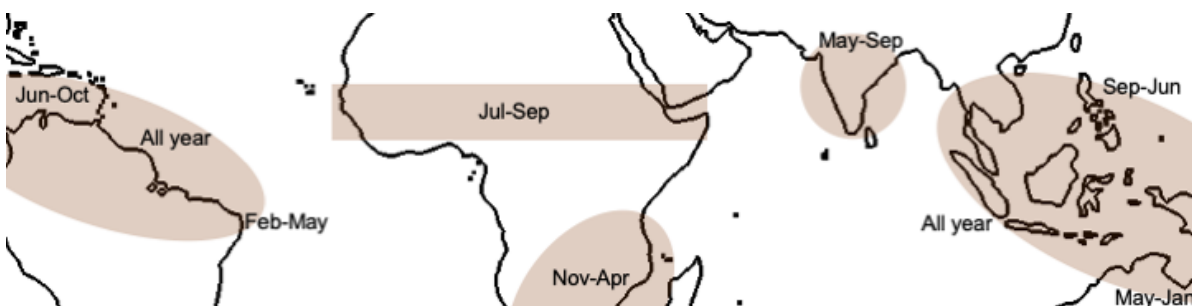


Figure 1.4 | Typical precipitation impacts of El Niño

Regions that tend to be drier during an El Niño year are shaded in brown. Adapted from (Met Office 2020)

Precipitation in a typical El Niño year is similar to a non-El Niño year with global mean precipitation only 2 mm yr^{-1} (0.2 %) above normal (Dai and Wigley 2000). However, El Niño has large impacts on tropical precipitation, and in many tropical areas 30-60 % of interannual precipitation variation is explained by El Niño (Dai and Wigley 2000). El Niño usually causes dry conditions in all seasons for a band of the tropical zone across South America, Africa, India and Southeast Asia (Dai and Wigley 2000). Particularly dry conditions are associated with El Niño in the northeast Amazon and east Africa (Figure 1.4). Strong precipitation anomalies in Southern Brazil have been linked to El Niño (Grimm et al. 1998), and drying can even begin the year before a defined El Niño event. El Niño droughts are stronger and more consistent than the wetting that occurs in opposite La Niña phase (Grimm et al. 1998). El Niño is also the main cause of droughts in Africa (Masih et al. 2014) and can cause droughts beyond the El Niño year itself. Analysis of El Niño events between 1960 and 1998 found stronger precipitation anomalies in South America than in Africa (Malhi and Wright 2004). There is some evidence that rising temperatures are increasing the variability of El Niño precipitation impacts, intensifying both the extreme wetting and extreme drying associated with El Niño (Collins et al. 2010, Liu et al. 2019, Zheng et al. 2019).

1.4.3 Fires

Perhaps the greatest El Niño impact to the global carbon cycle comes from increased fire frequency, particularly in fragmented landscapes. Greater aridity during El Niño increases the flammability of tropical forests and, with an ignition source, forest fires become more likely (Chen et al. 2017). Natural fires in moist tropical forests are rare and typically start near forest edges (Fonseca et al. 2017) where the microclimate is hotter and drier and human activity in adjacent land increases the chance of ignition occurring (Cochrane 2001). El Niño fires are most prevalent in Southeast Asia (van der Werf et al. 2004). Carbon emissions from fire during El Niño events are substantial and can account for more than 60 % of the CO_2 released to the atmosphere (van der Werf et al. 2004). Fire is not assessed here, nor in later chapters, but its significance is noted.

1.4.4 The tropical carbon cycle during El Niño

El Niño events can temporarily cause high rates of CO₂ release to the atmosphere and it is thought that the majority of this extra atmospheric CO₂ is due to reduced terrestrial uptake in tropical ecosystems that have experienced increased temperatures, droughts, fire and increased cloud cover (Malhi et al. 2002a). As such, El Niño events determine much of the interannual variation in the global carbon cycle (Wang et al. 1999). The exact mechanisms of this reduction in the tropical carbon sink are uncertain but could include; reduced photosynthesis, higher rates of biomass mortality and therefore increased necromass, increased fire frequency or intensity a combination of these factors (Malhi et al. 2018). Whether temperatures or drought drive these processes is also unknown, as is whether particular regions are responsible for most of this El Niño CO₂-release (Malhi et al. 2018). Tropical forests have been approximately net neutral for the last three decades, but during strong El Niño events, the tropics become a major net source (Mitchard 2018).

1.4.5 The 1982-83 El Niño

Atmospheric measurements of CO₂ concentration indicate that the 1982-83 El Niño led to a supplemental 6 Gt C in the atmosphere (Gaudry et al. 1987). The 1982-1983 El Niño caused drought in West Africa (Masih et al. 2014) and was the worst dry season since records began in Panama (Leigh et al. 1990) causing increased tree mortality but just for a short time as forests recovered by the wet season of 1984 (Leigh et al. 1990). Large, uncontrolled fires across East Kalimantan, Borneo were caused by the 1982-83 El Niño (Leighton and Wirawan 1986) and floods and destruction occurred in northern Peru (Caviedes 1984).

1.4.6 The 1997-98 El Niño

Prior to the very strong El Niño of 2015-2016, the last very strong El Niño was in 1997-98. Conditions were then unprecedented with record global air temperatures, extreme droughts in the tropics (e.g. (Nakagawa et al. 2000, Williamson et al. 2000b, Slik 2004)), major forest fires across Southeast Asia (Page et al. 2002, Fuller et al. 2004, van der Werf et al. 2004) and parts of Amazonia, and a global carbon anomaly of 2.13 ± 0.79 Pg C (van der Werf et al. 2004). Whilst drying had been observed in West Africa over the preceding 30 years and the 1982-1983 El Niño caused drought in the region (Masih et al. 2014), the 1997-98 El Niño did not seem to have an impact (Nicholson et al. 2000). Thus,

the very strong El Niño of 1997-98 had limited impacts in West Africa, but widespread impacts across the tropics.

1.4.7 The 2015-16 El Niño

Climate change in combination with the El Niño of 2015-16 meant ecosystems experienced the hottest temperatures for 125,000 years (Hoffman et al. 2017). Early research focused on South America indicates that the 2015-16 El Niño was longer in duration, warmer and there was a greater extent of extreme drought in Amazonia than 1997-98 (Jiménez-Muñoz et al. 2016). Yet, drought locations in 2015-16 were not consistent with 1997-1998; the drought typically seen with El Niño was only in eastern Amazonia whilst in western Amazonia there was an unusual wetting (Jiménez-Muñoz et al. 2016). Temperatures in tropical Africa in 2016 were 0.5 °C above the 1981-2010 mean, with similar temperature anomalies in tropical South America and Asia (Liu et al. 2017) and emissions from fire were the largest in Southeast Asia since 1997 (Huijnen et al. 2016). These new extremes of temperature and regional precipitation shifts indicate that the impacts of the 2015-16 El Niño might contrast with previous drought impacts.

1.5 Capturing the impacts of the 2015-16 El Niño with long-term forest plots

Long-term remeasurements of plot networks can capture ecological changes that span decades and large areas. The RAINFOR (Malhi et al. 2002b, Brienen et al. 2015) and AfriTRON (Lewis et al. 2009, 2013, Hubau et al. 2020) networks bring together resources and people to tackle new questions with long-term data over a large geographical extent. Following the methodology of (Phillips et al. 2010a), plots (1 hectare) are usually located on homogenous soil, relatively accessible with little human disturbance and have long term institutional support (RAINFOR manual includes plot establishment protocol (Phillips et al. 2010a)). When plots are established or remeasured, all trees greater than 10 cm diameter are identified to species, tagged and measured at 1.3 m above the ground unless, to avoid deformities or buttresses, another point of measurement is deemed more appropriate (Phillips et al. 2010a). This repeated methodology builds long-term datasets, forming a baseline against which the type and pace of ecological change can be evaluated, impacts interpreted, and future responses

predicted. Monitoring a plot for an extended period provides evidence of change in species composition, size distributions and demographic rates over time.

In regions with seasonal rainfall, timing of remeasurement is important. Ideally censuses should take place over whole year intervals, and at the time of year when there is least interannual variation in soil water availability. Therefore, in principle, for plots in areas that experience severe interannual variation in rainfall due to El Niño events, the best time of year to remeasure is during the wet season (Phillips et al. 2010a) but plots can be particularly difficult to access during the wet season so may be measured in the dry season. A reasonable compromise here that is often adopted is to avoid measuring at the end of the dry season, and thereby avoid diameter differences driven by seasonal hydrostatic variation masking growth signals.

The last very strong El Niño in 1997-98 was not captured by long term monitoring networks – neither RAINFOR nor AfriTRON formally existed at that point, and the density, frequency and consistency of measurement methodology of tropical permanent sampling plots were all less than today. But across the AfriTRON and RAINFOR networks many plots have been censused in 2014-15 and new emergency censuses were undertaken to remeasure some of them again in 2016-17, i.e. shortly before and shortly after the El Niño, specifically to capture the impact of a strong El Niño event. Plots therefore have more than two censuses before the El Niño census so long term plot trends and demographic rate changes can be specifically compared to the El Niño census interval. Moreover, using this set of measurements the potentially shifting baseline of community changes with underlying climate change can be accounted for when testing for effects of the recent climate anomalies.

Long-term plot data spanning the El Niño allow the resistance of tropical forests to climate change to be assessed, and the spatial coverage of the networks allows assessment of the climate anomaly across different baseline climates. Given that these networks that did not exist in the same capacity to assess the 1997-98 El Niño, for the first time, multiple census intervals exist allowing the impact of the 2015-16 El Niño on forest stands across the two largest areas of tropical forests on Earth to be assessed, across Africa and South America.

1.6 Aims and Objectives

The impact of the 2015-16 El Niño on tropical forests will depend on the strength of the climate anomaly in terms of temperature, precipitation and drought. Forests are large carbon stores as trees uptake carbon through photosynthesis and can store it within tissues for their lifetime. But drought and increasing temperature alter forest structure. Climate change over last few decades combined with the recent El Niño event mean ecosystems are experiencing the hottest temperatures for 125,000 years (Hoffman et al. 2017) . By combining plot data with climate data in this thesis I aim to assess the impact of the 2015-16 El Niño on: (1) intact tropical forest aboveground biomass and carbon stocks (2) stand-level structural and dynamic properties of biomass and carbon, i.e. the gains of carbon to the system from tree growth and recruitment and carbon losses from the system from tree mortality, and (3) changes in the aboveground biomass and the carbon sink over the El Niño.

Tropical forests of Africa and South America will be examined, first separately and then together to see if similar biomass and forest dynamics responses occur despite fundamentally different baseline climate and species composition. Using a series of objectives these aims will ultimately test and quantify the impact that the 2015-16 El Niño had an on tropical forests.

1.6.1 Objectives

1 Assess the climate and climate change over 2015-16 in the tropical forest biome

1.1 Characterise the tropical biome in the 2015-16 El Niño in terms of temperature, precipitation and departure from norms.

2 Assess how monitored plots' temperature and precipitation regime changed over 2015-16

2.1 Compile climate data at each plot during El Niño: anomalies and extremes of temperature precipitation and climate water deficit.

2.2 Define the climate anomaly for each plot compared to the long-term mean.

2.3 Differentiate between temperature and moisture anomalies.

3 Quantify the impacts of the 2015-16 El Niño on intact tropical forests in terms of aboveground biomass, carbon balance and stem dynamics

3.1 Assess net aboveground biomass change.

3.2 Assess growth impacts by comparing the El Niño census interval to all previous census intervals combined.

3.3 Assess mortality impacts by comparing the El Niño census interval to all previous census intervals combined.

3.4 Link ecological impacts of the 2015-16 El Niño to climate anomaly.

3.5 Test simply whether changes in growth and mortality are quantitatively related to the changes in local climate.

4 Resolve whether baseline climate confers resistance to climate anomalies

4.1 Compare baseline climate and impact of El Niño at each plot.

4.2 Determine whether ecosystems have acclimated to warmer temperatures or are more vulnerable because they are nearer a high temperature threshold.

4.3 Does temperature suppress the tropical biome?

5 Determine whether responses to El Niño vary by continent

5.1 Compare climate baseline and anomaly for South America and Africa.

5.2 Compare relative growth and mortality impacts for South America and Africa.

1.7 Thesis Outline

As aforementioned, the aims of this thesis are to quantify the climate anomaly of the 2015-16 El Niño and associated ecological impacts. This chapter has provided an overview of the literature to give context to the research, a rationale for the project and the aims and objectives to be addressed. The rest of this thesis consists of four chapters: three research manuscripts and a discussion.

The climate anomalies, baseline climate and ecological impacts of the 2015-16 El Niño in Africa are examined in Chapter 2, to achieve objectives 1-4 for Africa. The climate anomalies, baseline climate and ecological impacts of the 2015-16 El Niño in South America are examined in Chapter 3, to achieve objectives 1-4 for South America. In Chapter 4 the climate anomalies and ecological responses of the two continents are assessed and compared in terms of magnitude, meeting objective 5.

The main findings from chapters 2-4 are drawn together and discussed in Chapter 5. Chapter 5 contains further in-depth critical analysis of the results and further places them in the context of the literature. The key aims of the thesis are then re-examined to see if they have been achieved, and problems encountered during the research are discussed. Finally, the overall conclusions from the thesis are summarised.

Chapter 2

Resistance of African tropical forests to an extreme climate anomaly

Abstract

The response of tropical forests to environmental change is a critical uncertainty in predicting future climate change impacts. The 2015-16 El Niño Southern Oscillation resulted in record high temperatures and low precipitation in the tropics with substantial impacts on the global carbon cycle. Yet the role of African tropical forests is uncertain, particularly as their responses to temperature and short-term drought have yet to be determined using on-the-ground measurements. African tropical forests may be particularly sensitive because they exist in relatively dry conditions compared to Amazonian or Asian forests, or alternatively, they may be more resistant, because of an abundance of drought-adapted species. Here responses of structurally intact old-growth lowland tropical forests are reported from six countries within the African Tropical Rainforest Observatory Network (AfriTRON). One-hundred long-term inventory plots were measured at least twice prior to and once following the 2015-16 El Niño event. These 100 plots experienced the highest temperatures and driest conditions on record (+0.9°C and -76mm stronger maximum climatological water deficit than the mean conditions of 1980-2010). The record temperature did not significantly reduce carbon gains from tree growth or significantly increase carbon losses from tree mortality, but the record drought did significantly slow carbon gains from tree growth. Overall, the long-term increase in live biomass of these forests was reduced by 35 % due to the El Niño event, but these plots remained a carbon sink ($0.52 \pm 0.20 \text{ Mg C ha}^{-1} \text{ yr}^{-1}$), despite extreme environmental conditions. Analyses suggest African tropical forests may be more resistant to climatic extremes than Amazonian and Bornean forests.

2.1 Introduction

Tropical forests are a critical component of the global carbon cycle because they are extensive (Saatchi et al. 2011), carbon-dense (Sullivan et al. 2017) and highly productive (Malhi 2012). So, consistent impacts on these forests can have global consequences (Lewis 2006). Their global importance is seen via atmospheric measurements of CO₂, showing a near neutral exchange of carbon across the terrestrial tropics, hence the large carbon losses from deforestation and degradation are almost entirely offset by the significant carbon uptake from intact tropical forests and tropical forest regrowth (Gaubert et al. 2019). Independently, ground observations of structurally intact old-growth tropical forests also show this uptake, with forest biomass carbon increasing across remaining African (Lewis et al. 2009, Hubau et al. 2020), Amazonian (Brienen et al. 2015), and Asian (Qie et al. 2017) forests. Yet, unlike in Amazonia (Brienen et al. 2015, Feldpausch et al. 2016) and Asia (Qie et al. 2017) the impact of a severe drought or a drought and high-temperature event in African tropical forests has not been documented using ground data.

High temperatures test the physiological tolerance of tropical trees. Above optimal temperatures plants reduce their carbon uptake (Lloyd and Farquhar 2008). This includes closing stomata to avoid water loss, reducing internal CO₂ concentrations and reducing carbon assimilation in the leaf (Slot and Winter 2017). Higher temperatures increase vapour pressure deficits (Trenberth et al. 2014) and alongside reduced precipitation increase the chance of hydraulic failure (Rowland et al. 2015). Individually or in combination these impacts can slow growth and may eventually kill trees (McDowell et al. 2018). As well as reduced carbon uptake, plants use more carbon under higher temperatures: respiration rates tend to increase with short-term increases in temperature at both the leaf-level (Heskel et al. 2016) and in tropical forest communities (Clark et al. 2010), again reducing tree growth, and potentially leading to tree death via carbon starvation (Galbraith et al. 2010). Recent analyses of tropical forest plot data showed increased temperatures over the prior five years were associated with lower levels of carbon uptake from tree growth and higher levels of carbon loss from tree mortality (Hubau et al. 2020). Thus, with high temperature anomalies reduced tree growth and increased tree mortality are expected.

Drought also impacts trees as water deficits can slow tree growth, and if of sufficient strength or duration, can kill trees, either via hydraulic failure or carbon starvation. Hydraulic failure of the xylem has been found across species and biomes in response to

drought, whilst carbon starvation has been documented in some locations (Adams et al. 2017b). Inventory plot observations before, during and after droughts show the impacts of drought in Asia and Amazonia. In Asia, the 1997-98 El Niño temporarily halted the carbon sink in Bornean forests by increasing tree mortality (Slik 2004, Qie et al. 2017). In Amazonia, severe droughts in 2005 and 2010 elevated tree mortality and in 2010 also significantly reduced tree growth (Phillips et al. 2009, Feldpausch et al. 2016). The Amazon carbon sink was reversed by the 2005 drought, and while the sink later recovered it has since been consistently weaker than before the drought (Brienen et al. 2015), due to high-temperature impacts (Hubau et al. 2020). But while the impacts of short-term drought in their long-term context have been elucidated in Amazonia and Asia, in Africa so far there is a lack of any ground-based assessment of large-scale drought impacts due to a paucity of observations.

While the broad responses of African tropical forests to temperature and drought anomalies can be hypothesised from first principles and the responses of other continents, considerable uncertainties remain. On the one hand, there are grounds for expecting them to be especially vulnerable. African forests are already remarkably dry compared to Amazonian and Asian tropical forests, with almost 90% receiving $<2000 \text{ mm yr}^{-1}$ precipitation (Malhi and Wright 2004), the approximate amount necessary to maintain photosynthesis throughout the year (Guan et al. 2015). This low rainfall suggests African tropical forests may already be close to their physiological and ecological limits. As well as being drier they are also, on average, less species-rich than forests in Amazonia and Asia (Slik et al. 2015, Sullivan et al. 2017), and this lower diversity could conceivably drive lower resistance to climate anomalies (Tilman and Downing 1994).

Alternatively, the relatively dry conditions of African tropical forests may, counter-intuitively, actually confer drought resistance. African climate has oscillated between wetter conditions in interglacial periods, and cooler and drier conditions in glacial periods (deMenocal 2004), so the paleo-filtering of African species may have eliminated much of the most mesic-adapted biodiversity. African tropical forest diversity is actually similar to or higher than that of the Amazon when comparing equivalent forests with similar dry season lengths (Parmentier et al. 2007), suggesting most wet-adapted species have been lost and either the dry-adapted species remained or these lineages have diversified more, potentially conferring drought resistance. Indeed, long-term drought in West Africa led to tropical forests in Ghana increasing the abundance of deciduous species (Fauset et al. 2012, Aguirre-Gutiérrez et al. 2019). Similarly, the relatively cool conditions of African

tropical forests might imply resistance as they are further from a potential high temperature threshold for photosynthesis, or, if the temperature tolerance of species is based on local conditions, they might be more vulnerable. Overall, African tropical forests could plausibly be more or less vulnerable to temperature and drought anomalies than Amazonian or Asian tropical forests.

Understanding how intact African forests respond to climate anomalies is vital, not least because they have been providing a substantial long-term carbon sink, reducing the rate and magnitude of climate change (Lewis et al. 2009, Hubau et al. 2020).

Understanding the impacts of environmental change on African tropical forests is also important because of unique aspects of their structure. African forests typically have high aboveground biomass, and so high carbon storage per unit area - on average one-third more than Amazon forests (Feldpausch et al. 2012, Lewis et al. 2013, Sullivan et al. 2017). African forests are also composed of a smaller number of stems, approximately 425 ha^{-1} (≥ 10 cm diameter), compared to approximately 600 ha^{-1} in Amazonia and Asia (Lewis et al. 2013), so are unusually dominated by large trees. Hence, even small decreases in growth of the large dominant trees or modest increases in the mortality of these trees could lead to large carbon stock reductions and a loss of the carbon sink.

The 2015-16 El Niño event provides a first opportunity to assess the impact of high temperatures and strong water deficits on African tropical forests. While three very strong El Niños have occurred in the last 50 years, 1982-83, 1997-98 and 2015-16, only the latter occurred after a network of long-term inventory plots had been established in Africa and was poised to capture an El Niño event. Therefore, climate data is combined with measurements from 100 African Tropical Rainforest Observation Network (AfriTRON) long-term inventory plots to address the following questions: (1) Did African tropical forests experience unprecedented temperature anomalies in the 2015-16 El Niño? (2) Did African tropical forests experience unprecedented drought in the 2015-16 El Niño? (3) Which climate anomalies drove forest responses to the 2015-16 El Niño? and (4) What were the overall impacts on the monitored old-growth structurally intact tropical forests?

2.2 Methods

2.2.1 Climate Analysis

Here, the climate of the 2015-16 El Niño Southern Oscillation event is defined as the twelve-month period from May 2015 to April 2016. These twelve months capture the

two dry seasons per year African forests typically experience (Jun-Aug and Jan-Mar), and include peak temperatures which started in March 2015, as land surface temperature anomalies in Africa lag sea surface temperature anomalies that began in November 2014 (Liu et al. 2017), by four months (Malhi and Wright 2004). These twelve consecutive months are also those with the greatest SST anomalies (Liu et al. 2017). The same May-April twelve consecutive months are used to characterise the 1982-83 and 1997-98 El Niño events. To estimate the El Niño climate of African tropical forests here ‘tropical forest’ is defined as the Tropical and Subtropical Moist Broadleaf Forest Biome from the WWF Terrestrial Ecoregions of the World map (Olson et al. 2001). Analyses are restricted to mainland Africa.

2.2.2 Temperature, Precipitation and Drought Estimation

Each of the 1982-83, 1997-98 and 2015-16 El Niño events are first compared with the climate of the prior decade over African forests. This requires a continuous record from the early 1970s to 2017. Mean monthly temperatures (0.25 ° resolution) from the ERA-Interim reanalysis dataset are used for dates from 1979 to 2017 (Dee et al. 2011). For the years 1970 to 1978 monthly temperature is extracted from the 0.5 ° resolution CRU ts.4.01 dataset (Harris et al. 2014). The CRU dataset was resampled to match the resolution of ERA-I and harmonised to Celsius units. ERA-I and CRU are correlated for each month for the overlapping time period (1979-2016, i.e. January CRU vs. January ERA-I etc.) using all African tropical forest pixels, and the fit is used to correct the CRU data to match ERA-I (monthly correction coefficients, Figure A2.1). The 1970 to 2017 temperature record includes the monthly adjusted CRU data (1970 to 1978) and ERA-I monthly records from 1979 to 2017.

Each El Niño event is then compared with the prior decade but only for the monitored plot locations, by downscaling the climate data to 1 km² using WorldClim v2 (Fick and Hijmans 2017). Downscaling is achieved by resampling the 1970-2017 temperature record to match the resolution of WorldClim. Then the static 1970-2000 WorldClim temperature is used to correct the 1970-2017 record for each plot location by calculating the mean monthly temperature (μ) for the CRU-ERA-I record for the period 1970-2000. The monthly difference ($T_{diff} = T_{\mu} - T_{WorldClim}$) of the mean climate, T_{diff} is then used to create a plot-level monthly temperature 1970-2017: $T_{plot} = T - T_{diff}$. Temperature values were then additionally adjusted for any difference in altitude between the plot and the altitude of the 1 km grid cell used for WorldClim interpolation, using a lapse rate, so

that $T_{\text{plotalt}} = T_{\text{plot}} + 0.005 \times (A_{\text{WorldClim}} - A_{\text{plot}})$, where T is temperature ($^{\circ}\text{C}$) and A is altitude (m).

Similarly, continuous precipitation records are required from 1970 to 2017. The 0.25° resolution data from the Tropical Rainfall Measurement Mission (TRMM product 3B43 V7) is used from 1998 to 2017 (Huffman et al. 2007). Prior to 1998 monthly rainfall is extracted from the Global Precipitation Climatology Centre (GPCC) database (0.5° resolution, Version 7; (Schneider et al. 2011)), chosen as it has more African weather stations than CRU. The GPCC dataset is regridded to match the resolution of TRMM. TRMM and GPCC were then correlated for the overlapping time period (1998-2003, i.e. January TRMM vs. January GPCC) for all African tropical forest pixels, and the fit is used to correct the GPCC data to match TRMM (monthly correction coefficients, Figure A2.2). Hence, data from 1998-2017 are TRMM and prior to this, adjusted GPCC data.

Precipitation data extraction for plot locations followed a procedure similar to that used for temperature: downscaling to 1 km^2 resolution using WorldClim (v2 (Fick and Hijmans 2017)). The GPCC-TRMM precipitation record is resampled to match the resolution of WorldClim, and the mean (μ) GPCC-TRMM precipitation for the period 1970-2000 calculated for each month. As TRMM is known to overestimate precipitation in the driest months, and underestimate high rainfall events (Aragão et al. 2007), the monthly difference ($P_{\text{diff}} = P_{\mu} - P_{\text{WorldClim}}$) of the mean climate is calculated, and P_{diff} used to adjust monthly precipitation 1970-2017: $P_{\text{plot}} = P - P_{\text{diff}}$.

The drought intensity experienced by plots was estimated as the maximum cumulative water deficit (MCWD) as defined in Chapter 1 (Aragão et al. 2007). A constant monthly evapotranspiration of 100 mm is assumed (as in Hubau et al. 2020) so that MCWD is temperature independent, to assist discrimination between temperature and drought driving changes in growth and mortality.

For the pre-El Niño monitoring period of a plot the mean of the annual MCWD values is calculated, i.e. the baseline climate state. For the 2015-16 El Niño census interval the maximum annual MCWD value is selected, as it is the most extreme climate conditions within the El Niño sampling window for each plot that are interesting.

2.2.3 Plot Data Collection and Analysis

One hundred long-term inventory plots from AfriTRON (Lewis et al. 2009, 2013, Hubau et al. 2020) are analysed. Of the 100 plots, I remeasured 11 plots in Ghana and 8 plots in Liberia. I conducted the initial quality control assessment of these plots and 21

more and conducted the final quality control checks on all 100 plots. These 100 permanent sample plots are located in lowland (all <800 m), closed canopy, old-growth, structurally intact tropical forests. All plots have been inventoried at least twice prior to the 2015-16 El Niño event, and once afterwards. The 100 plots are in 26 distinct clusters across 6 countries: Cameroon, Democratic Republic of the Congo, Gabon, Ghana, Liberia and Republic of the Congo. The plots were established between 1979 and 2012, but only censuses from 1984 onwards are included to avoid potential impacts of the 1982-1983 El Niño. Median plot size is 1 ha, mean 0.90 ha (range 0.2-1 ha); mean initial census is January 2006 (July 1986 to April 2012), mean pre-El Niño census is April 2014 (range March 2013 to October 2015), and mean post-El Niño census is February 2017 (range October 2016-March 2017). The mean monitoring length pre-El Niño was 8.3 years and the mean length of the El Niño interval was 2.7 years. Data are curated at ForestPlots.net (Lopez-Gonzalez et al. 2011) version 2019.1 downloaded on 19 March 2019.

In each plot all trees ≥ 100 mm diameter are measured, tagged with a unique identifier, and identified to species, where possible. Tree diameter was measured at 1.3 m along the stem from the ground, or above buttresses, if present, using standardised methods (Phillips et al. 2010a). In some cases the point of diameter measurement (POM) had to be moved due to upward growth of buttresses or deformities. For these trees a single common estimate of growth before and after the POM-change was calculated, i.e. as if the tree had always been measured at the same POM (Talbot et al. 2014). Stems that reached a diameter ≥ 100 mm during the census interval were recorded as new recruits.

Field data were checked against standard rules to identify potential errors, identically for all 100 plots, consistent with previous large-scale analyses (Lewis et al. 2013, Brien et al. 2015, Qie et al. 2017, Hubau et al. 2020). Trees that increased in diameter >40 mm yr^{-1} or shrunk >5 mm over an interval were assessed, to determine if they may have been inaccurately measured in the field. For example, fast-growing species in a canopy gap could grow >40 mm yr^{-1} , or a rotten trunk could shrink >5 mm in an interval, but for those deemed potentially inaccurate the diameter was either interpolated or extrapolated using known measurements from the same stem from other censuses (0.03 % of all measurements). When only one accurate measurement was available growth was estimated by applying the mean growth rate (for diameter classes 100-199 mm and 200-399 mm) or median growth rate, for size classes with few stems (for diameters 400+ mm), (0.4 % of all measurements).

Tree aboveground mass is estimated using the allometric equation:

$$\text{AGB} = 0.0673 \times (\rho D^2 H)^{0.976} \quad (\text{Chave et al. 2014}),$$

where ρ is stem wood density (g cm^{-3}), D is stem diameter (cm) at 1.3 m or above buttresses, and H is height (m). Wood density measurements were compiled for 730 African species from 608 published sources, mostly were sourced from the Global Wood Density Database on the Dryad digital repository (datadryad.org) (Zanne et al. 2009, Chave et al. 2009) and each individual stem in a plot was matched to a species-specific mean wood density value, where possible. Species in both the tree inventory and wood density databases were standardized for orthography and synonymy using the African Plants Database (ville-ge.ch/cjb/bd/africa/) to maximize matches (Lewis et al. 2009). For incompletely identified individuals or individuals belonging to species not in the wood density database, the mean wood density value for genus is used if available, then family. For unidentified individuals, the mean wood density value of all individual trees in the plot is used (Lewis et al. 2009, Lopez-Gonzalez et al. 2011).

Tree heights were measured in 93 of the 100 plots; typically the 10 largest trees and 10 trees in each of the diameter classes 100-199 mm, 200-299 mm, 300-399 mm, 400-499, and 500-599 mm, with trees selected only when the top was visible (Sullivan et al. 2018). Three-parameter regional height-diameter Weibull equations were fit, using the `local.heights` function in the `BiomasaFP` R package, i.e. a fit for each plot with tree height data (Lopez-Gonzalez et al. 2015), and fits for each plot are in Table A2.1. For the other 7 plots, parameters were chosen from the appropriate region utilising the other plots' height data from that region: West Africa (Upper Guinea), West Central Africa (Western Congo) and East Central Africa (Eastern Congo) (Feldpausch et al. 2012). The parameters (Table A2.1) were used to estimate tree height from tree diameter for all stems for input into the allometric equation, above.

The aboveground biomass in live stems (AGB) was estimated, in $\text{Mg dry mass ha}^{-1}$, at each census of each plot; the additions of biomass to each plot over the census interval, as aboveground woody productivity (AGWP), in $\text{Mg dry mass ha}^{-1} \text{ yr}^{-1}$, and the losses of AGB from the plot, termed AGB mortality, also in $\text{Mg dry mass ha}^{-1} \text{ yr}^{-1}$, all calculated from tree-level AGB using the `BiomasaFP` R package (Lopez-Gonzalez et al. 2015). Plot-level carbon gains are increasingly underestimated as census length increases because trees that die have grown since they were last measured and unobserved recruits increase with census length. Unobserved recruits are trees that recruit into the system (i.e. cross the

100 mm diameter measurement threshold) and then die within that same census interval, so would be missed by the next plot remeasurement. To avoid census-interval effects carbon gains were estimated following Talbot et al. (Talbot et al. 2014), thus the carbon additions from trees that recruited and then died within the same interval (unobserved recruitment), and the carbon additions from trees that grew before they died within an interval (unobserved growth) were accounted for. Carbon losses are affected by similar processes, where the growth prior to tree death within the interval (unobserved growth), and the deaths of stems that were newly recruited within the interval (unobserved mortality) must be added. These usually add <3 % to plot-level carbon gains and losses and increase with census interval length. A mean of 1.4 % was added to plot-level carbon gains and losses and of 427 intervals, 40 % added <1 % and the maximum added to a plot was 16 %.

An analogous set of parameters to AGB carbon gains and carbon losses were calculated on a stems basis. Again, to avoid census-interval effects stem recruitment and stem mortality were estimated following Talbot et al. 2014. Time-weighted recruitment and mortality which represent the entire period of plot sampling are calculated and reduce the impact of the variability of recruitment and mortality over shorter timescales. The trees that recruited (unobserved recruitment) and then died (unobserved mortality) within the same interval are accounted for. Stem density (the number of stems ha⁻¹ at a census), stem recruitment (the number of new stems added in a census interval), and stem mortality (the number of stems lost in a census interval) were estimated.

The BiomassaFP R package (Lopez-Gonzalez et al. 2015) is used to calculate AGB, AGWP, AGB mortality, stem density, stem recruitment and stem mortality, including the calculation of the census interval corrections. Pre-El Niño means of these variables for each plot are time-weighted based on the census interval lengths within the pre-El Niño total census period. Throughout this thesis AGB, AGWP and AGB mortality are expressed in carbon terms as net carbon stocks, carbon gains and carbon losses and to convert biomass to carbon I use the mean carbon fraction for tropical angiosperms, 45.6 % (Martin et al. 2018). Plot-level per-capita stem mortality rates were calculated as annual mortality with units of percentage per year using the equation:

$$N_{s,t-1} = (1 - m_a) N_{s,t} \text{ (Kohyama et al. 2018)}$$

where N_s is the number of surviving trees and m_a is annual mortality.

The difference between the mean of the pre-El Niño monitoring period and the mean of the El Niño census interval for the net change in carbon stocks is termed Δ net carbon, for carbon gains is Δ carbon gains and for carbon losses is Δ carbon losses, and equivalents for stems are Δ net stems, Δ recruitment and Δ mortality for each plot. All analyses are weighted by sampling effort because larger plots and those monitored for longer are likely better estimates of carbon gains, carbon losses, and stem recruitment and mortality. An empirically estimated optimum weighting is used to weight each plot, using plot area and pre-El Niño monitoring length. Linear models are fitted that combine plot area and pre-El Niño monitoring length with differing root transformations, with the root transformation that removes any pattern in the residuals being chosen as the weighting function. When variables require weighting by both monitoring length and area, subtracting one avoids double-accounting (*sensu* (Lewis et al. 2009)). Selected weights were: Δ net carbon, $\text{Monitoring length}^{1/4} + \text{Area}^{1/7} - 1$; Δ carbon gains, $\text{Monitoring length}^{1/3}$; Δ carbon losses, $\text{Monitoring length}^{1/3}$; Δ net stems, $\text{Monitoring length}^{1/3}$; Δ recruitment, $\text{Monitoring length}^{1/4}$; and no weighting for Δ stem mortality. These weightings show no pattern in the residuals and suggest that the cube root best captures how monitoring length is related to sampling error. Area is only included in the net carbon weighting and has a very small power, indicating that the sampling error associated with area is small in this dataset. As most plots are relatively similar in size and census monitoring length, omitting weighting did not impact the main results.

The impacts of climate (temperature, MCWD and their interaction) on biomass carbon (Δ net carbon, Δ carbon gains, Δ carbon losses) and stems (Δ net stems, Δ recruitment, Δ mortality) were tested using linear models, Kendall's Tau correlation tests, t-tests and multiple linear regression using multi-model inference. I parse the potentially complex ecosystem response to the El Niño climate anomaly by using simple linear models of climate drivers and carbon and stem responses. In addition to the linear models I use one-tailed Kendall's Tau correlation tests which are suitable for nonparametric data and robust to the effects of outliers (Croux and Dehon 2010) to test for a negative impact of the El Niño on carbon and stem dynamics. Correlation tests can show a significant relationship even when the linear model is not significant as the ranking effect of in the correlation test reduces the impact of outliers. Overall impacts are calculated using paired t-tests which compare carbon and stem dynamics pre-El Niño and during the El Niño at the individual plot level. Multi-model inference is used to understand which of the underlying variables and interactions were most important. Baseline climate was included

in models to test whether plots that were already hotter (pre-El Niño temperature) or plots that were already drier (pre-El Niño MCWD) were more or less resistant to environmental change (trees in hotter or drier baseline climates may contain more hot or dry adapted species, but also may be closer to physiological temperature or moisture thresholds). Interactions were included in the models as one might expect, for example, greater impacts in locations that are hotter pre-El Niño and experience a greater temperature anomaly and so greater impacts on forests. Additionally, locations that are drier pre-El Niño and experience a greater MCWD anomaly and high temperatures may see greater impacts on forests as both changes may exacerbate water deficits. Variables were standardised using the scale function from the base R package by subtracting the mean and dividing by their standard deviation. Scaling of variables allows accurate effect size comparisons as when variables differ by orders of magnitude, one variable may have a greater impact purely because of its magnitude. Linear models with interactions were built with the scaled variables and multi-model inference was performed using the dredge and then model.avg functions of the MuMIn R package (Barton 2019). All possible combinations of effect terms was calculated and restricted to a 95% confidence set (AIC weightings of models sum to 0.95) thereby excluding highly unlikely models. Model averaged coefficients of terms with limited support exhibit shrinkage towards zero. We then model averaged the coefficients of terms (using the AIC weights of each model), meaning terms with limited support exhibit shrinkage towards zero (Symonds and Moussalli 2011). This multi-model inference was performed using the dredge and model.avg functions of the MuMIn R package (Barton 2019).

2.3 Results

2.3.1 Climate

The 50-year climate record shows that the long-term climate trends across African tropical forests are rising temperatures, decreasing precipitation and stronger seasonal moisture deficit (Figure 2.1). The three very strong El Niño events over the past 50 years are superimposed on these trends (Figure 2.1). Consequently, the 1982-83, 1997-98 and 2015-16 El Niño events each increased temperatures by 0.3, 0.3 and 0.6 °C respectively, compared to the temperature of the prior decade, indicating that the 2015-16 anomaly was larger than the previous two strong El Niño events (Table 2.1). Given the rising temperatures, the mean non-El Niño temperature in the 2010s is greater than the peak temperature during both the 1982-83 and 1997-98 El Niño events (Figure 2.1). Thus, in

the 2010s African forests experienced ongoing temperatures higher than the strongest El Niños of the past, and record temperatures in 2015-16 (Figure 2.1).

Across the African tropical forest domain the three El Niños also decreased precipitation, by $\sim 100 \text{ mm yr}^{-1}$, and increased drought compared to the prior decade, measured as MCWD, by $\sim 30 \text{ mm yr}^{-1}$ (Figure 2.1, Table 2.1). These impacts are superimposed on the long-term trends of declining precipitation and stronger MCWD-drought, with some evidence that the 2015-16 event was the most extreme, particularly for the plot locations (Figure 2.1, Table 2.1). Overall, the precipitation changes were less extreme than the change in MCWD-drought, which in turn were less extreme than the temperature changes (Figure 2.1, Table 2.1).

In the 2015-16 El Niño the 100 plots experienced record mean annual temperatures of $25.0 \pm 0.03 \text{ }^{\circ}\text{C}$ (95 % CIs), low total annual precipitation, average $1498 \pm 24 \text{ mm}$, and a record low MCWD, with mean $-261 \pm 2 \text{ mm}$ (Figure 2.1, Table 2.1). Comparing the plot census interval that captures the 2015-16 El Niño with the plot pre-El Niño census period, 96 of the 100 plots had higher mean monthly temperature over the El Niño census interval compared to their pre-El Niño census period, higher by a mean of $+0.31 \pm 0.04 \text{ }^{\circ}\text{C}$ (paired t-test $p < 0.0001$). All 100 plots had more negative MCWD (mean $-99 \pm 12 \text{ mm}$, $p < 0.0001$, Figure 2.2), and 65 plots also had lower total annual precipitation (mean $-46 \pm 34 \text{ mm yr}^{-1}$, $p < 0.01$, Figure 2.2). These anomalies are smaller than those for the 12-month El Niño year because the plot El Niño mean census length was 2.7 years, so the climate anomaly is diluted by the inclusion of months of more usual conditions. The 100 AfriTRON plot locations are hotter, wetter and less droughted than the region as a whole because the region also includes currently degraded fringes of the biome. Both the plots and region have similar trends of increasing temperature and decreasing rainfall (Figure 2.1).

Table 2.1 | Climate anomalies of three very strong El Niños for the African tropical forest region and plot locations. The 2015-16 El Niño was the hottest of the three most recent very strong El Niño events both absolutely and anomalously, in the region and the 100 plots. The drought was also the strongest MCWD drought of the three El Niño events, but of a similar magnitude as previous El Niño drought anomaly. A May to April year is used for climate analyses and displayed in the tables are means and 95 % confidence intervals.

El Niño	Mean annual temperature (°C)	Anomaly - decade	Anomaly – 1980-2010	Annual precipitation (mm)	Anomaly - decade	Anomaly – 1980-2010	MCWD (mm)	Anomaly - decade	Anomaly – 1980-2010
Region									
1982-83	23.5 ± 0.02	0.33 ± 0.02	0.08 ± 0.02	1513 ± 7	-95 ± 10	-84 ± 11	-220 ± 1	-31 ± 1	2 ± 2
1997-98	23.6 ± 0.02	0.32 ± 0.02	0.26 ± 0.02	1520 ± 8	-83 ± 11	-78 ± 12	-230 ± 1	-37 ± 2	-8 ± 2
2015-16	24.3 ± 0.02	0.57 ± 0.02	0.92 ± 0.02	1444 ± 9	-109 ± 13	-153 ± 12	-302 ± 1	-31 ± 2	-79 ± 2
Plot Locations									
1982-83	24.0 ± 0.03	0.36 ± 0.04	0 ± 0.04	1523 ± 22	-206 ± 9	-179 ± 9	-245 ± 3	-87 ± 3	-61 ± 4
1997-98	24.3 ± 0.03	0.37 ± 0.05	0.28 ± 0.05	1482 ± 23	-236 ± 9	-220 ± 10	-205 ± 3	-39 ± 4	-20 ± 4
2015-16	25.0 ± 0.03	0.47 ± 0.05	0.90 ± 0.05	1498 ± 24	-175 ± 11	-204 ± 10	-261 ± 2	-46 ± 3	-76 ± 3

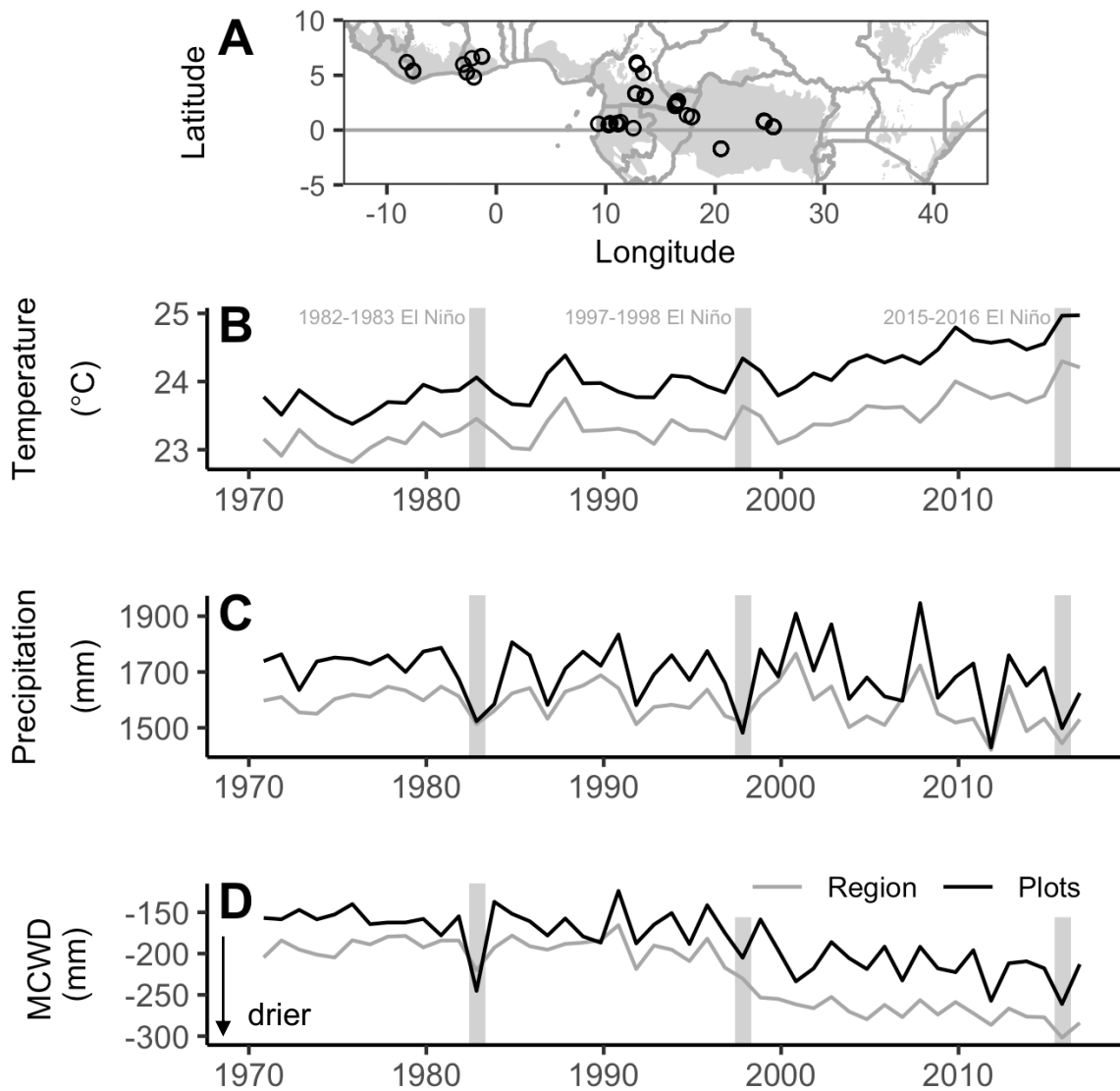


Figure 2.1 | Plot locations within African tropical forest region (A) and climate for plot locations and the African tropical forest region (B, C, D)

Temperatures were the highest recorded and water deficits the lowest recorded in both African tropical forests and in plot locations in 2015-16. Precipitation was also low. Plot locations within African tropical forests (A), and the horizontal line indicates the equator. African tropical forests (grey) are delimited by the Tropical and Subtropical Moist Broadleaf Forest Biome from the WWF Terrestrial Ecoregions of the World (Olson et al. 2001). Mean annual temperature (B), total annual precipitation (C) and maximum cumulative water deficit, MCWD, (D), values averaged for El Niño years May-April. $n=100$ plots, located in thirty 0.25° grid cells. Black lines are for plot locations, grey lines for the forest region. Grey vertical shading indicates the 1982-83, 1997-98, and 2015-16 very strong El Niño events.

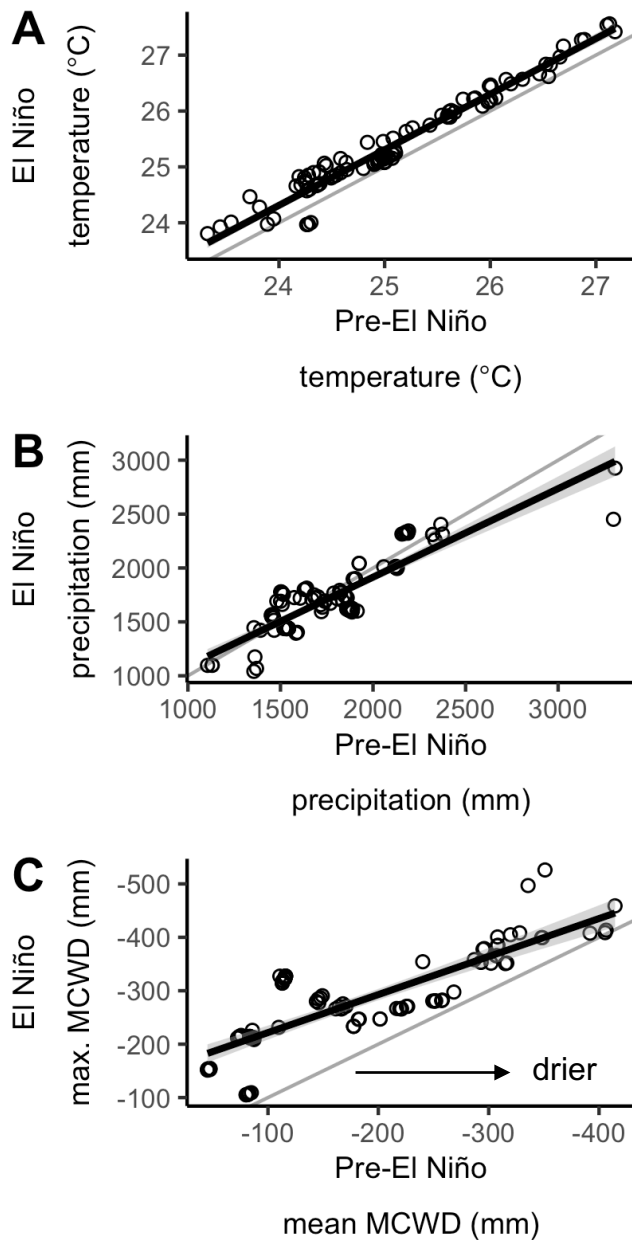


Figure 2.2 | Climate anomalies of 100 long-term inventory plots.

All plots warmed by about the same amount in the 2015-16 El Niño, but water deficits were greater in the wettest plots. Plot census interval pre-El Niño and El Niño temperature (A), plot census interval monthly precipitation (B), and plot census interval maximum cumulative water deficit MCWD (C). Black lines are significant linear models (A; $p < 0.0001$, B; $p < 0.0001$, C: $p < 0.0001$), grey lines indicate 1:1 relationship. Pre-El Niño and El Niño are defined by plot census dates.

2.3.2 Drivers of Biomass Carbon Dynamics

The record high temperatures of the 2015-16 El Niño had no detectable effect on forest carbon gains, losses or the carbon sink over the period of monitoring; higher temperatures were correlated with higher carbon gains (one-tailed Kendall's Tau; $p < 0.05$, Figure 2.3C), but were not correlated with losses ($p = 0.4$, Figure 2.3F) or the strength of the carbon sink ($p = 0.5$, Figure 2.3A). Considering drought, forests experiencing stronger MCWD showed a small but significant reduction in carbon gains ($p < 0.05$, Figure 2.3D), and a larger but non-significant increase in carbon losses ($p = 0.4$, Figure 2.3F), leading to a significant reduction in the carbon sink in the most strongly droughted plots ($p < 0.05$, Figure 2.3B). Thus, relative to pre-El Niño, forests subjected to a 100 mm increase in MCWD water deficit lost $0.3 \text{ Mg C ha}^{-1} \text{ yr}^{-1}$, dominated by carbon losses. Drought and not temperature drives the biomass changes seen in plots. Multi-model inference and model averaging confirms ΔMCWD is more important than $\Delta \text{temperature}$ in determining El Niño carbon dynamics responses (Figure 2.7).

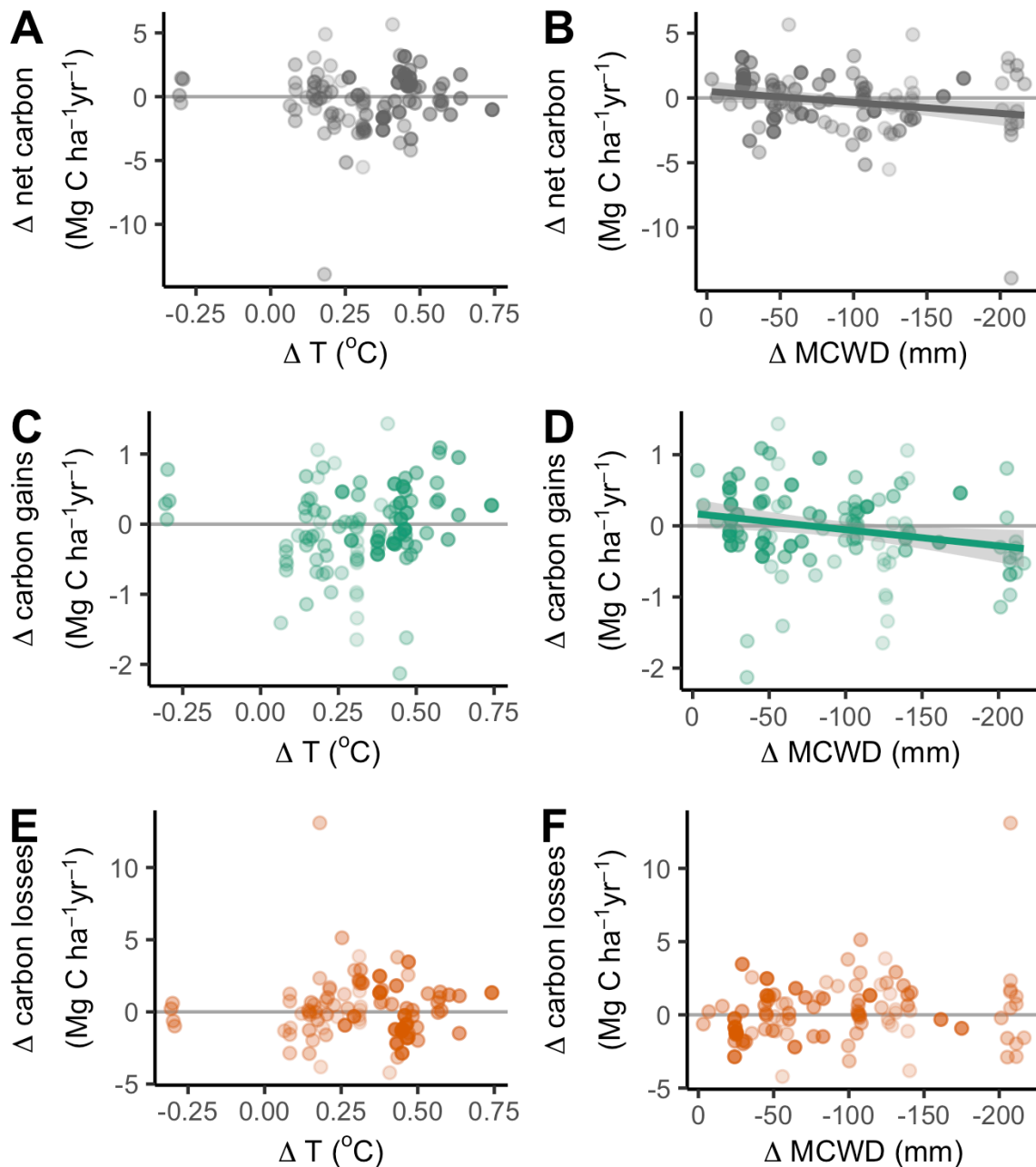


Figure 2.3 | Temperature (left) and drought (right) impacts on aboveground biomass carbon dynamics of 100 long-term forest plots

Temperature anomalies do not reduce carbon gains or increase losses, but drought anomalies reduce carbon gains. The net carbon change (A, B), carbon gains from tree growth and recruitment (C, D) and carbon losses from mortality (E, F) of the censuses capturing the El Niño event minus pre-El Niño plot monitoring period for 100 long-term inventory plots. The intensity of temperature change, Δ temperature (T) (A, C, E) is mean monthly temperature in El Niño minus mean monthly temperature pre-El Niño, using the census dates of the plot censuses. Relative intensity of the change in dry season strength is calculated as Δ maximum cumulative water deficit (MCWD) (B, D, F) which is the difference between maximum MCWD in El Niño and mean MCWD in pre-El Niño. Point shading from light to dark denotes greater weighting, with plots and line of best fit weighted by an empirically derived combination of pre-El Niño plot monitoring length and plot area for each response variable. Net change is in grey, gains are in green, losses orange. Solid lines represent significant linear models ($p < 0.05$). P-values of linear models and slopes of significant lines are as follows: A: $p = 0.8$, B: $y = -0.002x + 0.2$, $p < 0.05$, C: $p = 0.2$, D: $y = -0.002x + 0.2$, $p < 0.05$, E: $p = 0.9$, F: $p = 0.06$.

2.3.3 El Niño impact on Biomass Carbon Dynamics

Plot-level carbon dynamics over the 2015-16 El Niño were similar to those pre-El Niño. Carbon gains from tree growth and the recruitment of new trees were 1.4 % lower in the interval spanning the 2015-16 El Niño (mean 2014.3 to 2017.1) compared to the pre-El Niño census period (mean 2006.0 to 2014.3), a non-significant difference (2.54 ± 0.14 , 95 % CI, to 2.51 ± 0.14 Mg C ha⁻¹ yr⁻¹, paired t-test using weighted data, $p=0.2$, Figure 2.5). However, growth responses by size class indicate that small trees grew less in El Niño. Small trees had significantly lower median growth rates in the El Niño compared to the pre-El Niño measurement period (trees 100-199 mm diameter had a diameter decrease of 0.15 ± 0.11 mm yr⁻¹, $p<0.01$, a 0.11 % decrease), as did the medium size-class trees (200-399 mm diameter (decrease of 0.17 ± 0.14 mm yr⁻¹, $p<0.05$, a 0.06 % decrease). The median growth rate of large trees (400+ mm diameter) was also lower, but did not significantly decrease (0.14 ± 0.21 , $p=0.2$, a 0.02 % decrease). Hence the growth of smaller trees appeared to be more negatively impacted by the El Niño conditions than the large trees. There was a non-significant 15 % increase in carbon losses from mortality in the El Niño compared to the pre-El Niño census period (1.74 ± 0.11 to 1.98 ± 0.19 Mg C ha⁻¹ yr⁻¹, paired t-test using weighted data, $p=0.9$, Figure 2.3). Both trends combined to reduce the carbon sink by an average of 35 %, however, this was only a marginally significant reduction (0.81 ± 0.13 to 0.52 ± 0.20 Mg C ha⁻¹ yr⁻¹, paired t-test using weighted data, $p=0.07$, Figure 2.5). Furthermore, despite the extreme conditions the 100 plots remained a net carbon sink over the 2015-16 El Niño census interval, at 0.52 ± 0.20 Mg C ha⁻¹ yr⁻¹. Overall, the El Niño had modest impacts on the carbon dynamics of the 100 plots studied, while the trends were in the directions predicted no statistically significant changes were documented. Drought significantly impacted the carbon sink in plots (Figure 2.3), but not enough plots were severely droughted for that trend to drive the mean sink strength across the 100 plots down to zero, or to reverse it. Trends in net carbon, carbon gains and carbon losses were robust to the El Niño climate anomaly (Figure 2.4).

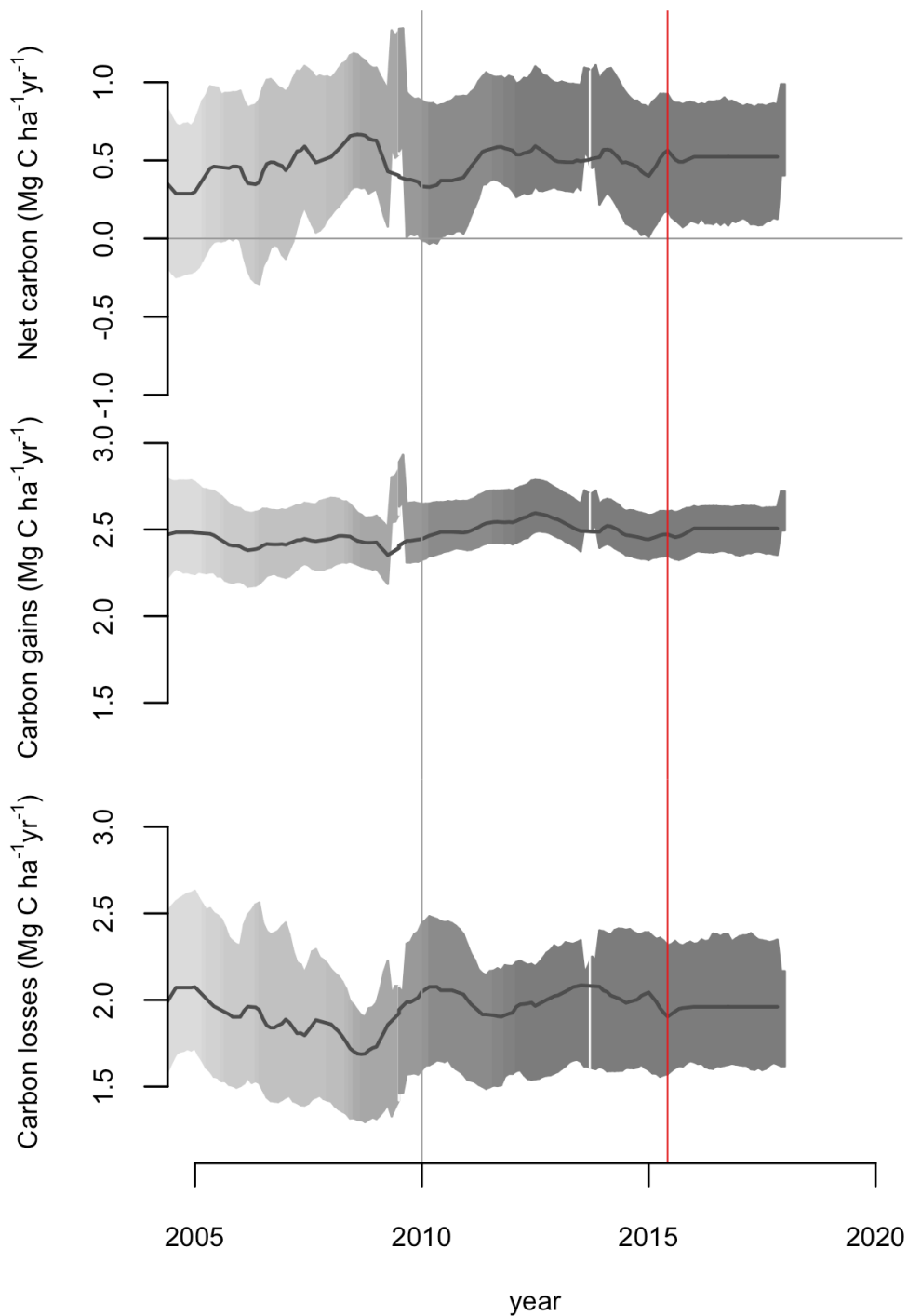


Figure 2.4 | Trends in net aboveground biomass carbon, carbon gains to the system from woody productivity and carbon losses from biomass mortality, for 100 long-term plots in Africa.

African tropical forests maintained their carbon uptake through the 2015-16 El Niño with no signs of a large or protracted impact of the El Niño on the carbon dynamics of African forests. The red line indicates the start of the 2015-16 El Niño climate anomaly and the shading of the confidence cloud indicates number the of plots included in the analysis, with a darker shading for more plots. This figure was produced using R code from Brienen et al. 2015 and Hubau et al. 2020.

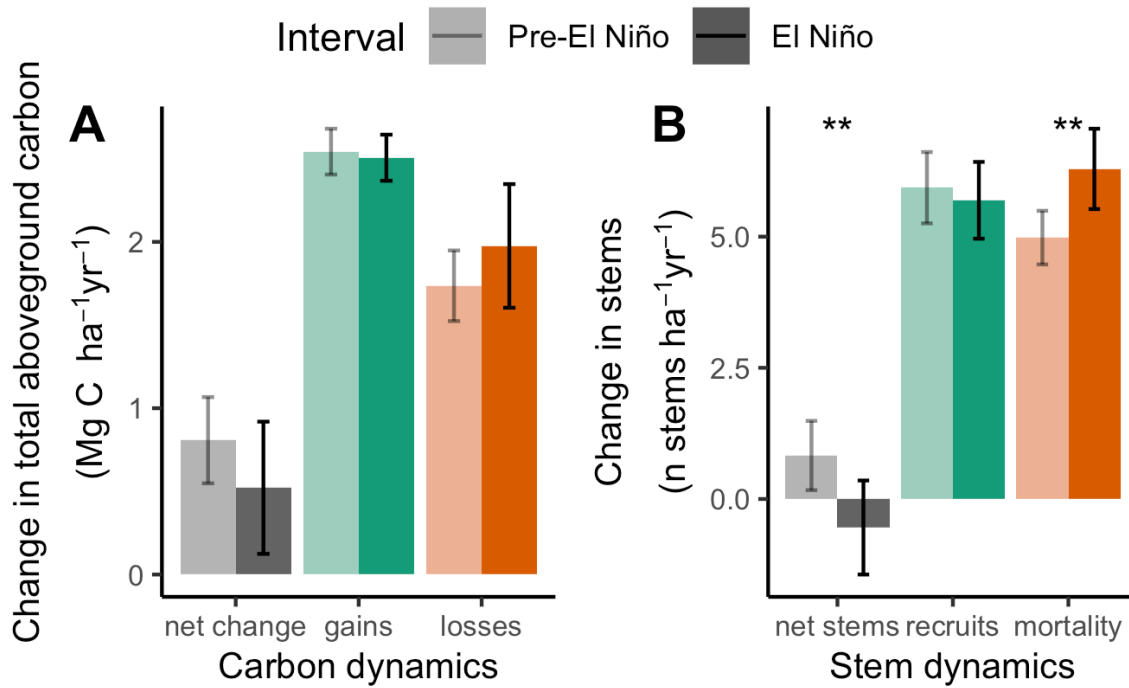


Figure 2.5 | Carbon (A) and stem dynamics (B), pre- (lighter shading) and during the 2015-16 El Niño (darker shading)

Carbon losses increase but not significantly from the pre-El Niño monitoring period to the El Niño census interval, stem mortality significantly increases reducing net stems. Pre- and El Niño carbon (A) and stems (B). Lighter shading is pre- El Niño and darker shading is during the El Niño. $n=100$ plots and error bars represent 95% confidence intervals. Significant differences are defined by paired t-tests with ** indicating $p<0.01$.

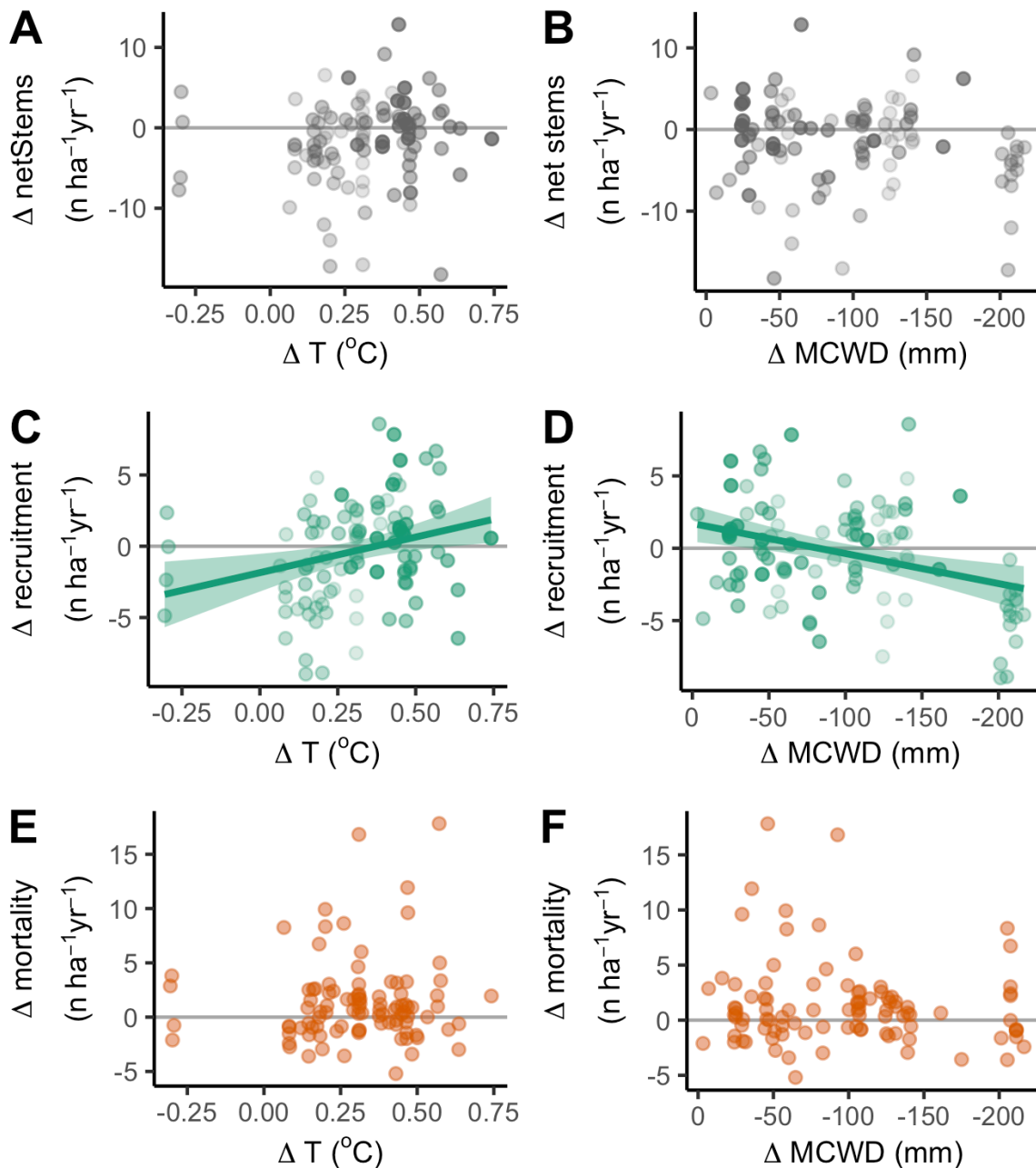


Figure 2.6 | Temperature (left) and drought (right) impacts on stem dynamics of 100 long-term forest plots

Recruitment increases with hotter temperature anomalies and decreases with stronger drought anomalies. The net stem change (A, B), stem gains from recruitment (C, D) and stem losses from mortality (E, F) of the censuses capturing the El Niño event minus pre-El Niño plot monitoring period for 100 long-term inventory plots. The intensity of temperature change, Δ temperature (T) (A, C, E) is mean monthly temperature in El Niño minus mean monthly temperature pre-El Niño, using the census dates of the plot censuses. Relative intensity of the change in dry season strength is calculated as Δ maximum cumulative water deficit (MCWD) (B, D, F) which is the difference between maximum MCWD in El Niño and mean MCWD in pre-El Niño. Point shading from light to dark denotes greater weighting, with plots and line of best fit weighted by an empirically derived combination of pre-El Niño plot monitoring length and plot area for each response variable. Net change is in grey, gains are in green, losses orange. Solid lines represent significant linear models ($p < 0.05$). P-values of linear models and slopes of significant lines are as follows: A: $p = 0.2$, B: $p = 0.2$, C: $5x - 1.9$, $p < 0.01$, D: $y = -0.02x + 1.7$, $p < 0.001$, E: $p = 0.6$, F: $p = 0.3$.

2.3.4 Stem Dynamics

An analysis of stem dynamics, rather than biomass carbon dynamics, and the potential drivers of change shows, surprisingly, stem recruitment increasing with increasing temperature (Kendall's Tau, $p < 0.01$, Figure 2.6C) and, as expected, decreasing with more negative MCWD ($p < 0.05$, Figure 2.6D). Indeed, recruitment is the process most responsive to climate anomaly, responding positively to temperature and negatively to drought (Figure 2.7). Somewhat surprisingly, stem mortality showed no significant relationship with either temperature or drought anomalies (Figure 2.6). The increase in stem recruitment with temperature could have been driven by recruitment of stems with low wood density, which might have benefited from more light reaching the understory, but there is no evidence of this as the median wood density of recruits did not change between pre- and El Niño intervals (0.63 g cm^{-3} pre-El Niño, 0.62 g cm^{-3} El Niño, paired t-test, $p = 0.5$).

Considering the dynamics of the 100 plots together, there was a non-significant decrease in stem recruitment during the El Niño event, with recruitment declining by 4 % (pre-El Niño $5.9 \pm 0.35 \text{ stem ha}^{-1} \text{ yr}^{-1}$ (95 % CI), El Niño $5.7 \pm 0.37 \text{ stem ha}^{-1} \text{ yr}^{-1}$; paired t-test on weighted data, $p = 0.8$, Figure 2.5). However, stem mortality significantly increased by 26 % (pre-El Niño $5.0 \pm 0.26 \text{ stems ha}^{-1} \text{ yr}^{-1}$, El Niño $6.3 \pm 0.39 \text{ stem ha}^{-1} \text{ yr}^{-1}$, $p < 0.01$). Together these led to a switch from an increase of $0.8 \pm 0.34 \text{ stems ha}^{-1} \text{ yr}^{-1}$ pre-El Niño to decline of $0.5 \pm 0.46 \text{ stems ha}^{-1} \text{ yr}^{-1}$, and a significant decrease in stem density over the El Niño ($p < 0.01$, Figure 2.5).

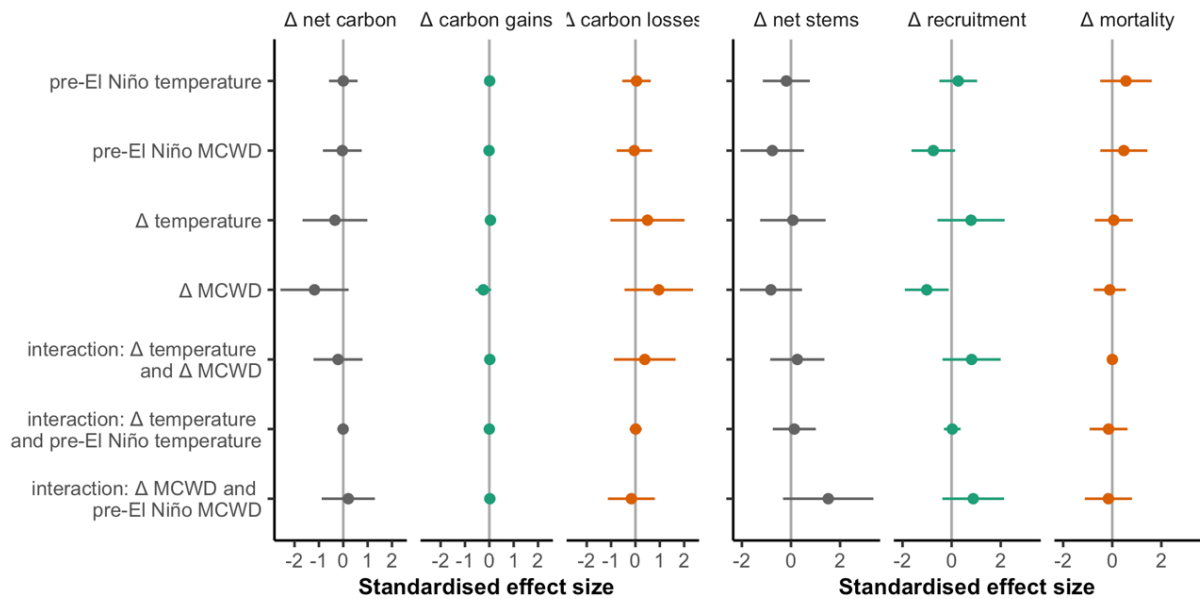


Figure 2.7 | Effect sizes of change in carbon and stems in 100 African tropical forest plots over the 2015-16 El Niño

Temperature and drought anomalies increased carbon losses, reducing net carbon, with a stronger impact of drought than temperature. Climate anomaly impacts on stems were more variable. Points show coefficients from linear models with multi-model inference. Coefficients are standardised so that they represent change in the response variable for one standard deviation change in the explanatory variable. Net change is in grey, gains are in green, losses orange. Error bars show 95 % CIs. The models explained 11 %, 8 % and 11 % of variation in Δ net carbon, Δ carbon gains and Δ carbon losses, and 18 %, 31 %, 13 % of variation in Δ net stems, Δ recruitment and Δ mortality, respectively. Coefficients are listed in tables A2.2 for carbon and A2.3 for stems.

A significant increase in stem mortality but no simultaneous increase in biomass carbon losses (Figure 2.5) implies a loss of smaller trees, which is what was found. Mortality rate increased overall, an increase of 0.3 ± 0.2 %, from 1.2 % to 1.5 %, (paired t-test, $p < 0.001$), and increases were similar for small (100-199 mm diameter: 0.3 ± 0.2 % from 1.3 % to 1.7 %, $p < 0.01$), medium (200-399 mm diameter: 0.3 ± 0.2 % from 1.2 % to 1.5 %, $p < 0.01$), and large trees (400+ mm diameter: 0.4 ± 0.3 % from 1.4 % to 1.8 %, $p = 0.07$). There are very few stems greater than 400 mm diameter, so the 0.4 % increase is an increase of 5 dead stems per year in the 2.7-year interval. Hence, most of the mortality is in smaller trees, explaining the significant increases in stem mortality without a large increase in carbon losses. Furthermore, the median diameter of dying trees decreased significantly from 190 mm diameter pre-El Niño to 174 mm in the El Niño census interval, a decline of 16 ± 14 mm (paired t-test, $p < 0.05$), so more trees died in the El Niño interval but they tended to be smaller, minimising any increased carbon losses during the interval. When broken down by size class, the median diameter of dying trees in the smallest size class, 100-199 mm diameter, decreased by 4 ± 4 mm (135.7 to 131.7,

$p=0.06$), while the median diameter of the other size classes did not change (200-399 mm diameter: 271 to 273 mm, $p=0.6$, 400+ mm diameter; 582 to 578 mm, $p=0.9$). The median size of surviving trees overall also does not change (179 to 179 mm diameter, $p=0.95$) and there is no change in the median wood density of dying (0.64 to 0.63 g cm⁻³, $p=0.6$) nor surviving trees (0.65 to 0.65 g cm⁻³, $p=0.7$). Thus, overall, stem mortality significantly increases over the El Niño census interval and it was predominantly smaller trees that died.

2.4 Discussion

African tropical forests experienced record temperature and drought in the 2015-16 El Niño, yet the 100 inventory plots monitored through this extreme climate anomaly maintained net carbon uptake over the 2.7-year period they were measured, at 0.52 ± 0.20 Mg C ha⁻¹ yr⁻¹. This suggests that African forests are resistant to short-term extreme anomalies, because the carbon sink is maintained, albeit at a lower rate. Yet, the extreme anomaly was shorter than the 2.7-year monitoring period. Assuming that the pre-El Niño sink continued prior to the El Niño event, and returned to this level afterward, suggests that there was a stronger impact of the anomaly on forest carbon dynamics than is apparent from the dataset. If the pre-El Niño sink occurred at all times except the El Niño 12 months, then the forests were still a sink, 0.11 Mg C ha⁻¹ yr⁻¹, but this value is indistinguishable from zero, i.e. the sink turned off, but these forests did not become a temporary carbon source. If the impacts were concentrated in just the strongest dry season months, then these forests were a short-term source of 0.47 Mg C ha⁻¹ yr⁻¹ for those three months. Under this potential scenario the immediate return of the forest to being a strong sink after being a very temporary source could then be interpreted as African tropical forests being resilient rather than resistant to environmental change. However, the lack of strong correlations between the carbon sink and temperature or drought anomalies suggest such extreme short-term carbon flux changes are unlikely. Furthermore, if these forests exhibited a large source and then recovered with a large sink they would show a signature of high carbon losses and an increase in carbon gains over the 2.7-year period, which was not found. Consistent with this interpretation of the results, independent data from remotely sensed CO₂ suggests that the regions of tropical forest where the plots are located were an ongoing sink throughout 2015 and 2016 (Palmer et al. 2019) or a modest source that is not driven by very short-term impacts of strong responses to drought (Liu et al. 2017). This independent evidence, and the fact that these forests have been a sink over 2.7 years while experiencing unprecedented heat and drought

conditions, reinforces the conclusion that African forests were resistant to the 2015-16 extreme climate anomaly. Thus, overall the analyses suggest that the carbon sink in African tropical forests was reduced by the 2015-16 El Niño event, but the record temperature and drought conditions did not cause the forests to lose aboveground biomass carbon.

2.4.1 Forest Responses

African forests appear to be more resistant to droughts than Amazonian or Bornean forests. The African data shows that the carbon impact of the drought in Africa was a reduction of $0.29 \text{ Mg C ha}^{-1} \text{ yr}^{-1}$ or 0.2 % of aboveground carbon stocks (pre-El Niño net carbon $0.81 \text{ Mg C ha}^{-1} \text{ yr}^{-1}$, El Niño net carbon $0.52 \text{ Mg C ha}^{-1} \text{ yr}^{-1}$, initial aboveground biomass carbon 164 Mg C ha^{-1}). Assuming the same biomass to carbon conversion of 45.6% as in this chapter and continental mean aboveground biomass stocks (Sullivan et al. 2017), then droughts in Amazonia had much larger impacts: during the 2005 drought they lost $0.73 \text{ Mg C ha}^{-1} \text{ yr}^{-1}$ or 0.5 % of their aboveground biomass carbon, from $0.41 \text{ Mg C ha}^{-1} \text{ yr}^{-1}$ pre-drought, to a loss of $0.32 \text{ Mg C ha}^{-1} \text{ yr}^{-1}$ (Phillips et al. 2009)). During the 2010 drought they lost even more carbon: $0.81 \text{ Mg C ha}^{-1} \text{ yr}^{-1}$, 0.6 % of aboveground biomass carbon, from $0.61 \text{ Mg C ha}^{-1} \text{ yr}^{-1}$ pre-drought, to a loss of $0.20 \text{ Mg C ha}^{-1} \text{ yr}^{-1}$ drought (Feldpausch et al. 2016)). In Borneo the 1997-98 El Niño caused a loss of $1.44 \text{ Mg C ha}^{-1} \text{ yr}^{-1}$, 0.7 % of aboveground biomass carbon, from $0.52 \text{ Mg C ha}^{-1} \text{ yr}^{-1}$ pre-El Niño, to a loss of $0.94 \text{ Mg C ha}^{-1} \text{ yr}^{-1}$ (Qie et al. 2017)). So, sample size is sufficient to detect a shutdown or reversal of the sink because $n=100$ plots in Africa, larger than the 55 plots from Amazonia remeasured to capture the 2005 drought, showing a shut-down of the sink (Phillips et al. 2009), and similar to the 97 plots showing a shut-down of Amazon sink in response to the 2010 drought (Feldpausch et al. 2016), and much larger than the 19 plots used to show a reversal of the sink during the 1997-98 El Niño in Bornean forests (Qie et al. 2017). Thus, the response of African tropical forests to recent droughts is at least 50 % less on both an absolute and relative basis than forests in Amazonia and Borneo.

The El Niño census interval is likely to have captured the impact of the climate anomaly on forest dynamics. Most trees die within a few months of tropical drought events (Phillips et al. 2009, Qie et al. 2017) and our El Niño census window was 2.7 years long, similar to the 2.0 year interval in Phillips et al. (2009) and the 3.5 year interval in Qie et al. (2017) that did detect a carbon sink shutdown in Amazonian and Asian forests

respectively. There is no evidence of a lagged response to drought on carbon gains in Amazonia or Africa (Hubau et al. 2020), no long-term increase in carbon losses from mortality in African forests implying a lack of response to past droughts (Hubau et al. 2020), nor rising carbon losses from mortality after the specific 1997-98 El Niño in African forests (Hubau et al. 2020). Furthermore, while remotely sensed data do not show a return to pre-El Niño carbon stocks in African forests, there was no continued reduction in stocks (Wigneron et al. 2020) and atmospheric and land surface model data tend to show some recovery of stocks (Bastos et al. 2018), both inconsistent with a hypothesised lagged tree mortality response to the 2015-16 El Niño event humid African forests.

Why then were the El Niño impacts small for African tropical forests? Muted African forest responses to the 2015-16 El Niño might be expected as some of the strongest water deficit anomalies occurred in the wettest plots (Figure 2.2) while peak temperature increases across African tropical forests were relatively short-lived. Nevertheless, these were unprecedented conditions regionally, and they failed to cause intact African tropical forests to lose any biomass on average. Additionally, the region-wide measurements suggest that African forests themselves are likely to be more drought-adapted than either Amazonian or Southeast Asian forests - due to past biogeographic history having favoured the persistence, expansion, and perhaps diversification of more drought-adapted species (deMenocal 2004, Parmentier et al. 2007), alongside adaptation to the relatively dry contemporary conditions across the continent (Malhi and Wright 2004). A recent analysis using inventory data also suggests that African forests are more drought-resistant, but not more heat-resistant than Amazonian forests (Hubau et al. 2020).

Plot measurement of only the live biomass monitors only the stocks of live carbon but there is also a flux of carbon to the atmosphere from necromass and soils, heterotrophic respiration. From an atmospheric perspective the full impact of the reduction in the live carbon sink from slowing carbon gains is experienced immediately, but the contribution from rising carbon losses is delayed because dead trees do not decompose instantaneously, meaning that the contribution of biomass losses to the net biome response to the El Niño is also likely to be muted. Additionally, soil carbon fluxes to the atmosphere in intact tropical forests are typically lower during drought conditions (Davidson et al. 2000, Rubio and Detto 2017) suggesting that the overall net biome response in African forests is muted because a small decrease in forest growth (i.e., reduced net primary productivity) may be somewhat offset by lower a soil carbon flux from lower heterotrophic respiration. Consistent with this, remotely sensed CO₂ data suggests

that the regions of tropical forest where the plots are located were an ongoing sink throughout 2015 and 2016 (Palmer et al. 2019). This independent evidence, and the fact that these forests have been a sink over 2.7 years while experiencing unprecedented heat and drought conditions, reinforces the conclusion that African forests were resistant to the 2015-16 extreme climate anomaly.

With relatively few stems and high biomass per hectare, African tropical forests are more dominated by large trees than those typically found in Amazonia or Asia (Lewis et al. 2013). Because of their structure, there is likely to be more severe asymmetric competition in African forests than in Amazonia or Asia, and small trees are much more subordinate in these ecosystems. In Africa in the 2015-16 El Niño, the response of large dominant trees was variable and not strongly directional, whereas small trees grew less and died more, perhaps due to more limited access to water than the large trees. These impacts on small trees show that African forests were suffering in the El Niño but responses were modest overall because large trees disproportionately influence forest stocks and total biomass (Enquist et al. 2020). African forests are structurally unique, possibly due to megafauna maintaining their large trees, and their large, long-lived trees may buffer ecosystem responses to environmental change (Enquist et al. 2020). Thus intriguingly, it may be the existence of a more complete megafauna that is conferring resistance to record-breaking climate anomalies.

The 2015-16 El Niño did not cause widespread mortality of large trees, because stem mortality rates did not significantly increase for the largest size class (pre-El Niño 1.4%, El Niño 1.8 %, paired t-test, $p=0.07$), unlike the increases seen as a result of previous droughts observed in Amazonia and Southeast Asia (Phillips et al. 2010b), experimental droughts in eastern Amazonia (Nepstad et al. 2007) and a meta-analysis, which included no plots in Africa (Bennett et al. 2015). Measurements are unlikely to have missed post-El Niño mortality given the El Niño 2.7-year census window, as most trees die within a few months of tropical drought events (Phillips et al. 2009, Qie et al. 2017). No increase in large tree mortality implies that rates of hydraulic failure only increased slightly, if at all, in African tropical forests in the 2015-2016 El Niño, again unusual when compared to Amazonian and Asian forests (Choat et al. 2012, Rowland et al. 2015). The lack of increase in large tree mortality further explains the limited impacts of the El Niño on African forest carbon stocks.

2.4.2 Regional Carbon Implications

A recent assessment of the long-term carbon sink in African forests is $0.46 \text{ Pg C yr}^{-1}$ ($0.37\text{-}0.56$ 95 % CIs) for the years 2000-2010 (Hubau et al. 2020), and the results suggest the sink reduced by 35 % over the 2.7 year El Niño census period, hence over the 2.7-year period the sink is estimated as $0.30 \text{ Pg C yr}^{-1}$ ($0.46 \times (1-0.35)$). The reduced sink captured by plot measurements is supported by a recent satellite-derived estimation of the carbon sink in African forests (Palmer et al. 2019). Palmer et al. (2019) analysed atmospheric CO_2 data to show that while Africa as a whole was a large source of carbon to the atmosphere over the El Niño, this was due to carbon release from Northern Africa. For the Congo Basin, in particular the West of the Congo Basin where most of the plots are located, the CO_2 data shows a carbon sink in this region in both 2015 and 2016, consistent with the ongoing carbon sink in 2015 and 2016 found here using the plot inventory data.

By contrast, Liu et al. (2017), also analysing atmospheric CO_2 data combined with a vegetation model came to a different conclusion, showing a source of $0.8 \pm 0.2 \text{ Pg C yr}^{-1}$ in the El Niño of 2015-16, compared the 2010-11 strong La Niña year for African forests. Liu et al.'s (2017) result is due to high surface temperature anomalies driving an increase in ecosystem respiration, which is not what was found here. Respiration increases in the plot data would manifest as reductions in carbon gains, yet carbon gains declined by just 1.4 %, not enough to stop or reverse the sink in the plots. While the flux identified by Liu et al. could come from soils, typically carbon releases are lower in dry periods due to lower biological activity (Saleska 2003). It should be noted that the Liu et al. respiration term is the residual after accounting for the estimates of the net biome exchange of carbon (from GOSAT and OCO-2), gross primary productivity and fire losses, thus is likely to be highly uncertain and potentially dominated by systematic errors in other terms.

In summary, this chapter shows that the unprecedented 2015-16 climate anomaly, including record air temperatures and water deficits, was insufficient to reverse the long-standing net carbon sink into intact forest biomass. This surprising resistance of structurally intact African forests and their continued carbon sink is also seen from at least one recent study of atmospheric CO_2 concentration data over Africa (Palmer et al. 2019), and when African forest responses are compared to the responses of Amazonian and Bornean forests to a strong drought (Phillips et al. 2009, Feldpausch et al. 2016, Qie et al. 2017). Resistance to rapid environmental change might be due to one of more of (i) the species present, as African forests are floristically distinct (Slik et al. 2018), (ii) their structure, as African tropical forests are dominated by large trees (Lewis et al. 2013),

which in turn may be a result of their retained megafauna (Enquist et al. 2020), (iii) the fact that African tree species have tolerated more extreme environmental change in glacial-to-interglacial cycles (Parmentier et al. 2007), or (iv) that the environmental conditions in African forests today are not as hot, nor warming as fast as Amazonian forests. Detection of the resistance of African tropical forests to unprecedented climate conditions was only possible because the AfriTRON ground monitoring network was already in place. Further progress will be made on understanding changes in African tropical forests if this network of plots continues to be monitored and is expanded to under-sampled areas alongside integration with new remote-sensing technologies.

Chapter 3

Drought and temperature sensitivity of South American tropical forests during an extreme climate anomaly

Abstract

South American tropical forests have provided a long-term carbon sink, but this sink is sensitive to drought, with past droughts in Amazonia in 2005 and 2010 causing biomass loss. While this implies that the increased frequency of droughts associated with climate change threatens the future of these forests, there is also evidence of communities shifting to become more drought-tolerant, so forests may already be adapting to climate change. One way to assess these differing hypothesised responses to ongoing climate change is to analyse the impacts of the 2015-16 El Niño Southern Oscillation, which resulted in record tropical warmth and altered precipitation and its impact across neotropical forests. Here responses of 137 long-term intact tropical forest inventory plots are reported across seven South American countries, each measured prior to and following the 2015-16 El Niño event. While the climatology of these forest plots varied, overall they experienced their highest recorded temperatures and strong water deficits (on average +1.2 °C and -57 mm stronger maximum climatological water deficit than the mean conditions of 1980-2010). During the record temperatures of the 2015-16 El Niño, the 137 forest plots went from being a significant carbon sink pre-El Niño to small source in the census that captures the El Niño. High temperature anomalies significantly increased carbon losses from tree mortality but did not significantly reduce carbon gains from tree growth, and the high drought anomalies significantly increased losses from mortality but did not reduce carbon gains from tree growth. The climatically hottest forests were significantly more prone to El Niño depression of carbon gains and the driest forests were significantly more prone to El Niño enhanced carbon losses from mortality of biomass and decreased recruitment. During the El Niño stem mortality rates increased for all trees, with no evidence of size selective mortality. The net biomass sink declined by $0.7 \pm 0.4 \text{ Mg C ha}^{-1} \text{ yr}^{-1}$ during the 2015-16 El Niño, similar to the impacts of the 2005 and 2010 droughts.

Thus, there is no evidence of shifts in species composition having provided drought resistance, rather the fact that carbon losses increased with temperature and the temperature threshold for rapid declines in biomass carbon gains highlight the vulnerability of many South American tropical forests to changing climate. Future extreme droughts are not guaranteed but high temperatures are, and as the extreme climate anomalies of the present become the normal climate of the future, every degree of warming may reduce the net carbon sink in South American tropical forests.

3.1 Introduction

Intact tropical forests are a key component of the Earth system, storing and sequestering large amounts of carbon, mean $1.19 \pm 0.41 \text{ Pg C yr}^{-1}$ from 1990-2007 (Pan et al. 2011). The most extensive and diverse tropical forests in the world are found in South America (e.g. (Ter Steege et al. 2013)) and measurements from long-term inventory plots suggest that Amazonian forests in particular have contributed a major carbon sink for decades, but that this carbon sink is declining (Brienen et al. 2015), and may cease in the future (Hubau et al. 2020). The declining sink is driven by a stalling of past increases of woody productivity and strongly accelerating tree mortality (Brienen et al. 2015) which are related to the impacts of increasing air temperatures, drought and internal forest dynamics (Hubau et al. 2020). In the short-term, the carbon sink in South American tropical forests is known to be vulnerable to both droughts (Phillips et al. 2009, Feldpausch et al. 2016, Hubau et al. 2020) and high air temperatures (Hubau et al. 2020). With record high temperatures on top of a long warming trend and a sequence of droughts, the 2015-16 El Niño provides a novel opportunity to assess tropical forest vulnerability to heat and to drought.

Tropical forest responses to temperature are likely to be complex. Potentially, increasing temperature should increase productivity since ecosystems in warmer climates tend to have higher productivity in terms of net primary production (Schuur 2003, Del Grosso et al. 2008), and this appears to hold across local tropical elevation gradients so is unlikely to simply be related to longer growing seasons (Raich et al. 1997, Fyllas et al. 2017, Malhi et al. 2017). If plants can tightly regulate stomatal conductance and increase water use efficiency then they should be able to perform better under high temperatures. However, higher temperatures also pose greater risks of thermal damage (Schreiber and Berry 1977) and greater hydraulic risks, as vapour pressure deficits (VPD) increase with temperature (Trenberth et al. 2014). At the top of the canopy VPD is greatest and decreases closer to the ground (Roberts et al. 1990b), so larger trees and taller forests are

more sensitive to VPD anomalies (Giardina et al. 2018). As temperatures increase, there must be a temperature beyond which productivity decreases in the lowland tropics. While tropical forest responses to drought have been well-documented, responses to temperature have not. Work so far has focused on mortality and associated hydraulic challenges (McDowell et al. 2018), largely neglecting potential simultaneous changes in productivity and growth (Bonal et al. 2016). Assessment of how South American tropical forests respond to recent, exceptional temperature anomalies can help fill this knowledge gap.

Droughts are likely to detrimentally affect all trees in a forest. Most tropical forests are water limited for most of the year, so from first principles increasing moisture is very likely to be beneficial. Lack of water impacts biomass primarily by tree mortality, and water deficits increase mortality risk for individual trees for most of the climate space (Allen et al. 2010, Phillips et al. 2010b). There is also evidence that the enhanced mortality risk with drought is unevenly distributed, with larger trees often more vulnerable to drought as they face greater hydraulic challenges (Bennett et al. 2015). So, it is expected that regions with more anomalous drought will have greater biomass mortality and a disproportionate number of large trees dying. Exceptions are likely though, notably in forests that typically have saturated soils – whether due to climatic reasons, where productivity is usually light-limited (Schoor 2003, Zuleta et al. 2017), or to edaphic factors where forests may exhibit some resistance to drought via lower tree mortality or higher recruitment (Sousa et al. 2020).

The 2015-16 El Niño is the third very strong drought in a decade in South America. Typical South American tropical forests are sensitive to drought (Nepstad et al. 2007, Phillips et al. 2009, Feldpausch et al. 2016). Indeed, the carbon sink of South American tropical forests has been paused by at least two severe droughts in the last twenty years. Thus, a long-term pattern of net carbon sequestration in intact Amazonian forests was temporarily halted due to the 2005 drought (Phillips et al. 2009) but then recovered, at a lower strength, soon after the climate anomaly (Brienen et al. 2015). The 2010 drought again reversed the baseline net sink, partly via increased mortality but also via reduced woody productivity (Feldpausch et al. 2016). For the Amazon region the 2010 drought was severe over a more extensive area than the 2005 drought (Lewis et al. 2011). The droughts of 2005 and 2010 were both non-El Niño droughts, and differ in spatial pattern to typical El Niño droughts which tend to be severe and widespread for the central Amazon (Jiménez-Muñoz et al. 2016). The last very strong El Niño in 1997-98 increased mortality

rates in Amazonia (Williamson et al. 2000a), there was also a very strong El Niño in 1982-83 and El Niño events tend to increase flower and seed production in Panama (Wright and Calderón 2006). Yet, with record hot temperatures and extreme drought and with a novel spatial pattern (Jiménez-Muñoz et al. 2016), the 2015-16 may have had the greatest impacts on Amazonian forests.

In spite of the recent impacts of severe droughts, other evidence points to considerable potential drought resistance in neotropical forests. In large parts of Amazonia, temperatures increased 1-2 °C and precipitation declined during the Mid-Holocene Dry Event approximately 9,000 to 4,000 years ago (Dick et al. 2013, Nascimento et al. 2019). Pollen records suggest that forests of the western Amazon were resilient to this long-term climate change with only a few species replacements and minor fluctuations in abundance (Nascimento et al. 2019). There is also contemporary evidence of very recent increases in temperature resistance (Yamori et al. 2014) and increases in drought resistance, as species composition has shifted towards more dry affiliated genera across Amazonia (Esquivel-Muelbert et al. 2019) and drought-induced mortality in Amazonia has been greater for wetter-affiliated genera (Esquivel-Muelbert et al. 2017). So, this chapter assesses whether South American tropical forests are becoming more drought-tolerant.

The level of drought and mean temperature prior to the climate anomaly, i.e. the baseline conditions, are likely important in determining forest responses to El Niño (Esquivel-Muelbert et al. 2019). If a universal temperature threshold for photosynthesis exists, forests closer to this threshold - those which are hotter and drier, may be expected to suffer more from a hot, dry climate anomaly. Alternatively, local adaptation of communities that have hotter or drier baseline climates might mean they do not suffer proportionately more from a hot dry climate anomaly. So, it is important to consider baseline climate when analysing ecosystem responses to climate anomalies. Most analyses focus on the impacts of the climate anomaly alone (Bonafant et al. 2016) and, in terms of plots, thus far there has not been enough temporal data nor replication to assess the importance of baseline conditions.

During the 2015-16 El Niño there were extreme temperatures and reduced precipitation across the tropics (Chapter 2 and Liu et al. 2017). In tropical South America in 2015, the mean annual precipitation was the lowest and the temperature highest on record (Jiménez-Muñoz et al. 2016). Early studies analysing reanalysis precipitation datasets (Jiménez-Muñoz et al. 2016) suggested that the 2015-16 El Niño drought was limited to the eastern Amazon, yet, (Yang et al. 2018a) found decreased precipitation

across a much broader area, and river discharge across the whole Amazon Basin was 40% lower than average between December 2015 and February 2016 (Van Schaik et al. 2018). Thus, there is still some uncertainty about the nature and extent of the 2015-16 climate anomaly across South American forests. Long-term measurements of forests are vital to help verify and understand the impact of the climate anomaly on South American tropical forests, but so far there is a lack of a large-scale field-based analysis of the impact of these unprecedented conditions.

Here, 137 long-term monitoring plots from across the RAINFOR network (Malhi et al. 2002b) are measured and analysed to assess the impact of the 2015-16 El Niño on South American tropical forests. These plots span Amazonia but also include forests at the fringes of the moist forest biome, encompassing forest communities in regions that are transitional with dry forests and Cerrado. With the largest on-the-ground dataset yet mobilised to address the impact of a single tropical drought, I investigate the impact of the 2015-16 El Niño high temperatures and drought on the temporal patterns of net aboveground biomass, productivity and biomass mortality of South American tropical forests. Therefore, climate data is combined with measurements from long-term inventory plots to address the following questions: (1) Did South American tropical forests experience unprecedented temperature anomalies in the 2015-16 El Niño? (2) Did South American tropical forests experience unprecedented drought in the 2015-16 El Niño? (3) How did the climate anomaly of 2015-16 compare to the extreme Amazon droughts of 2005 and 2010? (4) Which climate anomalies drove forest responses to the 2015-16 El Niño? (5) Were hotter forests more resistant or more vulnerable to the climate anomaly? (6) Were drier forests more resistant or more vulnerable to the climate anomaly? and (7) What were the overall impacts on the monitored old-growth structurally intact tropical forests?

3.2 Methods

Methods follow this in Chapter 2, to allow comparability, with changes or additional methods detailed below.

3.2.1 Climate Data

For temperature I used the ERA5 dataset (Copernicus Climate Change Service Climate Data Store (CDS) 2020) instead of ERA-I as used in Chapter 2, because the new ERA5 product has higher spatial (30 km) and temporal (1-hour) resolution. I also use the latest CRU monthly temperature data, version ts.4.03, instead version ts.4.01 used in

Chapter 2. Temperature products were combined as in Chapter 2, by matching overlapping months. Thus, in this chapter the temperature record for South America is a combination of the CRU ts.4.03 (1970-1978) and ERA5 (1979-2018) products rather than the combination of CRU ts.4.01 (1970-1978) and ERA-I (1979-2017) in Chapter 2. For precipitation I used the same products for this analysis as in the Chapter 2 analysis; GPCC (1970-1997) and TRMM (1998-2018).

The climate of the 2015-16 El Niño Southern Oscillation event is defined as the twelve-month period from May 2015 to April 2016, as for Africa in Chapter 2. These twelve consecutive months are also those with the greatest SST anomalies (Liu et al. 2017) and include peak temperatures for South America, as land surface temperature anomalies in South America lag sea surface temperature anomalies that began in November 2014 (Liu et al. 2017), by two months (Malhi and Wright 2004). These same May-April twelve consecutive months are also used to characterise the 1982-83 and 1997-98 El Niño events.

I analyse how carbon gains from productivity change with baseline temperatures. To compare results with the maximum temperature thresholds for carbon stocks found in (Sullivan et al. 2020) I used an additional temperature dataset to calculate maximum daily temperature. Data from WorldClim version 2 (Fick and Hijmans 2017) were extracted at plot locations and annual mean temperature (BIO1) and mean diurnal temperature range (BIO2) for 1970-2000 were used to calculate mean daily maximum temperature (BIO1 + BIO2/2) as an alternative long-term climate baseline in addition to pre-El Niño temperature.

The South American tropical forest region is defined using the Tropical and Subtropical Moist Broadleaf Forest Biome from the WWF Terrestrial Ecoregions of the World map (Olson et al. 2001), as for Africa in Chapter 2. The 137 South American forest plots include transitional forests at the edge of the moist tropical forest biome, which are sometimes beyond the limits of the Olsen polygon. Therefore, for maps visualising the climate anomaly a wider region is used - locations that have $> 1000 \text{ mm yr}^{-1}$ precipitation and are $< 1000 \text{ m}$ above sea level. So in Figure 3.1 and Table 3.1 the region is the same as in Chapter 2, and in further figures, just for visualisation, the area is expanded to include drier forest regions.

3.2.2 Plot Data Collection and Analysis

Long-term inventory plots were censused using standard RAINFOR methodology (Phillips et al. 2010a). All permanent sample plots used in the analysis are located in lowland (all <1000 m, 131 plots <800 m as for Africa in Chapter 2), closed canopy, old-growth, structurally intact tropical forests, had been censused at least twice prior to the 2015-16 El Niño event, and were censused once afterwards. The 137 plots meeting these criteria are distributed across 57 distinct clusters in seven countries: Bolivia, Brazil, Colombia, French Guiana, Guyana, Peru and Venezuela. I conducted the final quality control checks on all 137 plots. I include only plot censuses from 1984 onwards, as in Chapter 2, to exclude the impacts of the 1982-83 El Niño. Median plot size is 1 ha, mean 0.98 ha (range 0.2 - 6.25 ha); mean initial census is May 2004, mean pre-El Niño census is September 2014, and mean post-El Niño census is May 2017. The mean pre-El Niño monitoring length was 12.8 years and the mean length of the El Niño interval was 2.5 years, similar to mean census interval lengths for Africa in Chapter 2. Data are curated at ForestPlots.net (Lopez-Gonzalez et al. 2011) version 2019.1 downloaded on 19 August 2019. Tree heights were measured in all 137 plots; and methods for tree height are identical to Chapter 2.

As in Chapter 2, the mean of the El Niño census interval minus the mean of the pre-El Niño monitoring period and the result is Δ net carbon, Δ carbon gains and Δ carbon losses for each plot. Net carbon and carbon losses are for all plots ($n=137$). In this Chapter, as the mean El Niño census was slightly later post-El Niño, and El Niño carbon gains impacts are more likely to be seen with shorter census intervals, Δ carbon gains were restricted to plots that have been censused within one year of the maximum climate anomalies, so to be included they must have been measured before February 2017 ($n=62$ plots). Again, as in Chapter 2, the plots are weighted following the same procedure, but this resulted in slightly different weightings than for Africa. Selected weights were: Δ net carbon, $\text{Monitoring length}^{1/3} + \text{Area}^{1/3} - 1$; Δ carbon gains, $\text{Monitoring length}^{1/6} + \text{Area}^{1/5} - 1$; Δ carbon losses, $\text{Monitoring length}^{1/3} + \text{Area}^{1/3} - 1$.

Analyses in this chapter are very similar to the analyses performed in Chapter 2, but here in Chapter 3 I analyse data from 137 South American forest plots and the climate data at these plot locations. Additionally, to investigate temperature thresholds for carbon gains in this chapter I perform breakpoint regressions using the segmented R package (Muggeo 2003), bootstrapped with one hundred repetitions. As a high temperature threshold for photosynthesis exists theoretically, one could presume that two linear models would capture the temperature productivity relationship, a model prior to the temperature

threshold and a second beyond the temperature threshold both with different slopes. By fitting a breakpoint to the data I capture a potential temperature threshold. For the segmented analysis the breakpoint is estimated by the bootstrap restarting algorithm (Wood 2001). I test if the linear models either side of the breakpoint are significant and use Davies' test to determine whether lines on either side of the break point have significantly different slopes (Davies 1987, 2002).

3.3 Results

It was considerably hotter by 0.8 ± 0.04 °C (95 % CIs) and drier by -304 ± 16 mm yr⁻¹ across the South American tropical forest region during the 2015-16 El Niño compared to the previous decade (Figure 3.1, Table 3.1). The 50-year climate record shows that the long-term climate trends across South American tropical forests are rising temperatures and decreasing precipitation and seasonal moisture deficits (Figure 3.1). The three very strong El Niño events over the past 50 years are superimposed on these trends, so that the 2015-16 El Niño event led to record high temperatures and low precipitation and moisture deficits for South American tropical forests (Figure 3.1). The 1982-83, 1997-98 and 2015-16 very strong El Niño events each increased temperatures by 0.3, 0.8 and 0.8 °C, reduced precipitation by 138, 212 and 304 mm and decreased MCWD by 37, 45 and 60 mm, respectively, compared to the climate of the prior decade, indicating that the 2015-16 anomaly was larger than the previous two El Niño events in terms of drought (Figure 3.1, Table 3.1). The El Niño events have higher temperature anomalies than the non-El Niño droughts of 2005 and 2010, with 0.3, 0.8 and 0.8 °C compared to 0.3 and 0.1 °C (Table 3.1). The El Niño events also had greater decreases in precipitation, 138, 212 and 304 mm compared to increased precipitation during the non-El Niño droughts in 2005 and 2010, +67 and +63 mm. Mean water deficits are also much stronger for El Niño droughts with -37, -45 and -60 mm compared to -9 and 3 in non-El Niño droughts across the South American tropical forest region.

The 137 South American forest plot locations are hotter, drier and more droughted than the region as a whole because some of the plots are located outside of the core tropical forest region, in drier forests. Both the plots and region have similar trends of increasing temperature and decreasing rainfall (Figure 3.1). In the 2015-16 El Niño the 137 plot locations experienced record mean annual temperatures of 26.1 ± 0.03 °C, record low total annual precipitation, mean 1573 ± 20 mm, and low, but not record low, MCWD with mean -283 ± 2 mm (Table 3.1, Figure 3.3). Comparing the plot census interval that captures the 2015-16 El Niño with the plot pre-El Niño census period, 128 of the 137 plots

had higher mean monthly temperature over the El Niño census interval compared to their pre-El Niño censuses, higher by a mean of $+0.49 \pm 0.06$ °C (paired t-test, $p < 0.05$). Plots had greater water deficits during the El Niño census interval compared to their pre-El Niño monitoring period, 102 of the 137 plots had more negative MCWD, and 79 of the 137 plots had droughts greater than -25 mm (mean plot MCWD anomaly -48 ± 12 mm, paired t-test, $p < 0.001$), 107 plots also had lower total annual precipitation (mean -15 ± 4 mm yr⁻¹, paired t-test, $p < 0.0001$). The anomalies of temperature and MCWD were significantly correlated, as the temperature anomalies at plots increased water deficit anomalies became increased ($r = -0.17$, $p < 0.05$), and the anomalies of MCWD and precipitation were correlated; as precipitation anomalies increased, MCWD anomalies increased ($r = 0.42$, $p < 0.0001$). The mean El Niño census length of all plots was 2.5 years, so the climate anomalies corresponding to census measurement dates are smaller than those for the 12-month El Niño year because the climate anomaly is diluted by the inclusion of months of more usual conditions (Figure 3.3).

Table 3.1 | Climate anomalies of five drought events, including three very strong El Niño events, for the South American tropical forest region and plot locations. The 2015-16 El Niño was the hottest and driest drought event on record, both absolutely and anomalously, hotter and drier than the other two most recent very strong El Niño events and hotter and drier than two extreme droughts in the decade. The drought was also the strongest. A May-April year is used for climate analyses and n=137 plot locations. Displayed in the table are means and 95 % confidence intervals.

Drought Event	Mean annual temperature (°C)	Anomaly - decade	Anomaly – 1980-2010	Annual precipitation (mm)	Anomaly - decade	Anomaly – 1980-2010	MCWD (mm)	Anomaly - decade	Anomaly – 1980-2010
Region									
1982-83 El Niño	24.1 ± 0.03	0.3 ± 0.03	0.1 ± 0.04	2130 ± 9	-138 ± 14	-98 ± 14	-220 ± 1	-37 ± 2	-24 ± 2
1997-98 El Niño	24.7 ± 0.03	0.8 ± 0.04	0.7 ± 0.04	2008 ± 10	-212 ± 14	-220 ± 14	-241 ± 1	-45 ± 2	-45 ± 2
2005	24.4 ± 0.03	0.3 ± 0.04	0.3 ± 0.04	2280 ± 11	67 ± 16	52 ± 15	-203 ± 1	-9 ± 2	-8 ± 2
2010	24.4 ± 0.03	0.1 ± 0.04	0.3 ± 0.04	2309 ± 11	63 ± 16	81 ± 15	-194 ± 1	3 ± 2	2 ± 2
2015-16 El Niño	25.2 ± 0.03	0.8 ± 0.04	1.1 ± 0.04	1955 ± 11	-304 ± 16	-273 ± 15	-255 ± 1	-60 ± 2	-59 ± 2
Plot locations									
1982-83	25.0 ± 0.03	0.3 ± 0.03	0.04 ± 0.04	1902 ± 18	-136 ± 26	-16 ± 27	-236 ± 1	-7 ± 2	4 ± 2
1997-98	25.7 ± 0.03	0.9 ± 0.04	0.8 ± 0.04	1659 ± 17	-324 ± 25	-259 ± 26	-269 ± 1	-26 ± 2	-29 ± 2
2005	25.3 ± 0.03	0.2 ± 0.04	0.3 ± 0.04	1896 ± 22	55 ± 30	-22 ± 30	-245 ± 1	-4 ± 2	-5 ± 2
2010	25.4 ± 0.03	0.2 ± 0.04	0.4 ± 0.04	1960 ± 22	134 ± 31	42 ± 30	-246 ± 1	-4 ± 2	-6 ± 2
2015-16	26.1 ± 0.03	0.8 ± 0.04	1.2 ± 0.04	1573 ± 20	-279 ± 30	-345 ± 28	-283 ± 2	-45 ± 2	-42 ± 2

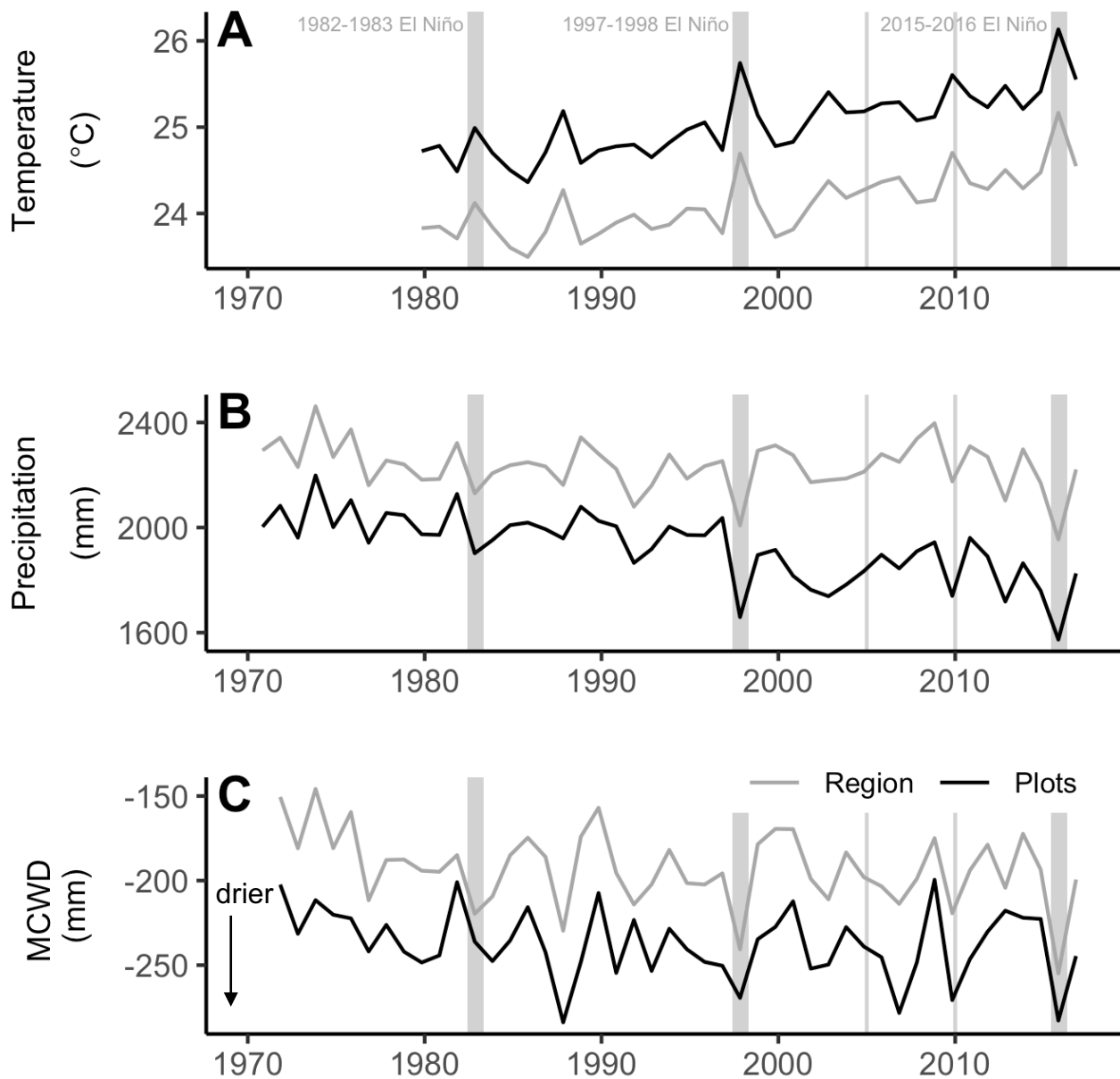
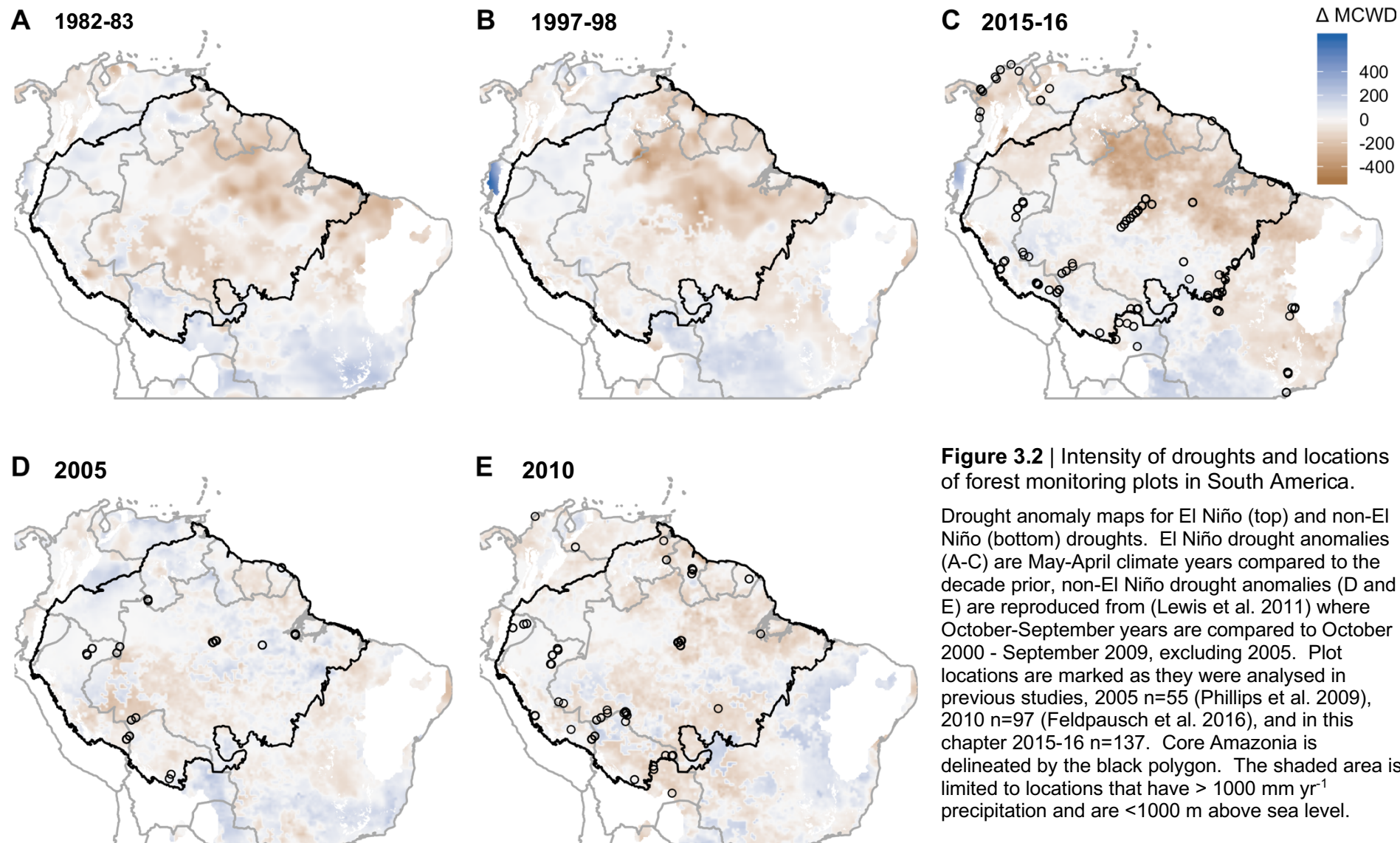


Figure 3.1 | Climate for plot locations (black) and the South American tropical forest region (grey)

South American tropical forests (grey) are delimited by the Tropical and Subtropical Moist Broadleaf Forest Biome from the WWF Terrestrial Ecoregions of the World (Olson et al. 2001). Mean annual temperature (A), total annual precipitation (B) and maximum cumulative water deficit, MCWD (C), values averaged for El Niño years May-April. $n=137$ plots. Black lines are for plot location, grey lines for the forest region. Grey vertical shading indicates the 1982-83, 1997-98, and 2015-16 very strong El Niño events and the vertical grey lines indicate the 2005 and 2010 droughts.



Of the five drought events examined in this chapter, the 2015-16 drought was the most extensive Amazonian drought (Figure 3.2). The total area that experienced a drought greater than 25 mm, i.e. Δ MCWD < -25, within core Amazonia, was: 4.2 million km² in the 2015-16 El Niño (Figure 3.2C), 4.0 million km² in the 1982-83 El Niño (Figure 3.2A), 3.9 million km² in the 1997-98 El Niño (Figure 3.2B) and as reported in (Lewis et al. 2011): 2.5 million km² in 2005 (Figure 3.2D) and 3.2 million km² in 2010 (Figure 3.2E). El Niño droughts are also more intense within Amazonia. The mean MCWD of pixels with Δ MCWD < -25 was -125 ± 1 mm in the 2015-16 El Niño (Figure 3.2C), -102 ± 1 mm in the 1982-83 El Niño (Figure 3.2A), -110 ± 1 mm in the 1997-98 El Niño (Figure 3.2B), and -85 ± 0 mm in 2005 (Figure 3.2D) and -73 ± 0 mm in 2010 (Figure 3.2E). So, when comparing drought across Amazonia, El Niño droughts are more extensive and more intense than non-ENSO droughts.

For the South American tropical forest region, in 2015-16 the epicentre of the drought was the north-east Amazon (Figure 3.2), while much of the south-west Amazon was wetter than the preceding decade. No plots were located at the epicentre of the 2015-16 drought and changes in net carbon reflect the distribution of drought with 47 % negative responses for plots east of -63° and 60 % negative to the west (Figure 3.10). This is due to carbon losses from aboveground biomass mortality being tightly linked to drought intensity, whilst carbon gains responses are more variable. The spatial pattern of droughts indicates that El Niño droughts have strong drying concentrated in the north and east Amazon, with limited drought in the south (Figure 3.2 panels A, B and C), whereas the non-El Niño droughts had drought in the south Amazon in 2005 (Figure 3.2D) and in the north and south Amazon in 2010 (Figure 3.2E).

The spatial pattern of drought, and locations of plots within that drought space dictate the drought-response captured by plot measurements. Of the 137 plots measured to capture the 2015-16 El Niño in this chapter, 73% experienced drought, while 67 % of the published plots measured to capture the 2010 drought experienced drought (Feldpausch et al. 2016) and 73 % of the published plots measured to capture the 2005 drought experienced drought (Phillips et al. 2009). The mean drought of the 137 plots in 2015-16 was -44 ± 12 mm, and by extracting the annual MCWD anomaly at plot locations (Figure 3.2), the mean MCWD anomaly at the 55 plots in Phillips et al. 2009 was -51 ± 12 in 2005 and at the 97 plots in Feldpausch et al. 2016 was -42 ± 11 in 2010. These percentages and mean MCWD anomalies suggest a similar proportion of plots were

droughted in the droughts of 2005, 2010 measured at the plots monitored at published locations, even though the published plot locations change and drought changes spatially.

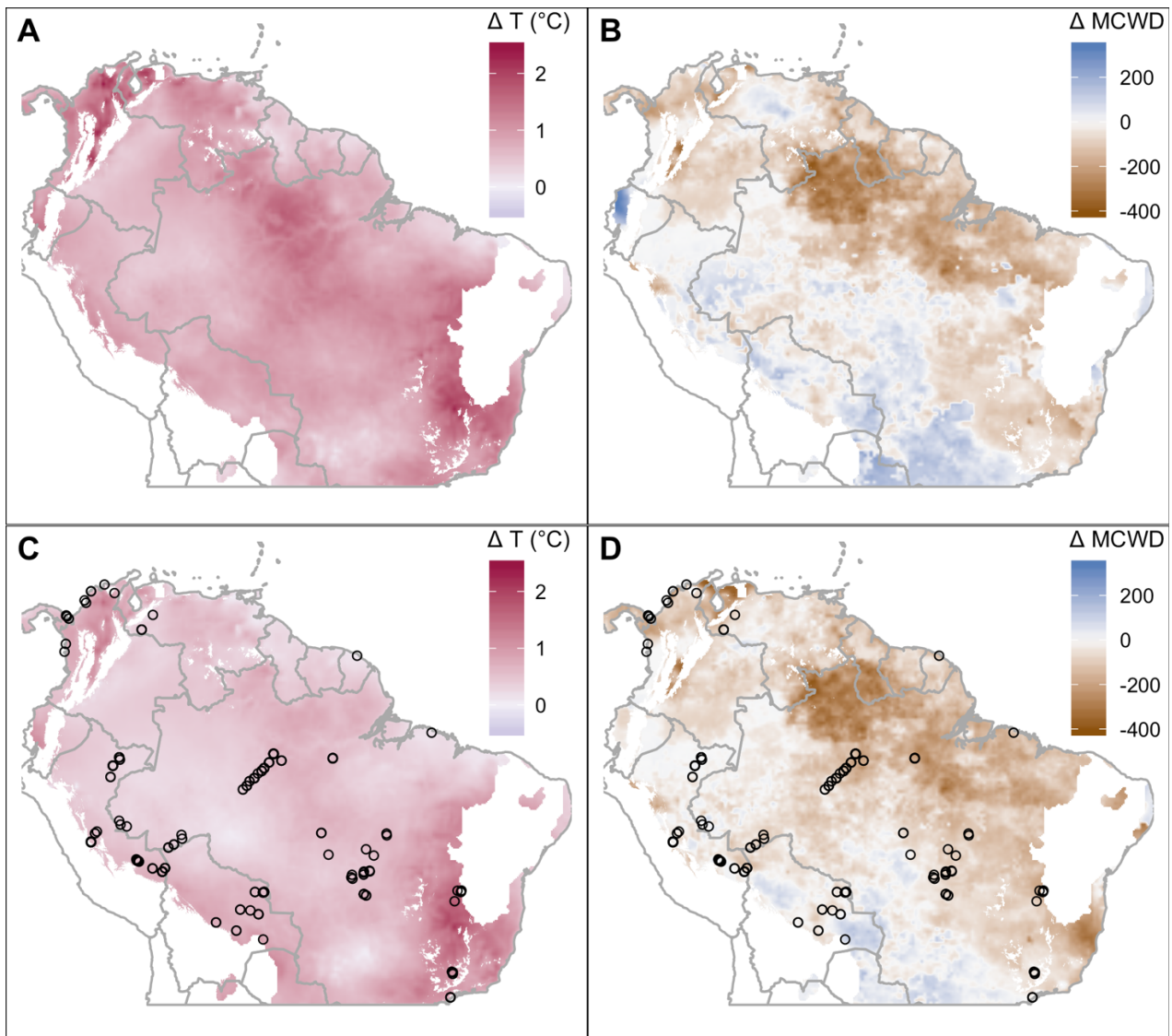


Figure 3.3 | Intensity of temperature (left) and drought (right) anomalies in 2015-16

The first row (A-B) is the anomaly for the El Niño year (May 2015 – April 2016) relative to the preceding decade (May 2005 - Apr 2015). The second row (C-D) is the anomaly for (September 2014 – May 2017) relative to (May 2004 - August 2014), the mean plot measurement dates. Plot locations are marked by black circles. The shaded area is limited to locations that have $> 1000 \text{ mm yr}^{-1}$ precipitation and are $< 1000 \text{ m}$ above sea level.

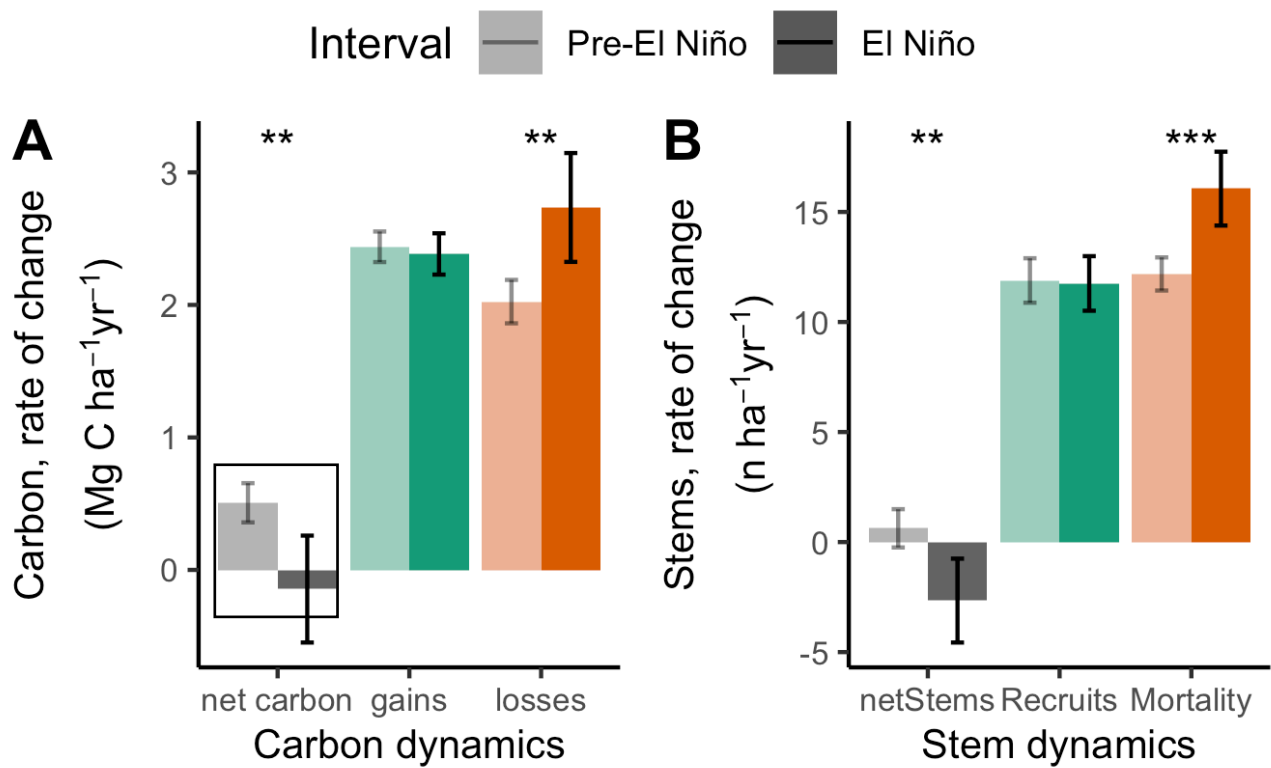


Figure 3.4 | Carbon (A) and stem dynamics (B), pre- (lighter shading) and during the 2015-16 El Niño (darker shading)

Carbon losses significantly increase from the pre-El Niño monitoring period to the El Niño census interval, reducing net carbon uptake, stem mortality also increases reducing net stems. Pre- and El Niño carbon (A) and stems (B). Lighter shading is pre-El Niño and darker shading is during the El Niño. $n=137$ plots and error bars represent 95% confidence intervals. Box around net carbon bars in panel A highlights that they are the same as the pair of bars with a box in Figure 3.5. Significant differences are defined by paired t-tests with ** indicating $p < 0.01$ and *** indicating $p < 0.001$

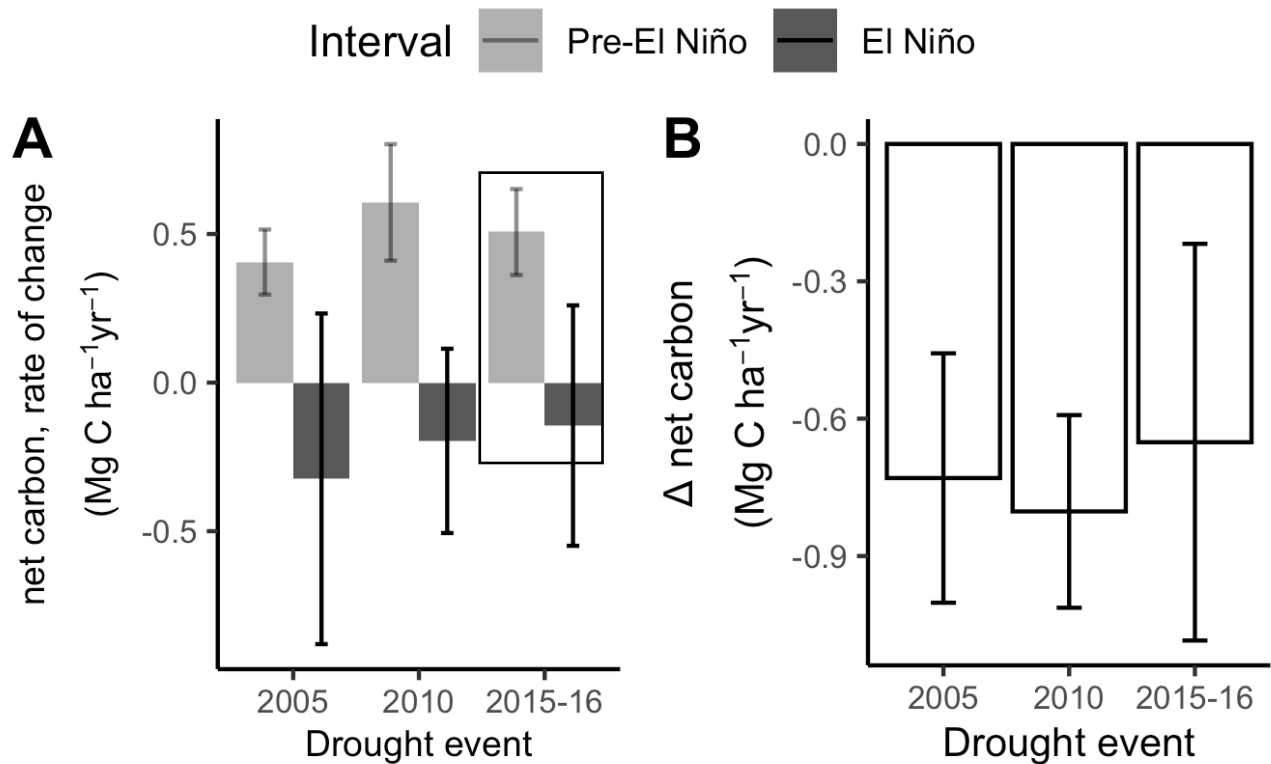


Figure 3.5 | Carbon dynamics, pre- and during the 2015-16 El Niño and in the context of 2005 and 2010 Amazon drought-responses

Declines in net carbon over three extreme droughts, including the 2015-16 El Niño, are similar. Pre-drought (lighter shading) and drought (darker shading) comparisons of $n=137$ plots, of which 75 % experienced drought more severe than the long term mean, and comparisons to the 2005; data from (Phillips et al. 2009) $n=55$ plots, 73 % of which experienced drought, and 2010; data from (Feldpausch et al. 2016) $n=97$, 67 % of which experienced drought. Error bars represent 95% confidence intervals. Box around 2015-16 bars in panel A highlights they are the same as the pair of bars with a box in Figure 3.4.

Over the censuses spanning the 2015-16 El Niño (mean 2014.7 to 2017.3) compared to the pre-El Niño period (mean 2004.3 to 2014.7) the carbon sink declined by 129 % (net carbon 0.5 to -0.1 Mg C ha⁻¹ yr⁻¹, Δ net carbon -0.7 ± 0.4 Mg C ha⁻¹ yr⁻¹, paired t-test, $p < 0.01$, Figure 3.4A). Seventy out of 137 plots had a net loss of aboveground biomass. The net change in carbon is composed of two process components; a significant increase in carbon losses due to biomass mortality (by 35 %, from 2.0 to 2.7 Mg C ha⁻¹ yr⁻¹, Δ carbon losses $+0.7 \pm 0.5$, $p < 0.01$) and no change in carbon gains from tree growth and new tree recruitment (from 2.4 to 2.4 Mg C ha⁻¹ yr⁻¹, Δ carbon gains -0.1 ± 0.2 , $p = 0.4$). Hence, during the record temperatures of the 2015-16 El Niño, the 137 forest plots went from being a significant carbon sink pre-El Niño to small source in the census that captures the El Niño.

Prior to the 2015-16 El Niño plots recorded a long-term net increase in aboveground biomass carbon, weighted by sampling effort, of 0.5 ± 0.1 Mg C ha⁻¹ yr⁻¹, between 2004.3 and 2014.7, consistent with the long-term Amazon carbon sink. By contrast, during the 2015-16 El Niño net the carbon balance declined significantly in monitored plots, to a small source, of -0.1 ± 0.2 Mg C ha⁻¹ yr⁻¹, a difference of -0.7 ± 0.4 Mg C ha⁻¹ yr⁻¹. The net carbon balance also significantly declined in previous droughts in South America, in 55 monitored plots in 2005 (-0.7 ± 0.6 Mg ha⁻¹ yr⁻¹ data from (Phillips et al. 2009)) and in 97 plots in 2010 (-0.8 ± 0.2 Mg ha⁻¹ yr⁻¹ data from (Feldpausch et al. 2016)), both times from a carbon sink to a small, non-significant, source (Figure 3.5).

Comparing the 2015-16 El Niño and 2005 and 2010 droughts, the change in net aboveground biomass carbon is similar (independent t-tests; 2005 vs 2010 $p = 0.7$, 2005 vs 2015-16 $p = 0.08$, 2010 vs 2015-16 $p = 0.6$, Figure 3.5B). Net aboveground biomass pre-drought was also similar (2005 vs 2010 $p = 0.4$, 2005 vs 2015-16 $p = 0.4$, 2010 vs 2015-16 $p = 0.4$, Figure 3.5A), as was net aboveground biomass in the interval that captures the drought (2005 vs 2010 $p = 0.9$, 2005 vs 2015-16 $p = 0.8$, 2010 vs 2015-16 $p = 0.6$, Figure 3.5A). In South America, there were similar water deficits at the actively monitored plot locations during the last three extreme droughts in 2005, 2010 and 2015-16, and the response of aboveground vegetation to these three extreme droughts where the plots were monitored was consistent. Of course, the drought was more extensive and more extreme in 2015-16 compared to previous droughts so the overall impact on the region may have been much larger in 2015-16 compared to previous drought events.

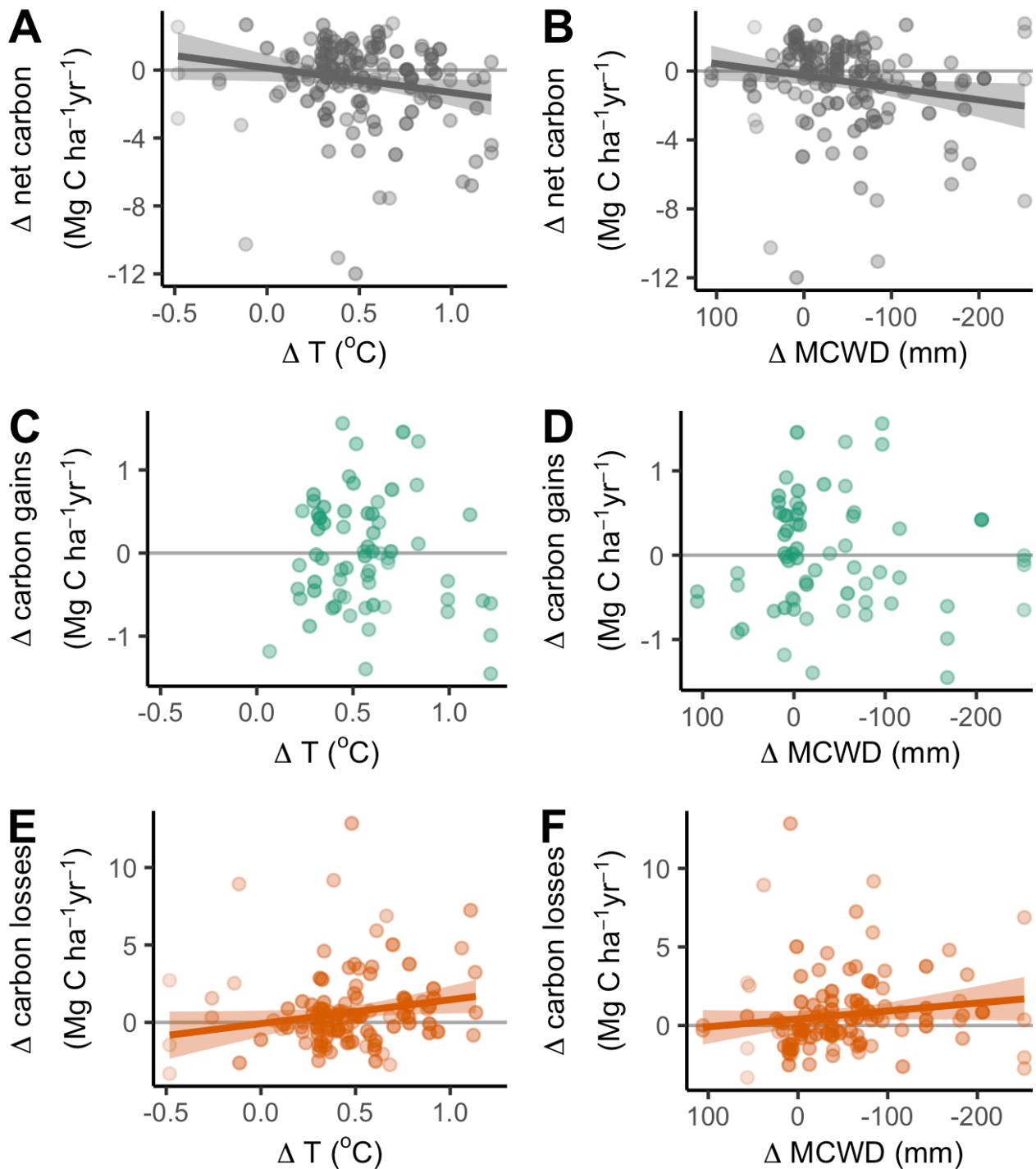


Figure 3.6 | Temperature (left) and drought (right) impacts on aboveground biomass carbon dynamics

Temperature anomalies and drought anomalies increase carbon losses and reduce net carbon. The net carbon change (**A**, **B**), carbon gains from tree growth and recruitment (**C**, **D**) and carbon losses from mortality (**E**, **F**) of the censuses capturing the El Niño event minus pre-El Niño plot monitoring period for 137 long-term inventory plots. The intensity of temperature change, Δ temperature (T) (**A**, **C**, **E**) is mean monthly temperature in El Niño minus mean monthly temperature pre-El Niño, using the census dates of the plot censuses. Relative intensity of the change in dry season strength is calculated as Δ maximum cumulative water deficit (MCWD) (**B**, **D**, **F**) which is the difference between maximum MCWD in El Niño and mean MCWD in pre-El Niño. Point shading from light to dark denotes greater weighting, with plots and line of best fit weighted by an empirically derived combination of pre-El Niño plot monitoring length and plot area for each response variable. Net change is in grey, gains are in green, losses orange. Solid lines represent significant linear models ($p < 0.05$). There are fewer points in C and D than in the other two

rows as carbon gains are restricted to plots that were measured within one year of the maximum climate anomaly, so to be included they must have been measured before February 2017. Slopes, intercepts and p-values for significant linear models are as follows: A: $y = -1.45x + 0.1$, $p < 0.05$, B: $y = -0.01x - 0.3$, $p < 0.05$, E: $y = 1.5x + 0.08$, $p < 0.05$, F: $y = 0.005x + 0.4$, $p < 0.05$.

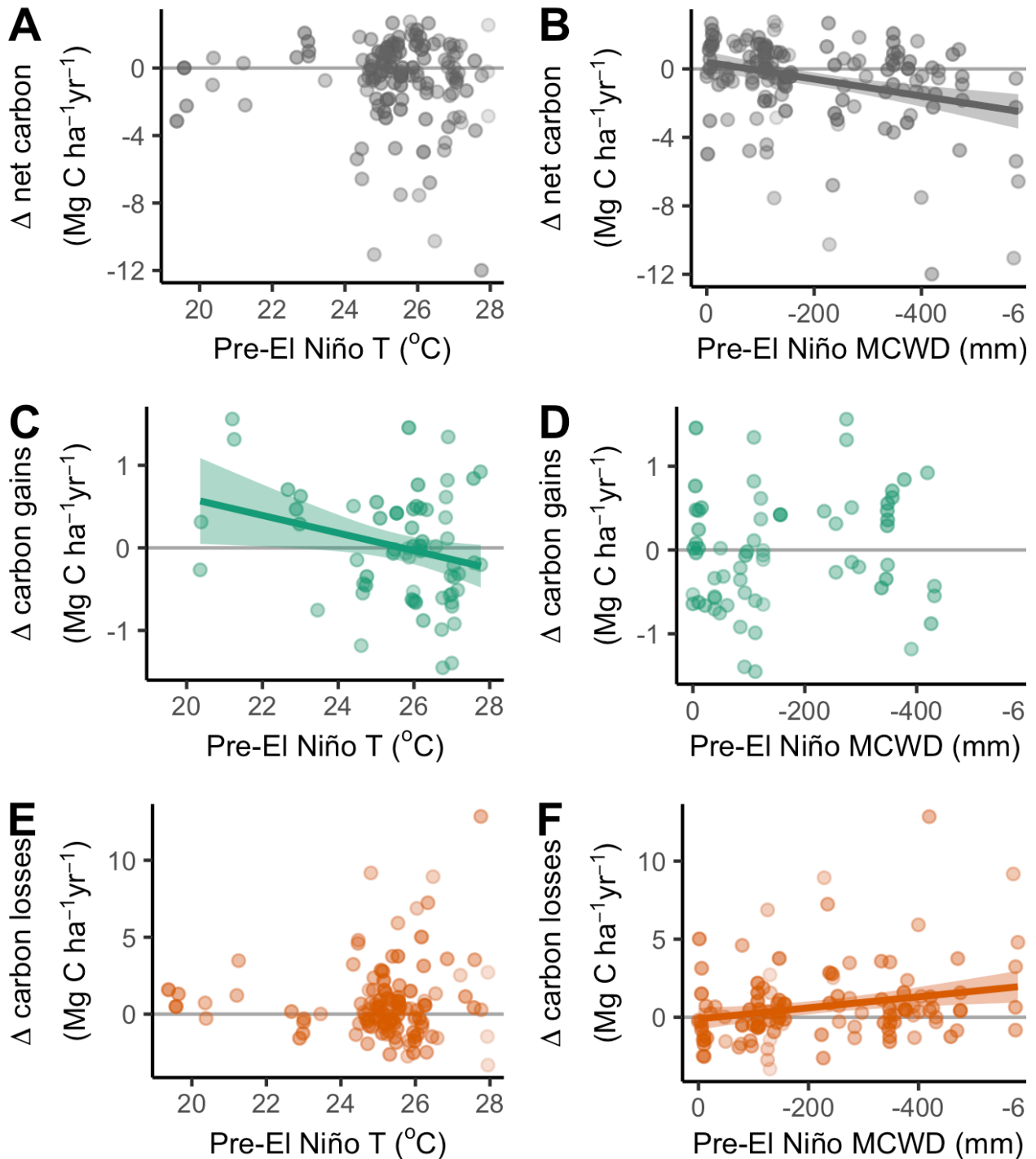


Figure 3.7 | Baseline temperature (left) and baseline drought (right) and anomalies of aboveground biomass carbon dynamics

Carbon gains significantly decrease with baseline temperature so plots with higher baseline temperatures had significantly lower carbon gains and baseline drier plots had significantly higher carbon losses and reduced net carbon. The net carbon change (A, B), carbon gains from tree growth and recruitment (C, D) and carbon losses from mortality (E, F) of the censuses capturing the El Niño event minus pre-El Niño plot

monitoring period for 137 long-term inventory plots. The pre-El Niño temperature (T) (**A, C, E**) is the mean of mean monthly temperature in the monitoring period prior to the El Niño, using the census dates of the plot censuses. The pre-El Niño maximum cumulative water deficit (MCWD) (**B, D, F**) is the mean MCWD in the monitoring period prior to the El Niño. Point shading from light to dark denotes greater weighting, with plots and line of best fit weighted by an empirically derived combination of pre-El Niño plot monitoring length and plot area for each response variable. Net change is in grey, gains are in green, losses orange. Solid lines represent significant linear models ($p < 0.05$). Slopes, intercepts and p-values for significant linear models are as follows: B: $y = -0.4x + 0.005$, $p < 0.001$, C: $y = 2.7x - 0.1$, $p < 0.05$, F: $y = 0.004x - 0.1$, $p < 0.01$.

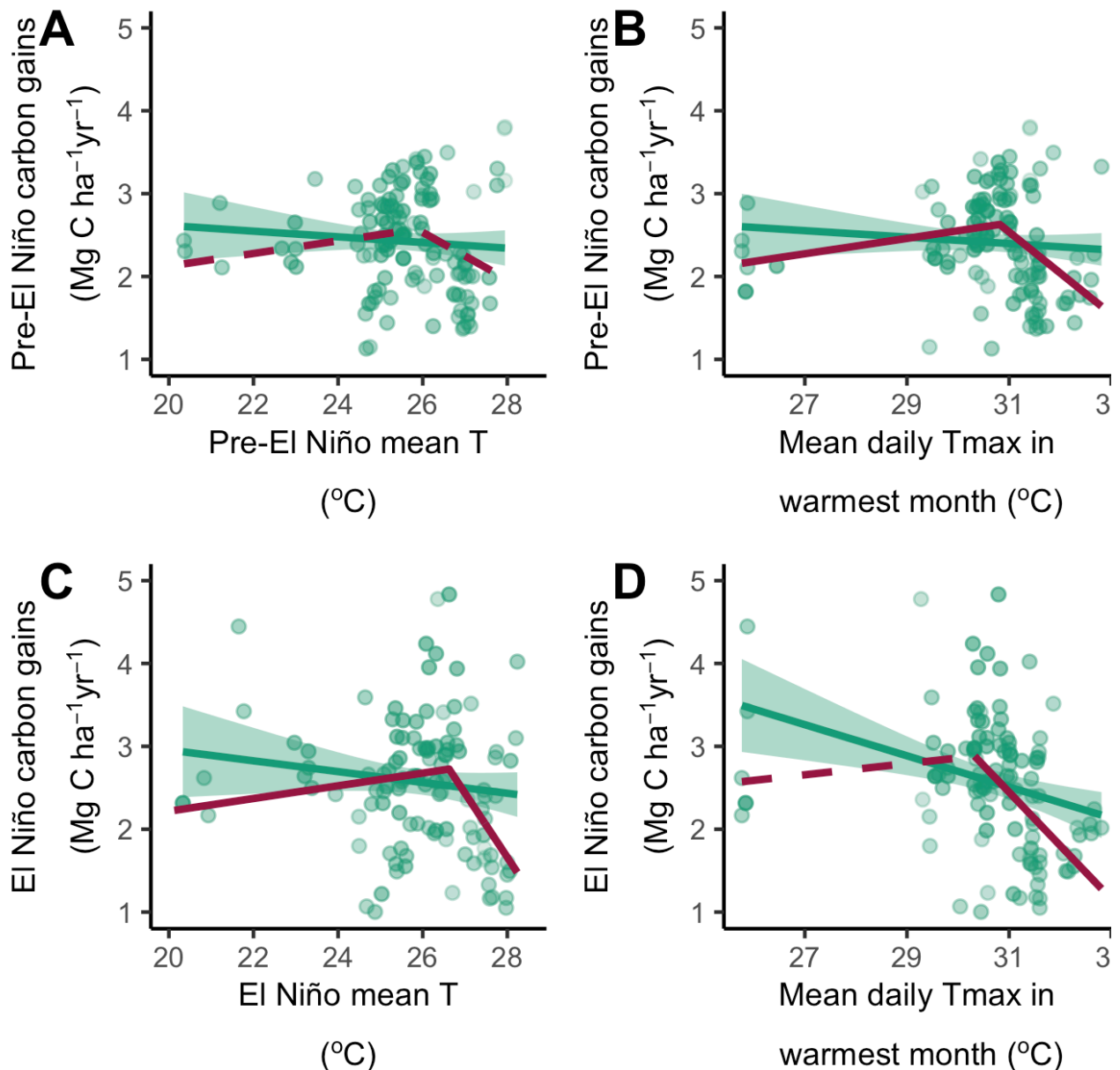


Figure 3.8 | Temperature-productivity thresholds

Temperatures increase productivity to a point, beyond which carbon gains decline with increasing temperatures. Baseline temperature and baseline carbon gains (A), long-term daily maximum temperature (from WorldClim v2) and baseline carbon gains (B), El Niño temperature and El Niño carbon gains (C), and long-term daily maximum temperature and El Niño carbon gains (D). Gains are shown in green, consistent with other figures. Point shading from light to dark denotes greater weighting, with plots and lines of best fit weighted by an empirically derived combination of pre-El Niño plot monitoring length and plot area. Significantly different slopes either side of breakpoint according to Davies' test A; $p < 0.05$,

B: $p < 0.001$, C: $p < 0.01$, D: $p < 0.001$, the linear models before and after the breakpoint are only sometimes significant, solid lines indicate significant linear models A: before breakpoint $p = 0.4$, after breakpoint $p = 0.2$, B: $p < 0.05$, $p < 0.01$, C: $p < 0.0001$, < 0.0001 , D: $p = 0.6$, $p < 0.0001$. Slopes of linear models before and after breakpoint, respectively A: $y = 0.08x + 0.6$, $y = -0.29x + 10$, B: $y = 0.09x - 0.2$, $y = -0.5x + 18$, C: $y = 0.08x + 0.7$, $y = -0.77x + 23$, D: $y = 0.07x + 0.8$, $y = -0.6x + 22$.

Temperature anomalies increase carbon losses from biomass mortality (two-tailed Kendall's Tau, $p < 0.05$, Figure 3.6E). Temperature anomalies have no effect on carbon gains from aboveground woody productivity ($p = 0.99$, Figure 3.6C) and temperature anomalies drive greater losses in net aboveground biomass carbon, but not significantly (linear model is significant $p < 0.05$, but Kendall's Tau is not $p = 0.06$, Figure 3.6A). Relative to pre-El Niño, forests subjected to a $0.5\text{ }^{\circ}\text{C}$ increase in temperature lost $0.6\text{ Mg C ha}^{-1}\text{ yr}^{-1}$ (Figure 3.6A).

Drought anomalies impact carbon losses from biomass mortality such that anomalously drier plots have greater increases in carbon losses (two-tailed Kendall's Tau, $p < 0.001$, Figure 3.6F), but drought anomalies have no significant effect on carbon gains ($p = 0.5$, Figure 3.6D). As drought impacts losses but not gains, net aboveground biomass carbon significantly reduced with drought anomaly over the El Niño i.e. the stronger the MCWD anomaly the more negative the net carbon response ($p < 0.05$, Figure 3.6B). Relative to pre-El Niño, forests subjected to a 100 mm increase in MCWD lost $0.9\text{ Mg C ha}^{-1}\text{ yr}^{-1}$.

Plots with hotter baseline climates pre-El Niño have reductions in carbon gains during the El Niño ($p = 0.05$, Figure 3.7C) and in a multivariate model with both baseline temperature and Δ temperature, baseline temperature has a negative effect on Δ carbon gains and Δ temperature has a positive effect (Figure 3.9). For Δ net carbon, both baseline climate and anomalies have negative effects, thus hotter and drier forests tended to lose more biomass carbon. Plots with stronger baseline water deficits lost more aboveground biomass carbon through mortality ($p < 0.01$, Figure 3.7F) and lost aboveground biomass carbon overall ($p < 0.01$, Figure 3.7B). So, drier plots with stronger dry seasons tended to lose more biomass carbon in the El Niño. There was no threshold effect for drought and carbon losses (pre- El Niño Davies' test $p = 0.4$, El Niño $p = 0.3$) unlike temperature and carbon gains.

The climatically hottest forests are significantly more prone to El Niño depression of carbon gains (Figure 3.7C) and the driest forests are significantly more prone to El Niño enhanced carbon losses from mortality of biomass and decreased recruitment (Figure 3.7F). As a consequence, these drier fringe forests, typically outside the core Amazon

area (Figure 3.2), significantly lost biomass during the El Niño period (Figure 3.7). While Figure 3.7 shows the mean climate of the census monitoring period pre-El Niño, these results also hold when I use a full 30-year climate record at plots. The driest quartile of plots pre-El Niño had significantly lower Δ net carbon (mean carbon losses of driest quartile of plots: $-1.8 \pm 0.6 \text{ Mg C ha}^{-1} \text{ yr}^{-1}$, mean of wettest quartile: $0.1 \pm 0.7 \text{ Mg C ha}^{-1} \text{ yr}^{-1}$, t-test; $p < 0.01$). This was because the driest quartile of plots pre-El Niño had significantly higher Δ carbon losses than the wettest quartile of plots in the El Niño, (mean of driest quartile $1.4 \pm 0.5 \text{ Mg C ha}^{-1} \text{ yr}^{-1}$, mean of wettest quartile $-0.2 \pm 0.3 \text{ Mg C ha}^{-1} \text{ yr}^{-1}$, $p < 0.05$), and no difference in Δ carbon gains ($p = 0.2$). The carbon dynamics of the hottest quartile of plots did not significantly differ from the coldest quartile of plots (Δ net carbon; $p = 0.9$, Δ carbon gains; $p = 0.2$, Δ carbon losses; $p = 0.4$), possibly because the temperature range (-0.5 to $1.2 \text{ }^\circ\text{C}$, $n = 137$) of the plots is much smaller than the MCWD range (-252 to 106 mm). Drier forests lost the most biomass in the 2015-16 El Niño.

Considering temperature and carbon gains relationships for both the pre-El Niño monitoring period (Figure 3.8A) and El Niño interval (Figure 3.8C), with increasing temperature carbon gains increase to a point, beyond which carbon gains decrease. Break-point regressions indicate temperature thresholds of $25.9 \pm 0.5 \text{ }^\circ\text{C}$ (95% CI) mean monthly temperature for the pre-El Niño mean carbon gains, (lines either side of breakpoint have significantly different slopes according to Davies' test, $p < 0.05$, Figure 3.8A), and $26.6 \pm 0.4 \text{ }^\circ\text{C}$ for the carbon gains of the El Niño census interval (Davies' test, $p < 0.01$, Figure 3.8C). Peak carbon gains are approximately $2.75 \text{ Mg C ha}^{-1} \text{ yr}^{-1}$, although both linear models either side of the breakpoint are significant only for the El Niño carbon gains, implying a strong reduction in carbon gains beyond the $\sim 26 \text{ }^\circ\text{C}$ threshold. The breakpoints of the pre-El Niño carbon gains and pre-El Niño mean temperature (Figure 3.8A) and El Niño carbon gains and El Niño mean temperature (Figure 3.8C) are not significantly different ($p = 0.3$), and during the El Niño a greater number of plots have mean annual temperatures beyond the breakpoint than pre-El Niño. These relationships are maintained when computed using mean daily maximum temperature instead of mean monthly temperature; pre-El Niño carbon gains have a breakpoint at $30.8 \pm 0.2 \text{ }^\circ\text{C}$ ($p < 0.001$, Figure 3.8B) and during El Niño carbon gains have a breakpoint at $30.3 \pm 0.3 \text{ }^\circ\text{C}$ ($p < 0.001$, Figure 3.8D), again these are not significantly different breakpoints ($p = 0.3$). Though, in this instance the linear models either side of the break points are both significant only for the pre-El Niño carbon gains. Overall, when considering the 137 plots together, there is no impact of temperature anomaly on carbon gains because reductions

in plots that exceed the breakpoint temperature threshold are compensated by cooler plots where the higher El Niño temperature boosts carbon gains (Figure 3.6).

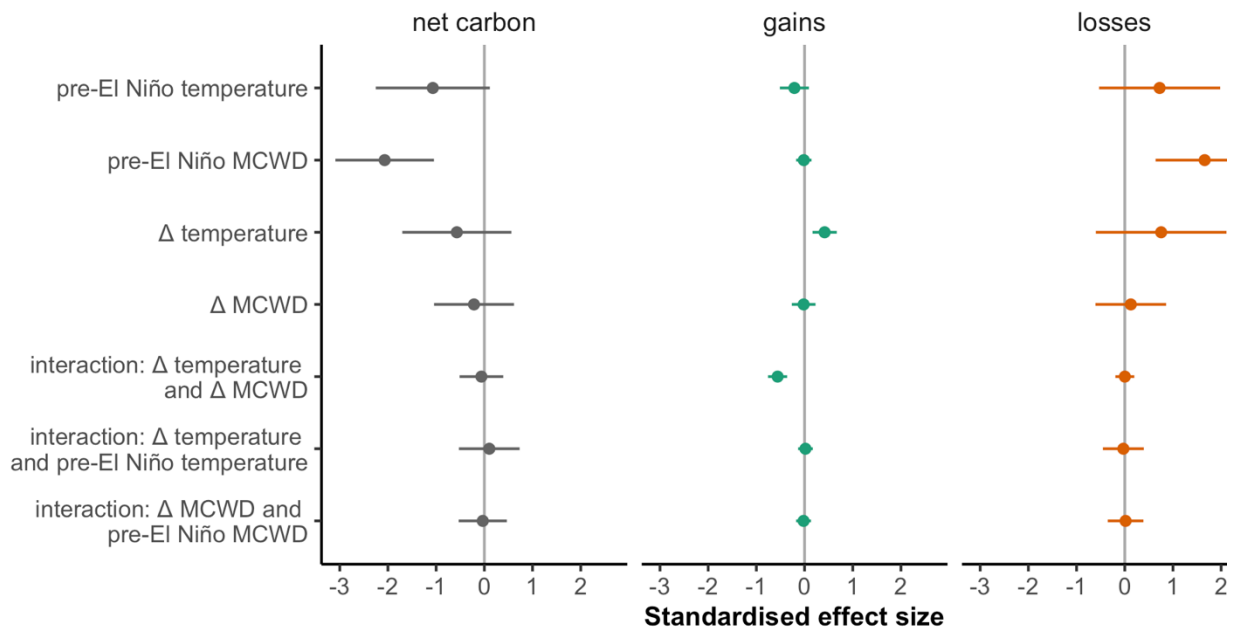


Figure 3.9 | Effect sizes of change in carbon in South American tropical forest plots over the 2015-16 El Niño

Temperature anomalies increased carbon gains, baseline drought increased carbon losses, temperature and drought anomalies interacted to reduce carbon gains where it was both anomalously hot and dry. Points show coefficients from linear models with multi-model inference. Coefficients are standardised so that they represent change in the response variable for one standard deviation change in the explanatory variable. Net change is in grey, gains are in green, losses orange. Error bars show 95 % CIs. The models explained 11 %, 30 % and 8 % of variation in Δ net carbon, Δ carbon gains and Δ carbon losses.

Stem mortality rates increased from the pre-El Niño monitoring period to the El Niño census interval, an increase of $0.6 \pm 0.3 \%$, from 2.1% to 2.8% , (paired t-test, $p < 0.0001$). This occurred in every size class, but especially in the large ($400+$ mm diameter: $1.2 \pm 0.6 \%$ from 2.4% to 3.2% , $p < 0.0001$) and medium trees ($200-399$ mm diameter: $0.9 \pm 0.3 \%$ from 1.7% to 2.7% , $p < 0.0001$), more so than in small trees ($100-199$ mm diameter: $0.5 \pm 0.4 \%$ from 2.5% to 3.0% , $p < 0.05$). There are many more trees in this smallest size class so even though the proportional change is smaller, the absolute number of dead trees is larger. There was no significant change in the size of dying trees overall (median diameter change pre-El Niño to El Niño $+1.0 \pm 5.9$ mm, paired t-test, $p = 0.2$), nor for each size class ($100-199$ mm diameter; $+0.5 \pm 1.5$ mm, $p = 0.7$; $200-399$ mm diameter, $+2.4 \pm 3.0$ mm, $p = 0.5$; $400+$ mm diameter, $+3.6 \pm 5.9$ mm, $p = 0.2$). So, during the El Niño stem mortality rates increased for all trees, with no compelling evidence of size selective mortality.

The size of live trees also did not change overall (median diameter change pre-El Niño to El Niño $+3.9 \pm 1.7$ mm, $p = 0.2$), but live trees in the larger size class increased in diameter ($400+$ mm diameter; $+20.2 \pm 17.3$, $p < 0.05$, $200-399$ mm diameter, $+4.6 \pm 4.5$ mm, $p = 0.05$), while the smallest size class did not change (median diameter, $100-199$ mm diameter; $+1.8 \pm 0.5$, $p = 0.2$). The wood density of dying trees did not change overall (median wood density -0.002 ± 0.02 g cm⁻³, $p = 0.8$), but increased for dying trees in the largest size class ($400+$ mm diameter; $+0.04 \pm 0.04$ g cm⁻³, $p < 0.05$) and did not change for trees in the smaller size class ($100-199$ mm diameter; -0.0004 ± 0.02 g cm⁻³, $p = 0.9$, $200-399$ mm diameter; $+0.006 \pm 0.01$ g cm⁻³, $p = 0.8$). Thus, more higher wood density trees died in the largest size class, potentially due to hydraulic constraints of height as these large trees with high wood density are likely to be the tallest trees in the plot. There was no change in the median wood density of live trees overall (-0.005 ± 0.03 g cm⁻³, $p = 0.5$), nor for trees of any size class ($100-199$ mm diameter; -0.002 ± 0.02 g cm⁻³, $p = 0.8$; $200-399$ mm diameter; -0.004 ± 0.03 g cm⁻³, $p = 0.7$; $400+$ mm diameter, $+0.02 \pm 0.007$ g cm⁻³, $p = 0.2$). Growth rates declined significantly in the El Niño, and median growth rates were significantly lower for all size classes ($100-199$ mm diameter; -0.15 ± 0.11 mm yr⁻¹, paired t-test, $p < 0.05$; $200-399$ mm diameter, -0.20 ± 0.15 mm yr⁻¹, $p < 0.05$; $400+$ mm diameter, -0.25 ± 0.22 mm yr⁻¹, $p < 0.05$) so trees grew more slowly, but it was not great enough to translate into significantly lower biomass gains overall. These size class analyses indicate that across the 137 plots, on average, trees of all sizes were detrimentally impacted by the El Niño and there is no evidence of predominant large tree mortality as seen in previous drought studies.

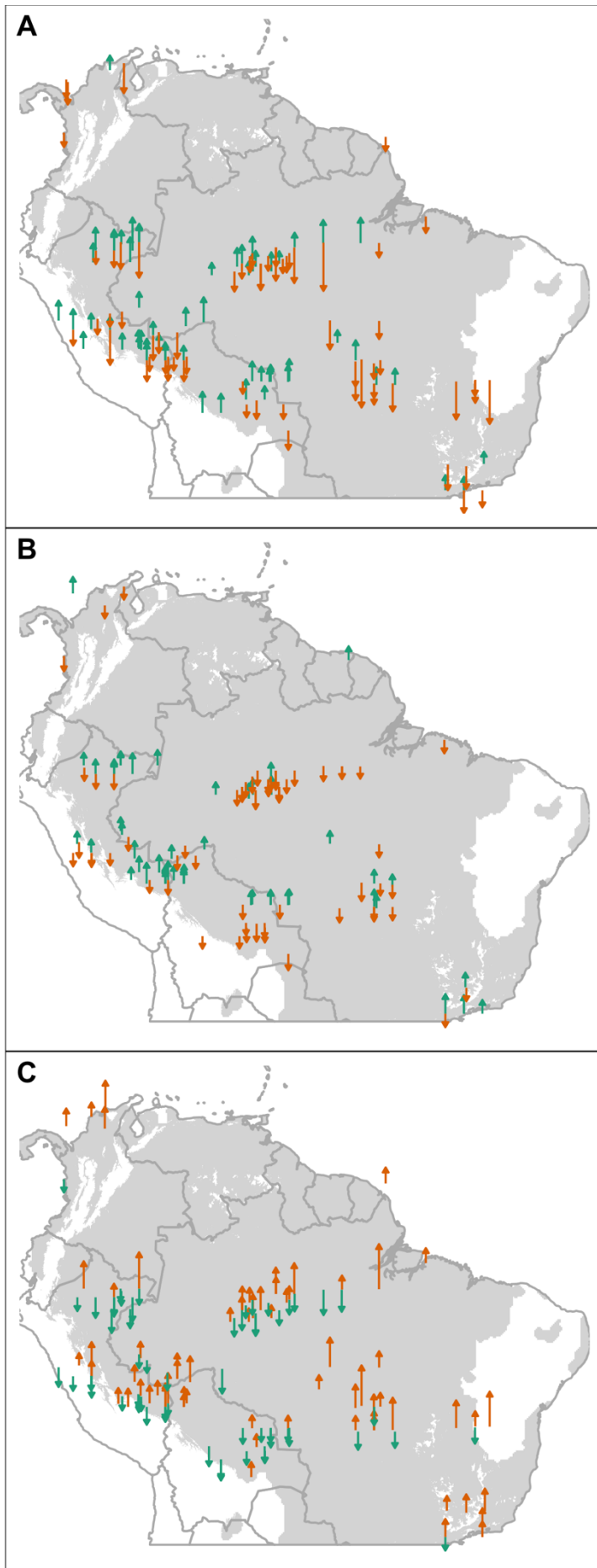


Figure 3.10 | Aboveground carbon change in neotropical moist forests

Negative impacts of the El Niño predominate in the central and southern Amazon. Arrows represent the direction of measured change and approximate location of each plot. Orange arrows indicate negative effects on biomass stocks (for example, decreasing net change, increasing losses) and green arrows indicate positive effects on biomass stocks (for example, increasing productivity). (A) Δ net carbon, El Niño – pre-El Niño aboveground net carbon. (B) Δ carbon gains, El Niño – pre-El Niño aboveground carbon gains. (C) Δ carbon losses, El Niño – pre-El Niño aboveground carbon losses. There are fewer arrows in (B) than in the other two panels as carbon gains are restricted to plots that were measured within one year of the maximum climate anomaly, so to be included they must have been measured before February 2017.

3.4 Discussion

The 2015-16 El Niño caused hotter temperatures across the neotropics and anomalous drought particularly in east Amazonia, while some locations were wetter than average. The record temperatures and drought led to increased carbon losses from biomass mortality, particularly in forests where the long-term climate was already relatively hot or dry (Figure 3.7). The results show clearly that the long-term climate conditions of forests strongly modified their biomass responses to the climate anomaly itself (Figure 3.7, Figure 3.8, Figure 3.9) and that there is a compounding effect of drought such that both baseline drought and drought anomaly increase biomass mortality. Baseline temperatures dictate forest response to temperature anomaly. Temperature switching occurs with stable or increasing temperatures increasing productivity in cooler forests and beyond a temperature threshold productivity declines with increasing temperatures in hotter forests. With widespread heat and variable drought, the 2015-16 El Niño was a good natural experiment with the opportunity to parse the effects of temperature and drought.

The 2015-16 El Niño was the hottest drought on record, with record low precipitation, and the drought was also widespread with 4.2 million km² of in Amazonia exposed to dry season anomalies that exceeded -25 mm. Compared to the very strong El Niño events of 1982-83 and 1997-98 and the major droughts of 2005 and 2010, the 2015-16 El Niño was hotter, had lower precipitation, slightly more negative MCWD (Figure 3.1, Table 3.1), and a greater area of drought (Figure 3.9). Several other studies also point to the 2015-16 El Niño drought as being the most extreme drought across South America for at least 50 years (Jiménez-Muñoz et al. 2016, Panisset et al. 2018). The 2015-16 El Niño drought was widespread according to observations of river discharge and terrestrial water storage (Yang et al. 2018a) and remotely sensed precipitation (Panisset et al. 2018), with some indication that the strongest drought in 2015-16 was limited to the eastern Amazon (Jiménez-Muñoz et al. 2016). The spatial pattern of precipitation anomalies in the 2015-16 El Niño were remarkably similar to CMIP5 RCP8.5 projected precipitation changes for 2100 (Duffy et al. 2015).

The 2015-16 El Niño climate anomaly reduced the net biomass sink of South American tropical forests by 129 % over the average 2.5-year census interval, a similar impact to previous (2005, 2010) drought-responses (Figure 3.10C). This 129 % loss translates to a reduction in net aboveground biomass of 0.7 Mg C ha⁻¹ yr⁻¹, indistinguishable from the reduction of 0.8 Mg C ha⁻¹ yr⁻¹ in the 2010 drought (Feldpausch et al. 2016), and the reduction of 0.7 Mg C ha⁻¹ yr⁻¹ in the 2005 drought, (Phillips et al.

2009), (Figure 3.5B). Measurements of the live carbon sink highlight a reduction in the live carbon biomass sink due to mortality, but these carbon losses will not enter the atmosphere immediately as carbon moves to the necromass pool and is decomposed over time. Soil carbon fluxes to the atmosphere in intact tropical forests are typically lower during drought conditions (Davidson et al. 2000, Rubio and Detto 2017).

The net exchange from all processes including fire and land use change (Palmer et al. 2019) suggest that South America remained a net carbon sink (0.26 Pg C) in 2015 and was a small net source of 0.2 Pg C in 2016 (Palmer et al. 2019), so about zero over the 2015-16 El Niño. In this chapter South American tropical forests were found to be a sink prior to the El Niño and a small source during the El Niño. Liu et al. 2017 suggest that El Niño impacts on South American forests dominated the global carbon cycle. Compared to the La Niña year of 2011, in 2015 South American forests were a source of 0.9 Pg C due to reduced productivity or possibly higher respiration costs during the El Niño (Liu et al. 2017). This is much smaller than the impacts detected in this chapter and whereas Liu et al. attribute the decline in growth to lower precipitation, results in this chapter indicate that declines in growth are linked to temperature, potentially highlighting problems with their underlying model which calculates respiration as a residual term. The 2015-16 El Niño affected trees of all sizes, rather than a disproportionate negative impact on large trees according to LiDAR (Leitold et al. 2018) and consistent with the size class analysis in this chapter that found growth was suppressed and mortality rates increased across size classes.

Relative to the pre-El Niño monitoring period, a total impact of -1.44 Pg C (-2.26 to -0.61) is estimated by scaling the mean net carbon impact (-0.7 ± 0.4 Mg C ha⁻¹ yr⁻¹) and confidence intervals by the total droughted area ($\sim 8.2 \times 10^8$ ha across South America, $\sim 4.2 \times 10^8$ ha in Amazonia), and census interval (2.5 years), using the same methods as (Phillips et al. 2009, Feldpausch et al. 2016). This is similar to the estimated total impacts of the 2005 drought, -1.21 Pg C (-2.01 to -0.57), and -1.07 Pg C (-2.04 to -0.24) in the 2010 drought (Phillips et al. 2009, Feldpausch et al. 2016). The estimated impact for 2015-16 may be conservative however because no plots monitored impacts at the drought epicentre. Carbon losses have been extremely high at the epicentre of droughts (Yang et al. 2018b) (Amazon 2005, lost 2.4 ± 1.8 Mg C ha⁻¹) so the location of plots within the drought space can dictate the strength of the forest response captured. Nevertheless, while there were only 55 plots sampled for the 2005 drought, for 2015-16 a total of 137

plots were available, so this increase of more than 100 % in sample size provides confidence in the robustness of the 2015-16 analysis.

On-the-ground analysis of long-term forest plots revealed that high temperature anomalies increased biomass carbon losses (Figure 3.6E). While tropical forests in South America are known to be temperature sensitive to long-term temperatures (Hubau et al. 2020, Sullivan et al. 2020), previous Amazon analyses did not examine the extent to which the impacts of anomalies interacted with climate baselines, and whether or not there were clear thresholds in terms of forest responses to climate. Biomass mortality has never-before been linked to such a short 2.5-year temperature anomaly in any previous studies of short-term climate anomalies in South America, nor in Africa in Chapter 2. In a warming world, sensitivity to rising temperatures means that these forests are vulnerable. There is no significant change in productivity with temperature overall (Figure 3.6C), but this masks the fact that in cooler sites productivity actually increased while in hotter sites productivity was suppressed, so that there is an interaction between forests' long-term climatologies and the temperature response of their short-term biomass dynamics. This switch in the response of neotropical forest productivity during the 2015-16 anomaly contingent on baseline temperature is mechanistically consistent with findings from two other analyses which use pan-tropical plot data (Hubau et al. 2020, Sullivan et al. 2020). Hotter tropical forests have lower carbon gains.

In South American tropical forests analysed in this chapter, the drier the long-term climate regime the greater the impact of a given increase of MCWD, and the hotter the long-term climate the lower the productivity and the higher the mortality. Furthermore, comparing the extreme quartiles, showed that drier plots had greater carbon losses and more negative net carbon than the wetter plots. Stronger MCWD anomalies had the greatest effects in forests with drier baseline climates. In these environments where water is so limiting the expectation might be for drought-tolerant species to be abundant (Engelbrecht et al. 2007, Esquivel-Muelbert et al. 2016). However, results point toward those forests which are climatologically close to the limits of the closed canopy tropical biome being more vulnerable to climate anomaly, as they are drier and possibly because they are closer to a potential temperature threshold. The climate changes where it is already hot and dry are driving biomass changes greater than the adaptive capacity of these ecosystems.

Temperature thresholds indicate that baseline temperatures are very important for drought responses in South America. Leaf and canopy level measurements from Tapajos,

Brazil have suggested that South American tropical forests might be close to a high temperature threshold (Doughty and Goulden 2008) as net ecosystem exchange declined when air temperatures were above approximately 28 °C. In this chapter, analysis using baseline mean monthly temperatures also suggest the existence of a productivity-temperature threshold, but that it might be lower, 25.5-27.0 °C (Figure 3.8 panels A and C). In terms of maximum rather than mean temperatures, Sullivan et al. (2020) derived a threshold for mean long-term daily maximum temperatures of 31.7-32.6 °C above which long-term carbon stocks decline. In this chapter, analysing quasi-annual departures in productivity, I find that short-term woody productivity declines above mean daily maximum temperatures of 30.0-31.0 °C (Figure 3.8 panels B and C). This chapter looks at the adaptability of the *in situ* species, so temperature thresholds are expected to be lower than the Sullivan et al. (2020) analysis which includes species composition differences. The temperature thresholds in this analysis are not statistically distinguishable between pre-El Niño and El Niño, but in the El Niño higher temperatures mean more plots exist beyond the threshold.

The nature of the 2015-16 El Niño climate anomaly in South America meant it was a natural experiment with the potential to test the vulnerability or resistance of tropical forests to drought and heat. Temperatures were higher everywhere, but drought varied, and some places were wetter. Analyses presented in this chapter suggest that South American tropical forests are vulnerable to temperature anomalies due to increased carbon losses and reduced carbon gains and are vulnerable to drought anomalies due to increased carbon losses. While measuring El Niño impacts from the ground up provides unique insight, each drought has its own climate and spatial signature and each drought impacts plots which have different recent climate and disturbance histories, so caution is warranted when comparing drought resistance at different times. Nevertheless, this chapter indicates a consistent drought response with no indications of either drought-resistance having increased over time due to the vulnerable trees already dying, species adaptation or shifts in community composition, or drought resistance having decreased with greater impacts of more recent droughts, despite repeated droughts. The committed carbon impacts of the 2005, 2010 and 2015-16 droughts total 3.72 Pg C. The Amazon carbon sink strength is approximately 0.45 Pg C yr⁻¹ (for the years 2000-2010 (Hubau et al. 2020)), so a decade of the Amazon carbon sink (4.5 Pg C) is almost completely wiped out by the impact of three severe droughts. This chapter in sum presents strong evidence of the vulnerability of South American tropical forests, particularly given the ongoing increase in global temperatures, since higher temperatures increased carbon losses and

restricted carbon gains, and it was the hotter drier forests that were the most impacted by the 2015-16 climate anomaly.

Chapter 4

Contrasting responses of African and South American tropical forests to an Extreme Climate Anomaly

Abstract

Intact tropical forests are an important component of the global carbon cycle as they uptake and store carbon from the atmosphere and have been functioning as a carbon sink for decades. Evidence suggests that while they are still carbon sinks, per unit area levels in both African and South American tropical carbon sinks have recently saturated. Superimposed on these trends, in hot or dry conditions, such as El Niño events, the carbon sink of intact tropical forests can be compromised. However, African and South American tropical forests may respond differently to these extreme climate anomalies because of systematic differences: African forests typically exist in both drier and cooler climates than South American forests, and African forests tend to be less dynamic, more dominated by a smaller number of large trees and are more carbon-dense than South American forests, also containing fewer species. Here climate data is combined with measurements from 237 long-term plots to compare El Niño responses of these fundamentally different forests on two continents. Higher temperature anomalies increased carbon losses, which is worrying given rising global temperatures. The response of carbon losses and net carbon to temperature anomaly were universal and could be predicted by the response of the other continent. Stronger drought anomalies also increased carbon losses, and per unit increase in drought anomaly, the increase in carbon loss was the same for both continents, however, South American tropical forests lose more carbon given the same drought anomaly. These results provide further evidence to suggest that South American tropical forests are vulnerable to both increasing temperatures and drought which drive increasing tree mortality rates. South American tropical forests, compared to African tropical forests, have species diversity but not drought

resistance, whereas of African tropical forest appear to have greater drought-resistance in El Niño climate anomalies, possibly due to their biogeographic history and current species composition.

4.1 Introduction

The tropical carbon sink is already vulnerable to high temperatures and periodic droughts, with its long-term future threatened by anthropogenic climate change (Hubau et al. 2020). The carbon sink is vulnerable because high temperatures and drought can cause hydraulic failure (Rowland et al. 2015, Choat et al. 2018) or carbon starvation (McDowell et al. 2018), killing trees. These same factors can also lead to reduced tree growth (Feldpausch et al. 2016). With anthropogenic temperature increases it is very likely there will be greater impacts of climate anomalies on tropical forests as warming increases vapour pressure deficits (Trenberth et al. 2014), and in combination with droughts, could cause widespread suppression of growth and increased tree mortality. One method of reducing the uncertainty in the magnitude of the future carbon sink is to assess how tropical forests respond to extreme climate anomalies in the shorter-term.

With a hotter baseline, and warming more quickly (Hubau et al. 2020), the South American tropical carbon sink might be most vulnerable to climate anomaly. African tropical forests are generally drier (Malhi and Wright 2004), cooler because they exist at higher elevations (Banin et al. 2012, Hubau et al. 2020), and have greater seasonal water deficits than forests in South America (Hubau et al. 2020). The forests of the two continents are connected by hydrology, and the Amazon basin, measured by discharge from the Amazon River, is usually wetter when the Congo basin, measured by discharge from the Congo River, is drier and vice versa (Eltahir et al. 2004). Seasonality is intensifying in both continents, with the intensity of the Amazon wet season increasing (Gloor et al. 2013) and the length of the dry season increasing in the Amazon (Fu et al. 2013) and the Congo (Jiang et al. 2019). The two continents' forests have different baseline climates so may respond differently to a common climate anomaly perturbation.

The tree species that compose the forests of Amazonia and Africa are different, which may alter forest responses to climate anomalies. Critically, the neotropics and Afrotropics also have contrasting long-term climate histories. South American tropical forests have persisted through glacial and interglacial periods with minimal changes in species and abundance according to pollen records (Dick et al. 2013, Nascimento et al. 2019). On the other hand, in glacial periods African tropical forests contracted to a small

number of refugia, as most of the continent was too dry for tropical forest species to persist. Hence the species-pool in African tropical forests has been filtered (deMenocal 2004), perhaps leading to the loss of the wet-adapted species and the adaptation and proliferation of the dry-adapted species. While South American forests are generally more diverse per unit area (Sullivan et al. 2017) and have more species in total (Slik et al. 2018) than African forests, for forests with similar dry season lengths, diversity is equivalent for African and South American tropical forests, and African forests may even be more diverse (Parmentier et al. 2007).

There are also continental differences in terms of forest structure. African tropical forests have fewer trees per hectare than forests in South America, with approximately 425 trees ha⁻¹ greater than 10 cm diameter in African forests versus 600 ha⁻¹ in Amazonian forests (Banin et al. 2012, Lewis et al. 2013, Hubau et al. 2020). African tropical forests are more dominated by large trees (Feldpausch et al. 2012, Lewis et al. 2013, Enquist et al. 2020) and for this reason carbon density is greater in Africa (Sullivan et al. 2017) and these large trees may buffer African tropical forests to climate change (Enquist et al. 2020). Carbon residence times are also longer in Africa (Galbraith et al. 2013, Hubau et al. 2020) where forests have lower carbon gains from recruitment, lower stem mortality and slower stem turnover. So, South American forests are more dynamic with faster turnover, higher recruitment and mortality.

Recent drought history of the continent may also differ. There have been at least two other severe droughts in the Amazon in the last twenty years. These droughts increased aboveground biomass mortality in 2005 (Phillips et al. 2009) and 2010, and in 2010 decreased productivity (Feldpausch et al. 2016); on both occasions pausing the intact forest carbon sink of the Amazon. Analysis of South American tropical forests and the 2015-16 El Niño in Chapter 3 indicates that South American forests are sensitive to both temperature and drought anomalies, with climate anomalies increasing carbon losses and reducing carbon gains. African tropical forests have experienced long-term decreases in precipitation and soil moisture since the 1980s, with dry season lengthening in the 2000s (Jiang et al. 2019). The abundance of deciduous species has increased in tropical forests in Ghana due to long-term drought in West Africa (Fauset et al. 2012, Aguirre-Gutiérrez et al. 2019). Analysis of the impacts of the 2015-16 El Niño climate anomaly in Chapter 2 indicate that African forests are sensitive to drought anomalies, but not to temperature anomalies, so African tropical forests may be more resistant to and less impacted by climate anomalies than South American forests.

Given the differences in baseline climate, long-term climate history, forest ecology and drought history, one might expect responses to the El Niño to differ between the two continents. On the other hand, it can be hypothesised that both continents' forests will have similar responses to environmental change because the physiological responses of photosynthesis and respiration to higher temperatures and periodic water shortages may be similar for all tropical rainforest trees. Therefore, it is imperative to compare the two continents. Assessments should also be per unit of temperature or drought increase, should consider the different baseline climate conditions and should report relative changes given the differences in aboveground biomass and other parameters between the two continents. Previous chapters in this thesis have indicated drought anomalies increase carbon losses of tropical forests in Africa and South America but point towards South American vulnerability and African tropical forest resistance to temperature anomalies. In this chapter whether these El Niño impacts differ by continent is analysed, the climate drivers are parsed and whether continent-specific responses are a result of the climate anomaly, baseline climate, forest structure or species composition is examined. Therefore, climate data is combined with measurements from long-term inventory plots across two continents to address the following questions: (1) Did tropical forests experience unprecedented temperature anomalies in the 2015-16 El Niño and does this vary by continent? (2) Did tropical forests experience unprecedented drought in the 2015-16 El Niño and does this vary by continent? (3) What were the overall impacts on the monitored old-growth structurally intact tropical forests and does this vary by continent? (4) Which climate anomalies drove forest responses to the 2015-16 El Niño and does this vary by continent? and (5) Were drier forests more resistant or more vulnerable to the climate anomaly?

4.2 Methods

Methods as in Chapter 2 apart from changes or additional methods detailed here.

4.2.1 Climate Data

Methods for the temperature record match Chapter 3. So, the temperature record for South America is identical to Chapter 3, and for comparison, in this chapter the ERA5 and CRU ts.4.03 temperature products are also used for Africa. Thus, the temperature record for Africa slightly differs from Chapter 2. The ERA5 product has higher spatial resolution than ERA-Interim, and the CRU product is a newer version of the same product. For analysis the El Niño year is May-April.

4.2.2 Plot Data Collection and Analysis

Long-term inventory plots were censused using standard RAINFOR methodology (Phillips et al. 2010a). All permanent sample plots used in the analysis are located in lowland, closed canopy, old-growth, structurally intact tropical forests, had been censused at least twice prior to the 2015-16 El Niño event, and were censused once afterwards. The 237 plots meeting these criteria are distributed across 88 distinct clusters in seven countries on two continents: Bolivia, Brazil, Colombia, French Guiana, Guyana, Peru, Venezuela, Cameroon, Democratic Republic of the Congo, Gabon, Ghana, Liberia and Republic of the Congo. To support temporal consistency among plots and avoid potential impacts of the 1982-83 El Niño, only censuses from 1984 onwards are included. Median plot size is 1 ha, mean 0.96 ha; mean initial census is October 2003, mean pre-El Niño census is July 2014, and mean post-El Niño census is April 2017. The mean pre-El Niño monitoring length was 10.8 years and the mean length of the El Niño interval was 2.75 years.

In all analyses the plots are weighted because larger and longer monitored plots are likely better estimates of carbon gains and losses. Using the same approach as in Chapters 2 and 3, but analysing the combined Africa and South America dataset, an empirically estimated weighting is used that combines plot area and pre-El Niño monitoring length. Residuals from linear models are related to plot area and to pre-El Niño monitoring length and the necessary root transformations are chosen to remove the pattern in the residuals. Selected weights for pooled data from both continents were: Δ net carbon, $\text{Monitoring length}^{1/3} + \text{Area}^{1/2} - 1$; Δ carbon gains, $\text{Monitoring length}^{1/3} + \text{Area}^{1/6} - 1$; Δ carbon losses, $\text{Monitoring length}^{1/3} + \text{Area}^{1/4} - 1$; Δ net stems, $\text{Monitoring length}^{1/3} + \text{Area}^{1/2} - 1$; Δ recruitment no weighting and Δ stem mortality, $\text{Area}^{1/6}$.

The data from both continents was pooled totalling 237 plots, allowing extra statistical power and a greater range of baseline climate, drought and temperature change during the El Niño. Analytical methods are described in Chapter 2 and Chapter 3. Here, in Chapter 4, linear models were fitted to the pooled dataset i.e. all 237 plots from two continents. Analysis of covariance was used to test whether continent regression lines differed in slope or intercept (McDonald 2014). Analysis of covariance tests two null hypotheses: (1) that the slopes of the regression lines are equal and (2) that the intercepts of the regression lines are the same. I used the Anova function and Type II approach from the R package car (Fox et al. 2020). I tested for the slope interaction first, and only if the slope was not significant did I test for different intercepts. The best model is selected by

Anova and plotted, and if the best model includes a continent interaction then a blue line is plotted for Africa and a red line for South America.

4.3 Results

Tropical forests on both continents were hotter in the 2015-16 El Niño with variable drought. Temperatures in the 2015-16 El Niño year increased by a mean of 0.8 ± 0.0 °C across African and South American tropical forests, compared to the decade prior. South American tropical forests had significantly hotter temperature anomalies as there was a significant difference between the temperature anomalies of the two continents, a mean of 0.6 °C, in African tropical forests and 0.8 °C in South American tropical forests, a difference of 0.2 ± 0.0 °C (t-test, $p < 0.0001$). Precipitation in the 2015-16 El Niño year decreased by a mean of -93 ± 0.1 mm yr⁻¹ across the two continents, compared to the decade prior. South American tropical forests had significantly greater precipitation anomalies as precipitation declined by 121 mm yr⁻¹ in South American tropical forests and by just 16 mm yr⁻¹ in African tropical forests, a difference of 104 ± 9 mm ($p < 0.0001$). Maximum cumulative water deficits, MCWD, in the 2015-16 El Niño year decreased by a mean of 39 ± 0.4 mm across the two continents, compared to the decade prior. South American forests also had significantly more negative MCWD anomalies, with a mean decrease of 41 mm in South America and 33 mm in Africa, a difference of 8 ± 3 mm ($p < 0.0001$). So, South American tropical forests had greater temperature and drought anomalies in the 2015-16 El Niño.

Considering the 237 forest plots monitored over the 2015-16 El Niño, compared to the monitoring period pre-El Niño, the South American ($n=137$) plots warmed significantly more than African ($n=100$) plots; mean temperature change in South America $+0.47 \pm 0.05$ °C, Africa $+0.34 \pm 0.03$ °C; (t-test, $p < 0.001$). Forest plots in South America had significantly greater precipitation decreases, a mean precipitation change of 176 ± 48 mm yr⁻¹; Africa -46 ± 34 mm yr⁻¹ ($p < 0.0001$). MCWD decreases were significantly less in South America than in Africa; mean MCWD change in South America -44 ± 12 mm; Africa -99 ± 12 mm ($p < 0.0001$), because the African plots cover the core of the closed canopy tropical forest biome and the main droughted area, whereas the main droughted area was not sampled in South America in 2015-16. The range of climate anomalies at plots also differs; African plots are warming but by a narrow range of $0 - 0.6$ °C whereas South American plots are warming by twice that range, $0 - 1.2$ °C. However, the range of plot precipitation anomalies is similar for South America (-864 to $+493$ mm yr⁻¹) and Africa (-

847 to +277 mm yr⁻¹). Plot MCWD anomalies show all African plots to be drier in the El Niño (Δ MCWD -217 to -3 mm), whereas the range is 61% larger in South American plots due to a number of plots wetting over the El Niño (Δ MCWD -252 to +106 mm).

Combining the plot data from both continents shows that over the El Niño census interval (average July 2014 to April 2017), compared to the prior period over which the plots were monitored (mean 10.8 years), the El Niño period was hotter by a mean of 0.41 ± 0.04 °C, had lower rainfall by 120 ± 32 mm yr⁻¹ and had stronger drought, with MCWD lower by 67 ± 9 mm. There are no significant interactions of continent with climate. Linear models are significant for the pooled data for all 237 plots for climate anomaly compared to baseline climate (Figure 4.1), when comparing climate anomalies (Figure 4.2) and when comparing baseline climate (Figure 4.3).

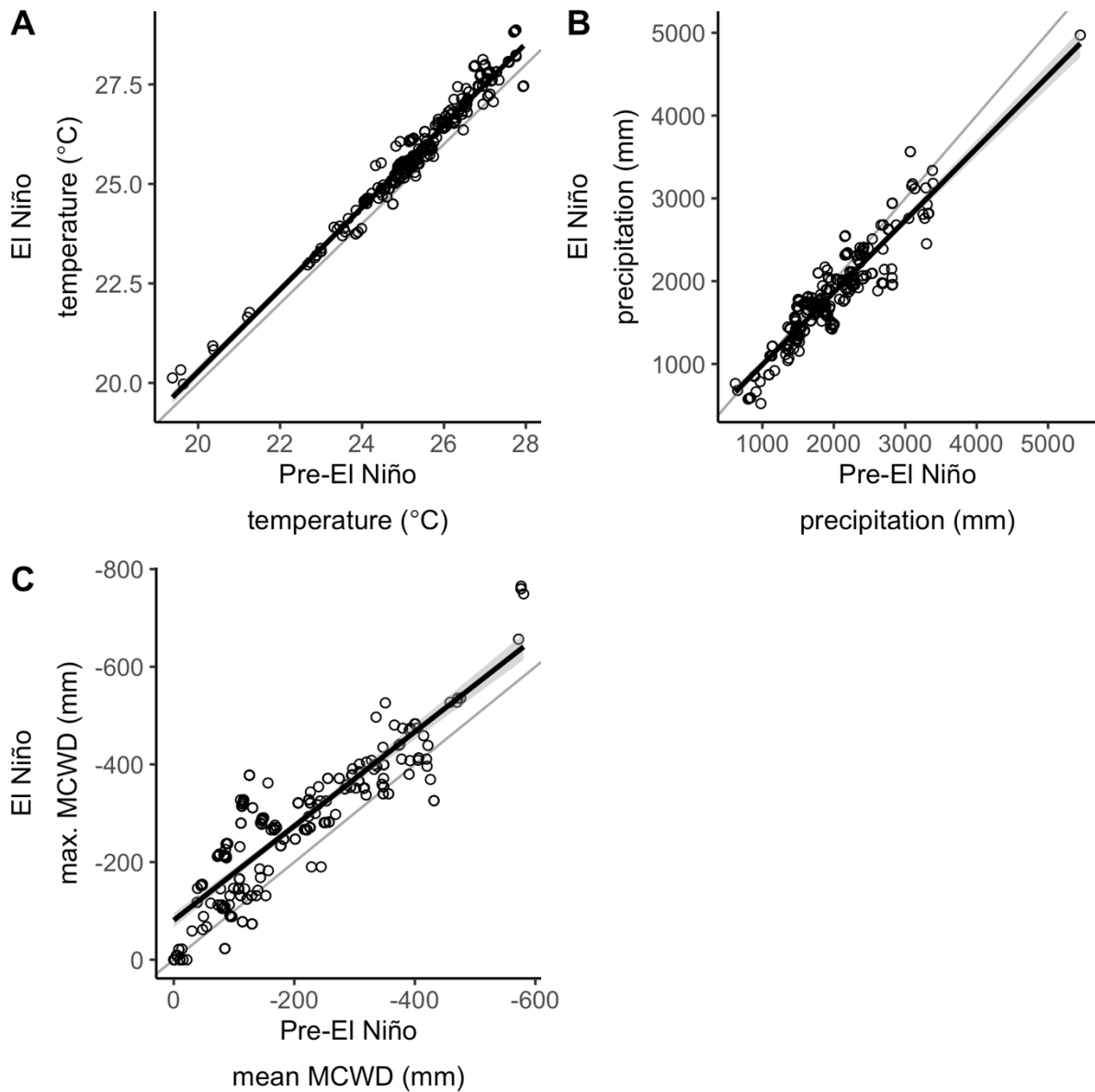


Figure 4.1 | Climate anomalies of 237 long-term forest plots

All plots warmed and dried by approximately the same amount in the 2015-16 El Niño. Plot census interval pre-El Niño and El Niño temperature (A), plot census interval monthly precipitation (B), and plot census interval maximum cumulative water deficit MCWD (C). Pre-El Niño and El Niño are defined by plot census dates. Black lines indicate significant linear models (A; $p < 0.0001$, B; $p < 0.0001$, C: $p < 0.0001$), grey lines indicate 1:1 relationship. A: $y = 1.03x - 0.33$, B: $y = 0.87x + 10$, C: $y = 0.96x - 81$.

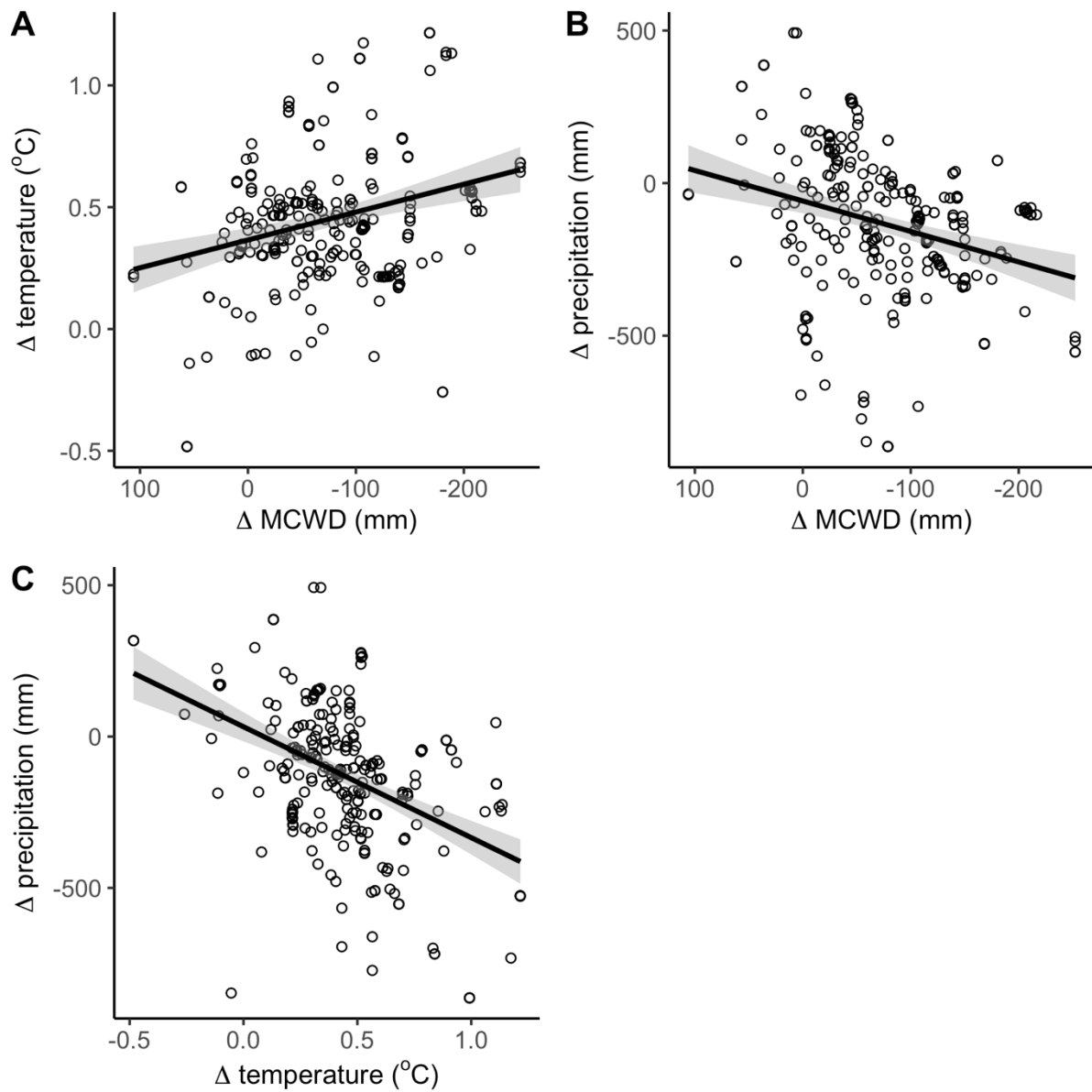


Figure 4.2 | El Niño climate anomalies at 237 plots

Plots with drier climate anomalies were also hotter in the 2015-16 El Niño. Solid lines indicate significant linear models, $p < 0.05$. A: $y = 0.001x + 0.37$, $p < 0.0001$, B: $y = -0.08x - 58$, $p < 0.0001$, C: $y = -31x + 36$, $p < 0.0001$.

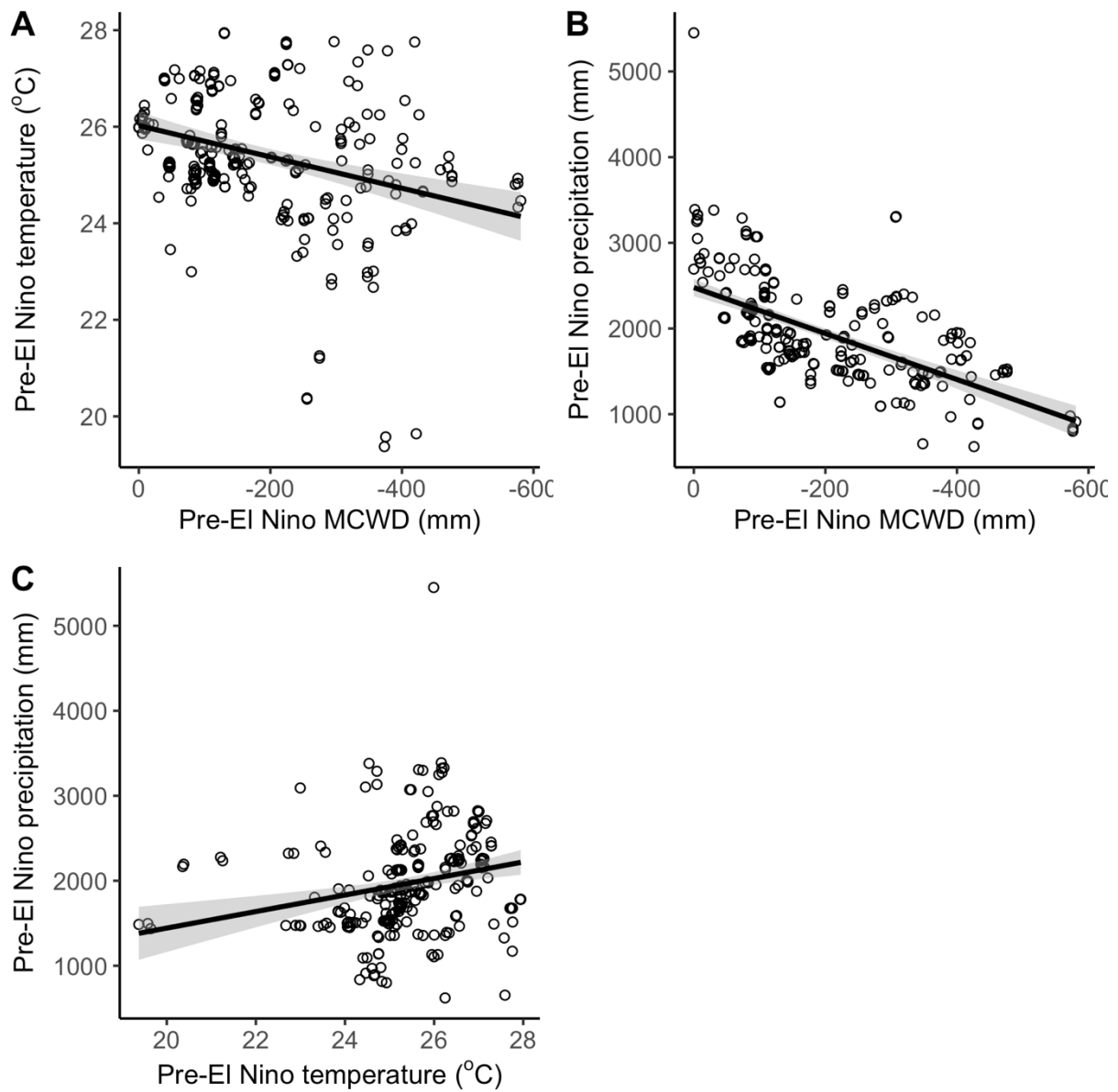


Figure 4.3 | Mean pre-EI Niño climate at 237 plots

Drier plots tend to be cooler. Solid lines indicate significant linear models, $p < 0.05$. $n = 237$ plots. A: $y = -0.003x + 26$, $p < 0.0001$, B: $y = -0.22x + 2478$, $p < 0.0001$, C: $y = 8.1x - 503$, $p < 0.0001$.

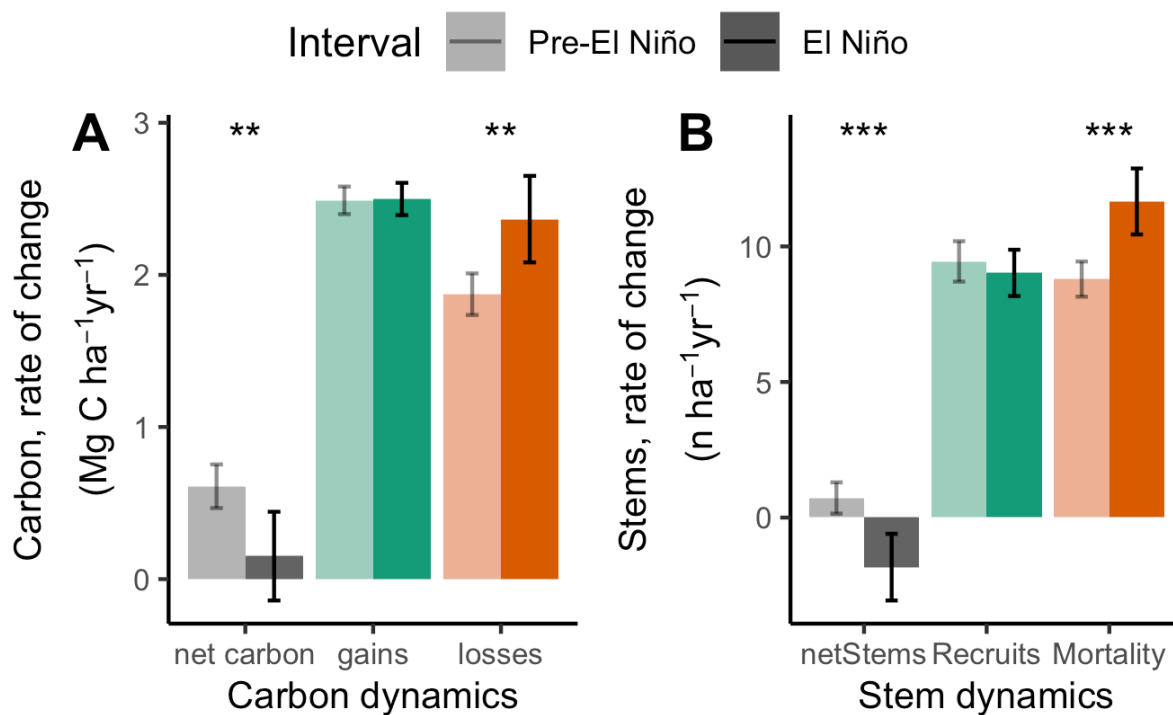


Figure 4.4 | Carbon (A) and stem dynamics (B), pre- (lighter shading) and during the 2015-16 El Niño

Carbon losses significantly increase from the pre-El Niño monitoring period to the El Niño census interval, reducing net carbon uptake. Stem mortality also significantly increases, reducing net stems. Pre- and El Niño carbon (A) and stems (B). Lighter shading is pre-El Niño and darker shading is during the El Niño. $n=237$ plots and error bars represent 95% confidence intervals. Significant differences are defined by paired t-tests with ** indicating $p < 0.01$ and *** indicating $p < 0.001$.

For the 237 plots combined there was a significant decrease in net carbon from 0.61 ± 0.14 Mg C ha⁻¹ yr⁻¹ in the pre-El Niño monitoring period to 0.15 ± 0.29 Mg C ha⁻¹ yr⁻¹ in the El Niño census interval, a decrease of 0.46 ± 0.30 Mg C ha⁻¹ yr⁻¹ (paired t-test with weighted data, $p < 0.01$, Figure 4.4A). This is driven by a significant increase in above ground carbon losses from 1.87 ± 0.14 Mg C ha⁻¹ yr⁻¹ to 2.37 ± 0.28 Mg C ha⁻¹ yr⁻¹, an increase of 0.49 ± 0.31 Mg C ha⁻¹ yr⁻¹ ($p < 0.01$) as carbon gains do not change significantly, from 2.49 ± 0.09 Mg C ha⁻¹ yr⁻¹ to 2.50 ± 0.11 Mg C ha⁻¹ yr⁻¹ ($p = 0.9$).

Climate anomalies affected carbon dynamics with greater losses of carbon in hotter and drier plots (Figure 4.5). Greater temperature anomalies were associated with significantly increased carbon losses (one-tailed Kendall's tau, $p < 0.05$, Figure 4.5E), and these increased losses with temperature drove losses of net carbon (linear model is significant but correlation test is not, $p = 0.2$, Figure 4.5A), as there are no significant

changes in carbon gains ($p=0.6$, Figure 4.5C). Stronger MCWD anomalies were associated with significantly greater reductions in carbon gains (linear model is not significant but correlation test is, $p<0.05$, Figure 4.5D), significantly greater increases in carbon losses ($p<0.01$, Figure 4.5F) and thus significantly greater reductions in net carbon ($p<0.01$, Figure 4.5B). Notably there is an interaction of continent with MCWD and carbon losses (Figure 4.5F). Slopes are similar (ANOVA, $p=0.6$), but intercepts are significantly different ($p<0.01$), with greater carbon losses per unit of drought in South America. There is also an interaction of continent with MCWD and net carbon (Figure 4.5B), again slopes are similar ($p=0.4$) but intercepts are significantly different ($p<0.01$), with greater reductions in net carbon per unit of drought in South America. Model averaging also highlights the importance of continent interactions. There is a significant effect of Δ MCWD and its interaction with continent on net carbon, carbon gains and carbon losses, and a significant effect of the interaction of Δ temperature with Δ MCWD and their interaction with continent on net carbon, carbon gains and carbon losses (Figure 4.10). So, both drought and temperature explain the loss of net carbon across the 237 plots during the El Niño. Carbon responses to temperature are conserved across continents, but carbon responses to drought differ for both carbon losses and net carbon.

Pre-El Niño baseline climate was also important as stronger pre-El Niño drought was associated with greater losses of carbon in El Niño (Figure 4.6) whilst baseline temperature had no effect. Overall, drier pre-El Niño MCWD was associated with greater increases in carbon losses in El Niño ($p<0.01$, Figure 4.6F), lower net carbon ($p<0.01$, Figure 4.6B), but no change in carbon gains ($p=0.9$, Figure 4.6D). Continent interacts with pre-El Niño MCWD and carbon losses (Figure 4.6F) and slopes are significantly different ($p<0.01$). For each unit of baseline drought, carbon losses in Africa are stable but carbon losses in South America increase with drier baseline climate. There is also an interaction of continent with pre-El Niño MCWD and net carbon, ($p<0.01$, Figure 4.6F), and slopes are significantly different.

With increasing temperature carbon gains increase until a point, beyond which carbon gains decrease. So, with all plots from both continents, temperature thresholds for carbon gains exist for both the pre-El Niño monitoring period (Figure 4.7A) and El Niño census interval (Figure 4.7C). Break point regressions indicate temperature thresholds of 23.9 ± 1.5 °C (95% CI) mean monthly temperature for the pre-El Niño mean carbon gains, (lines either side of breakpoint have significantly different slopes according to Davies' test, $p<0.05$, Figure 4.7A), and 26.6 ± 0.6 °C for the carbon gains of the El Niño census interval

(Davies' test, $p < 0.01$, Figure 4.7C). Peak carbon gains are approximately $2.75 \text{ Mg C ha}^{-1} \text{ yr}^{-1}$, as in Chapter 3, and the linear models either side of the breakpoint are significant for both the pre-El Niño (Figure 4.7A) and El Niño carbon gains (Figure 4.7C). The breakpoints of the pre-El Niño carbon gains and pre-El Niño mean temperature (Figure 3.8A) and El Niño carbon gains and El Niño mean temperature (Figure 3.8C) are significantly different ($p < 0.0001$), and the pre-El Niño threshold is lower than the results for the South America plots in Chapter 3. Temperature thresholds also exist when mean daily maximum temperature is used instead of mean monthly temperature; pre-El Niño carbon gains have a breakpoint at $30.8 \pm 0.5 \text{ }^\circ\text{C}$ ($p < 0.001$, Figure 4.7B) and during El Niño carbon gains have a breakpoint at $30.8 \pm 0.4 \text{ }^\circ\text{C}$ ($p < 0.001$, Figure 4.7D), which again are not significantly different breakpoints ($p = 0.8$). Apart from the pre-El Niño threshold (Figure 4.7A) the temperature thresholds are in line with temperature thresholds found in Chapter 3. For the mean daily maximum temperature (Figure 4.7 panels B and D) the linear models before the break points are not significant. Carbon gains increase until the temperature threshold, then decrease with a steeper line beyond the threshold, but most points are still before the temperature threshold so there is no relationship with temperature anomaly and carbon gains overall (Figure 4.5C). There were no threshold effects for drought and carbon losses (pre- El Niño Davies' test $p = 0.4$, El Niño $p = 0.8$) unlike temperature and carbon gains.

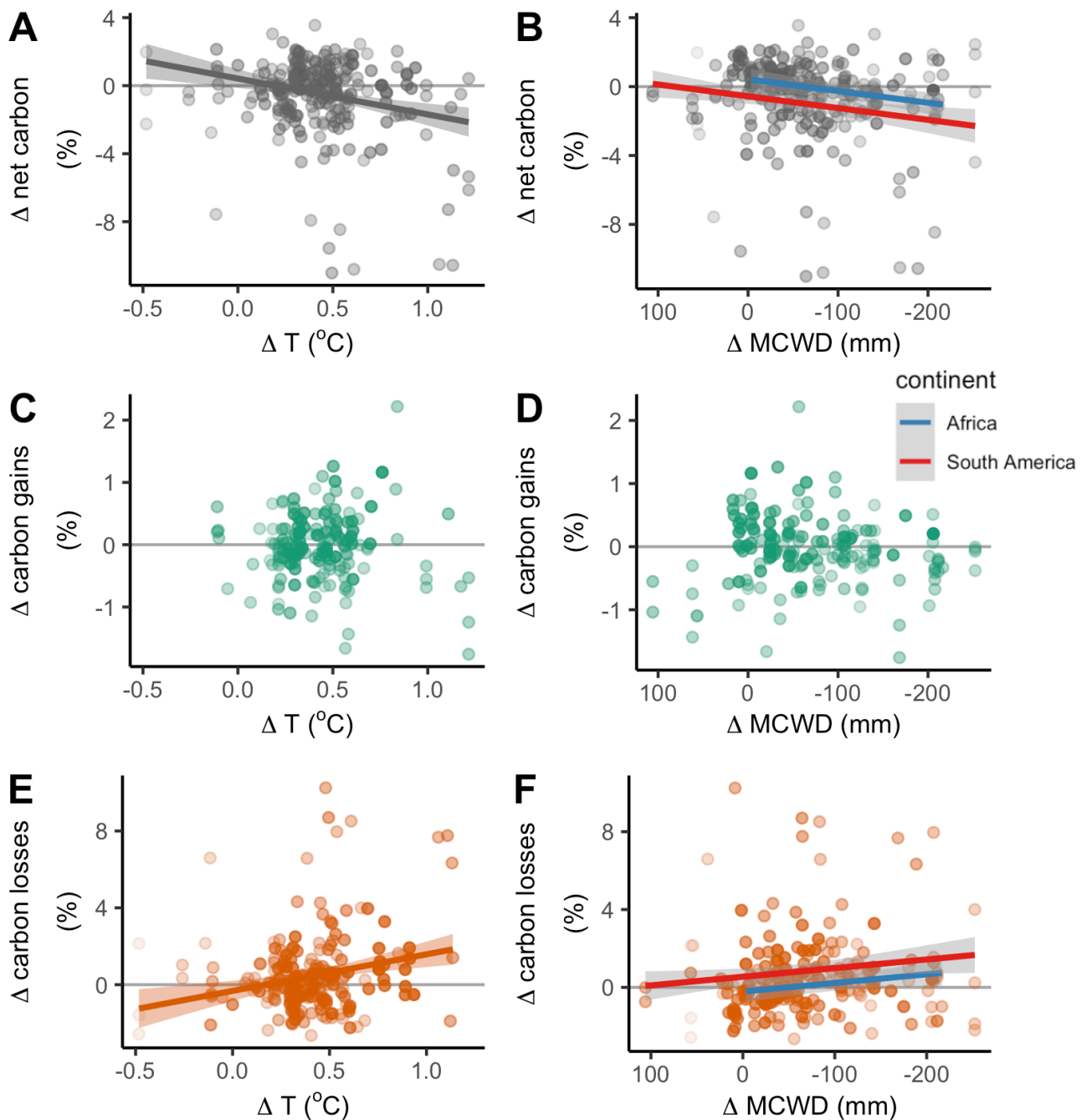


Figure 4.5 | Temperature (left) and drought (right) impacts on aboveground biomass carbon dynamics.

Temperature and drought anomalies significantly increase carbon losses and reduce net carbon, with the drought impact greater per unit of drought in South America than in Africa. The net carbon change (**A, B**), carbon gains from tree growth and recruitment (**C, D**) and carbon losses from mortality (**E, F**) of the censuses capturing the El Niño event minus pre-El Niño plot monitoring period for 237 long-term inventory plots. The intensity of temperature change, Δ temperature (T) (**A, C, E**) is mean monthly temperature in El Niño minus mean monthly temperature pre-El Niño, using the census dates of the plot censuses. Relative intensity of the change in dry season strength is calculated as Δ maximum cumulative water deficit (MCWD) (**B, D, F**) which is the difference between maximum MCWD in El Niño and mean MCWD in pre-El Niño. Point shading from light to dark denotes greater weighting, with plots and line of best fit weighted by an empirically derived combination of pre-El Niño plot monitoring length and plot area for each response variable. Net change is in grey, gains are in green, losses

orange. Solid lines represent significant linear models ($p < 0.05$). Analysis of covariance was used to test whether continent regression lines differed in slope or intercept and where either or both differed a blue line is plotted for Africa and a red line for South America. Otherwise, when the best model does not include a continent interaction, a single line is plotted. **A:** $-2.1x + 0.4$, $p < 0.001$, **B:** slopes are the same as the continent interaction is not significant $p = 0.4$, but intercepts differ between continents $p < 0.01$, Africa: $y = -0.008x + 0.5$ and South America: $y = -0.008x - 0.9$ with $p < 0.001$, **C:** $p = 0.6$, **D:** $p = 0.2$, **E:** $y = 1.9x - 0.3$, $p < 0.001$, **F:** slopes are the same as the continent interaction is not significant $p = 0.6$, but intercepts differ between continents $p < 0.01$, Africa: $y = 0.005x - 0.3$ and South America: $y = 0.005x + 0.7$ with $p < 0.01$.

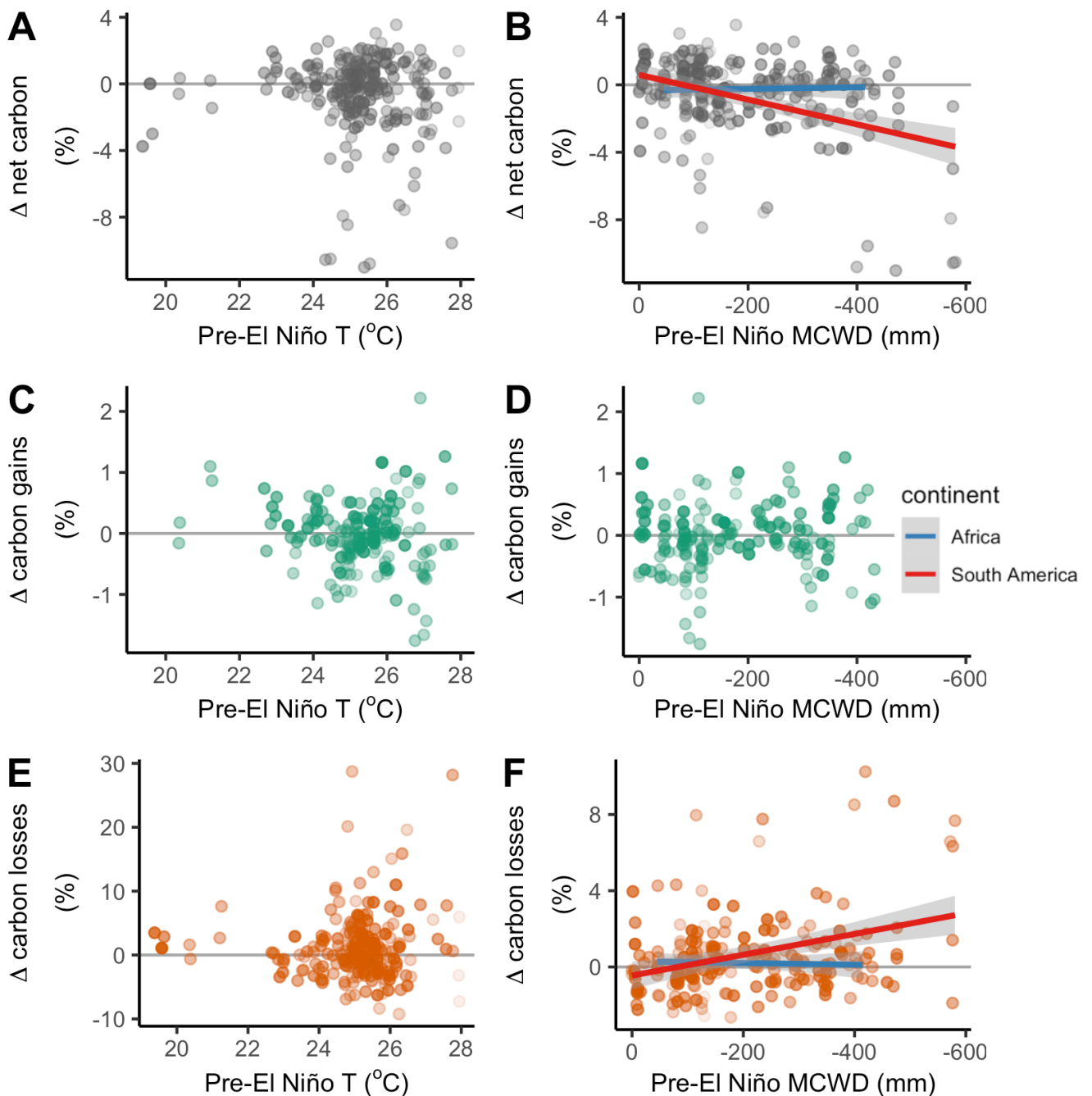


Figure 4.6 | Baseline temperature (left) and drought (right) and aboveground biomass carbon dynamics.

Baseline temperature does not influence carbon dynamics, but baseline drought increases carbon losses and reduces net carbon in South American forest plots. The net carbon change (**A**, **B**), carbon gains from tree growth and recruitment (**C**, **D**) and carbon losses from mortality (**E**, **F**) of the censuses capturing the El Niño event minus pre-El Niño plot monitoring period for 237 long-term inventory plots. The pre-El Niño temperature (T) (**A**, **C**, **E**) is the mean of mean monthly temperature in the monitoring period prior to the El Niño. The pre-El Niño maximum cumulative water deficit (MCWD) (**B**, **D**, **F**) is the mean MCWD in the monitoring period prior to the El Niño. Point shading from light to dark denotes greater weighting, with plots and line of best fit weighted by an empirically derived combination of pre-El Niño plot monitoring length and plot area for each response variable. Net change is in grey, gains are in green, losses orange.

Solid lines represent significant linear models ($p < 0.05$). Analysis of covariance was used to test whether continent regression lines differed in slope or intercept and where either or both differed a blue line is plotted for Africa and a red line for South America. Otherwise, when the best model does not include a continent interaction, a single line is plotted. **A:** $p = 0.5$, **B:** Significant continent interaction, $p < 0.01$, Africa: $y = 0.0004x - 0.3$ and South America: $y = -0.007x + 0.8$ with $p < 0.01$, **C:** $p = 0.1$, **D:** $p = 0.3$, **E:** $p = 0.4$, **F:** Significant continent interaction, $p < 0.01$, Africa: $y = -0.0003x + 0.2$ and South America: $y = 0.005x - 0.6$ with $p < 0.05$.

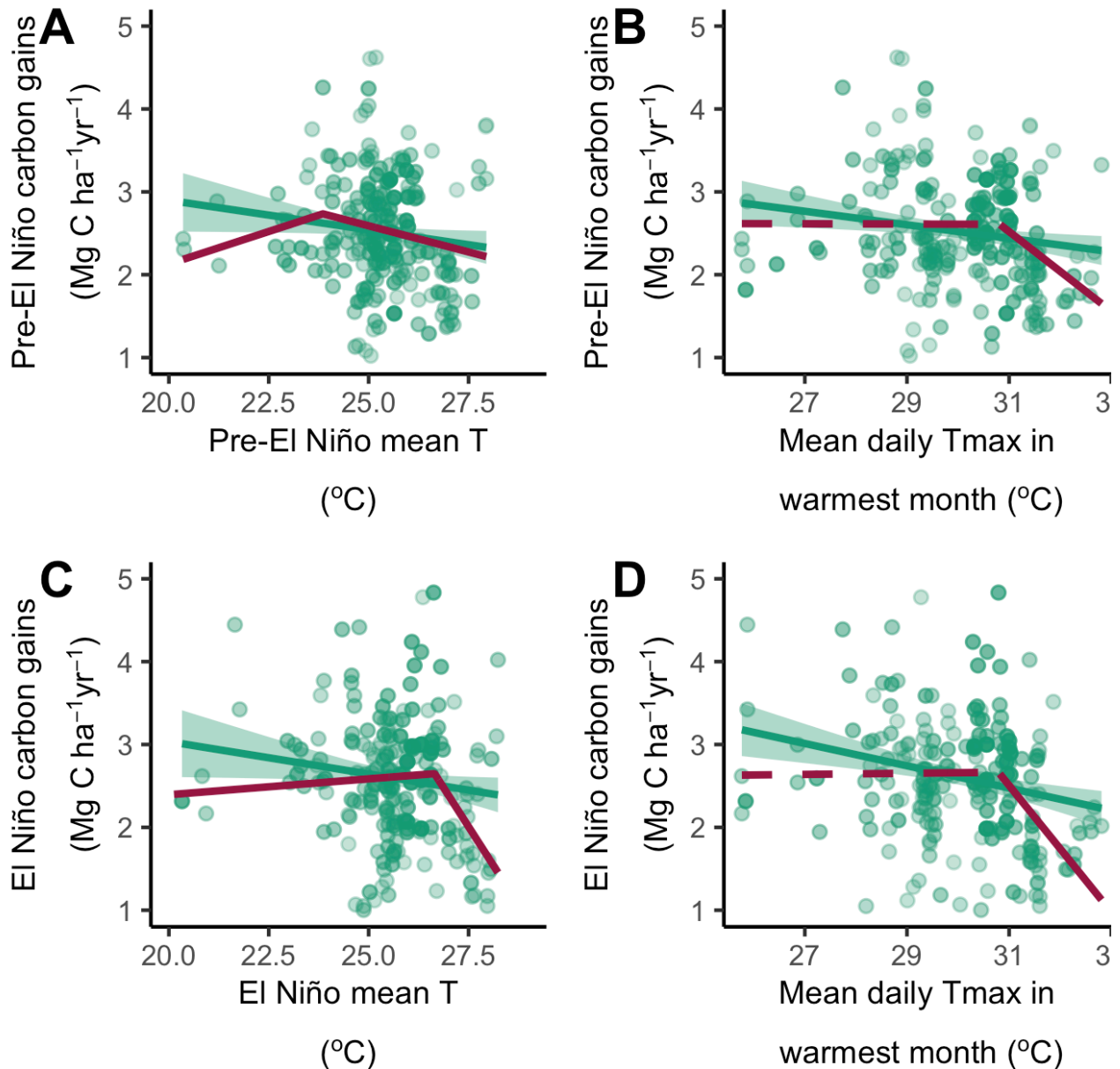


Figure 4.7 | Temperature-productivity thresholds

Temperatures increase productivity to a point, beyond which carbon gains decline with increasing temperatures. Baseline temperature and baseline carbon gains (A), long-term daily maximum temperature (from WorldClim v2) and baseline carbon gains (B), El Niño temperature and El Niño carbon gains (C), and long-term daily maximum temperature and El Niño carbon gains (D). Gains are shown in green, consistent with other figures. Point shading from light to dark denotes greater weighting, with plots and lines of best fit weighted by an empirically derived combination of pre-EI Niño plot monitoring length and plot area. Slopes are significantly different either side of breakpoint according to Davies' test A; $p < 0.05$, B: $p < 0.001$, C: $p < 0.01$, D: $p < 0.001$, the linear models before the breakpoint are significant, in A; $p < 0.05$, and C: $p < 0.0001$, but not B: $p = 0.9$, and D: $p = 0.7$, the linear models after the breakpoint are all significant A; $p < 0.05$, B: $p < 0.001$, C: $p < 0.001$, D: $p < 0.0001$. Solid lines indicate significant linear models,

$p < 0.05$. Slopes of linear models before and after breakpoint, respectively A: $y = 0.16x - 1$, $y = -0.13x + 6$, B: $y = -0.002x + 2.7$, $y = -0.5x + 17$, C: $y = 0.04x + 1.6$, $y = -0.75x + 23$, D: $y = 0.007x + 2.4$, $y = -0.8x + 26$.

The changes in stem dynamics over the 2015-16 El Niño mirrored the overall changes in carbon dynamics for the 237 plots combined. There was a significant decrease in net stems from an increase of 0.72 ± 0.14 stems $\text{ha}^{-1} \text{yr}^{-1}$ in the pre-El Niño monitoring period to a decrease of 2.83 ± 0.63 stems $\text{ha}^{-1} \text{yr}^{-1}$ in the El Niño census interval, a decrease of 2.55 ± 1.31 stems $\text{ha}^{-1} \text{yr}^{-1}$ (paired t-test with weighted data, $p < 0.001$, Figure 4.4B). This is driven by a significant increase in losses from stem mortality from 8.80 ± 0.33 stems $\text{ha}^{-1} \text{yr}^{-1}$ to 11.66 ± 0.62 stems $\text{ha}^{-1} \text{yr}^{-1}$, an increase of 2.83 ± 1.44 stems $\text{ha}^{-1} \text{yr}^{-1}$ ($p < 0.001$) as stem gains from recruitment do not change significantly, from 9.45 ± 0.38 stems $\text{ha}^{-1} \text{yr}^{-1}$ to 9.02 ± 0.44 stems $\text{ha}^{-1} \text{yr}^{-1}$ ($p = 0.5$).

Stem dynamics also responded to climate (Figure 4.8). Greater temperature anomalies were associated with increased stem gains (one-tailed Kendall's tau, $p < 0.01$, Figure 4.8C) and increased stem losses (significant linear model but not significant correlation test, $p = 0.1$, Figure 4.8E), and with both increased gains and losses there was no change in net stems with temperature ($p = 0.7$, Figure 4.8A). Stronger MCWD anomalies were associated with increases in stem losses ($p < 0.001$, Figure 4.8F), and reduced stem gains ($p < 0.0001$, Figure 4.8D) and greater losses of net stems ($p < 0.0001$, Figure 4.8B). There is an interaction of continent with MCWD and stem losses (Figure 4.8F). Slopes are similar (ANOVA, $p = 0.06$), but intercepts are significantly different ($p < 0.001$), with greater stem losses per unit of drought in South America, and the same for net carbon ($p = 0.2$, $p < 0.05$, Figure 4.8B). Model averaging shows a significant effect only of the interaction of Δ temperature with Δ MCWD and on stem gains from recruitment (Figure 4.10). So, it is drought impacts alone, and not temperature, that explains the net loss of stems seen across the 237 plots during the El Niño.

Baseline climate also influences stem dynamics (Figure 4.9). Hotter forests pre-El Niño had greater stem gains in El Niño ($p < 0.001$, Figure 4.9C), and increased net stems ($p < 0.01$, Figure 4.9A), as stem losses in the El Niño did not change with temperature anomaly ($p = 0.1$, Figure 4.9E). Although there was no change overall with stem losses and temperature anomaly, there is a significant interaction with continent; slopes are similar ($p = 0.8$), but intercepts are significantly different ($p < 0.05$, Figure 4.9E), so for forests with the same baseline temperature, South American forests lost proportionally more stems. Plots that were drier, with more negative MCWD pre-El Niño, had greater stem losses in

the El Niño ($p < 0.001$, Figure 4.9F), greater reductions in stem gains ($p < 0.0001$, Figure 4.9D) and reduced net stems ($p < 0.0001$, Figure 4.9B). There is an interaction between continent, pre-El Niño MCWD and stem gains as slopes are significantly different ($p < 0.05$, Figure 4.9D) and forests in Africa have stable stem gains across a range of baseline drought while forests in South America have increased gains with lower baseline drought and decreased gains with higher baseline drought. For net stems there is also a continent interaction, as again net stems are stable across a range of baseline drought in Africa, and greater reductions in net stems for South America are associated with stronger baseline drought ($p < 0.01$, Figure 4.9B).

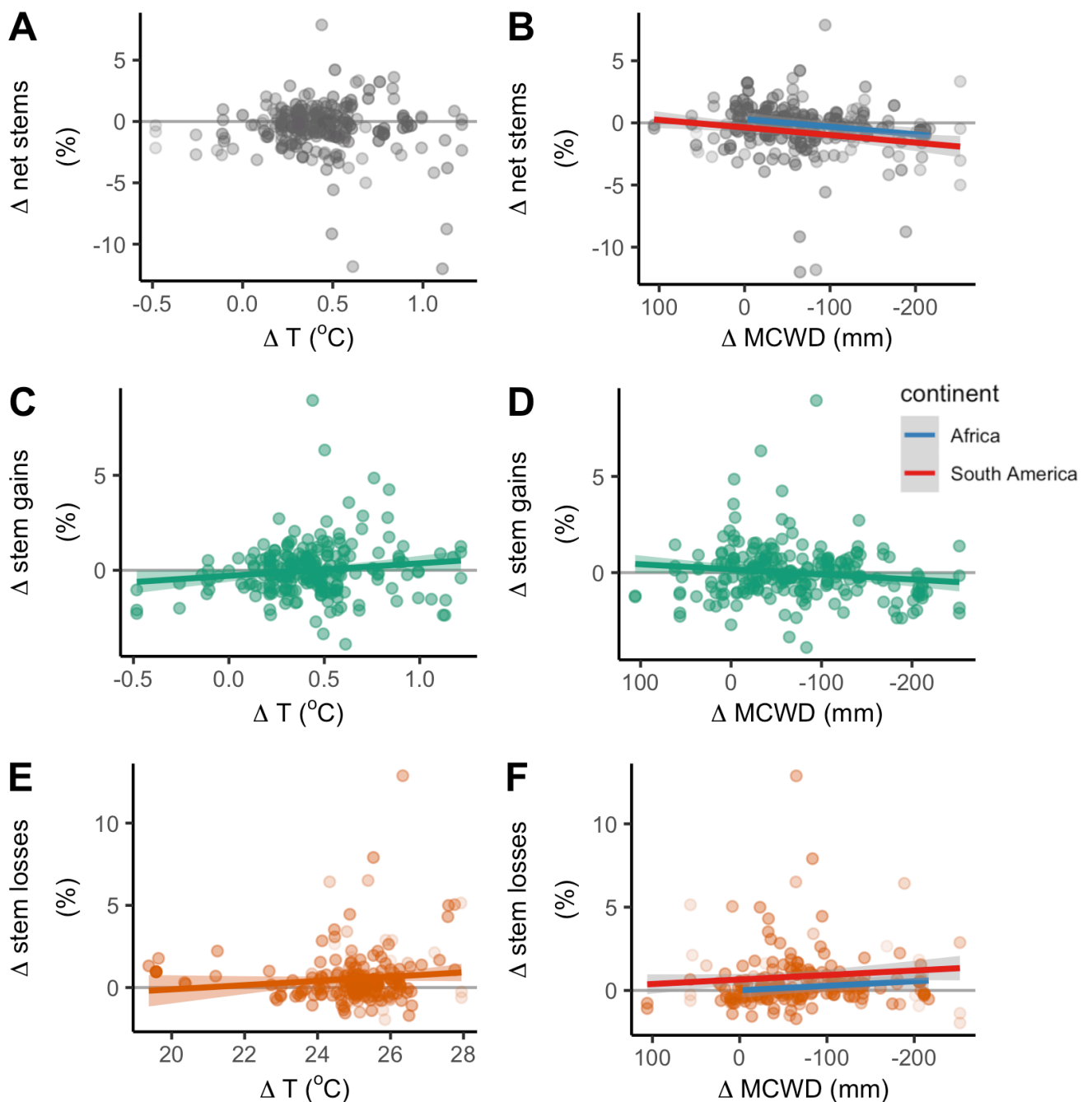


Figure 4.8 | Temperature (left) and drought (right) impacts on stem dynamics of 237 long-term forest plots.

Stem gains and stem losses increase significantly with temperature anomaly, stem gains decrease and stem losses increase with drought anomaly, with net stem losses. The net stem change (**A**, **B**), stem gains from recruitment (**C**, **D**) and stem losses from mortality (**E**, **F**) of the censuses capturing the El Niño event minus the pre-El Niño plot monitoring period. The temperature change, Δ temperature (T) (**A**, **C**, **E**) is mean monthly temperature in the El Niño census interval minus the mean monthly temperature pre-El Niño, using the census dates of the plot censuses. Relative intensity of the change in dry season strength is calculated as Δ maximum cumulative water deficit (MCWD) (**B**, **D**, **F**) which is the difference between maximum MCWD in El Niño and mean MCWD in pre-El Niño. Point shading from light to dark denotes greater weighting, with plots and line of best fit weighted by an empirically derived combination of pre-El Niño plot monitoring length and plot area for each response variable. Net change is in grey, gains are in green, losses orange. Solid lines indicate significant linear models

$p < 0.05$. Analysis of covariance was used to test whether continent regression lines differed in slope or intercept and where either or both differed a blue line is plotted for Africa and a red line for South America. Otherwise, when the best model does not include a continent interaction, a single line is plotted. A: $p = 0.1$, B: slopes are the same as the continent interaction is not significant $p = 0.2$, but intercepts differ between continents $p < 0.05$, Africa: $y = -0.007x + 0.4$ and South America: $y = -0.007x - 0.6$ with $p < 0.01$, C: $y = 0.7x - 0.3$, $p < 0.05$, D: $y = -0.003x + 0.2$, $p < 0.05$, E: $y = 1.5x - 0.04$, $p < 0.001$, F: slopes are the same as the continent interaction is not significant $p = 0.06$, but intercepts differ between continents $p < 0.001$, Africa: $y = -0.003x - 0.001$ and South America: $y = -0.003x + 0.6$ with $p < 0.05$.

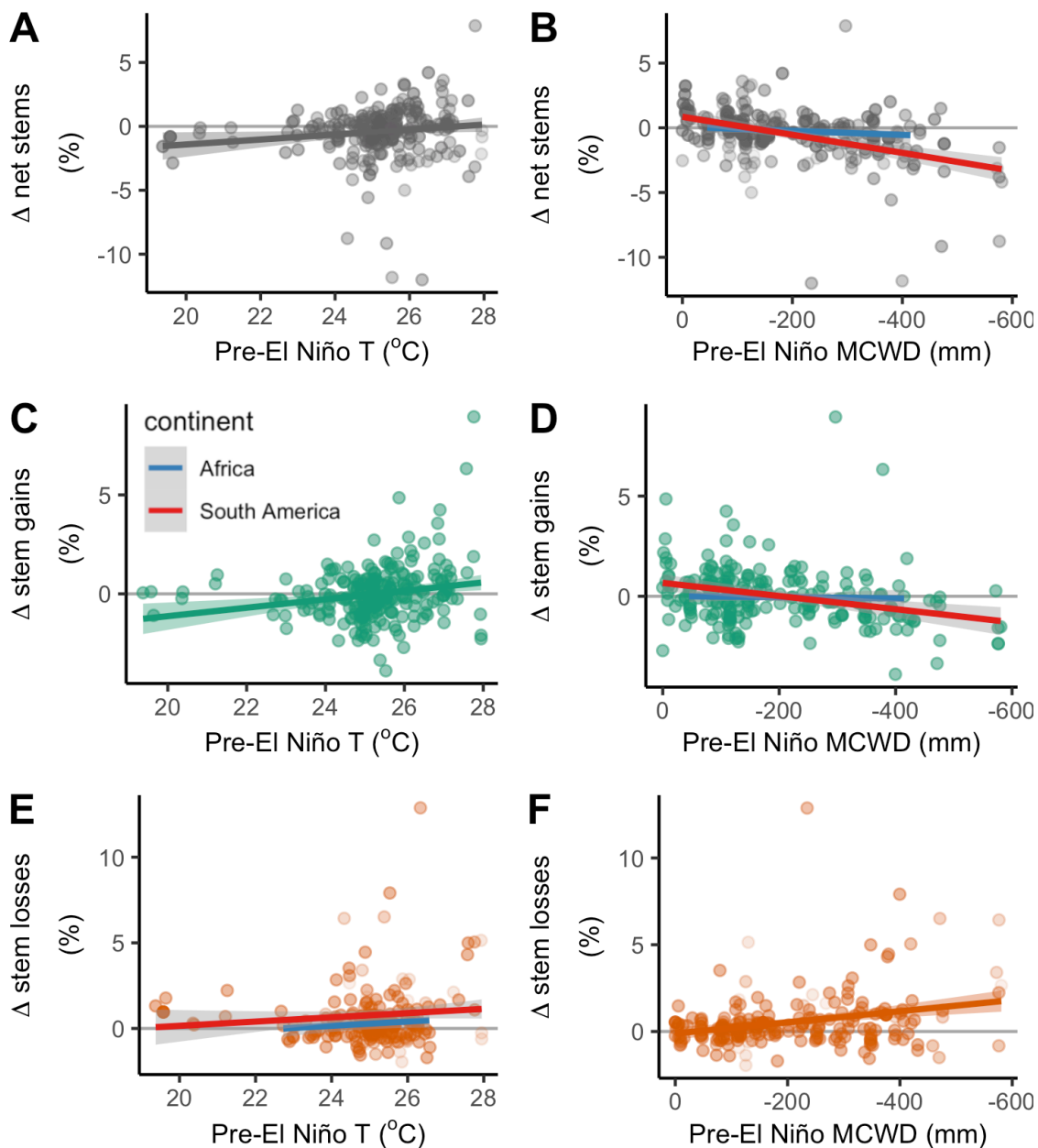


Figure 4.9 | Baseline temperature (left) and drought (right) and stem dynamics.

Stem gains and net stems increase with baseline temperature, stem losses also increase with baseline temperature, with greater losses in South America for the same baseline temperature. Stem losses increase with baseline drought and stem gains decrease, especially in South America. The change in net stems (**A**, **B**), stem gains from recruitment (**C**, **D**) and stem losses from mortality (**E**, **F**) of the censuses capturing the El Niño event minus pre-El Niño plot monitoring period for 237 long-term inventory plots. The pre-El Niño temperature (T) (**A**, **C**, **E**) is the mean of mean monthly temperature in the monitoring period prior to the El Niño. The pre-El Niño maximum cumulative water deficit (MCWD) (**B**, **D**, **F**) is the mean MCWD in the monitoring period prior to the El Niño. Point shading from light to dark denotes greater weighting, with plots and line of best fit weighted by an empirically derived combination of pre-El Niño plot monitoring length and plot area for each response variable. Net change is in grey, gains are in green, losses orange. Solid lines represent significant linear models ($p < 0.05$). Analysis of covariance was used to test whether continent regression lines differed in slope or intercept and where either or both differed a blue line is plotted for Africa and a red line for South America. Otherwise, when the best model does not include a continent interaction, a single line is plotted. **A**: $y = 0.2x - 5$, $p < 0.05$, **B**: Significant continent interaction, $p < 0.01$, Africa: $y = 0.0004x - 0.3$ and South America: $y = -0.007x + 0.8$, with $p < 0.01$, **C**:

$y=0.2x-5$, $p<0.01$, **D**: Significant continent interaction, $p<0.05$, Africa: $y= -0.0003x +0.02$ and South America: $y= -0.003x +0.7$, with $p<0.001$, **E**: slopes are the same as the continent interaction is not significant $p=0.8$, but intercepts differ between continents $p<0.05$, Africa: $y=0.1x - 2.6$ and South America: $y=0.1x +0.5$ with $p<0.05$, **F**: $y= 0.003x -0.1$, $p<0.0001$.

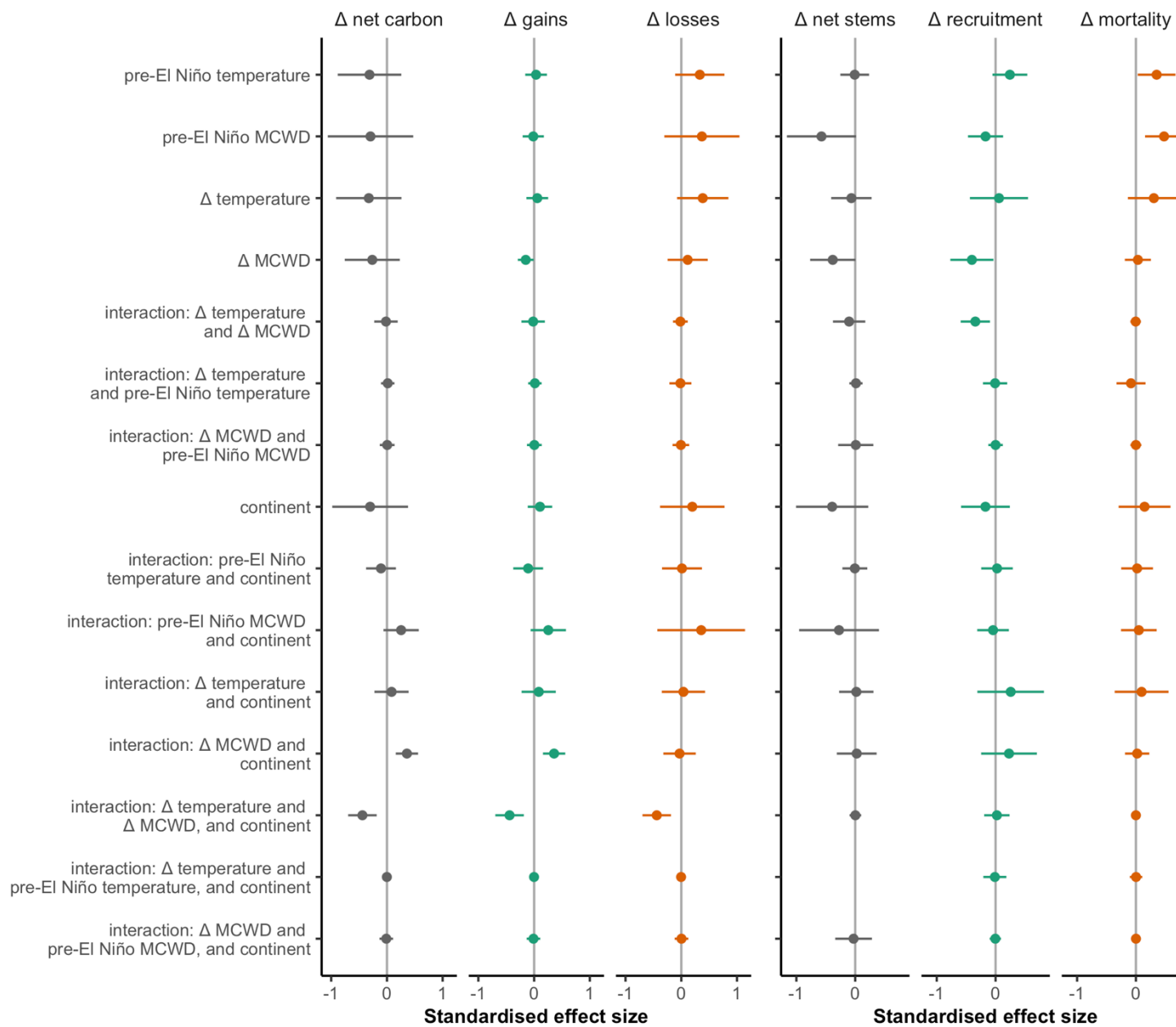


Figure 4.10 | Effect sizes of change in carbon and stems in tropical forest plots over the 2015-16 El Niño

Drought significantly reduced carbon gains and recruitment, and there was an interaction of continent with temperature and drought. Points show coefficients from linear models with multi-model inference and error bars show 95 % CIs. Coefficients are standardised so that they represent change in the response variable for one standard deviation change in the explanatory variable. Net change is in grey, gains are in green, losses orange. Error bars show 95 % CIs. The full models explained 22 %, 19 % and 13 % of variation in Δ net carbon, Δ carbon gains and Δ carbon losses and 25 %, 23 % and 18 % of variation in Δ net stems, Δ recruitment and Δ stem mortality, respectively, as proportional changes (%).

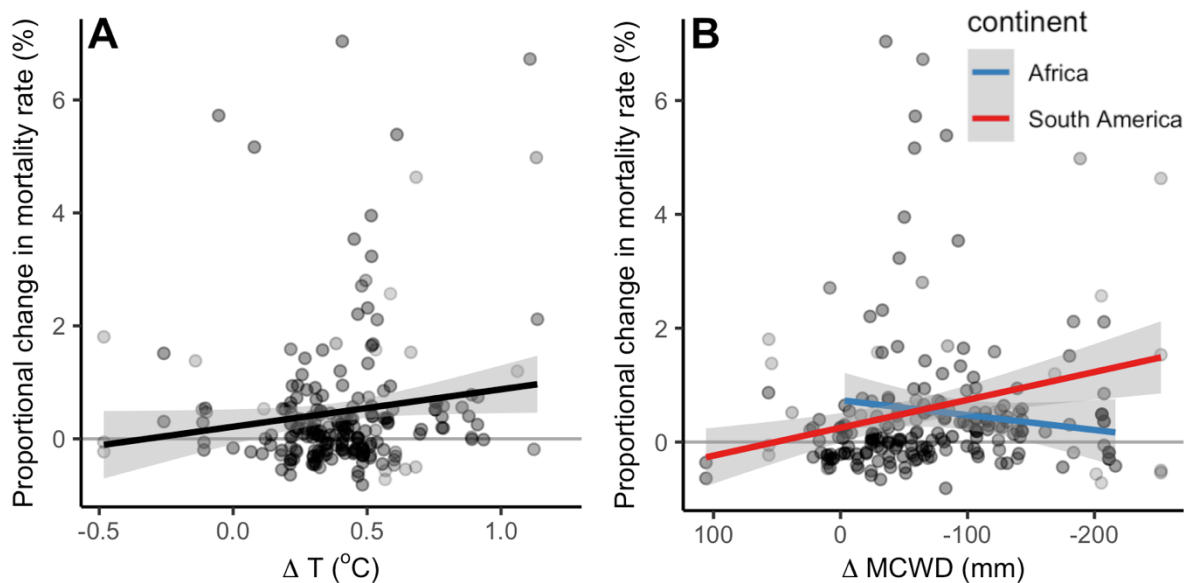


Figure 4.11 | Temperature (left) and drought (right) impacts on per capita stem mortality rate.

Stem mortality rate significantly increases with temperature. There is a continent interaction and mortality rate significantly increases with drought in South America but not in Africa. Solid lines indicate significant linear models $p < 0.05$. Analysis of covariance was used to test whether continent regression lines differed in slope or intercept and where either or both differed a blue line is plotted for Africa and a red line for South America. Otherwise, when the best model does not include a continent interaction, a single line is plotted. **A**: $y = 0.7x + 0.2$, $p < 0.05$, **B**: Significant continent interaction, $p < 0.001$, Africa: $y = -0.003x + 0.7$ and South America: $y = -0.008x - 0.5$, with $p < 0.05$.

Annual mortality rate increases across all plots from 1.7 ± 0.1 % in the pre-El Niño monitoring period to 2.3 ± 0.2 % in the El Niño census interval (Wilcoxon signed rank test, $p < 0.0001$). Mortality rates respond to climate anomalies (Figure 4.11) as forests experiencing stronger temperature anomalies have significant increases in mortality rate (one-tailed Kendall's tau, $p < 0.05$, Figure 4.11A). Forests experiencing stronger MCWD anomalies have significant increases in mortality rate too ($p < 0.05$, Figure 4.11B), but there is also a significant interaction of continent with Δ MCWD and mortality rate (ANOVA, $p < 0.001$, Figure 4.11B), such that mortality rates increase with drought in South America and decrease in Africa ($p < 0.05$, Figure 4.11B), although this could be a function of the greater spread of the South American Δ MCWD data.

Mortality rate significantly increases for every size class (Table 4.1). For the smallest size class (trees with diameter 100-199 mm) mortality rates were 0.4 ± 0.02 % higher in El Niño than pre-El Niño (Wilcoxon signed rank test, $p < 0.01$), for the medium size

class (trees with diameter 200-399 mm) mortality rates were 0.7 ± 0.2 % higher ($p < 0.0001$) and for the largest size class (trees with diameter 400+ mm) mortality rates were 0.9 ± 0.4 % higher ($p < 0.0001$). So, there is no evidence of size-selective mortality, rather mortality increases for trees of all sizes.

Table 4.1 | Mean plot-level per capita stem mortality rates of 237 plots

Diameter (mm)	Mortality rate (%)	
	Pre-El Niño	El Niño
100-199	2.0 ± 0.2	2.5 ± 0.3
200-399	1.5 ± 0.1	2.2 ± 0.2
400+	2.0 ± 0.2	2.7 ± 0.32

Median growth rates were significantly lower for trees of all sizes during the El Niño. For the smallest size class (trees with diameter 100-199 mm) median growth rates were 0.15 ± 0.08 mm yr⁻¹ less in El Niño than pre-El Niño (paired t-test, $p < 0.001$), for the medium size class (trees with diameter 200-399 mm) growth rates were 0.19 ± 0.11 mm yr⁻¹ less ($p < 0.001$) and for the largest size class (trees with diameter 400+ mm) growth rates were 0.21 ± 0.15 mm yr⁻¹ less ($p < 0.01$).

4.4 Discussion

Intact tropical forests in Africa and South America differ in composition, structure, climate and biogeographic history. Yet, long-term forest plot responses to the temperature anomaly of the 2015-16 El Niño are conserved across continents. Responses to drought differ between the two continents and are moderated by baseline drought and its interaction with continent. A stronger baseline drought increases carbon losses in the El Niño, indicating that plots with stronger dry seasons are more vulnerable to drought, rather than more resistant.

In the 2015-16 El Niño, for both Africa and South America, there were greater drought-induced changes in carbon losses than carbon gains. Greater responses of carbon losses from biomass mortality, stem mortality and mortality rates, compared to carbon gains from woody productivity and recruitment, indicate that both continents suffered a severe drought. Carbon losses increase with increasing pre-El Niño MCWD in South America, but do not in Africa. This may be a consequence of species composition resulting from their contrasting paleoclimate and biogeographic histories. Species filtering in Africa through glacial-interglacial periods (deMenocal 2004) likely selected for the

drought-tolerant species which remained and may have diversified. The lack of species filtering through glacial-interglacial periods in South America implies minimal changes in the survival of species and abundance there today (Dick et al. 2013, Nascimento et al. 2019). South American tropical forests, compared to African tropical forests, have species diversity but not drought resistance.

Temperature anomaly impacts are via carbon losses and net carbon, so the temperature impact is through tree mortality rather than growth, as there is no overall carbon gains response with temperature. As in Chapter 3, it is just the temperature anomaly, and not the pre-El Niño temperature that is linked to increasing carbon losses (Figure 4.5, Figure 3.6). Recent work suggests that hydraulic safety margins are the best determinant of vulnerability to mortality in severe drought (Powers et al. 2020). It is likely that hydraulically vulnerable species are more prevalent in South America than Africa as the species pool has not been filtered to the same extent through glacial-interglacial periods (deMenocal 2004). Temperature has been linked to tree mortality (Anderegg et al. 2013) experimentally (Adams et al. 2017a) and in the field in the Southwestern USA and in the tropics (Adams et al. 2009, Williams et al. 2013, Hubau et al. 2020). An effect of temperature reducing carbon gains was not seen here overall (Figure 4.5C), unlike in other studies (Clark et al. 2013, Hubau et al. 2020). This may be because of smaller sample sizes, or a long census interval that captures the El Niño, or perhaps productivity was reduced but the effect was dwarfed by the increased productivity of recruits which increased with temperature (Figure 4.9C). The temperature thresholds analysis indicates that productivity was reduced at plots with mean monthly temperatures above 26.6 °C, or daily maximum temperatures above 30.8 °C (Figure 4.7). South American tropical forests, with hotter baseline temperatures and warming more quickly (Hubau et al. 2020), and hotter El Niño temperature anomalies shown in this chapter, are closer to a potential physiological temperature threshold than African tropical forests. Baseline temperatures do not have an effect on carbon losses across continents, but temperature anomalies increase carbon losses and reduce net carbon.

Hotter temperature anomalies are exacerbated in drier plots. In wetter plots there is more latent heating, and less sensible heating, so some of the heat energy is dissipated in the state change of evaporating water. In drier plots there is more sensible heating, and less latent heating, so temperatures will increase even more in the drier plots (Wilson et al. 2002, McGloin et al. 2019). Forest plots of the same temperature are drier in South America (Figure 4.3A), so greater sensible heating is likely taking place in South America,

which might help to explain the increases in mortality with drought as the drought effect might be exacerbated by temperature even though the temperature effect is not significant. These drier locations may also have very hot days and very cold nights, and less cloud cover, all of which could increase the desiccation effect.

The spatial distribution of plots means potential spatial autocorrelation. Spatial autocorrelation should be investigated, but may not cause bias (Diniz-Filho et al. 2003). Some forest plots exist within clusters and can be within 1 km of each other, within the same climate grid cell, and so it is possible that they may have experienced the same climate anomaly. One would expect plots with the same climate anomaly to respond similarly in terms of carbon gains or losses, and if so, clusters may artificially inflate the statistical power of the current analysis. A possible solution is analysing at the cluster scale rather than the plot scale however, plots within a cluster can be very different to one-another, e.g. monodominant and multi-species plots exist in close proximity and analysing at the cluster level would lose some important information as to how plots that are climatologically and compositionally similar respond to perturbation slightly differently. In the overall analysis I used paired t-tests testing for changes at each individual plot, so the main results are unlikely to change even when accounting for any spatial correlation.

There is a greater El Niño impact in South America than Africa, driven by carbon losses. Using microwave satellite data to measure aboveground carbon Wigneron et al. 2020 suggest South American tropical forests were a greater source of CO₂ than African tropical forests from 2014 to 2017. They also find that the carbon uptake of both continents had not recovered from the 2015-16 El Niño by 2017 due to tree mortality, both consistent with the findings in this chapter. As suggested in previous chapters of this thesis, most of the land carbon emissions in 2015-16 were not from closed canopy forests, so remotely sensed CO₂ indicating Africa dominated global emissions does not conflict with results in this chapter (Palmer et al. 2019). A third study that used remotely sensed CO₂ also found South America to be the largest carbon source of the tropical continents using (Liu et al. 2017). In Chapter 2 it was drought anomalies that reduced carbon gains and, in this chapter, for a combined set of plots from Africa and South America, temperature and drought anomalies increased carbon losses, but the drought effect was stronger in South America than in Africa.

Temperature responses are universal across tropical forests on two continents. Given rising global temperatures, that temperature is driving increased carbon losses from biomass mortality is very concerning. As global temperatures continue to rise tropical

forests are likely to lose increasing amounts of carbon. Drought responses vary by continent, with higher carbon losses from mortality in South America than in Africa, probably due to the species present and the contrasting paleoclimate history of the continents. Hence, the high species diversity and higher species richness of South American forests does not confer resistance to either drought or high temperatures.

Chapter 5

Conclusions

5.1 Research Synthesis

This thesis investigates the climate of the 2015-16 El Niño and associated impacts on aboveground biomass carbon and stem dynamics for intact forests in two distinct tropical regions – Africa and South America. The primary goals of the research were to: quantify the climate and climate change caused by the 2015-16 El Niño in the tropical forest biome (1) and at monitored plots (2), understand changes in aboveground biomass, carbon balance and stem dynamics (3), determine whether baseline climate confers resistance to climate anomaly (4) and establish if responses to the climate anomaly vary by continent (5). To achieve these objectives, I collected field data from 20 plots in Africa, compiled census measurements from a further over 217 long-term forest plots in Africa and South America and combined these plot measurements with climate data. I quantify the impact of the climate anomaly on the aboveground biomass carbon balance of intact forests and evaluate the impacts of the El Niño event on long-term processes; multi-year impacts on growth and mortality.

Notably, I show for the first time that drought reduced growth in Africa. Studies tend to link drought to increased carbon losses rather than reduced carbon gains (Bonal et al. 2016), and the results of Chapter 2 are important because it is the first formal assessment of drought responses in Africa. In Africa, plots remained a carbon sink despite extreme temperatures and drought anomalies but African forests are not completely resistant to drought as drought anomalies reduced carbon gains, a reduction of $0.2 \text{ Mg C ha}^{-1} \text{ yr}^{-1}$ for a drought anomaly of -200 mm (Figure 2.3). These results significantly advance understanding of how African tropical forests respond to temperature and moisture anomalies as the carbon sink impacts are now quantified; a net carbon loss of one-third. In South America the net carbon impact was nearly four times greater, a 130 % decrease in net carbon from a sink pre-El Niño, to a small but not significant source during the El Niño. In South American tropical forests temperature and drought anomalies both

increased carbon losses and reduced net carbon but did not affect growth (Chapter 3). Additionally, I present the first evidence that baseline climate moderates forest responses to climate anomaly. Baseline temperatures are particularly important in South America where productivity at cooler plots is stable or increases in the El Niño, but productivity decreases at hotter plots. This indicates that some tropical forests in South America are close to the limits of their thermal tolerance and suggests that high temperatures without drought could cause widespread tree mortality. There is also a compounding effect of drought in South America, as plots that are the baseline driest and have stronger MCWD anomalies in the El Niño have greater reductions in carbon gains and greater increases in losses (Figure 4.10). These drier plots are not more resistant because they are already dry but are in fact more impacted by El Niño drought. Continent effects are exerted via baseline MCWD, with seasonally drier forests in South America having greater El Niño carbon losses, but across a range of baseline drought El Niño carbon losses are stable in Africa (Figure 4.6).

In tropical forests across two continents net carbon decreased with both temperature and drought anomalies as carbon losses increased (Figure 4.5, Table 5.1) and carbon gains decreased beyond temperature thresholds (Figure 4.7). That tropical forests are vulnerable to both temperature and drought anomalies is a critical finding because future droughts will be periodic, but temperatures are certainly rising, and tropical forests are likely to lose carbon with temperature increases alone. Furthermore, temperature responses to the El Niño are conserved across continents but continents differ in their response to drought, as carbon losses and stem mortality are greater in South America. Similar temperature responses across both continents perhaps indicates that a shared physiological mechanism is determining this temperature threshold, perhaps directly via the photosynthetic enzymes or indirectly through reduced stomatal conductance. There are large increases in carbon losses from biomass mortality in South America for the driest plots, contrasting with the remarkable stability of the African tropical carbon sink (Figure 4.6). The contrasting continental responses are possibly due to the presence of more drought-adapted species in Africa than in South America as a result of hotter drier climate in the past interglacials in Africa selecting for drought-tolerant species.

Table 5.1 | Summary of the key impacts of the 2015-16 El Niño climate anomaly on carbon dynamics of tropical forests

P-values are from linear models and one-tailed Kendall's Tau correlation tests, respectively, and are only reported when $p < 0.05$, ns=nonsignificant.

Key Impacts	Africa	South America	Combined
Temperature anomaly on net carbon	ns, ns	$p < 0.05$, ns	$p < 0.001$, ns
Temperature anomaly on carbon gains	ns, $p < 0.05$ (gains increase)	ns, ns	ns, ns
Temperature anomaly on carbon losses	ns, ns	$p < 0.05$, $p < 0.05$	$p < 0.001$, $p < 0.05$
Drought anomaly on net carbon	$p < 0.05$, $p < 0.05$	$p < 0.05$, $p < 0.05$	$p < 0.01$, $p < 0.01$
Drought anomaly on carbon gains	$p < 0.05$, $p < 0.05$	ns, ns	ns, $p < 0.05$
Drought anomaly on carbon losses	ns, $p < 0.05$	ns, $p < 0.001$	ns, $p < 0.01$
Baseline temperature on net carbon	ns, ns	ns, ns	ns, ns
Baseline temperature on carbon gains	ns, ns	$p < 0.05$, ns	ns, ns
Baseline temperature on carbon losses	ns, ns	ns, ns	ns, ns
Baseline drought on net carbon	ns, ns	$p < 0.001$, $p < 0.001$	$p < 0.0001$, $p < 0.001$
Baseline drought on carbon gains	ns, ns	ns, ns	ns, ns
Baseline drought on carbon losses	ns, ns	$p < 0.01$, $p < 0.01$	$p < 0.0001$, $p < 0.001$

5.1.1 Climate and climate change in the tropical forest biome

The 2015-16 El Niño caused unprecedented high temperatures, low precipitation and strong water deficits across the tropical biome. Temperature increases were widespread but there was a greater spatial variability of drought across the tropics, with most areas drying but some areas wetting in the El Niño. Regions that dried included West Africa and the Western Congo basin, whilst some parts of the Eastern Congo were wetter. The Northeast and Eastern Amazon dried whilst the southwest Amazon was wetter. Spatial signatures of the 2015-16 El Niño drought differed from the 2005 and 2010 Amazon droughts but were similar to past El Niño droughts. In 2005 the drought epicentre

was in the Southwest Amazon and in 2010 the drought was more widespread across the Southern Amazon.

The long-term forest plots had slightly hotter climates than the tropical moist forest region as a whole, and during the El Niño had similar temperature increases compared to the region but were more droughted perhaps because El Niño droughts coincided with dry seasons. Plots in South America were drier than the region. The MCWD reduction was on average twice as much in the African plots as the South American plots. MCWD increases uniformly across South American plots but the wettest plots in Africa experienced the greatest drought. The hotter temperatures and variable drought among plots likely well reflect climate of the future.

5.1.2 Temperature and drought impacts on carbon and stem dynamics

The long-term increase in live aboveground biomass of African forests was reduced in the El Niño event, by 35 % (Figure 2.5), but plots remained a carbon sink despite extreme environmental conditions. The South American tropical carbon sink declined by 129 % (Figure 3.4), from a significant sink pre-El Niño, to a small but not significant source in the plot census interval capturing the El Niño.

Drought anomalies reduced net carbon stocks in Africa, as they reduced carbon gains and increased carbon losses (Figure 2.3). Temperature anomalies in Africa increased carbon gains but did not negatively impact carbon dynamics. In South America both temperature and drought anomalies reduced net carbon (Figure 3.6) due to temperature and drought anomalies increasing carbon losses from aboveground biomass mortality. Temperature and drought anomalies in South America did not impact carbon gains. So, drought significantly reduced carbon losses on both continents and gains only in Africa, whereas for temperature, carbon losses only increased in South America. Overall, these trends led to reduced carbon stocks by a mean of 75 % across both continents (Figure 4.4).

5.1.3 Baseline climate can modulate climate anomaly response

Baseline climate modulates carbon responses in South America but has minimal impact for African tropical forests (Figure 4.6). In colder forests productivity increased with greater temperature anomalies and in hotter forests productivity decreased with greater temperature anomalies (Figure 4.7). The threshold was a maximum temperature of 30.8 °C and the decline after this threshold was much greater than the increase in productivity

up until that point. Also, in South America in the El Niño plots with baseline stronger water deficits lost more aboveground biomass carbon (Figure 4.6) and there was a compounding effect of drought such that both baseline drought and drought anomaly increased biomass mortality (Figure 4.5).

5.1.4 Are El Niño responses to temperature and drought consistent across two continents?

Forest responses to the El Niño are similar across the two continents for temperature anomaly and carbon losses but marginally significant for temperature anomaly and net carbon and not for temperature anomaly and carbon gains (Figure 4.5, Table 5.1). The responses of one continent can be predicted based on the other, suggesting a convergence of temperature-response, at least to an El Niño temperature anomaly. This is the first evidence of a universal tropical forest response to temperature anomaly which allows calculations such as for a 1 °C anomaly net carbon losses are 1.7 % ha⁻¹ yr⁻¹.

There is a significant effect of continent on the relationships between MCWD anomaly and net carbon, pre-El Niño MCWD and net carbon, and pre-El Niño MCWD and carbon losses from aboveground biomass mortality (Figure 4.5, Figure 4.6). So, for the same drought anomaly, South American forests lose 0.4 % more carbon.

Drought significantly increased stem losses in both continents, as did temperature. Temperature anomaly increased stem gains, so there was no overall impact of temperature on net stems, but drought anomaly did reduce net stems. Drought reduces net stems by 1 % more in South America for the same drought anomaly.

5.2 Research Implications

Overall, the results from the inventory plots indicate that intact tropical forests have some resistance to El Niño climate anomalies. Even in the most impacted 10% of the 237 plots monitored as part of this study lost only 6.0 ± 1.1 % of their aboveground biomass carbon. El Niño is a quasi-regular climate phenomenon that recurs, so exposure to this type of drought in the past may have allowed adaptation, hence the resistance to El Niño droughts.

Results comparing the continents shows African forests are more resistant to El Niño events due to greater drought-resistance (lower carbon losses), and no baseline climate impact on carbon gains (Chapter 2). Results in this thesis point towards the

vulnerability of South American tropical forests, particularly those that have hotter and drier climates. Intact forest plots in South America with higher mean temperatures respond more negatively to warming than their cooler counterparts and forests with greater seasonal water deficits respond more negatively to drought (Chapter 3). The compounding effects of baseline climate and anomaly in South America suggests that anthropogenic warming is increasingly detrimental for forests, and that it is very important to limit global temperature increases to less than 1.5 °C. With 1.5 °C warming the net carbon impacts in South America will be a loss of at least -2.1 Mg C ha yr⁻¹ (Figure 3.6A) as this is calculated without the effect of baseline climate. To ensure that tropical forests to continue to perform their climate regulating functions, net zero emissions must be reached as soon as possible.

Newer dynamic global vegetation models (DGVMs) try to represent the varied plant functional types tropical forests trees (Fisher et al. 2018). This thesis has demonstrated that there are distinct continental differences in how tropical forests are responding to changing climate, specifically in how African and South American forests respond to drought. These functional differences could likely be incorporated into models without adding substantial complexity and may provide notable improvements to accuracy of model outputs. Results in this thesis could be used to test the capacity of DGVMs to accurately represent tropical forests, firstly by testing whether DGVMs are able to produce the contrasting continental responses to the 2015-16 El Niño – a reduction of the carbon sink by one-third in Africa and its shut-down in South America. Now data is available to compare against model outputs, this simple set up may be a useful way to explore model responses to forcing. Different mortality dynamics for Africa and South America could be investigated by altering mortality losses on the two continents. This might lead to an earlier ending of the carbon sink in Amazonia than in Africa, as predicted by Hubau et al. (2020) as mortality losses determine carbon residence time in models (Galbraith et al. 2013). I also show a threshold for reductions in carbon gains when temperatures are exceeded, and this should be easy to explore with models. Further challenges for DGVMs might include incorporating the elasticity of resistance with to changing species composition. Results in this thesis can help test the ability of models to accurately represent the intact tropical biome, and models could help address the longer-term implications of my findings.

5.3 Future Directions

Continued investment in monitoring plot networks across Africa and South America is vital to understand how forests will continue to respond to climate in a changing world. As plots continue to be measured, and there is more than one post-El Niño remeasurement census, resilience can be formally assessed. Resilience is the capacity of an ecosystem to recover from a disturbance, after incurring losses, whereas resistance is the capacity of an ecosystem to endure disturbance without loss. With multiple post-El Niño censuses forest recovery from disturbance can be measured, rather than just the impact of the disturbance. So, it can be understood whether those forests which are more resistant are also more resilient. Especially important will be assessing whether, and how quickly, South American tropical forests recover from large biomass carbon losses and whether the carbon sink decline identified and predicted in Hubau et al. 2020 will continue into the future. These plot networks must also be ready to capture the next large El Niño event which will likely bring record temperatures given ongoing warming.

Forest plot responses to an extreme climate anomaly can be used to test the diversity-resistance paradigm, as biodiversity is thought to increase ecosystem resistance to climate anomaly perturbation, with evidence to support this idea from grasslands (Isbell et al. 2015). In this thesis, tropical forests in Africa, which are typically less species-rich, are more resistant to climate anomaly than their typically more diverse South American counterparts. Resistance of African tropical forests and vulnerability of some South American forests contrasts with what would be expected with diversity and resistance, but it would be valuable to understand this pattern within each continent.

In analyses presented in this thesis there is an increase in stem recruitment with temperature, not just of light wooded species that tend to grow quickly, but species of all wood densities. During drought, small trees might benefit from light release as the larger, dominant trees lose their leaves or die. Understanding the species composition of these recruits and testing if there is a compositional shift occurring in the forest understory will be valuable as this may affect the climate vulnerability of the long-term carbon sink. Also important is understanding the composition of the overstory; the percentage of deciduous, semideciduous or brevideciduous species, which large trees in the overstory are likely to die in temperature and drought anomalies and whether the deaths of trees in the overstory can be linked to the increase in stem recruitment. Climate driven compositional changes

may confer greater resistance to extreme climate events and there have been long-term climate driven shifts in the floristic composition of tropical forests in the Amazon and Ghana (Fauset et al. 2012, Esquivel-Muelbert et al. 2019, Aguirre-Gutiérrez et al. 2019). Compositional changes may modify carbon responses, so understanding which species do well and which suffer is important for understanding if forests have the capacity to future-proof themselves.

There has been a long-term increase of carbon losses from tree mortality in South America, and an increase in carbon losses in Africa after 2010 in the most intensively monitored plots (Hubau et al. 2020). So, the intact tropical carbon sink has saturated and is decreasing but there is still a large sink, especially in Africa. African productivity is still rising with indications that temperature has not yet limited growth in Africa. Results presented in this thesis, overall, support the results in Hubau et al. 2020 with Africa being more resistant to drought than the Amazon and temperature anomalies having consistent impacts on gains and losses across both continents. This thesis provides some evidence that forests, at least in Africa, are resistant to climate anomalies.

5.4 Summary

This thesis shows that intact tropical moist forest plots in Africa and South America responded differently to the 2015-16 El Niño climate anomaly. In Africa plots remained a carbon sink despite extreme temperatures and drought anomalies, although the sink was reduced by 35 % because drought reduced carbon gains from tree growth. In South America plots were a carbon sink prior to the El Niño but the sink reduced 129 % to be a small, but not significant, source during the El Niño interval, because both temperature and drought increased carbon losses from biomass mortality. Baseline climate exacerbated the carbon losses in South American forests but not in African forests – the first evidence that baseline climate is important when considering climate anomalies. Overall, with the pooled data from both continents, temperature anomalies increased carbon losses. Forests on both continents were vulnerable to temperature, with no effect in Africa alone perhaps because baseline temperatures are not yet hot enough. Drought also increased carbon losses, and for the same amount of drought carbon losses were greater in South America. These results significantly advance understanding of how African and South American tropical forests respond to high temperature and water deficit anomalies. Both continents are already sensitive to drought, but South American forests are more drought-sensitive, and carbon losses of both continents are temperature-

sensitive. Responses to the 2015-16 El Niño climate anomaly show that the net carbon sink in intact tropical forests in Africa and South America may decline further in the hotter and periodically drier climates of the near future.

References

- Adams, H. D., G. A. Barron-gafford, R. L. Minor, A. A. Gardea, L. Patrick, D. J. Law, D. D. Breshears, N. G. McDowell, and T. E. Huxman. 2017a. Temperature response surfaces for mortality risk of tree species with future drought. *Environmental Research Letters* 12:115014.
- Adams, H. D., M. Guardiola-Claramonte, G. A. Barron-Gafford, J. C. Villegas, D. D. Breshears, C. B. Zou, P. A. Troch, and T. E. Huxman. 2009. Temperature sensitivity of drought-induced tree mortality portends increased regional die-off under global-change-type drought. *Proceedings of the National Academy of Sciences of the United States of America* 106:7063–7066.
- Adams, H. D., M. J. B. Zeppel, W. R. L. Anderegg, H. Hartmann, S. M. Landh usser, D. T. Tissue, T. E. Huxman, P. J. Hudson, T. E. Franz, C. D. Allen, L. D. L. Anderegg, G. A. Barron-Gafford, D. J. Beerling, D. D. Breshears, T. J. Brodrribb, H. Bugmann, R. C. Cobb, A. D. Collins, L. T. Dickman, H. Duan, B. E. Ewers, L. Galiano, D. A. Galvez, N. Garcia-Forner, M. L. Gaylord, M. J. Germino, A. Gessler, U. G. Hacke, R. Hakamada, A. Hector, M. W. Jenkins, J. M. Kane, T. E. Kolb, D. J. Law, J. D. Lewis, J.-M. Limousin, D. M. Love, A. K. Macalady, J. Mart nez-Vilalta, M. Mencuccini, P. J. Mitchell, J. D. Muss, M. J. O'Brien, A. P. O'Grady, R. E. Pangle, E. A. Pinkard, F. I. Piper, J. A. Plaut, W. T. Pockman, J. Quirk, K. Reinhardt, F. Ripullone, M. G. Ryan, A. Sala, S. Sevanto, J. S. Sperry, R. Vargas, M. Vennetier, D. A. Way, C. Xu, E. A. Yezpez, and N. G. McDowell. 2017b. A multi-species synthesis of physiological mechanisms in drought-induced tree mortality. *Nature Ecology & Evolution* 1:1285–1291.
- Aguirre-Guti rrez, J., I. Oliveras, S. Rifai, S. Fauset, S. Adu-Bredu, K. Affum-Baffoe, T. R. Baker, T. R. Feldpausch, A. Gvozdevaite, W. Hubau, N. J. B. Kraft, S. L. Lewis, S. Moore,  . Niinemets, T. Peprah, O. L. Phillips, K. Ziemińska, B. Enquist, and Y. Malhi. 2019. Drier tropical forests are susceptible to functional changes in response to a long-term drought. *Ecology Letters* 22:855–865.
- Allen, C. D., D. D. Breshears, and N. G. McDowell. 2015. On underestimation of global vulnerability to tree mortality and forest die-off from hotter drought in the Anthropocene. *Ecosphere* 6:art129.
- Allen, C. D., A. K. Macalady, H. Chenchouni, D. Bachelet, N. McDowell, M. Vennetier, T. Kitzberger, A. Rigling, D. D. Breshears, E. H. (Ted) Hogg, P. Gonzalez, R. Fensham, Z. Zhang, J. Castro, N. Demidova, J.-H. Lim, G. Allard, S. W. Running, A. Semerci, and N. Cobb. 2010. A global overview of drought and heat-induced tree mortality reveals emerging climate change risks for forests. *Forest Ecology and Management* 259:660–684.
- Anderegg, W. R. L., L. D. L. Anderegg, J. A. Berry, and C. B. Field. 2014. Loss of whole-tree hydraulic conductance during severe drought and multi-year forest die-off. *Oecologia* 175:11–23.
- Anderegg, W. R. L., A. P. Ballantyne, W. K. Smith, J. Majkut, S. Rabin, C. Beaulieu, R. Birdsey, J. P. Dunne, R. A. Houghton, R. B. Myneni, Y. Pan, J. L. Sarmiento, N. Serota, E. Shevliakova, P. Tans, and S. W. Pacala. 2015a. Tropical nighttime warming as a dominant driver of variability in the terrestrial carbon sink. *Proceedings of the National Academy of Sciences of the United States of America* 112:15591–6.
- Anderegg, W. R. L., J. A. Hicke, R. A. Fisher, C. D. Allen, J. Aukema, B. Bentz, S. Hood, J. W. Lichstein, A. K. Macalady, N. McDowell, Y. Pan, K. Raffa, A. Sala, J. D. Shaw, N. L. Stephenson, C. Tague, and M. Zeppel. 2015b. Tree mortality from drought, insects, and their interactions in a changing climate. *New Phytologist* 208:674–683.
- Anderegg, W. R. L., J. M. Kane, and L. D. L. Anderegg. 2013. Consequences of widespread tree mortality triggered by drought and temperature stress. *Nature Climate Change* 3:30–36.
- Arag o, L. E. O. C., L. O. Anderson, M. G. Fonseca, T. M. Rosan, L. B. Vedovato, F. H. Wagner, C. V. J. Silva, C. H. L. Silva Junior, E. Arai, A. P. Aguiar, J. Barlow, E. Berenguer, M. N. Deeter, L. G. Domingues, L. Gatti, M. Gloor, Y. Malhi, J. A. Marengo, J. B. Miller, O. L. Phillips, and S. Saatchi. 2018. 21st Century drought-related fires counteract the decline of Amazon deforestation carbon emissions. *Nature Communications* 9:1–12.
- Arag o, L. E. O. C., Y. Malhi, R. M. Roman-Cuesta, S. Saatchi, L. O. Anderson, and Y. E. Shimabukuro. 2007. Spatial patterns and fire response of recent Amazonian droughts. *Geophysical Research Letters* 34:L07701.
- Arag o, L. E. O. C., B. Poulter, J. B. Barlow, L. O. Anderson, Y. Malhi, S. Saatchi, O. L. Phillips, and E.

- Gloor. 2014. Environmental change and the carbon balance of Amazonian forests. *Biological Reviews* 89:913–931.
- Baccini, A., S. J. Goetz, W. S. Walker, N. T. Laporte, M. Sun, D. Sulla-Menashe, J. Hackler, P. S. A. Beck, R. Dubayah, M. A. Friedl, S. Samanta, and R. A. Houghton. 2012. Estimated carbon dioxide emissions from tropical deforestation improved by carbon-density maps. *Nature Climate Change* 2:182–185.
- Banin, L., T. R. Feldpausch, O. L. Phillips, T. R. Baker, J. Lloyd, K. Affum-Baffoe, E. J. M. M. Arets, N. J. Berry, M. Bradford, R. J. W. Brienen, S. Davies, M. Drescher, N. Higuchi, D. W. Hilbert, A. Hladik, Y. Iida, K. A. Salim, A. R. Kassim, D. A. King, G. Lopez-Gonzalez, D. Metcalfe, R. Nilus, K. S. H. Peh, J. M. Reitsma, B. Sonké, H. Taedoumg, S. Tan, L. White, H. Wöll, and S. L. Lewis. 2012. What controls tropical forest architecture? Testing environmental, structural and floristic drivers. *Global Ecology and Biogeography* 21:1179–1190.
- Barlow, J., T. A. Gardner, I. S. Araujo, T. C. Ávila-Pires, A. B. Bonaldo, J. E. Costa, M. C. Esposito, L. V. Ferreira, J. Hawes, M. I. M. Hernandez, M. S. Hoogmoed, R. N. Leite, N. F. Lo-Man-Hung, J. R. Malcolm, M. B. Martins, L. A. M. Mestre, R. Miranda-Santos, A. L. Nunes-Gutjahr, W. L. Overal, L. Parry, S. L. Peters, M. A. Ribeiro, M. N. F. Da Silva, C. Da Silva Motta, and C. A. Peres. 2007. Quantifying the biodiversity value of tropical primary, secondary, and plantation forests. *Proceedings of the National Academy of Sciences of the United States of America* 104:18555–18560.
- Barlow, J., G. D. Lennox, J. Ferreira, E. Berenguer, A. C. Lees, R. Mac Nally, J. R. Thomson, S. F. de B. Ferraz, J. Louzada, V. H. F. Oliveira, L. Parry, R. Ribeiro de Castro Solar, I. C. G. Vieira, L. E. O. C. Aragão, R. A. Begotti, R. F. Braga, T. M. Cardoso, R. C. de O. Jr, C. M. Souza Jr, N. G. Moura, S. S. Nunes, J. V. Siqueira, R. Pardini, J. M. Silveira, F. Z. Vaz-de-Mello, R. C. S. Veiga, A. Venturieri, and T. A. Gardner. 2016. Anthropogenic disturbance in tropical forests can double biodiversity loss from deforestation. *Nature* 535:144–147.
- Barton, K. 2019. MuMIn: Multi-Model Inference, Version 1.43.6.
- Bastos, A., P. Friedlingstein, S. Sitch, C. Chen, A. Mialon, J.-P. Wigneron, V. K. Arora, P. R. Briggs, J. G. Canadell, P. Ciais, F. Chevallier, L. Cheng, C. Delire, V. Haverd, A. K. Jain, F. Joos, E. Kato, S. Lienert, D. Lombardozzi, J. R. Melton, R. Myneni, J. E. M. S. Nabel, J. Pongratz, B. Poulter, C. Rödenbeck, R. Séférian, H. Tian, C. van Eck, N. Viovy, N. Vuichard, A. P. Walker, A. Wiltshire, J. Yang, S. Zaehle, N. Zeng, and D. Zhu. 2018. Impact of the 2015/2016 El Niño on the terrestrial carbon cycle constrained by bottom-up and top-down approaches. *Philosophical Transactions of the Royal Society B: Biological Sciences* 373:20170304.
- Bennett, A. C., N. G. McDowell, C. D. Allen, and K. J. Anderson-Teixeira. 2015. Larger trees suffer most during drought in forests worldwide. *Nature Plants* 1:15139.
- Bonal, D., B. Burban, C. Stahl, F. Wagner, and B. Hérault. 2016. The response of tropical rainforests to drought—lessons from recent research and future prospects. *Annals of Forest Science* 73:27–44.
- Bonan, G. B., M. Williams, R. A. Fisher, and K. W. Oleson. 2014. Modeling stomatal conductance in the Earth system: linking leaf water-use efficiency and water transport along the soil-plant-atmosphere continuum. *Geoscientific Model Development Discussions* 7:3085–3159.
- Breshears, D. D., H. D. Adams, D. Eamus, N. G. McDowell, D. J. Law, R. E. Will, A. P. Williams, and C. B. Zou. 2013. The critical amplifying role of increasing atmospheric moisture demand on tree mortality and associated regional die-off. *Frontiers in Plant Science* 4:2–5.
- Brienen, R. J. W., O. L. Phillips, T. R. Feldpausch, E. Gloor, T. R. Baker, J. Lloyd, G. Lopez-Gonzalez, A. Monteagudo-Mendoza, Y. Malhi, S. L. Lewis, R. Vásquez Martínez, M. Alexiades, E. Álvarez Dávila, P. Alvarez-Loayza, A. Andrade, L. E. O. C. Aragão, A. Araujo-Murakami, E. J. M. M. Arets, L. Arroyo, G. A. Aymard C., O. S. Bánki, C. Baraloto, J. Barroso, D. Bonal, R. G. A. Boot, J. L. C. Camargo, C. V. Castilho, V. Chama, K. J. Chao, J. Chave, J. A. Comiskey, F. Cornejo Valverde, L. da Costa, E. A. de Oliveira, A. Di Fiore, T. L. Erwin, S. Fauset, M. Forsthofer, D. R. Galbraith, E. S. Grahame, N. Groot, B. Hérault, N. Higuchi, E. N. Honorio Coronado, H. Keeling, T. J. Killeen, W. F. Laurance, S. Laurance, J. Licona, W. E. Magnussen, B. S. Marimon, B. H. Marimon-Junior, C. Mendoza, D. A. Neill, E. M. Nogueira, P. Núñez, N. C. Pallqui Camacho, A. Parada, G. Pardo-Molina, J. Peacock, M. Peña-Claros, G. C. Pickavance, N. C. A. Pitman, L. Poorter, A. Prieto, C. A. Quesada, F. Ramírez, H. Ramírez-Angulo, Z. Restrepo, A. Roopsind, A. Rudas, R. P. Salomão, M. Schwarz, N. Silva, J. E. Silva-Espejo, M. Silveira, J. Stropp, J. Talbot, H. ter Steege, J. Teran-Aguilar, J. Terborgh, R. Thomas-Caesar, M. Toledo, M. Torello-Raventos, R. K. Umetsu, G. M. F. van der Heijden, P. van der Hout, I. C. Guimarães Vieira, S. A. Vieira, E. Vilanova, V. A. Vos, and R. J. Zagt. 2015. Long-term decline of the Amazon carbon sink. *Nature* 519:344–348.

- Cabrol, N. A., U. Feister, D. P. Häder, H. Piazena, E. A. Grin, and A. Klein. 2014. Record solar UV irradiance in the tropical Andes. *Frontiers in Environmental Science* 2:15–20.
- Cai, W., G. Wang, A. Santoso, M. J. McPhaden, L. Wu, F.-F. Jin, A. Timmermann, M. Collins, G. Vecchi, M. Lengaigne, M. H. England, D. Dommenges, K. Takahashi, and E. Guilyardi. 2015. Increased frequency of extreme La Niña events under greenhouse warming.
- Caviedes, C. N. 1984. El Niño 1982-83. *Geographical Review* 74:267–290.
- Chave, J., D. Coomes, S. Jansen, S. L. Lewis, N. G. Swenson, and A. E. Zanne. 2009. Towards a worldwide wood economics spectrum. *Ecology Letters* 12:351–366.
- Chave, J., M. Rejou-Mechain, A. Burquez, E. Chidumayo, M. S. Colgan, W. B. C. Delitti, A. Duque, T. Eid, P. M. Fearnside, R. C. Goodman, M. Henry, A. Martinez-Yrizar, W. A. Mugasha, H. C. Muller-Landau, M. Mencuccini, B. W. Nelson, A. Ngomanda, E. M. Nogueira, E. Ortiz-Malavassi, R. Pelissier, P. Ploton, C. M. Ryan, J. G. Saldarriaga, and G. Vieilledent. 2014. Improved allometric models to estimate the aboveground biomass of tropical trees. *Global Change Biology* 20:3177–3190.
- Chen, C., T. Park, X. Wang, S. Piao, B. Xu, R. K. Chaturvedi, R. Fuchs, V. Brovkin, P. Ciais, R. Fensholt, H. Tømmervik, G. Bala, Z. Zhu, R. R. Nemani, and R. B. Myneni. 2019. China and India lead in greening of the world through land-use management. *Nature Sustainability* 2:122–129.
- Choat, B., T. J. Brodribb, C. R. Brodersen, R. A. Duursma, R. López, and B. E. Medlyn. 2018. Triggers of tree mortality under drought. *Nature* 558:531–539.
- Choat, B., S. Jansen, T. J. Brodribb, H. Cochard, S. Delzon, R. Bhaskar, S. J. Bucci, T. S. Feild, S. M. Gleason, U. G. Hacke, A. L. Jacobsen, F. Lens, H. Maherali, J. Martínez-Vilalta, S. Mayr, M. Mencuccini, P. J. Mitchell, A. Nardini, J. Pittermann, R. B. Pratt, J. S. Sperry, M. Westoby, I. J. Wright, and A. E. Zanne. 2012. Global convergence in the vulnerability of forests to drought. *Nature* 491:752–5.
- Clark, D. A., D. B. Clark, and S. F. Oberbauer. 2013. Field-quantified responses of tropical rainforest aboveground productivity to increasing CO₂ and climatic stress, 1997-2009. *Journal of Geophysical Research: Biogeosciences* 118:783–794.
- Clark, D. A., S. C. Piper, C. D. Keeling, and D. B. Clark. 2003. Tropical rain forest tree growth and atmospheric carbon dynamics linked to interannual temperature variation during 1984-2000. *Proceedings of the National Academy of Sciences* 100:5852–5857.
- Clark, D. B., D. A. Clark, and S. F. Oberbauer. 2010. Annual wood production in a tropical rain forest in NE Costa Rica linked to climatic variation but not to increasing CO₂. *Global Change Biology* 16:747–759.
- Collins, M., S.-I. An, W. Cai, A. Ganachaud, E. Guilyardi, F. F. Jin, M. Jochum, M. Lengaigne, S. Power, A. Timmermann, G. Vecchi, and A. Wittenberg. 2010. The impact of global warming on the tropical Pacific Ocean and El Niño. *Nature Geoscience* 3:391–397.
- Condit, R. 1998. Ecological Implications of Changes in Drought Patterns: Shifts in Forest Composition in Panama. *Climatic Change* 39:413–427.
- Copernicus Climate Change Service Climate Data Store (CDS). 2020. Copernicus Climate Change Service (C3S) (2017): ERA5: Fifth generation of ECMWF atmospheric reanalyses of the global climate.
- Croux, C., and C. Dehon. 2010. Influence functions of the Spearman and Kendall correlation measures. *Statistical Methods & Applications* 19:497–515.
- Dai, A., and T. M. L. Wigley. 2000. Global patterns of ENSO-induced precipitation. *Geophysical Research Letters* 27:1283–1286.
- Davidson, E. A., L. V. Verchot, J. Henrique Cattânio, I. L. Ackerman, and J. E. M. Carvalho. 2000. Effects of soil water content on soil respiration in forests and cattle pastures of eastern Amazonia. *Biogeochemistry* 48:53–69.
- Davies, R. B. 2002. Hypothesis Testing When a Nuisance Parameter Is Present Only under the Alternative: Linear Model Case. *Biometrika* 89:484–489.
- Davies, R. B. . 1987. Hypothesis Testing when a Nuisance Parameter is Present Only Under the Alternatives. *Biometrika* 74:33–43.
- Dee, D. P., S. M. Uppala, A. J. Simmons, P. Berrisford, P. Poli, S. Kobayashi, U. Andrae, M. A. Balmaseda, G. Balsamo, P. Bauer, P. Bechtold, A. C. M. Beljaars, L. van de Berg, J. Bidlot, N. Bormann, C. Delsol, R. Dragani, M. Fuentes, A. J. Geer, L. Haimberger, S. B. Healy, H. Hersbach, E. V. Hólm, L. Isaksen, P. Kållberg, M. Köhler, M. Matricardi, A. P. McNally, B. M. Monge-Sanz, J.-J. Morcrette, B.-K. Park, C.

- Peubey, P. de Rosnay, C. Tavorato, J.-N. Thépaut, and F. Vitart. 2011. The ERA-Interim reanalysis: configuration and performance of the data assimilation system. *Quarterly Journal of the Royal Meteorological Society* 137:553–597.
- deMenocal, P. B. 2004. African climate change and faunal evolution during the Pliocene–Pleistocene. *Earth and Planetary Science Letters* 220:3–24.
- Dexter, K. G., M. Lavin, B. M. Torke, A. D. Twyford, T. A. Kursar, P. D. Coley, C. Drake, R. Hollands, and R. T. Pennington. 2017. Dispersal assembly of rain forest tree communities across the Amazon basin. *Proceedings of the National Academy of Sciences* 114:2645–2650.
- Dexter, K. G., B. Smart, C. Baldauf, T. R. Baker, and M. P. Bessike. 2015. Floristics and biogeography of vegetation in seasonally dry tropical regions. *International Forestry Review* 17:10–32.
- Dick, C. W., S. L. Lewis, M. Maslin, and E. Bermingham. 2013. Neogene origins and implied warmth tolerance of Amazon tree species. *Ecology and Evolution* 3:162–169.
- Diniz-Filho, J. A. F., L. M. Bini, and B. A. Hawkins. 2003. Spatial autocorrelation and red herrings in geographical ecology. *Global Ecology and Biogeography* 12:53–64.
- Donoghue, M. J., and M. J. Donoghue. 2008. A phylogenetic perspective on the distribution of plant diversity. *Pnas* 105:11549–11555.
- Doughty, C. E., and M. L. Goulden. 2008. Are tropical forests near a high temperature threshold? *Journal of Geophysical Research: Biogeosciences* 113:n/a-n/a.
- Doughty, C. E., Y. Malhi, A. Araujo-Murakami, D. B. Metcalfe, J. E. Silva-Espejo, L. Arroyo, J. P. Heredia, E. Pardo-Toledo, L. M. Mendizabal, V. D. Rojas-Landivar, M. Vega-Martinez, M. Flores-Valencia, R. Sibling-Rivero, L. Moreno-Vare, L. Jessica Viscarra, T. Chuviru-Castro, M. Osinaga-Becerra, and R. Ledezma. 2014. Allocation trade-offs dominate the response of tropical forest growth to seasonal and interannual drought. *Ecology* 95:2192–2201.
- Duffy, P. B., P. Brando, G. P. Asner, and C. B. Field. 2015. Projections of future meteorological drought and wet periods in the Amazon. *Proceedings of the National Academy of Sciences* 112:13172–13177.
- Eltahir, E. A. B., B. Loux, T. K. Yamana, and A. Bombliès. 2004. A see-saw oscillation between the Amazon and Congo basins. *Geophysical Research Letters* 31:1–4.
- Engelbrecht, B. M. J., L. S. Comita, R. Condit, T. A. Kursar, M. T. Tyree, B. L. Turner, and S. P. Hubbell. 2007. Drought sensitivity shapes species distribution patterns in tropical forests. *Nature* 447:80–82.
- Enquist, B. J., A. J. Abraham, M. B. J. Harfoot, Y. Malhi, and C. E. Doughty. 2020. The megabiota are disproportionately important for biosphere functioning. *Nature Communications* 11:699.
- Esquivel-Muelbert, A., T. R. Baker, K. G. Dexter, S. L. Lewis, H. ter Steege, G. Lopez-Gonzalez, A. Monteagudo Mendoza, R. Brien, T. R. Feldpausch, N. Pitman, A. Alonso, G. van der Heijden, M. Peña-Claros, M. Ahuite, M. Alexiades, E. Álvarez Dávila, A. A. Murakami, L. Arroyo, M. Aulestia, H. Balslev, J. Barroso, R. Boot, A. Cano, V. Chama Moscoso, J. A. Comiskey, F. Cornejo, F. Dallmeier, D. C. Daly, N. Dávila, J. F. Duivenvoorden, A. J. Duque Montoya, T. Erwin, A. Di Fiore, T. Fredericksen, A. Fuentes, R. García-Villacorta, T. Gonzales, J. E. Guevara Andino, E. N. Honorio Coronado, I. Huamantupa-Chuquimaco, T. J. Killeen, Y. Malhi, C. Mendoza, H. Mogollón, P. M. Jørgensen, J. C. Montero, B. Mostacedo, W. Nauray, D. Neill, P. N. Vargas, S. Palacios, W. Palacios Cuenca, N. C. Pallqui Camacho, J. Peacock, J. F. Phillips, G. Pickavance, C. A. Quesada, H. Ramírez-Angulo, Z. Restrepo, C. Reynel Rodríguez, M. R. Paredes, R. Sierra, M. Silveira, P. Stevenson, J. Stropp, J. Terborgh, M. Tirado, M. Toledo, A. Torres-Lezama, M. N. Umaña, L. E. Urrego, R. Vasquez Martinez, L. V. Gamarra, C. I. A. Vela, E. Vilanova Torre, V. Vos, P. von Hildebrand, C. Vriesendorp, O. Wang, K. R. Young, C. E. Zartman, and O. L. Phillips. 2016. Seasonal drought limits tree species across the Neotropics. *Ecography*:1–12.
- Esquivel-Muelbert, A., A. C. Bennett, M. J. P. Sullivan, J. C. A. Baker, Y. Gavish, M. O. Johnson, Y. Wang, A. Chambers-Ostler, M. L. Giannichi, L. Gomes, M. Kalamandeen, K. C. Pattayak, and S. Fauset. 2019. A spatial and temporal risk assessment of the impacts of El Niño on the tropical forest carbon cycle: Theoretical framework, scenarios, and implications. *Atmosphere* 10.
- Esquivel-Muelbert, A., D. Galbraith, K. G. Dexter, T. R. Baker, L. Lewis, P. Meir, L. Rowland, A. Carlos, D. Nepstad, and O. L. Phillips. 2017. Biogeographic distributions of neotropical trees reflect their directly measured drought tolerances. *Scientific Reports*:1–11.
- Esquivel-Muelbert, A., T. R. Baker, K. G. Dexter, S. L. Lewis, R. J. W. Brien, T. R. Feldpausch, J. Lloyd, A. Monteagudo-Mendoza, L. Arroyo, E. Álvarez-Dávila, N. Higuchi, B. S. Marimon, B. H. Marimon-Junior,

- M. Silveira, E. Vilanova, E. Gloor, Y. Malhi, J. Chave, J. Barlow, D. Bonal, N. Davila Cardozo, T. Erwin, S. Fauset, B. Hérault, S. Laurance, L. Poorter, L. Qie, C. Stahl, M. J. P. Sullivan, H. ter Steege, V. A. Vos, P. A. Zuidema, E. Almeida, E. Almeida de Oliveira, A. Andrade, S. A. Vieira, L. Aragão, A. Araujo-Murakami, E. Arets, G. A. Aymard C, C. Baraloto, P. B. Camargo, J. G. Barroso, F. Bongers, R. Boot, J. L. Camargo, W. Castro, V. Chama Moscoso, J. Comiskey, F. Cornejo Valverde, A. C. Lola da Costa, J. del Aguila Pasquel, A. Di Fiore, L. Fernanda Duque, F. Elias, J. Engel, G. Flores Llampazo, D. Galbraith, R. Herrera Fernández, E. Honorio Coronado, W. Hubau, E. Jimenez-Rojas, A. J. N. Lima, R. K. Umetsu, W. Laurance, G. Lopez-Gonzalez, T. Lovejoy, O. Aurelio Melo Cruz, P. S. Morandi, D. Neill, P. Núñez Vargas, N. C. Pallqui Camacho, A. Parada Gutierrez, G. Pardo, J. Peacock, M. Peña-Claros, M. C. Peñuela-Mora, P. Petronelli, G. C. Pickavance, N. Pitman, A. Prieto, C. Quesada, H. Ramírez-Angulo, M. Réjou-Méchain, Z. Restrepo Correa, A. Roopsind, A. Rudas, R. Salomão, N. Silva, J. Silva Espejo, J. Singh, J. Stropp, J. Terborgh, R. Thomas, M. Toledo, A. Torres-Lezama, L. Valenzuela Gamarra, P. J. van de Meer, G. van der Heijden, P. van der Hout, R. Vasquez Martinez, C. Vela, I. C. G. Vieira, and O. L. Phillips. 2019. Compositional response of Amazon forests to climate change. *Global Change Biology* 25:39–56.
- Fauset, S., T. R. Baker, S. L. Lewis, T. R. Feldpausch, K. Affum-Baffoe, E. G. Foli, K. C. Hamer, and M. D. Swaine. 2012. Drought-induced shifts in the floristic and functional composition of tropical forests in Ghana. *Ecology Letters* 15:1120–1129.
- Fedorov, A. V, and S. G. Philander. 2000. Is El Nino Changing ? *Science* 288:1997–2002.
- Feldpausch, T. R., J. Lloyd, S. L. Lewis, R. J. W. Brienen, M. Gloor, A. Monteagudo Mendoza, G. Lopez-Gonzalez, L. Banin, K. Abu Salim, K. Affum-Baffoe, M. Alexiades, S. Almeida, I. Amaral, A. Andrade, L. E. O. C. Aragão, A. Araujo Murakami, E. J. M. M. Arets, L. Arroyo, G. A. Aymard C., T. R. Baker, O. S. Bánki, N. J. Berry, N. Cardozo, J. Chave, J. A. Comiskey, E. Alvarez, A. de Oliveira, A. Di Fiore, G. Djagbletey, T. F. Domingues, T. L. Erwin, P. M. Fearnside, M. B. França, M. A. Freitas, N. Higuchi, Y. Iida, E. Jiménez, A. R. Kassim, T. J. Killeen, W. F. Laurance, J. C. Lovett, Y. Malhi, B. S. Marimon, B. H. Marimon-Junior, E. Lenza, A. R. Marshall, C. Mendoza, D. J. Metcalfe, E. T. A. Mitchard, D. A. Neill, B. W. Nelson, R. Nilus, E. M. Nogueira, A. Parada, K. S.-H. Peh, A. Pena Cruz, M. C. Peñuela, N. C. A. Pitman, A. Prieto, C. A. Quesada, F. Ramírez, H. Ramírez-Angulo, J. M. Reitsma, A. Rudas, G. Saiz, R. P. Salomão, M. Schwarz, N. Silva, J. E. Silva-Espejo, M. Silveira, B. Sonké, J. Stropp, H. E. Taedoumg, S. Tan, H. ter Steege, J. Terborgh, M. Torello-Raventos, G. M. F. van der Heijden, R. Vásquez, E. Vilanova, V. A. Vos, L. White, S. Willcock, H. Woell, and O. L. Phillips. 2012. Tree height integrated into pantropical forest biomass estimates. *Biogeosciences* 9:3381–3403.
- Feldpausch, T. R., O. L. Phillips, R. J. W. Brienen, E. Gloor, J. Lloyd, Y. Malhi, A. Alarcón, E. Á. Dávila, A. Andrade, L. E. O. C. Aragao, L. Arroyo, G. A. C. Aymard, T. R. Baker, C. Baraloto, J. Barroso, D. Bonal, W. Castro, V. Chama, J. Chave, T. F. Domingues, S. Fauset, N. Groot, E. H. Coronado, S. Laurance, W. F. Laurance, S. L. Lewis, J. C. Licona, B. S. Marimon, C. M. Bautista, D. A. Neill, E. A. Oliveira, C. O. Santos, N. C. P. Camacho, A. Prieto, C. A. Quesada, F. Ramírez, A. Rudas, G. Saiz, R. P. Salomão, M. Silveira, H. Steege, J. Stropp, J. Terborgh, G. M. F. Heijden, R. V. Martinez, E. Vilanova, and V. A. Vos. 2016. Amazon forest response to repeated droughts. *Global Biogeochemical Cycles*:1–19.
- Feng, X., A. Porporato, and I. Rodriguez-Iturbe. 2013. Changes in rainfall seasonality in the tropics. *Nature Climate Change* 3:811–815.
- Fetcher, N. 1979. Water relations of five tropical forest trees on Barro Colorado Island, Panama. *Oecologia* 40:229–233.
- Fetcher, N., S. F. Oberhauer, and B. R. Strain. 1985. Vegetation effects on microclimate in lowland tropical forest in Costa Rica.
- Fick, S. E., and R. J. Hijmans. 2017. WorldClim 2: new 1-km spatial resolution climate surfaces for global land areas. *International Journal of Climatology* 37:4302–4315.
- Field, C. B., R. B. Jackson, and H. A. Mooney. 1995. Stomatal responses to increased CO₂: implications from the plant to the global scale. *Plant, Cell & Environment* 18:1214–1225.
- Fisher, R. A., C. D. Koven, W. R. L. Anderegg, B. O. Christoffersen, M. C. Dietze, C. E. Farrior, J. A. Holm, G. C. Hurtt, R. G. Knox, P. J. Lawrence, J. W. Lichstein, M. Longo, A. M. Matheny, D. Medvigy, H. C. Muller-Landau, T. L. Powell, S. P. Serbin, H. Sato, J. K. Shuman, B. Smith, A. T. Trugman, T. Viskari, H. Verbeeck, E. Weng, C. Xu, X. Xu, T. Zhang, and P. R. Moorcroft. 2018. Vegetation demographics in Earth System Models: A review of progress and priorities. *Global Change Biology* 24:35–54.
- Foley, J. a, G. P. Asner, M. H. Costa, M. T. Coe, H. K. Gibbs, E. a Howard, S. Olson, J. Patz, N.

- Ramankutty, R. Defries, and P. Snyder. 2007. Amazonia loss of Amazon revealed : ecosystem Basin forest goods degradation and and in the The Ecological Society. *Frontiers in Ecology and the Environment* 5:25–32.
- Fox, J., S. Weisberg, B. Price, D. Adler, D. Bates, G. Baud-Bovy, B. Bolker, S. Ellison, D. Firth, M. Friendly, G. Gorjanc, S. Graves, R. Heiberger, P. Krivitsky, R. Laboissiere, M. Maechler, G. Monette, D. Murdoch, H. Nilsson, D. Ogle, B. Ripley, W. Venables, S. Walker, D. Winsemius, A. Zeileis, and R-Core. 2020. *car: Companion to Applied Regression, Version 3.0-7*.
- Fu, R., L. Yin, W. Li, P. A. Arias, R. E. Dickinson, L. Huang, S. Chakraborty, K. Fernandes, B. Liebmann, R. Fisher, and R. B. Myneni. 2013. Increased dry-season length over southern Amazonia in recent decades and its implication for future climate projection. *Proceedings of the National Academy of Sciences of the United States of America* 110:18110–18115.
- Fuller, D. O., T. C. Juessup, and A. Salim. 2004. Loss of forest cover in Kalimantan, Indonesia, since the 1997-1998 El Niño. *Conserv. Biol.* 10:249–254.
- Fyllas, N. M., L. P. Bentley, A. Shenkin, G. P. Asner, O. K. Atkin, S. Díaz, B. J. Enquist, W. Farfan-Rios, E. Gloor, R. Guerrieri, W. H. Huasco, Y. Ishida, R. E. Martin, P. Meir, O. Phillips, N. Salinas, M. Silman, L. K. Weerasinghe, J. Zaragoza-Castells, and Y. Malhi. 2017. Solar radiation and functional traits explain the decline of forest primary productivity along a tropical elevation gradient. *Ecology Letters* 20:730–740.
- Galbraith, D., P. E. Levy, S. Sitch, C. Huntingford, P. Cox, M. Williams, and P. Meir. 2010. Multiple mechanisms of Amazonian forest biomass losses in three dynamic global vegetation models under climate change. *New Phytologist* 187:647–665.
- Galbraith, D., Y. Malhi, K. Affum-Baffoe, A. D. A. Castanho, C. E. Doughty, R. A. Fisher, S. L. Lewis, K. S. H. Peh, O. L. Phillips, C. A. Quesada, B. Sonké, and J. Lloyd. 2013. Residence times of woody biomass in tropical forests. *Plant Ecology and Diversity* 6:139–157.
- Gaubert, B., B. B. Stephens, S. Basu, F. Chevallier, F. Deng, E. A. Kort, P. K. Patra, W. Peters, C. Rödenbeck, T. Saeki, D. Schimel, I. Van der Laan-Luijkx, S. Wofsy, and Y. Yin. 2019. Global atmospheric CO₂ inverse models converging on neutral tropical land exchange, but disagreeing on fossil fuel and atmospheric growth rate. *Biogeosciences* 16:117–134.
- Gaudry, A., P. Monfray, G. Polian, and G. Lambert. 1987. The 1982-1983 El Niño: a 6 billion ton CO₂ release. *Tellus B: Chemical and Physical Meteorology* 39:209–213.
- Gentry, A. H. 1988. Tree species richness of upper Amazonian forests. *Ecology* 85:156–159.
- Giardina, F., A. G. Konings, D. Kennedy, S. H. Alemohammad, R. S. Oliveira, M. Uriarte, and P. Gentine. 2018. Tall Amazonian forests are less sensitive to precipitation variability. *Nature Geoscience* 11:405–409.
- Glantz, M. H. 2001. *Currents of Change: Impacts of El Niño and La Niña on Climate and Society*. Page Cambridge University Press. Cambridge University Press.
- Gloor, M., J. Barichivich, G. Ziv, R. Brienen, J. Schöngart, and P. Peylin. 2015. Recent Amazon climate as background for possible ongoing and future changes of Amazon humid forests. *Global Biogeochemical Cycles* 29:1384–1399.
- Gloor, M., R. J. W. Brienen, D. Galbraith, T. R. Feldpausch, J. Schöngart, J. L. Guyot, J. C. Espinoza, J. Lloyd, and O. L. Phillips. 2013. Intensification of the Amazon hydrological cycle over the last two decades. *Geophysical Research Letters* 40:1729–1733.
- Grimm, A. M., S. E. T. Ferraz, and J. Gomes. 1998. Precipitation anomalies in southern Brazil associated with El Niño and La Niña events. *Journal of Climate* 11:2863–2880.
- Del Grosso, S., W. Parton, T. Stohlgren, D. Zheng, D. Bachelet, S. Prince, K. Hibbard, and R. Olson. 2008. Global potential net primary production predicted from vegetation class, precipitation and temperature. *Ecology* 89:2117–2126.
- Guan, K., M. Pan, H. Li, A. Wolf, J. Wu, D. Medvigy, K. K. Caylor, J. Sheffield, E. F. Wood, Y. Malhi, M. Liang, J. S. Kimball, S. R. Saleska, J. Berry, J. Joiner, and A. I. Lyapustin. 2015. Photosynthetic seasonality of global tropical forests constrained by hydroclimate. *Nature Geoscience* 8:284–289.
- Guha, A., T. Banik, R. Roy, and B. K. De. 2017. The effect of El Niño and La Niña on lightning activity: its relation with meteorological and cloud microphysical parameters. *Natural Hazards* 85:403–424.
- Hacke, U. G., J. S. Sperry, W. T. Pockman, S. D. Davis, and K. A. McCulloh. 2001. Trends in wood density

and structure are linked to prevention of xylem implosion by negative pressure. *Oecologia* 126:457–461.

- Hansen, M. C., P. V. Potapov, R. Moore, M. Hancher, S. A. Turubanova, A. Tyukavina, D. Thau, S. V. Stehman, S. J. Goetz, T. R. Loveland, A. Kommareddy, A. Egorov, L. Chini, C. O. Justice, and J. R. G. Townshend. 2013. High-resolution global maps of 21st-century forest cover change. *Science* 342:850–853.
- Hansen, M. C., S. V. Stehman, and P. V. Potapov. 2010. Quantification of global gross forest cover loss. *Proceedings of the National Academy of Sciences of the United States of America* 107:8650–5.
- Harris, I., P. D. Jones, T. J. Osborn, and D. H. Lister. 2014. Updated high-resolution grids of monthly climatic observations - the CRU TS3.10 Dataset. *International Journal of Climatology* 34:623–642.
- Heskel, M. A., O. S. O'Sullivan, P. B. Reich, M. G. Tjoelker, L. K. Weerasinghe, A. Penillard, J. J. G. Egerton, D. Creek, K. J. Bloomfield, J. Xiang, F. Sinca, Z. R. Stangl, A. Martinez-de la Torre, K. L. Griffin, C. Huntingford, V. Hurry, P. Meir, M. H. Turnbull, and O. K. Atkin. 2016. Convergence in the temperature response of leaf respiration across biomes and plant functional types. *Proceedings of the National Academy of Sciences* 113:3832–3837.
- Hoffman, J. S., P. U. Clark, A. C. Parnell, and F. He. 2017. Regional and global sea-surface temperatures during the last interglaciation. *Science* 355:276–279.
- Honorio Coronado, E. N., K. G. Dexter, R. T. Pennington, J. Chave, S. L. Lewis, M. N. Alexiades, E. Alvarez, A. Alves de Oliveira, I. L. Amaral, A. Araujo-Murakami, E. J. M. M. Arets, G. A. Aymard, C. Baraloto, D. Bonal, R. Brienen, C. Cerón, F. Cornejo Valverde, A. Di Fiore, W. Farfan-Rios, T. R. Feldpausch, N. Higuchi, I. Huamantupa-Chuquimaco, S. G. Laurance, W. F. Laurance, G. Lopez-Gonzalez, B. S. Marimon, B. H. Marimon-Junior, A. Monteagudo Mendoza, D. Neill, W. Palacios Cuenca, M. C. Peñuela Mora, N. C. A. Pitman, A. Prieto, C. A. Quesada, H. Ramirez Angulo, A. Rudas, A. R. Ruschel, N. Salinas Revilla, R. P. Salomón, A. Segalin de Andrade, M. R. Silman, W. Spironello, H. ter Steege, J. Terborgh, M. Toledo, L. Valenzuela Gamarra, I. C. G. Vieira, E. Vilanova Torre, V. Vos, and O. L. Phillips. 2015. Phylogenetic diversity of Amazonian tree communities. *Diversity and Distributions* 21:1295–1307.
- Hoorn, C., F. P. Wesselingh, H. ter Steege, M. A. Bermudez, A. Mora, J. Sevink, I. Sanmartín, A. Sanchez-Meseguer, C. L. Anderson, J. P. Figueiredo, C. Jaramillo, D. Riff, F. R. Negri, H. Hooghiemstra, J. Lundberg, T. Stadler, T. Särkinen, and A. Antonelli. 2010. Amazonia Through Time: Andean uplift, climate change, landscape evolution and biodiversity. *Science* 330:927–931.
- Hubau, W., S. L. Lewis, O. L. Phillips, K. Affum-Baffoe, H. Beeckman, A. Cuní-Sanchez, A. K. Daniels, C. E. N. Ewango, S. Fauset, J. M. Mukinzi, D. Sheil, B. Sonké, M. J. P. Sullivan, T. C. H. Sunderland, H. Taedoumg, S. C. Thomas, L. J. T. White, K. A. Abernethy, S. Adu-Bredu, C. A. Amani, T. R. Baker, L. F. Banin, F. Baya, S. K. Begne, A. C. Bennett, F. Benedet, R. Bitariho, Y. E. Bocko, P. Boeckx, P. Boundja, R. J. W. Brienen, T. Brncic, E. Chezeaux, G. B. Chuyong, C. J. Clark, M. Collins, J. A. Comiskey, D. A. Coomes, G. C. Dargie, T. de Haulleville, M. N. D. Kamdem, J.-L. Doucet, A. Esquivel-Muelbert, T. R. Feldpausch, A. Fofanah, E. G. Foli, M. Gilpin, E. Gloor, C. Gonmadje, S. Gourlet-Fleury, J. S. Hall, A. C. Hamilton, D. J. Harris, T. B. Hart, M. B. N. Hockemba, A. Hladik, S. A. Ifo, K. J. Jeffery, T. Jucker, E. K. Yakusu, E. Kearsley, D. Kenfack, A. Koch, M. E. Leal, A. Levesley, J. A. Lindsell, J. Lisingo, G. Lopez-Gonzalez, J. C. Lovett, J.-R. Makana, Y. Malhi, A. R. Marshall, J. Martin, E. H. Martin, F. M. Mbayu, V. P. Medjibe, V. Mihindou, E. T. A. Mitchard, S. Moore, P. K. T. Munishi, N. N. Bengone, L. Ojo, F. E. Ondo, K. S. H. Peh, G. C. Pickavance, A. D. Poulsen, J. R. Poulsen, L. Qie, J. Reitsma, F. Rovero, M. D. Swaine, J. Talbot, J. Taplin, D. M. Taylor, D. W. Thomas, B. Toirambe, J. T. Mukendi, D. Tuagben, P. M. Umunay, G. M. F. van der Heijden, H. Verbeeck, J. Vleminckx, S. Willcock, H. Wöll, J. T. Woods, and L. Zomagho. 2020. Asynchronous carbon sink saturation in African and Amazonian tropical forests. *Nature* 579:80–87.
- Hubau, W., T. De Mil, J. Van den Bulcke, O. L. Phillips, B. Angoboy Ilondea, J. Van Acker, M. J. P. Sullivan, L. Nsenga, B. Toirambe, C. Couralet, L. F. Banin, S. K. Begne, T. R. Baker, N. Bourland, E. Chezeaux, C. J. Clark, M. Collins, J. A. Comiskey, A. Cuní-Sanchez, V. Deklerck, S. Dierickx, J.-L. Doucet, C. E. N. Ewango, T. R. Feldpausch, M. Gilpin, C. Gonmadje, J. S. Hall, D. J. Harris, O. J. Hardy, M.-N. D. Kamdem, E. Kasongo Yakusu, G. Lopez-Gonzalez, J.-R. Makana, Y. Malhi, F. M. Mbayu, S. Moore, J. Mukinzi, G. Pickavance, J. R. Poulsen, J. Reitsma, M. Rousseau, B. Sonké, T. Sunderland, H. Taedoumg, J. Talbot, J. Tshibamba Mukendi, P. M. Umunay, J. Vleminckx, L. J. T. White, L. Zomagho, S. L. Lewis, and H. Beeckman. 2019. The persistence of carbon in the African forest understory. *Nature Plants*.
- Huffman, G. J., D. T. Bolvin, E. J. Nelkin, D. B. Wolff, R. F. Adler, G. Gu, Y. Hong, K. P. Bowman, and E. F.

- Stocker. 2007. The TRMM Multisatellite Precipitation Analysis (TMPA): Quasi-Global, Multiyear, Combined-Sensor Precipitation Estimates at Fine Scales. *Journal of Hydrometeorology* 8:38–55.
- Huijnen, V., M. J. Wooster, J. W. Kaiser, D. L. A. Gaveau, J. Flemming, M. Parrington, A. Inness, D. Murdiyarso, B. Main, and M. Van Weele. 2016. Fire carbon emissions over maritime southeast Asia in 2015 largest since 1997. *Scientific Reports* 6:1–8.
- IPCC. 2012. Managing the risks of extreme events and disasters to advance climate change adaptation. Page Ipcc.
- IPCC. 2018. Global warming of 1.5 °C. Page An IPCC Special Report on the impacts of global warming of 1.5°C above pre-industrial levels and related global greenhouse gas emission pathways, in the context of strengthening the global response to the threat of climate change, sustainable development.
- Isbell, F., D. Craven, J. Connolly, M. Loreau, B. Schmid, C. Beierkuhnlein, T. M. Bezemer, C. Bonin, H. Bruelheide, E. De Luca, A. Ebeling, J. N. Griffin, Q. Guo, Y. Hautier, A. Hector, A. Jentsch, J. Kreyling, V. Lanta, P. Manning, S. T. Meyer, A. S. Mori, S. Naeem, P. A. Niklaus, H. W. Polley, P. B. Reich, C. Roscher, E. W. Seabloom, M. D. Smith, M. P. Thakur, D. Tilman, B. F. Tracy, W. H. Van Der Putten, J. Van Ruijven, A. Weigelt, W. W. Weisser, B. Wilsey, and N. Eisenhauer. 2015. Biodiversity increases the resistance of ecosystem productivity to climate extremes. *Nature* 526:574–577.
- Issartel, J., and C. Coiffard. 2011. Extreme longevity in trees: Live slow, die old? *Oecologia* 165:1–5.
- IUSS Working Group WRB. 2006. World reference base for soil resources 2006. Rome.
- Jackson, R. B. 2005. Trading Water for Carbon with Biological Carbon Sequestration. *Science* 310:1944–1947.
- James, R., R. Washington, and D. P. Rowell. 2013. Implications of global warming for African climate. *Phil Trans R Soc B*:368.
- Jiang, Y., L. Zhou, C. J. Tucker, A. Raghavendra, W. Hua, Y. Y. Liu, and J. Joiner. 2019. Widespread increase of boreal summer dry season length over the Congo rainforest. *Nature Climate Change* 4:1–8.
- Jiménez-Muñoz, J. C., C. Mattar, J. Barichivich, A. Santamaría-Artigas, K. Takahashi, Y. Malhi, J. A. Sobrino, and G. van der Schrier. 2016. Record-breaking warming and extreme drought in the Amazon rainforest during the course of El Niño 2015–2016. *Scientific Reports* 6:33130.
- Jones, I. L., C. A. Peres, M. Benchimol, L. Bunnefeld, and D. H. Dent. 2017. Woody lianas increase in dominance and maintain compositional integrity across an Amazonian dam-induced fragmented landscape. *PLoS ONE* 12:1–19.
- Keenan, R. J., G. A. Reams, F. Achard, J. V. de Freitas, A. Grainger, and E. Lindquist. 2015. Dynamics of global forest area: Results from the FAO Global Forest Resources Assessment 2015. *Forest Ecology and Management* 352:9–20.
- Keenan, T. F., D. Y. Hollinger, G. Bohrer, D. Dragoni, J. W. Munger, H. P. Schmid, and A. D. Richardson. 2013. Increase in forest water-use efficiency as atmospheric carbon dioxide concentrations rise. *Nature* 499:324–327.
- Kohyama, T. S., T. I. Kohyama, and D. Sheil. 2018. Definition and estimation of vital rates from repeated censuses: Choices, comparisons and bias corrections focusing on trees. *Methods in Ecology and Evolution* 9:809–821.
- Kume, T., N. Tanaka, K. Kuraji, H. Komatsu, N. Yoshifuji, T. M. Saitoh, M. Suzuki, and T. Kumagai. 2011. Ten-year evapotranspiration estimates in a Bornean tropical rainforest. *Agricultural and Forest Meteorology* 151:1183–1192.
- Leigh, E. G., D. M. Windsor, A. S. Rand, and R. B. Foster. 1990. The Impact of the “El Niño” Drought of 1982–83 on a Panamanian Semideciduous Forest. *Elsevier Oceanography Series* 52:473–486.
- Leighton, N., and M. Wirawan. 1986. Catastrophic drought and fire in Borneo tropical rain forest associated with the 1982–1983 El Niño southern oscillation event. *Tropical rain forests and the world atmosphere*.
- Leitold, V., D. C. Morton, M. Longo, M. N. dos-Santos, M. Keller, and M. Scaranello. 2018. El Niño drought increased canopy turnover in Amazon forests. *New Phytologist*:959–971.
- Lewis, S. L. 2006. Tropical forests and the changing earth system. *Philosophical Transactions of the Royal Society B: Biological Sciences* 361:195–210.
- Lewis, S. L., P. M. Brando, O. L. Phillips, G. M. F. van der Heijden, and D. Nepstad. 2011. The 2010 Amazon drought. *Science (New York, N.Y.)* 331:554.

- Lewis, S. L., D. P. Edwards, and D. Galbraith. 2015. Increasing human dominance of tropical forests. *Science* 349:827–832.
- Lewis, S. L., G. Lopez-Gonzalez, B. Sonké, K. Affum-Baffoe, T. R. Baker, L. O. Ojo, O. L. Phillips, J. M. Reitsma, L. White, J. A. Comiskey, M.-N. D. K. C. E. N. Ewango, T. R. Feldpausch, A. C. Hamilton, M. Gloor, T. Hart, A. Hladik, J. Lloyd, J. C. Lovett, J.-R. Makana, Y. Malhi, F. M. Mbago, H. J. Ndangalasi, J. Peacock, K. S.-H. Peh, D. Sheil, T. Sunderland, M. D. Swaine, J. Taplin, D. Taylor, S. C. Thomas, R. Votere, and H. Wöll. 2009. Increasing carbon storage in intact African tropical forests. *Nature* 457:1003–1006.
- Lewis, S. L., Y. Malhi, and O. L. Phillips. 2004. Fingerprinting the impacts of global change on tropical forests. *Philosophical Transactions of the Royal Society B: Biological Sciences* 359:437–462.
- Lewis, S. L., B. Sonke, T. Sunderland, S. K. Begne, G. Lopez-Gonzalez, G. M. F. van der Heijden, O. L. Phillips, K. Affum-Baffoe, T. R. Baker, L. Banin, J.-F. Bastin, H. Beeckman, P. Boeckx, J. Bogaert, C. De Canniere, E. Chezeaux, C. J. Clark, M. Collins, G. Djagbletey, M. N. K. Djuikouo, V. Droissart, J.-L. Doucet, C. E. N. Ewango, S. Fauset, T. R. Feldpausch, E. G. Foli, J.-F. Gillet, A. C. Hamilton, D. J. Harris, T. B. Hart, T. de Haulleville, A. Hladik, K. Hufkens, D. Huygens, P. Jeanmart, K. J. Jeffery, E. Kearsley, M. E. Leal, J. Lloyd, J. C. Lovett, J.-R. Makana, Y. Malhi, A. R. Marshall, L. Ojo, K. S.-H. Peh, G. Pickavance, J. R. Poulsen, J. M. Reitsma, D. Sheil, M. Simo, K. Steppe, H. E. Taedoumg, J. Talbot, J. R. D. Taplin, D. Taylor, S. C. Thomas, B. Toirambe, H. Verbeeck, J. Vleminckx, L. J. T. White, S. Willcock, H. Woell, and L. Zemagho. 2013. Above-ground biomass and structure of 260 African tropical forests. *Philosophical Transactions of the Royal Society B: Biological Sciences* 368:20120295–20120295.
- Lindenmayer, D. B., and W. F. Laurance. 2017. The ecology, distribution, conservation and management of large old trees. *Biological Reviews* 92:1434–1458.
- Liu, J., K. W. Bowman, D. S. Schimel, N. C. Parazoo, Z. Jiang, M. Lee, A. A. Bloom, D. Wunch, C. Frankenberg, Y. Sun, C. W. O'Dell, K. R. Gurney, D. Menemenlis, M. Gierach, D. Crisp, and A. Eldering. 2017. Contrasting carbon cycle responses of the tropical continents to the 2015–2016 El Niño. *Science* 358:eaam5690.
- Liu, N., C. Liu, and T. Lavigne. 2019. The variation of the intensity, height and size of precipitation systems with El Niño–Southern Oscillation in the tropics and subtropics. *Journal of Climate*:JCLI-D-18-0766.1.
- Lloyd, J., and G. D. Farquhar. 2008. Effects of rising temperatures and [CO₂] on the physiology of tropical forest trees. *Philosophical Transactions of the Royal Society B: Biological Sciences* 363:1811–1817.
- Lopez-Gonzalez, G., S. L. Lewis, M. Burkitt, and O. L. Phillips. 2011. ForestPlots.net: a web application and research tool to manage and analyse tropical forest plot data. *Journal of Vegetation Science* 22:610–613.
- Lopez-Gonzalez, G., M. J. P. Sullivan, and T. R. Baker. 2015. BiomasaFP: Tools for analysing data downloaded from ForestPlots.net. R package version.
- Malhi, Y. 2012. The productivity, metabolism and carbon cycle of tropical forest vegetation. *Journal of Ecology* 100:65–75.
- Malhi, Y., T. A. Gardner, G. R. Goldsmith, M. R. Silman, and P. Zelazowski. 2014. Tropical Forests in the Anthropocene. *Annual Review of Environment and Resources* 39:125–159.
- Malhi, Y., C. A. J. Girardin, G. R. Goldsmith, C. E. Doughty, N. Salinas, D. B. Metcalfe, W. Huaraca Huasco, J. E. Silva-Espejo, J. del Aguilla-Pasquell, F. Farfán Amézquita, L. E. O. C. Aragão, R. Guerrieri, F. Y. Ishida, N. H. A. Bahar, W. Farfan-Rios, O. L. Phillips, P. Meir, and M. Silman. 2017. The variation of productivity and its allocation along a tropical elevation gradient: a whole carbon budget perspective. *New Phytologist* 214:1019–1032.
- Malhi, Y., P. Meir, and S. Brown. 2002a. Capturing Carbon and Conserving Biodiversity. *Phil Trans R Soc* 360:1567–1591.
- Malhi, Y., O. L. Phillips, J. Lloyd, T. Baker, J. Wright, S. Almeida, L. Arroyo, T. Frederiksen, J. Grace, N. Higuchi, T. Killeen, W. F. Laurance, C. Leaña, S. Lewis, P. Meir, A. Monteagudo, D. Neill, P. Núñez Vargas, S. N. Panfil, S. Patiño, N. Pitman, C. A. Quesada, A. Rudas-Ll., R. Salomão, S. Saleska, N. Silva, M. Silveira, W. G. Sombroek, R. Valencia, R. Vásquez Martínez, I. C. G. Vieira, and B. Vinceti. 2002b. An international network to monitor the structure, composition and dynamics of Amazonian forests (RAINFOR). *Journal of Vegetation Science* 13:439.
- Malhi, Y., L. Rowland, L. E. O. C. Araga, and R. A. Fisher. 2018. New insights into the variability of the

- tropical land carbon cycle from the El Niño of 2015/2016. *Philosophical Transactions of the Royal Society B: Biological Sciences* 373.
- Malhi, Y., and J. Wright. 2004. Spatial patterns and recent trends in the climate of tropical rainforest regions. *Philosophical Transactions of the Royal Society of London. Series B: Biological Sciences* 359:311–329.
- van Mantgem, P. J., N. L. Stephenson, J. C. Byrne, L. D. Daniels, J. F. Franklin, P. Z. Fulé, M. E. Harmon, A. J. Larson, J. M. Smith, A. H. Taylor, and T. T. Veblen. 2009. Widespread increase of tree mortality rates in the western United States. *Science (New York, N.Y.)* 323:521–4.
- Martin, A. R., M. Doraisami, and S. C. Thomas. 2018. Global patterns in wood carbon concentration across the world's trees and forests. *Nature Geoscience* 11:915–920.
- Masih, I., S. Maskey, F. E. F. Mussá, and P. Trambauer. 2014. A review of droughts on the African continent: a geospatial and long-term perspective. *Hydrol. Earth Syst. Sci* 18:3635–3649.
- Mattson, W. J., and R. A. Haack. 1987. The role of drought in outbreaks of plant-eating insects. *Bioscience* 37:110–118.
- McDonald, J. H. 2014. Analysis of Covariance. Pages 220–228 *Handbook of Biological Statistics*. 3rd Ed. Sparky House Publishing, Baltimore, Maryland.
- McDowell, N., C. D. Allen, K. Anderson-Teixeira, P. Brando, R. Brienen, J. Chambers, B. Christoffersen, S. Davies, C. Doughty, A. Duque, F. Espirito-Santo, R. Fisher, C. G. Fontes, D. Galbraith, D. Goodsman, C. Grossiord, H. Hartmann, J. Holm, D. J. Johnson, A. R. Kassim, M. Keller, C. Koven, L. Kueppers, T. Kumagai, Y. Malhi, S. M. McMahon, M. Mencuccini, P. Meir, P. Moorcroft, H. C. Muller-Landau, O. L. Phillips, T. Powell, C. A. Sierra, J. Sperry, J. Warren, C. Xu, and X. Xu. 2018. Drivers and mechanisms of tree mortality in moist tropical forests. *New Phytologist* 219:851–869.
- McDowell, N. G. 2011. Mechanisms Linking Drought, Hydraulics, Carbon Metabolism, and Vegetation Mortality. *Source: Plant Physiology* 155:1051–1059.
- McDowell, N. G., and C. D. Allen. 2015. Darcy's law predicts widespread forest mortality under climate warming. *Nature Climate Change* in press.
- McDowell, N. G., A. P. Williams, C. Xu, W. T. Pockman, L. T. Dickman, S. Sevanto, R. Pangle, J. Limousin, J. Plaut, D. S. Mackay, J. Ogee, J. C. Domec, C. D. Allen, R. A. Fisher, X. Jiang, J. D. Muss, D. D. Breshears, S. A. Rauscher, and C. Koven. 2016. Multi-scale predictions of massive conifer mortality due to chronic temperature rise. *Nature Climate Change* 6:295–300.
- McDowell, N., W. T. Pockman, C. D. Allen, D. D. Breshears, N. Cobb, T. Kolb, J. Plaut, J. Sperry, A. West, D. G. Williams, and E. A. Yepez. 2008. Mechanisms of plant survival and mortality during drought: why do some plants survive while others succumb to drought? *The New phytologist* 178:719–39.
- McGloin, R., L. Šigut, M. Fischer, L. Foltýnová, S. Chawla, M. Trnka, M. Pavelka, and M. V. Marek. 2019. Available Energy Partitioning During Drought at Two Norway Spruce Forests and a European Beech Forest in Central Europe. *Journal of Geophysical Research: Atmospheres* 124:3726–3742.
- McGregor, G. R., and S. Nieuwolt. 1998. *Tropical climatology: an introduction to the climates of the low latitudes*. Wiley.
- Meinzer, F. C., D. M. Johnson, B. Lachenbruch, K. A. McCulloh, and D. R. Woodruff. 2009. Xylem hydraulic safety margins in woody plants: Coordination of stomatal control of xylem tension with hydraulic capacitance. *Functional Ecology* 23:922–930.
- Met Office. 2020. ENSO impacts. <https://www.metoffice.gov.uk/research/climate/seasonal-to-decadal/gpc-outlooks/el-nino-la-nina/enso-impacts>.
- Metcalfe, D. B., P. Meir, L. E. O. C. Aragão, R. Lobo-do-Vale, D. Galbraith, R. A. Fisher, M. M. Chaves, J. P. Maroco, A. C. L. da Costa, S. S. de Almeida, A. P. Braga, P. H. L. Gonçalves, J. de Athaydes, M. da Costa, T. T. B. Portela, A. A. R. de Oliveira, Y. Malhi, and M. Williams. 2010. Shifts in plant respiration and carbon use efficiency at a large-scale drought experiment in the eastern Amazon. *New Phytologist* 187:608–621.
- Mitchard, E. T. A. 2018. The tropical forest carbon cycle and climate change. *Nature* 559:527–534.
- Mori, A. S. 2019. Local and biogeographic determinants and stochasticity of tree population demography. *Journal of Ecology* 107:1276–1287.
- Muggeo, V. M. R. 2003. Estimating regression models with unknown break-points. *Statistics in Medicine* 22:3055–3071.

- Nakagawa, M., K. Tanaka, T. Nakashizuka, T. Ohkubo, T. Kato, T. Maeda, K. Sato, H. Miguchi, H. Nagamasu, K. Ogino, S. Teo, A. A. Hamid, and L. H. Seng. 2000. Impact of severe drought associated with the 1997–1998 El Niño in a tropical forest in Sarawak. *Journal of Tropical Ecology* 16:355–367.
- Nascimento, M. N., G. S. Martins, R. C. Cordeiro, B. Turcq, L. S. Moreira, and M. B. Bush. 2019. Vegetation response to climatic changes in western Amazonia over the last 7,600 years. *Journal of Biogeography*:1–18.
- Nemani, R. R. 2003. Climate-Driven Increases in Global Terrestrial Net Primary Production from 1982 to 1999. *Science* 300:1560–1563.
- Nepstad, D. C., I. M. Tohver, D. Ray, and P. Moutinho. 2007. Mortality of Large Trees and Lianas following Experimental Drought in an Amazon Forest. *Ecology* 88:2259–2269.
- Nicholson, S. E., B. Some, and B. Kone. 2000. An analysis of recent rainfall conditions in West Africa, including the rainy seasons of the 1997 El Niño and the 1998 La Niña years. *Journal of Climate* 13:2628–2640.
- NOAA. 2018. Global Climate Report - Annual 2017. National Centers for Environmental Information 2016:1–11.
- Olson, D. M., E. Dinerstein, E. D. Wikramanayake, N. D. Burgess, G. V. N. Powell, E. C. Underwood, J. A. D'Amico, I. Itoua, H. E. Strand, J. C. Morrison, C. J. Loucks, T. F. Allnutt, T. H. Ricketts, Y. Kura, J. F. Lamoreux, W. W. Wettengel, P. Hedao, and K. R. Kassem. 2001. Terrestrial Ecoregions of the World: A New Map of Life on Earth. *BioScience* 51:933–938.
- Page, S. E., F. Siegert, J. O. Rieley, H.-D. V. Boehm, A. Jaya, and S. Limin. 2002. The amount of carbon released from peat and forest fires in Indonesia during 1997. *Nature* 420:61–65.
- Palmer, P. I., L. Feng, D. Baker, F. Chevallier, H. Bösch, and P. Somkuti. 2019. Net carbon emissions from African biosphere dominate pan-tropical atmospheric CO₂ signal. *Nature Communications* 10:3344.
- Pan, Y., R. a Birdsey, J. Fang, R. Houghton, P. E. Kauppi, W. a Kurz, O. L. Phillips, A. Shvidenko, S. L. Lewis, J. G. Canadell, P. Ciais, R. B. Jackson, S. W. Pacala, a D. McGuire, S. Piao, A. Rautiainen, S. Sitch, and D. Hayes. 2011. A Large and Persistent Carbon Sink in the World's Forests. *Science* 333:988–993.
- Panisset, J. S., R. Libonati, C. M. P. Gouveia, F. Machado-Silva, D. A. França, J. R. A. França, and L. F. Peres. 2018. Contrasting patterns of the extreme drought episodes of 2005, 2010 and 2015 in the Amazon Basin. *International Journal of Climatology* 38:1096–1104.
- Parmentier, I., Y. Malhi, B. Senterre, R. J. Whittaker, A. Alonso, M. P. B. Balinga, A. Bakayoko, F. Bongers, C. Chatelain, J. A. Comiskey, R. Cortay, M.-N. D. Kamdem, J.-L. Doucet, L. Gautier, W. D. Hawthorne, Y. A. Issembe, F. N. Kouamé, L. A. Kouka, M. E. Leal, J. Lejoly, S. L. Lewis, L. Nusbaumer, M. P. E. Parren, K. S.-H. Peh, O. L. Phillips, D. Sheil, B. Sonké, M. S. M. Sosef, T. C. H. Sunderland, J. Stropp, H. Ter Steege, M. D. Swaine, M. G. P. Tchouto, B. S. Van Gernerden, J. L. C. H. Van Valkenburg, and H. Wöll. 2007. The odd man out? Might climate explain the lower tree α -diversity of African rain forests relative to Amazonian rain forests? *Journal of Ecology* 95:1058–1071.
- Phillips, O. L., L. E. O. C. Aragao, S. L. Lewis, J. B. Fisher, J. Lloyd, G. Lopez-Gonzalez, Y. Malhi, A. Monteagudo, J. Peacock, C. A. Quesada, G. van der Heijden, S. Almeida, I. Amaral, L. Arroyo, G. Aymard, T. R. Baker, O. Banki, L. Blanc, D. Bonal, P. Brando, J. Chave, A. C. A. de Oliveira, N. D. Cardozo, C. I. Czimczik, T. R. Feldpausch, M. A. Freitas, E. Gloor, N. Higuchi, E. Jimenez, G. Lloyd, P. Meir, C. Mendoza, A. Morel, D. A. Neill, D. Nepstad, S. Patino, M. C. Penuela, A. Prieto, F. Ramirez, M. Schwarz, J. Silva, M. Silveira, A. S. Thomas, H. t. Steege, J. Stropp, R. Vasquez, P. Zelazowski, E. A. Davila, S. Andelman, A. Andrade, K.-J. Chao, T. Erwin, A. Di Fiore, E. H. C., H. Keeling, T. J. Killeen, W. F. Laurance, A. P. Cruz, N. C. A. Pitman, P. N. Vargas, H. Ramirez-Angulo, A. Rudas, R. Salamao, N. Silva, J. Terborgh, and A. Torres-Lezama. 2009. Drought Sensitivity of the Amazon Rainforest. *Science* 323:1344–1347.
- Phillips, O. L., T. R. Baker, T. R. Feldpausch, and R. J. W. Brienen. 2010a. RAINFOR field manual for plot establishment and remeasurement.
- Phillips, O. L., G. van der Heijden, S. L. Lewis, G. López-González, L. E. O. C. Aragão, J. Lloyd, Y. Malhi, A. Monteagudo, S. Almeida, E. A. Dávila, I. Amaral, S. Andelman, A. Andrade, L. Arroyo, G. Aymard, T. R. Baker, L. Blanc, D. Bonal, Á. C. A. de Oliveira, K.-J. Chao, N. D. Cardozo, L. da Costa, T. R. Feldpausch, J. B. Fisher, N. M. Fyllas, M. A. Freitas, D. Galbraith, E. Gloor, N. Higuchi, E. Honorio, E. Jiménez, H. Keeling, T. J. Killeen, J. C. Lovett, P. Meir, C. Mendoza, A. Morel, P. N. Vargas, S. Patiño, K. S.-H. Peh, A. P. Cruz, A. Prieto, C. A. Quesada, F. Ramírez, H. Ramírez, A. Rudas, R. Salamão, M.

- Schwarz, J. Silva, M. Silveira, J. W. Ferry Slik, B. Sonké, A. S. Thomas, J. Stropp, J. R. D. Taplin, R. Vásquez, and E. Vilanova. 2010b. Drought-mortality relationships for tropical forests. *New Phytologist* 187:631–646.
- Phillips, O. L., R. Vésquez Martínez, L. Arroyo, T. R. Baker, T. Killeen, S. L. Lewis, Y. Malhi, A. Monteagudo Mendoza, D. Neill, P. Núñez Vargas, M. Alexiades, C. Cerón, A. Di Flore, T. Erwin, A. Jardim, W. Palacios, M. Saldias, and B. Vinceti. 2002. Increasing dominance of large lianas in Amazonian forests. *Nature* 418:770–774.
- Piao, S., S. Sitch, P. Ciais, P. Friedlingstein, P. Peylin, X. Wang, A. Ahlström, A. Anav, J. G. Canadell, N. Cong, C. Huntingford, M. Jung, S. Levis, P. E. Levy, J. Li, X. Lin, M. R. Lomas, M. Lu, Y. Luo, Y. Ma, R. B. Myneni, B. Poulter, Z. Sun, T. Wang, N. Viovy, S. Zaehle, and N. Zeng. 2013. Evaluation of terrestrial carbon cycle models for their response to climate variability and to CO₂ trends. *Global Change Biology* 19:2117–2132.
- Powers, J. S., G. Vargas-G, T. J. Brodribb, N. B. Schwartz, D. Perez-Aviles, C. M. Smith-Martin, J. M. Becknell, F. Aureli, R. Blanco, E. Calderón-Morales, J. C. Calvo-Alvarado, A. J. Calvo-Obando, M. M. Chavarría, D. Carvajal-Vanegas, C. Dionisio Jiménez-Rodríguez, E. Murillo Chacon, C. M. Schaffner, L. K. Werden, X. Xu, and D. Medvigy. 2020. A catastrophic tropical drought kills hydraulically vulnerable tree species. *Global Change Biology:gcb*.15037.
- Putz, F. E., and K. H. Redford. 2010. The importance of defining “Forest”: Tropical forest degradation, deforestation, long-term phase shifts, and further transitions. *Biotropica* 42:10–20.
- Qie, L., S. L. Lewis, M. J. P. Sullivan, G. Lopez-Gonzalez, G. C. Pickavance, T. Sunderland, P. Ashton, W. Hubau, K. Abu Salim, S.-I. Aiba, L. F. Banin, N. Berry, F. Q. Brearley, D. F. R. P. Burslem, M. Dančák, S. J. Davies, G. Fredriksson, K. C. Hamer, R. Hédl, L. K. Kho, K. Kitayama, H. Krisnawati, S. Lhota, Y. Malhi, C. Maycock, F. Metali, E. Mirmanto, L. Nagy, R. Nilus, R. Ong, C. A. Pendry, A. D. Poulsen, R. B. Primack, E. Rutishauser, I. Samsuodin, B. Saragih, P. Sist, J. W. F. Slik, R. S. Sukri, M. Svátek, S. Tan, A. Tjoa, M. van Nieuwstadt, R. R. E. Vernimmen, I. Yassir, P. S. Kidd, M. Fitriadi, N. K. H. Ideris, R. M. Serudin, L. S. Abdullah Lim, M. S. Saparudin, and O. L. Phillips. 2017. Long-term carbon sink in Borneo’s forests halted by drought and vulnerable to edge effects. *Nature Communications* 8:1966.
- Le Quéré, C., R. M. Andrew, J. G. Canadell, S. Sitch, J. Ivar Korsbakken, G. P. Peters, A. C. Manning, T. A. Boden, P. P. Tans, R. A. Houghton, R. F. Keeling, S. Alin, O. D. Andrews, P. Anthoni, L. Barbero, L. Bopp, F. Chevallier, L. P. Chini, P. Ciais, K. Currie, C. Delire, S. C. Doney, P. Friedlingstein, T. Gkritzalis, I. Harris, J. Hauck, V. Haverd, M. Hoppema, K. Klein Goldewijk, A. K. Jain, E. Kato, A. Körtzinger, P. Landschützer, N. Lefèvre, A. Lenton, S. Lienert, D. Lombardozzi, J. R. Melton, N. Metzl, F. Millero, P. M. S. Monteiro, D. R. Munro, J. E. M. S. Nabel, S. I. Nakaoka, K. O’Brien, A. Olsen, A. M. Omar, T. Ono, D. Pierrot, B. Poulter, C. Rödenbeck, J. Salisbury, U. Schuster, J. Schwinger, R. Séférian, I. Skjelvan, B. D. Stocker, A. J. Sutton, T. Takahashi, H. Tian, B. Tilbrook, I. T. Van Der Laan-Luijkx, G. R. Van Der Werf, N. Viovy, A. P. Walker, A. J. Wiltshire, and S. Zaehle. 2016. Global Carbon Budget 2016. *Earth System Science Data* 8:605–649.
- Le Quéré, C., R. M. Andrew, P. Friedlingstein, S. Sitch, J. Pongratz, A. C. Manning, J. I. Korsbakken, G. P. Peters, J. G. Canadell, R. B. Jackson, T. A. Boden, P. P. Tans, O. D. Andrews, V. K. Arora, D. C. E. Bakker, L. Barbero, M. Becker, R. A. Betts, L. Bopp, F. Chevallier, L. P. Chini, P. Ciais, C. E. Cosca, J. Cross, K. Currie, T. Gasser, I. Harris, J. Hauck, V. Haverd, R. A. Houghton, C. W. Hunt, G. Hurtt, T. Ilyina, A. K. Jain, E. Kato, M. Kautz, R. F. Keeling, K. Klein Goldewijk, A. Körtzinger, P. Landschützer, N. Lefèvre, A. Lenton, S. Lienert, I. Lima, D. Lombardozzi, N. Metzl, F. Millero, P. M. S. Monteiro, D. R. Munro, J. E. M. S. Nabel, S.-I. Nakaoka, Y. Nojiri, X. A. Padin, A. Peregón, B. Pfeil, D. Pierrot, B. Poulter, G. Rehder, J. Reimer, C. Rödenbeck, J. Schwinger, R. Séférian, I. Skjelvan, B. D. Stocker, H. Tian, B. Tilbrook, F. N. Tubiello, I. T. Van Der Laan-Luijkx, G. R. Van Der Werf, S. Van Heuven, N. Viovy, N. Vuichard, A. P. Walker, A. J. Watson, A. J. Wiltshire, S. Zaehle, and D. Zhu. 2018. Global Carbon Budget 2017. *Earth Syst. Sci. Data* 10:405–448.
- Quesada, C. A., J. Lloyd, M. Schwarz, S. Patiño, T. R. Baker, C. Czimczik, N. M. Fyllas, L. Martinelli, G. B. Nardoto, J. Schmerler, A. J. B. Santos, M. G. Hodnett, R. Herrera, F. J. Luizão, A. Arneeth, G. Lloyd, N. Dezzio, I. Hilke, I. Kuhlmann, M. Raessler, W. A. Brand, H. Geilmann, J. O. M. Filho, F. P. Carvalho, R. N. A. Filho, J. E. Chaves, O. F. Cruz, T. P. Pimentel, and R. Paiva. 2010. Variations in chemical and physical properties of Amazon forest soils in relation to their genesis. *Biogeosciences* 7:1515–1541.
- Quesada, C. A., O. L. Phillips, M. Schwarz, C. I. Czimczik, T. R. Baker, S. Patiño, N. M. Fyllas, M. G. Hodnett, R. Herrera, S. Almeida, E. Alvarez Dávila, A. Arneeth, L. Arroyo, K. J. Chao, N. Dezzio, T. Erwin, A. Di Fiore, N. Higuchi, E. Honorio Coronado, E. M. Jimenez, T. Killeen, A. T. Lezama, G. Lloyd, G. López-González, F. J. Luizão, Y. Malhi, A. Monteagudo, D. A. Neill, P. Núñez Vargas, R. Paiva, J.

- Peacock, M. C. Peñuela, A. Peña Cruz, N. Pitman, N. Priante Filho, A. Prieto, H. Ramírez, A. Rudas, R. Salomão, A. J. B. Santos, J. Schmerler, N. Silva, M. Silveira, R. Vásquez, I. Vieira, J. Terborgh, and J. Lloyd. 2012. Basin-wide variations in Amazon forest structure and function are mediated by both soils and climate. *Biogeosciences* 9:2203–2246.
- Raich, J. W., A. E. Russell, and P. M. Vitousek. 1997. Primary productivity and ecosystem development along an elevational gradient on Mauna Loa, Hawai'i. *Ecology* 78:707–721.
- Richards, P. W., R. P. D. Walsh, I. C. Baillie, and P. Greig-Smith. 1996. *The Tropical Rain Forest: An Ecological Study*. Cambridge University Press.
- Roberts, J., O. M. R. Cabral, and L. F. de Aguiar. 1990a. Stomatal and boundary-layer conductances in an Amazonian terra firme rain forest. *Journal of Applied Ecology* 27:336–353.
- Roberts, J., O. M. R. Cabral, and L. F. De Aguiar. 1990b. Stomatal and Boundary-Layer Conductance in an Amazonian terra Firme Rain Forest. *Journal of Applied Ecology* 27:336–353.
- Rowland, L., A. C. L. Da Costa, D. R. Galbraith, R. S. Oliveira, O. J. Binks, A. A. R. Oliveira, A. M. Pullen, C. E. Doughty, D. B. Metcalfe, S. S. Vasconcelos, L. V. Ferreira, Y. Malhi, J. Grace, M. Mencuccini, and P. Meir. 2015. Death from drought in tropical forests is triggered by hydraulics not carbon starvation. *Nature* 528:119–122.
- Rubio, V. E., and M. Detto. 2017. Spatiotemporal variability of soil respiration in a seasonal tropical forest. *Ecology and Evolution* 7:7104–7116.
- Ryan, M. G., N. Phillips, and B. J. Bond. 2006. The hydraulic limitation hypothesis revisited. *Plant, Cell & Environment* 29:367–381.
- Saatchi, S. S., N. L. Harris, S. Brown, M. Lefsky, E. T. a Mitchard, W. Salas, B. R. Zutta, W. Buermann, S. L. Lewis, S. Hagen, S. Petrova, L. White, M. Silman, and A. Morel. 2011. Benchmark map of forest carbon stocks in tropical regions across three continents. *Proceedings of the National Academy of Sciences* 108:9899–9904.
- Saleska, S. R. 2003. Carbon in Amazon Forests: Unexpected Seasonal Fluxes and Disturbance-Induced Losses. *Science* 302:1554–1557.
- Van Schaik, E., L. Killaars, N. E. Smith, G. Koren, L. P. H. Van Beek, W. Peters, and I. T. Van Der Laan-Luijckx. 2018. Changes in surface hydrology, soil moisture and gross primary production in the Amazon during the 2015/2016 El Niño.
- Schippers, P., F. Sterck, M. Vlam, and P. A. Zuidema. 2015. Tree growth variation in the tropical forest: Understanding effects of temperature, rainfall and CO₂. *Global Change Biology* 21:2749–2761.
- Schneider, U., A. Becker, P. Finger, A. Meyer-Christoffer, B. Rudolf, and M. Ziese. 2011. GPCP Full Data Reanalysis Version 6.0 at 0.5°: Monthly Land-Surface Precipitation from Rain-Gauges built on GTS-based and Historic Data.
- Schnitzer, S. A., and F. Bongers. 2011. Increasing liana abundance and biomass in tropical forests: Emerging patterns and putative mechanisms. *Ecology Letters* 14:397–406.
- Schreiber, U., and J. A. Berry. 1977. Heat-induced changes of chlorophyll fluorescence in intact leaves correlated with damage of the photosynthetic apparatus. *Planta* 136:233–238.
- Schuur, E. A. G. 2003. Productivity and global climate revisited: The sensitivity of tropical forest growth to precipitation. *Ecology* 84:1165–1170.
- Settele, J., R. Scholes, R. Betts, S. Bunn, P. Leadley, D. Nepstad, J. Overpeck, and M. A. T. (contributing lead Authors). 2014. Figure 4-7 in Chapter 4, Terrestrial and Inland Water Systems. In: Intergovernmental Panel on Climate Change (IPCC), C. Field et al. (Eds.), In: *Climate Change 2014: Impacts, Adaptation and Vulnerability: Contribution of Working Group II to the Fifth Assesment Report of the Intergovernmental Panel on Climate Change*. Cambridge University Press.
- Sevanto, S., N. G. McDowell, L. T. Dickman, R. Pangle, and W. T. Pockman. 2014. How do trees die? A test of the hydraulic failure and carbon starvation hypotheses. *Plant, Cell and Environment* 37:153–161.
- Slette, I. J., A. K. Post, M. Awad, T. Even, A. Punzalan, S. Williams, M. D. Smith, and A. K. Knapp. 2019. How ecologists define drought, and why we should do better. *Global Change Biology*:gcb.14747.
- Slik, J. W. F. 2004. El Niño droughts and their effects on tree species composition and diversity in tropical rain forests. *Oecologia* 141:114–120.
- Slik, J. W. F., V. Arroyo-Rodríguez, S.-I. Aiba, P. Alvarez-Loayza, L. F. Alves, P. Ashton, P. Balvanera, M. L. Bastian, P. J. Bellingham, E. van den Berg, L. Bernacci, P. da C. Bispo, L. Blanc, K. Böhning-Gaese, F.

B. , Pascal Boeckx, B. Boyle, M. Bradford, F. Q. Brearley, M. B.-N. Hockemba, S. Bunyavejchewin, D. C. L. Matos, M. Castillo-Santiago, E. L. M. Catharino, S.-L. Chai, Y. Chen, R. K. Colwell, R. L. Chazdon, C. Clark, D. B. Clark, D. A. Clark, H. Culmsee, K. Damas, H. S. Dattaraja, G. Dauby, P. Davidar, S. J. DeWalt, J.-L. Doucet, A. Duque, G. Durigan, K. A. O. Eichhorn, P. V. Eisenlohr, E. Eler, C. Ewango, N. Farwig, K. J. Feeley, L. Ferreira, R. Field, A. T. de O. Filho, C. Fletcher, O. Forshed, G. Franco, G. Fredriksson, T. Gillespie, J.-F. Gillet, G. Amarnath, D. M. Griffith, J. Grogan, N. Gunatilleke, D. Harris, R. Harrison, A. Hector, J. Homeier, N. Imai, A. Itoh, P. A. Jansen, C. A. Joly, B. H. J. de Jong, K. Kartawinata, E. Kearsley, D. L. Kelly, D. Kenfack, M. Kessler, K. Kitayama, R. Kooyman, E. Larney, Y. Laumonier, S. Laurance, W. F. Laurance, M. J. Lawes, I. L. do Amaral, S. G. Letcher, J. Lindsell, X. Lu, A. Mansor, A. Marjokorpi, E. H. Martin, H. Meilby, F. P. L. Melo, D. J. Metcalfe, V. P. Medjibe, J. P. Metzger, J. Millet, D. Mohandass, J. C. Montero, M. de M. Valeriano, B. Mugerwa, H. Nagamasu, R. Nilus, S. O.-G. Onrizal, N. Page, P. Parolin, M. Parrenn, N. Parthasarathy, E. Paudel, A. Permana, M. T. F. Piedade, N. C. A. Pitman, L. Poorter, A. D. Poulsen, J. Poulsen, J. Powers, R. C. Prasad, J.-P. Puyravaud, J.-C. Razafimahaimodison, J. Reitsma, J. R. dos Santos, W. R. Spironello, H. Romero-Saltos, F. Rovero, A. H. Rozak, K. Ruokolainen, E. Rutishauser, F. Saiter, P. Saner, B. A. Santos, F. Santos, S. K. Sarker, M. Satdichanh, C. B. Schmitt, J. Schöngart, M. Schulze, M. S. Sukanuma, D. Sheil, E. da S. Pinheiro, P. Sist, T. Stevart, R. Sukumar, I.-F. Sun, T. Sunderland, H. S. Suresh, E. Suzuki, M. Tabarelli, J. Tang, N. Targhetta, I. Theilade, D. W. Thomas, P. Tchouto, J. Hurtado, R. Valencia, J. L. C. H. van Valkenburg, T. Van Do, R. Vasquez, H. Verbeeck, V. Adegunle, S. A. Vieira, C. O. Webb, T. Whitfeld, S. A. Wich, J. Williams, F. Wittmann, H. Wöll, X. Yang, C. Y. A. Yao, S. L. Yap, T. Yoneda, R. A. Zahawi, R. Zakaria, R. Zang, R. L. de Assis, B. G. Luize, and E. M. Venticinque. 2015. An estimate of the number of tropical tree species. *Proceedings of the National Academy of Sciences* 112:E4628–E4629.

Slik, J. W. F., J. Franklin, V. Arroyo-Rodríguez, R. Field, S. Aguilar, N. Aguirre, J. Ahumada, S.-I. Aiba, L. F. Alves, A. K. A. Avella, F. Mora, G. A. Aymard C., S. Báez, P. Balvanera, M. L. Bastian, J.-F. Bastin, P. J. Bellingham, E. van den Berg, P. da Conceição Bispo, P. Boeckx, K. Boehning-Gaese, F. Bongers, B. Boyle, F. Brambach, F. Q. Brearley, S. Brown, S.-L. Chai, R. L. Chazdon, S. Chen, P. Chhang, G. Chuyong, C. Ewango, I. M. Coronado, J. Cristóbal-Azkarate, H. Culmsee, K. Damas, H. S. Dattaraja, P. Davidar, S. J. DeWalt, H. Din, D. R. Drake, A. Duque, G. Durigan, K. Eichhorn, E. S. Eler, T. Enoki, A. Ensslin, A. B. Fandohan, N. Farwig, K. J. Feeley, M. Fischer, O. Forshed, Q. S. Garcia, S. C. Garkoti, T. W. Gillespie, J.-F. Gillet, C. Gonmadje, I. Granzow-de la Cerda, D. M. Griffith, J. Grogan, K. R. Hakeem, D. J. Harris, R. D. Harrison, A. Hector, A. Hemp, J. Homeier, M. S. Hussain, G. Ibarra-Manríquez, I. F. Hanum, N. Imai, P. A. Jansen, C. A. Joly, S. Joseph, K. Kartawinata, E. Kearsley, D. L. Kelly, M. Kessler, T. J. Killeen, R. M. Kooyman, Y. Laumonier, S. G. Laurance, W. F. Laurance, M. J. Lawes, S. G. Letcher, J. Lindsell, J. Lovett, J. Lozada, X. Lu, A. M. Lykke, K. Bin Mahmud, N. P. D. Mahayani, A. Mansor, A. R. Marshall, E. H. Martin, D. Calderado Leal Matos, J. A. Meave, F. P. L. Melo, Z. H. A. Mendoza, F. Metali, V. P. Medjibe, J. P. Metzger, T. Metzker, D. Mohandass, M. A. Munguía-Rosas, R. Muñoz, E. Nurtjahy, E. L. de Oliveira, Onrizal, P. Parolin, M. Parren, N. Parthasarathy, E. Paudel, R. Perez, E. A. Pérez-García, U. Pommer, L. Poorter, L. Qie, M. T. F. Piedade, J. R. R. Pinto, A. D. Poulsen, J. R. Poulsen, J. S. Powers, R. C. Prasad, J.-P. Puyravaud, O. Rangel, J. Reitsma, D. S. B. Rocha, S. Rolim, F. Rovero, A. Rozak, K. Ruokolainen, E. Rutishauser, G. Rutten, M. N. Mohd. Said, F. Z. Saiter, P. Saner, B. Santos, J. R. dos Santos, S. K. Sarker, C. B. Schmitt, J. Schoengart, M. Schulze, D. Sheil, P. Sist, A. F. Souza, W. R. Spironello, T. Sposito, R. Steinmetz, T. Stevart, M. S. Sukanuma, R. Sukri, A. Sultana, R. Sukumar, T. Sunderland, Supriyadi, H. S. Suresh, E. Suzuki, M. Tabarelli, J. Tang, E. V. J. Tanner, N. Targhetta, I. Theilade, D. Thomas, J. Timberlake, M. de Morisson Valeriano, J. van Valkenburg, T. Van Do, H. Van Sam, J. H. Vandermeer, H. Verbeeck, O. R. Vetaas, V. Adegunle, S. A. Vieira, C. O. Webb, E. L. Webb, T. Whitfeld, S. Wich, J. Williams, S. Wisser, F. Wittmann, X. Yang, C. Y. Adou Yao, S. L. Yap, R. A. Zahawi, R. Zakaria, and R. Zang. 2018. Phylogenetic classification of the world's tropical forests. *Proceedings of the National Academy of Sciences* 115:1837–1842.

Slot, M., and K. Winter. 2017. Photosynthetic acclimation to warming in tropical forest tree Seedlings. *Journal of Experimental Botany* 68:2275–2284.

Smith, W. K., S. C. Reed, C. C. Cleveland, A. P. Ballantyne, W. R. L. Anderegg, W. R. Wieder, Y. Y. Liu, and S. W. Running. 2016. Large divergence of satellite and Earth system model estimates of global terrestrial CO₂ fertilization. *Nature Climate Change* 6:306–310.

Sousa, T. ., J. Schietti, F. Coelho de Souza, A. Esquivel-Muelbert, I. . Ribeiro, T. Emílio, P. A. C. . Pequeno, O. Phillips, and F. R. . Costa. 2020. Palms and trees resist extreme drought in Amazon forests with shallow water tables. *Journal of Ecology*:1365-2745.13377.

Ter Steege, H., N. C. A. Pitman, D. Sabatier, C. Baraloto, R. P. Salomão, J. E. Guevara, O. L. Phillips, C. V.

Castilho, W. E. Magnusson, J. F. Molino, A. Monteagudo, P. N. Vargas, J. C. Montero, T. R. Feldpausch, E. N. H. Coronado, T. J. Killeen, B. Mostacedo, R. Vasquez, R. L. Assis, J. Terborgh, F. Wittmann, A. Andrade, W. F. Laurance, S. G. W. Laurance, B. S. Marimon, B. H. Marimon, I. C. G. Vieira, I. L. Amaral, R. Brienens, H. Castellanos, D. C. López, J. F. Duivenvoorden, H. F. Mogollón, F. D. D. A. Matos, N. Dávila, R. García-Villacorta, P. R. S. Diaz, F. Costa, T. Emilio, C. Levis, J. Schietti, P. Souza, A. Alonso, F. Dallmeier, A. J. D. Montoya, M. T. F. Piedade, A. Araujo-Murakami, L. Arroyo, R. Gribel, P. V. A. Fine, C. A. Peres, M. Toledo, G. A. Aymard C., T. R. Baker, C. Cerón, J. Engel, T. W. Henkel, P. Maas, P. Petronelli, J. Stropp, C. E. Zartman, D. Daly, D. Neill, M. Silveira, M. R. Paredes, J. Chave, D. D. A. Lima Filho, P. M. Jørgensen, A. Fuentes, J. Schöngart, F. C. Valverde, A. Di Fiore, E. M. Jimenez, M. C. P. Mora, J. F. Phillips, G. Rivas, T. R. Van Andel, P. Von Hildebrand, B. Hoffman, E. L. Zent, Y. Malhi, A. Prieto, A. Rudas, A. R. Ruschell, N. Silva, V. Vos, S. Zent, A. A. Oliveira, A. C. Schutz, T. Gonzales, M. T. Nascimento, H. Ramirez-Angulo, R. Sierra, M. Tirado, M. N. U. Medina, G. Van Der Heijden, C. I. A. Vela, E. V. Torre, C. Vriesendorp, O. Wang, K. R. Young, C. Baider, H. Balslev, C. Ferreira, I. Mesones, A. Torres-Lezama, L. E. U. Giraldo, R. Zagt, M. N. Alexiades, L. Hernandez, I. Huamantupa-Chuquimaco, W. Milliken, W. P. Cuenca, D. Pauletto, E. V. Sandoval, L. V. Gamarra, K. G. Dexter, K. Feeley, G. Lopez-Gonzalez, and M. R. Silman. 2013. Hyperdominance in the Amazonian tree flora. *Science* 342.

Sterck, F. J., L. Poorter, and F. Schieving. 2016. Leaf Traits Determine the Growth - Survival Trade - Off across Rain Forest Tree Species Author (s): F . J . Sterck , L . Poorter and F . Schieving Published by : The University of Chicago Press for The American Society of Naturalists Stable URL : <http://167:758-765>.

Stocker, T. F., D. Qin, G.-K. Plattner, M. M. B. Tignor, S. K. Allen, J. Boschung, A. Nauels, Y. Xia, V. Bex, P. M. Midgley, L. V. Alexander, N. L. Bindoff, F.-M. Breon, J. A. Church, U. Cubasch, S. Emori, P. Forster, P. Friedlingstein, N. Gillett, J. M. Gregory, D. L. Hartmann, E. Jansen, B. Kirtman, R. Knutti, K. Kumar Kanikicharla, P. Lemke, J. Marotzke, V. Masson-Delmotte, G. A. Meehl, I. I. Mokhov, S. Piao, Q. Dahe, V. Ramaswamy, D. Randall, M. Rhein, M. Rojas, C. Sabine, D. Shindell, L. D. Talley, D. G. Vaughan, S.-P. Xie, M. R. Allen, O. Boucher, D. Chambers, J. Hesselbjerg Christensen, P. Ciais, P. U. Clark, M. Collins, J. C. Comiso, V. Vasconcellos de Menezes, R. A. Feely, T. Fichet, A. M. Fiore, G. Flato, J. Fuglestedt, G. Hegerl, P. J. Hezel, G. C. Johnson, G. Kaser, V. Kattsov, J. Kennedy, A. M. G. Klein Tank, C. Le Quere, G. Myhre, T. Osborn, A. J. Payne, J. Perlwitz, S. Power, M. Prather, S. R. Rintoul, J. Rogelj, T. F. RStocker, M. Rusticucci, M. Schulz, J. Sedlacek, P. A. Stott, R. Sutton, P. W. Thorne, and D. Wuebbles. 2013. *Climate Change 2013: The Physical Science Basis. Contribution of Working Group I to the Fifth Assessment Report of the Intergovernmental Panel on Climate Change.*

Sullivan, M. J. P., S. L. Lewis, K. Affum-Baffoe, C. Castilho, F. Costa, A. C. Sanchez, C. E. N. Ewango, W. Hubau, B. Marimon, A. Monteagudo-Mendoza, L. Qie, B. Sonké, R. V. Martinez, T. R. Baker, R. J. W. Brienens, T. R. Feldpausch, D. Galbraith, M. Gloor, Y. Malhi, S.-I. Aiba, M. N. Alexiades, E. C. Almeida, E. A. de Oliveira, E. Á. Dávila, P. A. Loayza, A. Andrade, S. A. Vieira, L. E. O. C. Aragão, A. Araujo-Murakami, E. J. M. M. Arets, L. Arroyo, P. Ashton, G. Aymard C., F. B. Baccaro, L. F. Banin, C. Baraloto, P. B. Camargo, J. Barlow, J. Barroso, J.-F. Bastin, S. A. Batterman, H. Beeckman, S. K. Begne, A. C. Bennett, E. Berenguer, N. Berry, L. Blanc, P. Boeckx, J. Bogaert, D. Bonal, F. Bongers, M. Bradford, F. Q. Brearley, T. Brncic, F. Brown, B. Burban, J. L. Camargo, W. Castro, C. Céron, S. C. Ribeiro, V. C. Moscoso, J. Chave, E. Chezeaux, C. J. Clark, F. C. de Souza, M. Collins, J. A. Comiskey, F. C. Valverde, M. C. Medina, L. da Costa, M. Dančák, G. C. Dargie, S. Davies, N. D. Cardozo, T. de Haulleville, M. B. de Medeiros, J. del Aguila Pasquel, G. Derroire, A. Di Fiore, J.-L. Doucet, A. Dourdain, V. Droissart, L. F. Duque, R. Ekoungoulou, F. Elias, T. Erwin, A. Esquivel-Muelbert, S. Fauset, J. Ferreira, G. F. Llampazo, E. Foli, A. Ford, M. Gilpin, J. S. Hall, K. C. Hamer, A. C. Hamilton, D. J. Harris, T. B. Hart, R. Hédli, B. Herault, R. Herrera, N. Higuchi, A. Hladik, E. H. Coronado, I. Huamantupa-Chuquimaco, W. H. Huasco, K. J. Jeffery, E. Jimenez-Rojas, M. Kalamandeen, M. N. K. Djuikouo, E. Kearsley, R. K. Umetsu, L. K. Kho, T. Killeen, K. Kitayama, B. Klitgaard, A. Koch, N. Labrière, W. Laurance, S. Laurance, M. E. Leal, A. Levesley, A. J. N. Lima, J. Lisingo, A. P. Lopes, G. Lopez-Gonzalez, T. Lovejoy, J. C. Lovett, R. Lowe, W. E. Magnusson, J. Malumbres-Olarte, Á. G. Manzatto, B. H. Marimon, A. R. Marshall, T. Marthews, S. M. de Almeida Reis, C. Maycock, K. Melgaço, C. Mendoza, F. Metali, V. Mihindou, W. Milliken, E. T. A. Mitchard, P. S. Morandi, H. L. Mossman, L. Nagy, H. Nascimento, D. Neill, R. Nilus, P. N. Vargas, W. Palacios, N. P. Camacho, J. Peacock, C. Pendry, M. C. Peñuela Mora, G. C. Pickavance, J. Pipoly, N. Pitman, M. Playfair, L. Poorter, J. R. Poulsen, A. D. Poulsen, R. Preziosi, A. Prieto, R. B. Primack, H. Ramírez-Angulo, J. Reitsma, M. Réjou-Méchain, Z. R. Correa, T. R. de Sousa, L. R. Bayona, A. Roopsind, A. Rudas, E. Rutishauser, K. Abu Salim, R. P. Salomão, J. Schietti, D. Sheil, R. C. Silva, J. S. Espejo, C. S. Valeria, M. Silveira, M. Simo-Droissart, M. F. Simon, J. Singh, Y. C. Soto Shareva, C. Stahl, J. Stropp, R. Sukri, T. Sunderland, M. Svátek, M. D. Swaine, V. Swamy, H. Taedoumg, J. Talbot, J.

- Taplin, D. Taylor, H. ter Steege, J. Terborgh, R. Thomas, S. C. Thomas, A. Torres-Lezama, P. Umunay, L. V. Gamarra, G. van der Heijden, P. van der Hout, P. van der Meer, M. van Nieuwstadt, H. Verbeeck, R. Vernimmen, A. Vicentini, I. C. G. Vieira, E. V. Torre, J. Vleminckx, V. Vos, O. Wang, L. J. T. White, S. Willcock, J. T. Woods, V. Wortel, K. Young, R. Zagt, L. Zomagho, P. A. Zuidema, J. A. Zwerts, and O. L. Phillips. 2020. Long-term thermal sensitivity of Earth's tropical forests. *Science* 368:869–874.
- Sullivan, M. J. P., S. L. Lewis, W. Hubau, L. Qie, T. R. Baker, L. F. Banin, J. Chave, A. Cuni-Sanchez, T. R. Feldpausch, G. Lopez-Gonzalez, E. Arets, P. Ashton, J.-F. Bastin, N. J. Berry, J. Bogaert, R. Boot, F. Q. Brearley, R. Brienen, D. F. R. P. Burslem, C. Canniere, M. Chudomelová, M. Dančák, C. Ewango, R. Hédli, J. Lloyd, J.-R. Makana, Y. Malhi, B. S. Marimon, B. H. M. Junior, F. Metali, S. Moore, L. Nagy, P. N. Vargas, C. A. Pendry, H. Ramírez-Angulo, J. Reitsma, E. Rutishauser, K. A. Salim, B. Sonké, R. S. Sukri, T. Sunderland, M. Svátek, P. M. Umunay, R. V. Martinez, R. R. E. Vernimmen, E. V. Torre, J. Vleminckx, V. Vos, and O. L. Phillips. 2018. Field methods for sampling tree height for tropical forest biomass estimation. *Methods in Ecology and Evolution* 9:1179–1189.
- Sullivan, M. J. P., J. Talbot, S. L. Lewis, O. L. Phillips, L. Qie, S. K. Begne, J. Chave, A. Cuni-Sanchez, W. Hubau, G. Lopez-Gonzalez, L. Miles, A. Monteagudo-Mendoza, B. Sonké, T. Sunderland, H. ter Steege, L. J. T. White, K. Affum-Baffoe, S. Aiba, E. C. de Almeida, E. A. de Oliveira, P. Alvarez-Loayza, E. Á. Dávila, A. Andrade, L. E. O. C. Aragão, P. Ashton, G. A. Aymard C., T. R. Baker, M. Balinga, L. F. Banin, C. Baraloto, J.-F. Bastin, N. Berry, J. Bogaert, D. Bonal, F. Bongers, R. Brienen, J. L. C. Camargo, C. Cerón, V. C. Moscoso, E. Chezeaux, C. J. Clark, Á. C. Pacheco, J. A. Comiskey, F. C. Valverde, E. N. H. Coronado, G. Dargie, S. J. Davies, C. De Canniere, M. N. Djuikouo K., J.-L. Doucet, T. L. Erwin, J. S. Espejo, C. E. N. Ewango, S. Fauset, T. R. Feldpausch, R. Herrera, M. Gilpin, E. Gloor, J. S. Hall, D. J. Harris, T. B. Hart, K. Kartawinata, L. K. Kho, K. Kitayama, S. G. W. Laurance, W. F. Laurance, M. E. Leal, T. Lovejoy, J. C. Lovett, F. M. Lukasu, J.-R. Makana, Y. Malhi, L. Maracahipes, B. S. Marimon, B. H. M. Junior, A. R. Marshall, P. S. Morandi, J. T. Mukendi, J. Mukinzi, R. Nilus, P. N. Vargas, N. C. P. Camacho, G. Pardo, M. Peña-Claros, P. Pétronelli, G. C. Pickavance, A. D. Poulsen, J. R. Poulsen, R. B. Primack, H. Priyadi, C. A. Quesada, J. Reitsma, M. Réjou-Méchain, Z. Restrepo, E. Rutishauser, K. A. Salim, R. P. Salomão, I. Samsedin, D. Sheil, R. Sierra, M. Silveira, J. W. F. Slik, L. Steel, H. Taedoumg, S. Tan, J. W. Terborgh, S. C. Thomas, M. Toledo, P. M. Umunay, L. V. Gamarra, I. C. G. Vieira, V. A. Vos, O. Wang, S. Willcock, and L. Zomagho. 2017. Diversity and carbon storage across the tropical forest biome. *Scientific Reports* 7:39102.
- Symonds, M. R. E., and A. Moussalli. 2011. A brief guide to model selection, multimodel inference and model averaging in behavioural ecology using Akaike's information criterion. *Behavioral Ecology and Sociobiology* 65:13–21.
- Talbot, J., S. L. Lewis, G. Lopez-Gonzalez, R. J. W. Brienen, A. Monteagudo, T. R. Baker, T. R. Feldpausch, Y. Malhi, M. Vanderwel, A. Araujo Murakami, L. P. Arroyo, K.-J. Chao, T. Erwin, G. van der Heijden, H. Keeling, T. Killeen, D. Neill, P. Núñez Vargas, G. A. Parada Gutierrez, N. Pitman, C. A. Quesada, M. Silveira, J. Stropp, and O. L. Phillips. 2014. Methods to estimate aboveground wood productivity from long-term forest inventory plots. *Forest Ecology and Management* 320:30–38.
- Terrer, C., R. B. Jackson, I. C. Prentice, T. F. Keenan, C. Kaiser, S. Vicca, J. B. Fisher, P. B. Reich, B. D. Stocker, B. A. Hungate, J. Peñuelas, I. McCallum, N. A. Soudzilovskaia, L. A. Cernusak, A. F. Talhelm, K. Van Sundert, S. Piao, P. C. D. Newton, M. J. Hovenden, D. M. Blumenthal, Y. Y. Liu, C. Müller, K. Winter, C. B. Field, W. Viechtbauer, C. J. Van Lissa, M. R. Hoosbeek, M. Watanabe, T. Koike, V. O. Leshyk, H. W. Polley, and O. Franklin. 2019. Nitrogen and phosphorus constrain the CO₂ fertilization of global plant biomass. *Nature Climate Change* 9:684–689.
- Tilman, D., and J. A. Downing. 1994. Biodiversity and stability in grasslands. *Nature* 367:363–365.
- Tjoelker, M. G., J. Oleksyn, and P. B. Reich. 2001. Modelling respiration of vegetation: evidence for a general temperature-dependent Q₁₀. *Global Change Biology* 7:223–230.
- Trenberth, K. E., J. M. Caron, D. P. Stepaniak, and S. Worley. 2002. Evolution of El Niño-Southern Oscillation and global atmospheric surface temperatures. *Journal of Geophysical Research D: Atmospheres* 107:5–1.
- Trenberth, K. E., A. Dai, G. van der Schrier, P. D. Jones, J. Barichivich, K. R. Briffa, and J. Sheffield. 2014. Global warming and changes in drought. *Nature Climate Change* 4:17–22.
- Tyrrell, N. L., D. Dommenges, C. Frauen, S. Wales, and M. Rezný. 2015. The influence of global sea surface temperature variability on the large-scale land surface temperature. *Clim Dyn* 44:2159–2176.
- University of East Anglia Climatic Research Unit, I. C. Harris, and P. D. Jones. 2020. CRU TS4.03: Climatic

Research Unit (CRU) Time-Series (TS) version 4.03 of high-resolution gridded data of month-by-month variation in climate (Jan. 1901- Dec. 2018).
<https://catalogue.ceda.ac.uk/uuid/10d3e3640f004c578403419aac167d82>.

- Vitousek, P. M., and R. L. Sanford. 1986. Nutrient cycling in moist tropical forest. *Annual review of ecology and systematics*. Vol. 17:137–167.
- Wang, H. J., R. H. Zhang, J. Cole, and F. Chavez. 1999. El Niño and the related phenomenon southern oscillation (ENSO): The largest signal in interannual climate variation. *Proceedings of the National Academy of Sciences of the United States of America* 96:11071–11072.
- Wang, X., R. L. Edwards, A. S. Auler, H. Cheng, X. Kong, Y. Wang, F. W. Cruz, J. A. Dorale, and H. W. Chiang. 2017. Hydroclimate changes across the Amazon lowlands over the past 45,000 years. *Nature* 541:204–207.
- van der Werf, G. R., J. Randerson, G. Collatz, L. Giglio, P. Kasibhatla, A. Arellano, S. Olsen, and E. Kasischke. 2004. Continental-Scale Partitioning of Fire Emissions During the 1997 to 2001 El Niño/La Niña Period. *Science* 303:73–76.
- Wigneron, J.-P., L. Fan, P. Ciais, A. Bastos, M. Brandt, J. Chave, S. Saatchi, A. Baccini, and R. Fensholt. 2020. Tropical forests did not recover from the strong 2015–2016 El Niño event. *Science Advances* 6:eaay4603.
- Williams, A. P., C. D. Allen, A. K. Macalady, D. Griffin, C. A. Woodhouse, D. M. Meko, T. W. Swetnam, S. A. Rauscher, R. Seager, H. D. Grissino-Mayer, J. S. Dean, E. R. Cook, C. Gangodagamage, M. Cai, and N. G. McDowell. 2013. Temperature as a potent driver of regional forest drought stress and tree mortality. *Nature Climate Change* 3:292–297.
- Williamson, G. B., W. F. Laurance, A. A. Oliveira, P. Delamônica, C. Gascon, T. E. Lovejoy, and L. Pohl. 2000a. Amazonian tree mortality during the 1997 El Niño drought. *Conservation Biology* 14:1538–1542.
- Williamson, G. B., W. F. Laurance, A. A. Oliveira, C. Gascon, T. E. Lovejoy, and L. Pohl. 2000b. Tree Mortality during the 1997 El Niño Drought. *Conservation Biology* 14:1538–1542.
- Willson, R. C., and A. V. Mordvinov. 2003. Secular total solar irradiance trend during solar cycles 21–23. *Geophysical Research Letters* 30:n/a-n/a.
- Wilson, K. B., D. D. Baldocchi, M. Aubinet, P. Berbigier, C. Bernhofer, H. Dolman, E. Falge, C. Field, A. Goldstein, A. Granier, A. Grelle, T. Halldor, D. Hollinger, G. Katul, B. E. Law, A. Lindroth, T. Meyers, J. Moncrieff, R. Monson, W. Oechel, J. Tenhunen, R. Valentini, S. Verma, T. Vesala, and S. Wofsy. 2002. Energy partitioning between latent and sensible heat flux during the warm season at FLUXNET sites. *Water Resources Research* 38:30-1-30–11.
- Wood, S. N. 2001. Minimizing Model Fitting Objectives That Contain Spurious Local Minima by Bootstrap Restarting. *Biometrics* 57:240–244.
- Wright, S. J., and O. Calderón. 2006. Seasonal, El Niño and longer term changes in flower and seed production in a moist tropical forest. *Ecology Letters* 9:35–44.
- Wythers, K. R., P. B. Reich, M. G. Tjoelker, and P. B. Bolstad. 2005. Foliar respiration acclimation to temperature and temperature variable Q10 alter ecosystem carbon balance. *Global Change Biology* 11:435–449.
- Yamori, W., K. Hikosaka, and D. A. Way. 2014. Temperature response of photosynthesis in C3, C4, and CAM plants: Temperature acclimation and temperature adaptation. *Photosynthesis Research* 119:101–117.
- Yang, J., H. Tian, S. Pan, G. Chen, B. Zhang, and S. Dangal. 2018a. Amazon drought and forest response: Largely reduced forest photosynthesis but slightly increased canopy greenness during the extreme drought of 2015/2016. *Global Change Biology* 24:1919–1934.
- Yang, Y., S. S. Saatchi, L. Xu, Y. Yu, S. Choi, N. Phillips, R. Kennedy, M. Keller, Y. Knyazikhin, and R. B. Myneni. 2018b. Post-drought decline of the Amazon carbon sink. *Nature Communications* 9:3172.
- Yanoviak, S. P., E. M. Gora, P. M. Bitzer, J. C. Burchfield, H. C. Muller-Landau, M. Detto, S. Paton, and S. P. Hubbell. 2019. Lightning is a major cause of large tree mortality in a lowland Neotropical forest. *New Phytologist*.
- Yin, Y., A. A. Bloom, J. Worden, S. Saatchi, Y. Yang, M. Williams, J. Liu, Z. Jiang, H. Worden, K. Bowman, C. Frankenberg, and D. Schimel. 2020. Fire decline in dry tropical ecosystems enhances decadal land carbon sink. *Nature Communications* 11.

- Zanne, A. E., G. Lopez-Gonzalez, D. A. Coomes, J. Ilic, S. Jansen, S. L. Lewis, R. B. Miller, N. G. Swenson, M. C. Wiemann, and J. Chave. 2009. Data from: Towards a worldwide wood economics spectrum. Dryad Digital Repository.
- Zelazowski, P., Y. Malhi, C. Huntingford, S. Sitch, and J. B. Fisher. 2011. Changes in the potential distribution of humid tropical forests on a warmer planet. *Philosophical Transactions of the Royal Society A: Mathematical, Physical and Engineering Sciences* 369:137–160.
- Zhang, Y.-J., F. C. Meinzer, G.-Y. Hao, F. G. Scholz, S. J. Bucci, F. S. C. Takahashi, R. Villalobos-Vega, J. P. Giraldo, K.-F. Cao, W. A. Hoffmann, and G. Goldstein. 2009. Size-dependent mortality in a Neotropical savanna tree: the role of height-related adjustments in hydraulic architecture and carbon allocation. *Plant, Cell & Environment* 32:1456–1466.
- Zheng, X. T., C. Hui, S. P. Xie, W. Cai, and S. M. Long. 2019. Intensification of El Niño Rainfall Variability Over the Tropical Pacific in the Slow Oceanic Response to Global Warming. *Geophysical Research Letters* 46:2253–2260.
- Ziegler, C., S. Coste, C. Stahl, S. Delzon, S. Levionnois, J. Cazal, H. Cochard, A. Esquivel-Muelbert, J. Y. Goret, P. Heuret, G. Jaouen, L. S. Santiago, and D. Bonal. 2019. Large hydraulic safety margins protect Neotropical canopy rainforest tree species against hydraulic failure during drought. *Annals of Forest Science* 76.
- Zuleta, D., A. Duque, D. Cardenas, H. C. Muller-Landau, and S. Davies. 2017. Drought induced mortality patterns and rapid biomass recovery in a terra firme forest in the Colombian Amazon. *Ecology*.

Appendices

Figure A2.1 | Monthly correlation coefficients for temperature

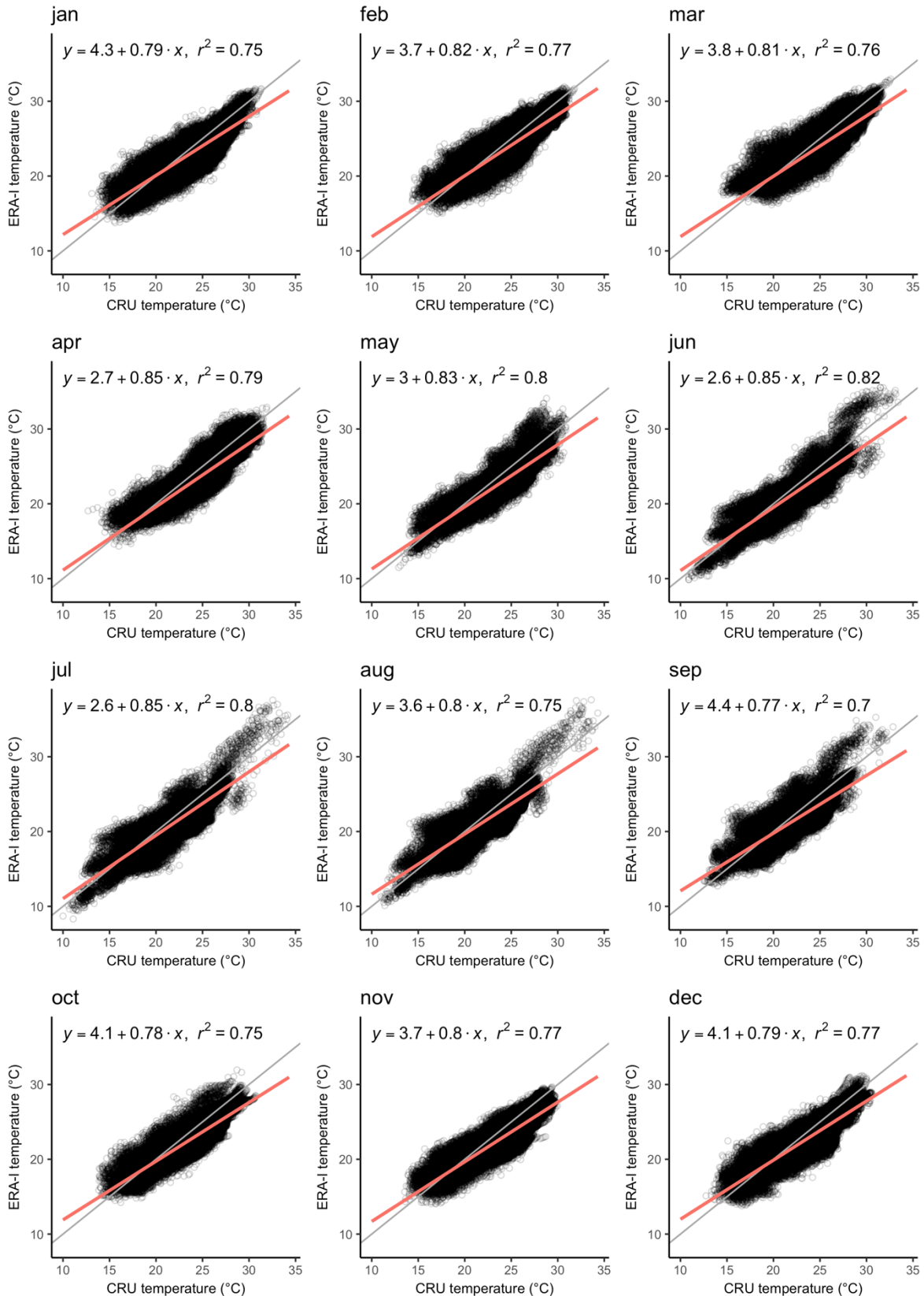


Figure A2.2 | Monthly correlation coefficients for precipitation

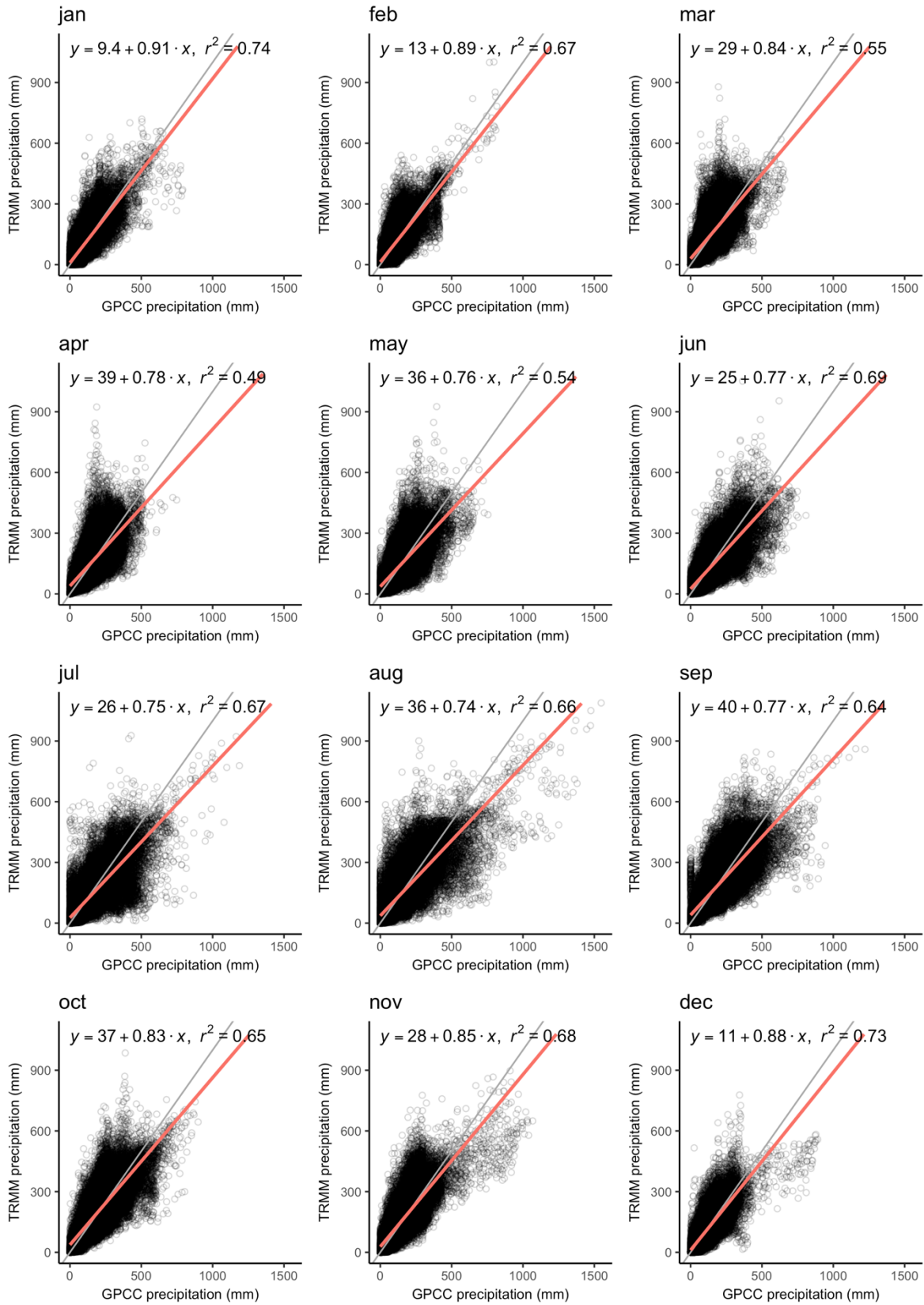


Table A2.1 | Parameters used to estimate tree height from tree diameter

Plot Code	a	b	c
ANK-01	52.7	0.05	0.72
ANK-02	52.7	0.05	0.72
ANK-03	52.7	0.05	0.72
ASN-02	52.7	0.05	0.72
BOB-01	52.7	0.05	0.72
BOB-02	52.7	0.05	0.72
BOB-03	52.7	0.05	0.72
CAP-09	52.7	0.05	0.72
CAP-10	52.7	0.05	0.72
CVL-01	52.7	0.05	0.72
CVL-11	52.7	0.05	0.72
DAD-03	52.7	0.05	0.72
DAD-04	52.7	0.05	0.72
DJK-01	44.6	0.05	0.83
DJK-02	44.6	0.05	0.83
DJK-03	44.6	0.05	0.83
DJK-04	44.6	0.05	0.83
DJK-05	44.6	0.05	0.83
DJK-06	44.6	0.05	0.83
DJL-01	44.6	0.05	0.83
DJL-02	44.6	0.05	0.83
DJL-03	44.6	0.05	0.83
DJL-04	44.6	0.05	0.83
DJL-05	44.6	0.05	0.83
DJL-06	44.6	0.05	0.83
DNG-01	44.6	0.05	0.83
DNG-02	44.6	0.05	0.83
GBO-02	52.7	0.05	0.72
GBO-04	52.7	0.05	0.72
GBO-08	52.7	0.05	0.72
GBO-11	52.7	0.05	0.72
GBO-15	52.7	0.05	0.72
GBO-19	52.7	0.05	0.72
HAB-03	44.6	0.05	0.83
HAB-06	44.6	0.05	0.83
HAB-07	44.6	0.05	0.83
IVI-01	44.6	0.05	0.83

IVI-02	44.6	0.05	0.83
KOL-01	44.6	0.05	0.83
KOL-02	79.2	0.04	0.55
KOL-03	79.2	0.04	0.55
KOL-04	44.6	0.05	0.83
KSN-01	48.2	0.05	0.71
KSN-02	48.2	0.05	0.71
KSN-05	48.2	0.05	0.71
KSN-06	48.2	0.05	0.71
LTL-01	79.2	0.04	0.55
MDC-01	44.6	0.05	0.83
MDC-02	44.6	0.05	0.83
MDC-03	44.6	0.05	0.83
MDC-04	44.6	0.05	0.83
MDC-05	44.6	0.05	0.83
MDJ-01	44.6	0.05	0.83
MDJ-03	44.6	0.05	0.83
MDJ-07	44.6	0.05	0.83
MDJ-10	44.6	0.05	0.83
MNG-03	44.6	0.05	0.83
MNG-04	44.6	0.05	0.83
NNN-01	44.6	0.05	0.83
NNN-02	44.6	0.05	0.83
NNN-03	44.6	0.05	0.83
NNN-04	44.6	0.05	0.83
NNN-05	44.6	0.05	0.83
NNN-06	44.6	0.05	0.83
NNP-01	44.6	0.05	0.83
NNP-02	44.6	0.05	0.83
NNP-05	44.6	0.05	0.83
OVG-01	44.6	0.05	0.83
SAN-22	44.6	0.05	0.83
SAN-24	44.6	0.05	0.83
SNG-01	48.2	0.05	0.71
SNG-02	48.2	0.05	0.71
SNG-03	48.2	0.05	0.71
SNG-04	48.2	0.05	0.71
SNG-05	48.2	0.05	0.71
SNG-06	48.2	0.05	0.71

SNG-07	48.2	0.05	0.71
SNG-08	48.2	0.05	0.71
SNG-09	48.2	0.05	0.71
YGB-08	48.2	0.05	0.71
YGB-14	48.2	0.05	0.71
YGB-15	48.2	0.05	0.71
YGB-16	48.2	0.05	0.71
YGB-17	48.2	0.05	0.71
YGB-18	48.2	0.05	0.71
YGB-24	48.2	0.05	0.71
YGB-25	48.2	0.05	0.71
YGB-26	48.2	0.05	0.71
YGB-27	48.2	0.05	0.71
YGB-28	48.2	0.05	0.71
YOK-06	48.2	0.05	0.71
YOK-07	48.2	0.05	0.71
YOK-08	48.2	0.05	0.71
YOK-09	48.2	0.05	0.71
YOK-10	48.2	0.05	0.71
YOK-16	48.2	0.05	0.71
YOK-17	48.2	0.05	0.71
YOK-18	48.2	0.05	0.71
YOK-19	48.2	0.05	0.71
YOK-20	48.2	0.05	0.71

Table A2.2 | Coefficients of model-averaged multiple regression models of net carbon, carbon gains and carbon losses

Variable	Δ net carbon				Δ carbon gains				Δ carbon losses			
	Estimate	SE	Z	P	Estimate	SE	Z	P	Estimate	SE	Z	P
Intercept	-0.69	0.57	1.20	0.23	-0.10	0.13	0.75	0.45	0.65	0.53	1.22	0.22
Pre-El Niño temperature	0.00	0.30	0.01	0.99	0.01	0.07	0.18	0.85	0.04	0.30	0.15	0.88
Pre-El Niño MCWD	-0.04	0.40	0.09	0.93	-0.01	0.09	0.14	0.89	-0.05	0.37	0.12	0.90
Δ temperature	-0.34	0.68	0.50	0.62	0.04	0.11	0.38	0.71	0.50	0.77	0.64	0.52
Δ MCWD	-1.18	0.71	1.65	0.10	-0.25	0.16	1.51	0.13	0.96	0.71	1.33	0.18
Interaction: Δ temperature and Δ MCWD	-0.22	0.51	0.42	0.67	0.02	0.08	0.24	0.81	0.38	0.64	0.59	0.55
Interaction: Δ temperature and pre-El Niño temperature	-0.01	0.55	0.06	0.95	0.00	0.02	0.24	0.98	0.01	0.13	0.07	0.94
Interaction: Δ MCWD and pre-El Niño MCWD	0.21	0.55	0.37	0.71	0.02	0.08	0.25	0.80	-0.17	0.49	0.34	0.73

Table A2.3 | Coefficients of model-averaged multiple regression models of net stems, recruitment and stem mortality

Variable	Δ net stems				Δ recruitment				Δ mortality			
	Estimate	SE	Z	P	Estimate	SE	Z	P	Estimate	SE	Z	P
Intercept	-0.75	0.67	1.10	0.27	0.26	0.43	0.59	0.55	1.24	0.45	2.72	<0.01
Pre-El Niño temperature	-0.19	0.49	0.39	0.70	0.27	0.39	0.68	0.49	0.56	0.53	1.04	0.30
Pre-El Niño MCWD	-0.76	0.65	1.15	0.24	-0.75	0.45	1.64	0.10	0.47	0.49	0.96	0.34
Δ temperature	0.08	0.68	0.11	0.91	0.79	0.70	1.13	0.26	0.06	0.39	0.16	0.87
Δ MCWD	-0.82	0.64	1.27	0.20	-1.01	0.45	2.22	<0.05	-0.10	0.33	0.30	0.76
Interaction: Δ temperature and Δ MCWD	0.26	0.56	0.46	0.65	0.82	0.60	1.35	0.18	0.00	0.07	0.05	0.96
Interaction: Δ temperature and pre-El Niño temperature	0.13	0.45	0.30	0.76	0.03	0.17	0.15	0.88	-0.15	0.39	0.38	0.70
Interaction: Δ MCWD and pre-El Niño MCWD	1.52	0.93	1.62	0.11	0.88	0.64	1.37	0.17	-0.16	0.49	0.32	0.75